

Cover Page



Universiteit Leiden



The handle <http://hdl.handle.net/1887/35155> holds various files of this Leiden University dissertation.

Author: Hussaarts, Leonie

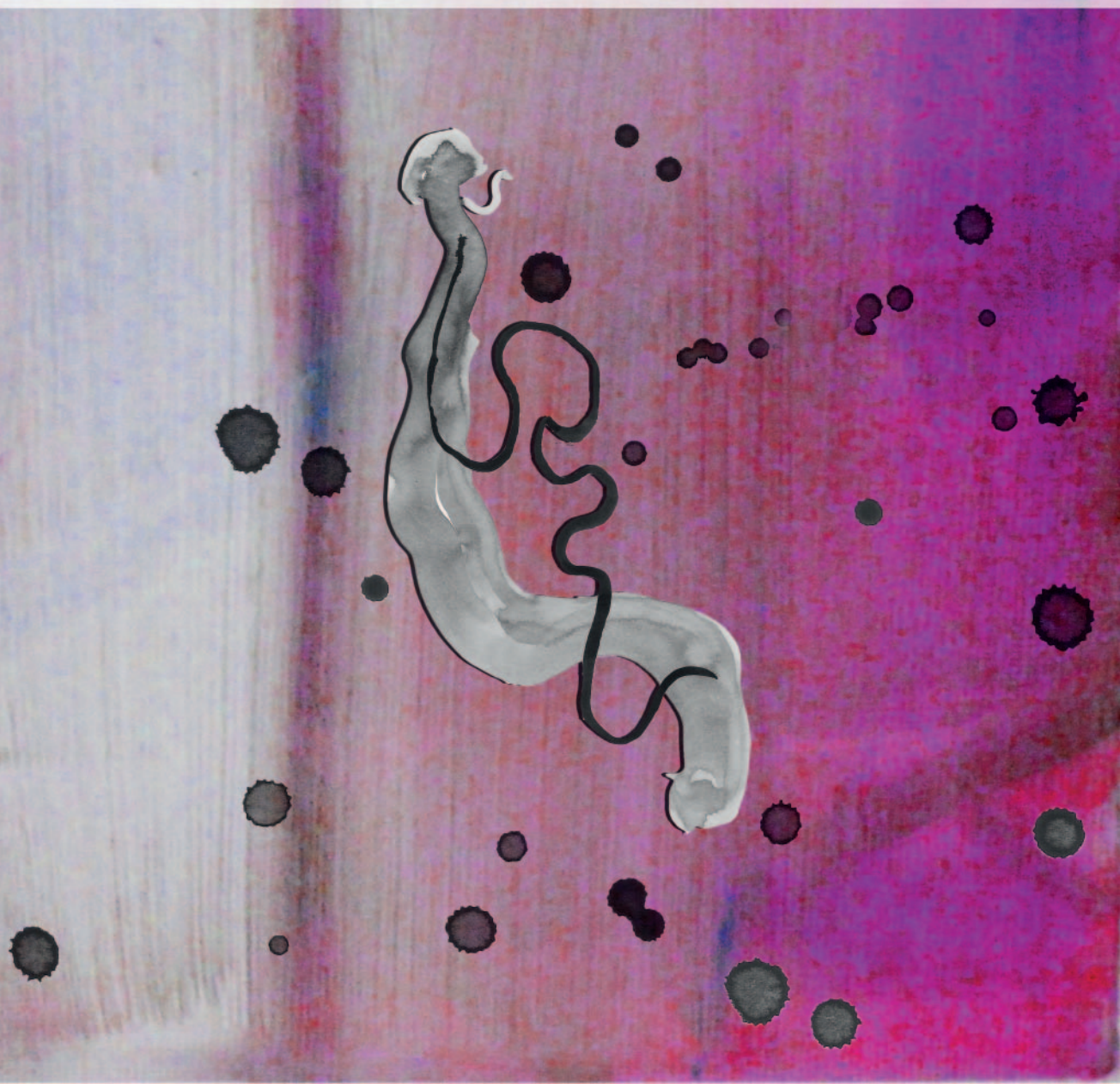
Title: Immune modulation by schistosomes : mechanisms of T helper 2 polarization and implications for metabolic disorders

Issue Date: 2015-09-10

IMMUNE MODULATION BY SCHISTOSOMES:

mechanisms of T helper 2 polarization and
implications for metabolic disorders

Leonie Husaarts



IMMUNE MODULATION BY SCHISTOSOMES:

mechanisms of T helper 2 polarization and
implications for metabolic disorders

ISBN: 978-94-6182-556-8

© 2015 Leonie Husaarts

The work presented in this thesis was performed at the Department of Parasitology,
at the Leiden University Medical Center in the Netherlands.

Printing of this thesis was financially supported by ChipSoft and BD Biosciences.

Cover design and artwork: Martijn den Ouden (www.martijndenouden.nl)

Layout and Printing: Off Page (www.offpage.nl)

IMMUNE MODULATION BY SCHISTOSOMES:

mechanisms of T helper 2 polarization and
implications for metabolic disorders

Proefschrift

ter verkrijging van
de graad van Doctor aan de Universiteit Leiden,
op gezag van Rector Magnificus prof.mr. C.J.J.M. Stolker,
volgens besluit van het College voor Promoties
ter verdedigen op donderdag 10 september 2015
klokke 11.15 uur

door

Leonie Husaarts
geboren te Delft in 1987

PROMOTIECOMMISSIE

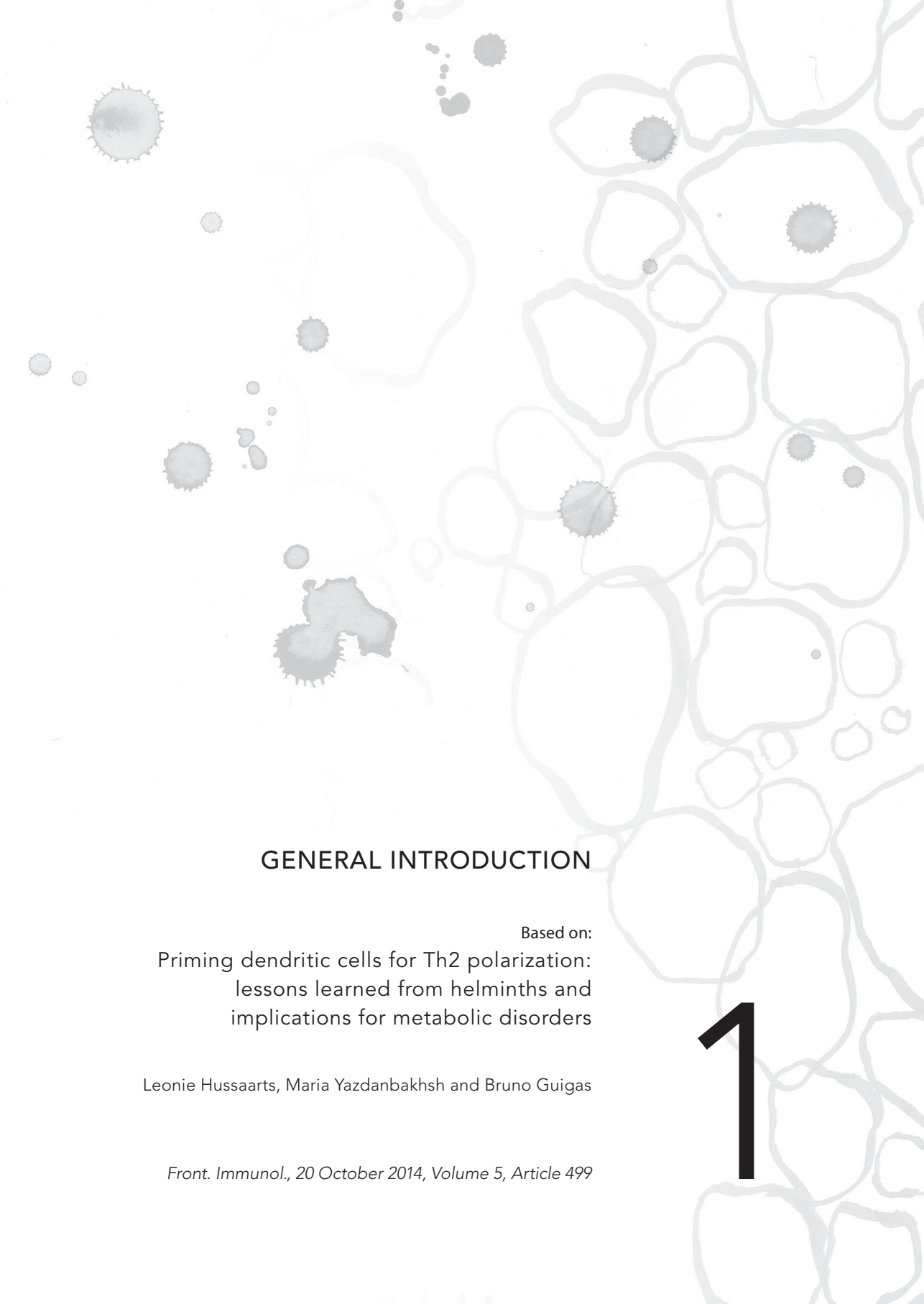
Promotor: Prof. Dr. M. Yazdanbakhsh

Co-promotor: Dr. B. Guigas

Overige leden: Dr. D. Jankovic (National Institutes of Health, Bethesda, MD, USA)
Prof. Dr. C. van Kooten
Prof. Dr. M.P.J. de Winther (Academic Medical Center, Amsterdam)

TABLE OF CONTENTS

Chapter 1	General introduction	7
Chapter 2	Schistosome-derived omega-1 drives Th2 polarization by suppressing protein synthesis following internalization by the mannose receptor	25
Chapter 3	Rapamycin and omega-1: mTOR-dependent and -independent Th2 skewing by human dendritic cells	51
Chapter 4	Analysis of human dendritic cell maturation and polarization using label-free quantitative proteomics	63
Chapter 5	Chronic helminth infection and helminth-derived egg antigens promote adipose tissue M2 macrophages and improve insulin sensitivity in obese mice	87
Chapter 6	Mannose receptor deficiency protects against high-fat diet-induced insulin resistance and decreases classical activation of liver and adipose tissue macrophages	111
Chapter 7	Summarizing discussion	133
Addendum	Nederlandse samenvatting	149
	Dankwoord / Acknowledgements	153
	Curriculum Vitae	155
	List of publications	157



GENERAL INTRODUCTION

Based on:
Priming dendritic cells for Th2 polarization:
lessons learned from helminths and
implications for metabolic disorders

Leonie Hussaarts, Maria Yazdanbakhsh and Bruno Guigas

Front. Immunol., 20 October 2014, Volume 5, Article 499

1

1. IMMUNE RESPONSES

Mammalian immune responses are a result of interplay between the non-specific innate immune system and the adaptive immune system. The innate immune system provides a first line of defense, while the adaptive immune system is antigen-specific and required for long-term protection against infections. CD4⁺ T helper (Th) are members of the adaptive immune system that regulate immunity and inflammation through the secretion of specific cytokines. Different classes of pathogens require activation of specific Th cell subsets, and immune responses are therefore often classified based on the central Th cell subsets involved.

In case of rapidly replicating microorganisms, such as bacteria and viruses, an antimicrobial type 1 immune response is invoked. The principal regulators of the type 1 immune response are Th1 cells, which secrete the pro-inflammatory cytokine interferon- γ (IFN- γ). IFN- γ stimulates macrophage activation, antigen uptake and presentation, and intracellular killing of microbes. The type 2 immune response, on the other hand, encompasses the host response to parasitic worms (also known as helminths), and is characterized by the presence of Th2 cells, which secrete interleukin-4 (IL-4), IL-5 and IL-13 to mediate B cell activation and IgE antibody production. Furthermore, type 2 immune responses are characterized by an expanding group of innate immune cells, including eosinophils, mast cells, group 2 innate lymphoid cells, and alternatively activated macrophages. Together, these cells control infection and/or mediate parasite expulsion through smooth muscle contraction and mucus production (reviewed in (1;2)). In addition to Th1 and Th2 cells, different T helper cell subsets have been discovered over the past ten years, including Th17 which protect against protect against extracellular bacteria and fungi, and Th22 and Th9 cells, which have a range of functional activities (3).

Aside from anti-helminth immunity, it has become increasingly clear that type 2 immune responses have additional functions. For example, literature has described a close association between type 2 immune responses and wound repair (4-7). Strikingly, recent evidence indicates that multiple facets of the type 2 immune response can also regulate metabolism and protect against insulin resistance. For just one example, the prototypical Th2 cytokine IL-4 can regulate the balance between fatty acid and glucose oxidation in hepatocytes (8). Conversely, pro-inflammatory immune responses have been shown to participate in the pathogenesis of diet-induced diabetes (9;10). By studying the molecular mechanisms that govern helminth-induced Th2 polarization, we may therefore learn valuable lessons for both the protection against helminth infection and pathways involved in metabolic regulation.

2. AN INTRODUCTION TO SCHISTOSOMES

Schistosomes are helminths frequently used to study T helper 2 polarization, not only because of their prevalence, but also because of their ability to infect both mice and humans. Schistosomes are the causative agent of schistosomiasis and chronically infect over 200 million people worldwide (11). There are five species of schistosomes, of which *Schistosoma japonicum*, *S. mansoni*, and *S. haematobium* are the most common. The life cycles of these three

schistosomes are largely comparable. Briefly, when infected individuals urinate or defecate in water, eggs are excreted that hatch to release miracidiae, which can penetrate the fresh water snail. In the snail, the miracidiae develop into sporocysts, which generate cercariae that can infect the human host. Upon infection, the cercariae lose their tail and become schistosomulae, which enter circulation and migrate through several tissues to the hepatic portal vein, where the mature male and female worms form pairs. Schistosome pairs then migrate to the mesenteric veins (*S. japonicum* and *S. mansoni*), or to the venous plexus of the bladder (*S. haematobium*), where the female starts to produce hundreds of eggs per day. The eggs penetrate through the tissues to the intestine or the bladder, and are again released with feces or urine. Not all eggs go through this process though. Depending on the species, the blood flow carries many eggs to the liver, where they induce granuloma formation, or to the bladder, where they can promote bladder cancer (11).

Since mice are highly susceptible to *S. mansoni* infection, the host immune response to this species has been the most widely studied (12). The first weeks after infection, during schistosomulae migration, are characterized by a T helper 1 (Th1) response. After 5-6 weeks post infection, with the onset of egg deposition in the liver and intestines, the immune response changes. The Th1 component decreases and a strong egg-specific Th2 response, characterized by IL-4, IL-5 and IL-13 cytokine expression, develops (11). The development of the Th2 response is essential for reducing morbidity of the host by excessive Th1-like inflammatory reactions: wild type (C57BL/6) mice enter a chronic phase of egg accumulation 8 weeks post infection, however IL-4-deficient mice die of uncontrolled Th1-associated inflammatory reactions to parasites (13).

Although it is clear that the induction of Th2 responses serves an important host-protective role during the initial stage of infection, persistent type 2 cytokine responses may also result in immunopathology and morbidity (14;15). Egg-induced granuloma formation is detrimental to the host as it is associated with the induction of IL-13-dependent liver fibrosis. As such, schistosome-infected mice in which IL-13 is blocked fail to develop liver fibrosis, which leads to prolonged survival of these mice (16-18). Therefore, to prevent Th2-associated damage to the host, controlling the Th2 response is at least equally important as its generation. Th2 cell control becomes visibly active around week 12 post infection, when the chronic phase of infection emerges. Egg production continues but the Th2 response diminishes and newly formed liver granulomas have a smaller size than those formed at earlier times during infection (11). At this stage, control of the Th2 response is provided by regulatory T cells (Treg cells) (19;20), alternatively activated macrophages (7;21), and regulatory B cells (22).

3. DENDRITIC CELLS AND T HELPER 2 POLARIZATION

The mechanisms that initiate the Th2 response in helminth infection are still not fully understood, although it is clear that dendritic cells (DCs) (23), the most efficient antigen-presenting cells (APCs) in the immune system, play a crucial role (24). DCs are located in peripheral tissues, where they continuously sample the environment to capture antigens from invading microbes. Upon recognition of pathogen-associated molecular patterns (PAMPs), DCs

undergo phenotypic changes that allow them to migrate to the lymph nodes and to provide the signals required for the activation of T cells (25;26). The importance of DCs in Th2 skewing is highlighted by studies showing that depletion of CD11c⁺ DCs interferes with the induction of a Th2 response to *S. mansoni* and *Helimosomoides polygyrus* (27-29). Interestingly, it has become increasingly clear that distinct DC subsets induce different Th responses (reviewed in (24;30)), and in the last few years, several studies analyzed the role of DC subsets in the initiation of Th2 responses to helminth infection.

3.1 Dendritic cell subsets associated with Th2 polarization

Two independent groups recently showed that the development of a Th2 response to *Nippostrongylus brasiliensis* depends on dermal CD301b⁺ DCs (31;32). Specifically, depletion of CD301b⁺ DCs prior to infection reduces IL-4 production by CD4⁺ T cells, without affecting the percentage of T follicular helper (Tfh) cells or germinal center B cells (31). Mechanistically, Th2-inducing PDL2⁺CD301b⁺ DCs were shown to depend on DC-specific expression of the transcription factor interferon regulatory factor 4 (IRF4) (32). In line with these findings, CD11c^{int}MHCII^{hi} dermal DCs expressing PDL2 and CD301b were also identified as a Th2-priming DC subset in *N. brasiliensis* infection (33). Of note, CD301b⁺ DCs alone are insufficient to generate a Th2 response *in vitro* (32) or *in vivo* (31), suggesting that additional requirements exist. For example, optimal localization of DCs within the lymph node may play a crucial role. In *H. polygyrus* infection, CXCR5-expressing CD11c⁺ DCs migrate to the lymph node and localize adjacent to B cell follicles (34). Depletion of CXCR5 or B cell-derived lymphotoxin alters the localization of the DCs and, as a consequence, impairs the development of Tfh and Th2 cells (34). In addition, it has been suggested that DCs require signals from basophils (35) and group 2 innate lymphoid cells (ILC2s) (36) to prime Th2 responses to allergens. Together, these studies suggest that specific DC subsets, as well as the microenvironment in which these subsets encounter CD4⁺ T cells, are important for Th2 development *in vivo*.

3.2 Sensing helminth-derived antigens

DCs are equipped with pattern recognition receptors (PRRs) that recognize a wide array of PAMPs. The classical paradigm describes that triggering of PRRs, including the Toll-like receptors (TLRs), RIG-I-like receptors, NOD-like receptors, scavenger receptors, and C-type lectin receptors (CLRs), induces DC maturation and subsequent antigen-specific activation of T helper cells (37).

While signaling through most TLRs induces Th1/Th17 responses (38), Th2-inducing helminth-derived molecules have also been described to interact with DCs through TLR2, 3 and 4 (39-42). Although the schistosome-related glycan LNFPIII, which contains Lewis X (Le^x) trisaccharides, requires TLR4 for Th2 skewing (43), various studies suggest that TLRs are dispensable for Th2 polarization by helminth antigens. For example, bone marrow-derived DCs (BMDCs) from TLR2- and TLR4-knockout mice can still skew Th2 when pulsed with *S. mansoni* soluble egg antigens (SEA) (44), and the TLR adaptor protein MyD88 is not required for Th2 skewing by SEA-stimulated splenic DCs (45). Interestingly, human monocyte-derived dendritic cells (moDCs) stimulated

with phosphatidylserine lipids from schistosomes induce IL-10-producing T cells through TLR2 (40). Therefore, helminth products may employ TLRs for the induction of regulatory responses, but it seems that other PRRs are required for the initiation of a Th2 response.

Indeed, CLRs that sense helminth glycans play an important role in Th2 skewing. For example, SEA is internalized by moDCs through DC-specific ICAM-3-grabbing nonintegrin (DC-SIGN), macrophage galactose-type lectin (MGL) and mannose receptor (MR) (46), and binds to Dectin-2 on BMDCs (47). Binding of SEA to DC-SIGN was shown to depend on Le^x (48), and a recent study showed that blocking DC-SIGN-associated signaling inhibits Th2 skewing (49). Likewise, excretory/secretory products from the tapeworm *Taenia crassiceps* (TcES) bind MR and MGL on BMDCs (50), and the Th2-skewing capacity of TcES is glycan-dependent (51). In sum, these studies indicate that helminth-derived antigen preparations can bind a variety of PRRs, which may induce distinct intracellular events that promote Th2 polarization.

3.3 Intracellular mechanisms associated with Th2 polarization

PRR-mediated signaling classically induces DC maturation via mitogen-activated protein kinases (MAPK) (52). However, in contrast to microbial ligands, helminth products often fail to induce classical signs of maturation and are well-known to downregulate TLR-mediated maturation (46;53-59). Indeed, unlike many TLR ligands, Th2-inducing compounds fail to phosphorylate p38 MAPK but instead promote phosphorylation of p42/p44 MAPK (ERK1/2) (reviewed in (60)). ERK1/2 stabilizes c-Fos, and inhibiting either c-FOS or ERK1/2 enhances IL-12 production by moDCs (61), suggesting that activation of this pathway suppresses Th1-polarizing cytokines. Likewise, TSLP promotes ERK1/2 phosphorylation (62) and fails to induce IL-12 production by myeloid DCs (63;64).

It was noted that the NF- κ B signaling pathway also seems involved in Th2 polarization, as SEA- or LNFPIII-stimulated BMDCs from NF- κ B1 knockout mice fail to prime a Th2 response (65;66). Furthermore, it was recently demonstrated that Le^x residues, via DC-SIGN, activate LSP1 in moDCs, leading to nuclear accumulation of the atypical NF- κ B family member Bcl3 and downregulation of IL-12 mRNA. These events also seem required for SEA-induced T cell polarization, since silencing either LSP1 or Bcl3 interferes with Th2 skewing (49). Similarly, the Th2-inducing capacity of TSLP was shown to involve activation of NF- κ B and STAT5 (62;67).

Lastly, SEA can signal through spleen tyrosine kinase (Syk) downstream of Dectin-2, activating the Nlrp3 inflammasome and increasing TLR-triggered release of IL-1 β by BMDCs. However, infection of various inflammasome-deficient mice with *S. mansoni* demonstrated that activation of this pathway does not seem to favor any particular Th response (47). Thus, helminth antigens can activate signaling, and certain members of the NF- κ B and ERK pathways in particular seem to play a role in Th2 polarization.

In addition to signaling-dependent mechanisms, a number of studies identified a role for cysteine protease inhibitors secreted by filarial nematodes (cystatins) in regulating host immune responses by interfering with antigen processing (reviewed in (68)). Therefore, helminths may employ both signaling-dependent and independent mechanisms to condition DCs for Th2 skewing (**figure 1**).

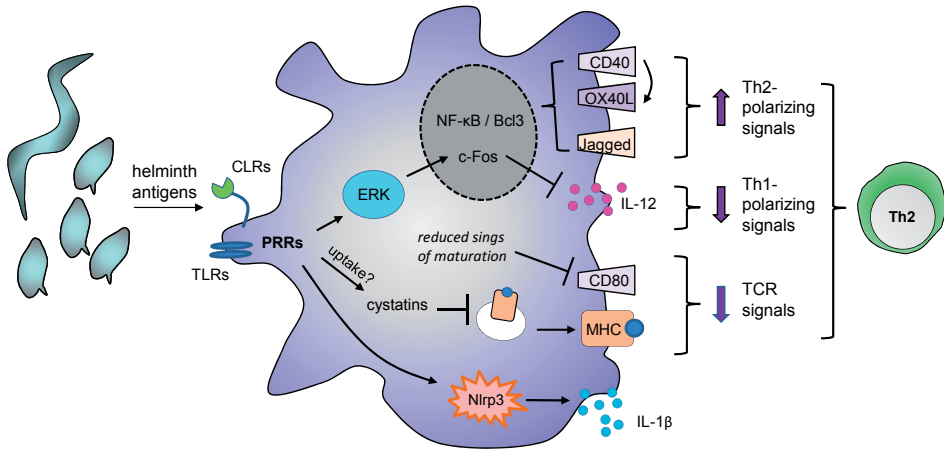


Figure 1. Possible mechanisms by which helminth molecules modulate DCs for Th2 polarization. Helminth antigens are recognized by DCs through ligation of pattern recognition receptors (PRRs), such as Toll-like receptors (TLRs) and C-type lectin receptors (CLRs). Depending on the antigen, binding promotes phosphorylation of ERK1/2, nuclear accumulation of NF- κ B or Bcl3, and/or activation of the Nlrp3 inflammasome which mediates IL-1 β secretion. Phosphorylation of ERK1/2 stabilizes c-Fos, leading to downregulation of IL-12 expression. In addition, DCs can upregulate expression of Th2-associated CD40 and Jagged, which are under the control of NF- κ B and ERK1/2, respectively (74;75). Upon encounter of T cells expressing CD40L, signaling through CD40 promotes OX40L expression in an autocrine manner. Alternatively, PRRs may mediate uptake of antigens that interfere with antigen presentation on MHCs, such as cystatins. In addition, helminth products fail to upregulate classical markers of maturation. Altogether, these events favor DC-mediated Th2 polarization.

3.4 Primed DCs and initiation of T cell polarization

A major difference between Th1 and Th2 development is that a Th1 response requires persistent production of Th1-polarizing cytokines, like IL-12, which are exclusively produced by APCs. By contrast, once primed DCs induce IL-4 production by a few activated T helper cells, the Th2 response is self-sustained through autocrine production of IL-4 (69;70). Therefore, in order to understand mechanisms of Th2 polarization, it is critical to identify the DC-associated polarizing signals that control early IL-4 production by activated T cells.

3.4.1 Soluble factors and surface molecules

As discussed above, DCs stimulated with helminth molecules or TSLP fail to express IL-12. Moreover, injection of IL-12 can block the development of a Th2 response to *S. mansoni* eggs (71). These findings led to the so-called 'default concept', which states that Th2 differentiation spontaneously occurs in the absence of a Th1-priming signal like IL-12. However, mice lacking IL-12 do not develop a Th2 response to microbial pathogens (72), and blocking the mTOR pathway in moDCs skews a potent Th2 response without affecting IL-12 (73), suggesting that there are active signals involved in Th2 differentiation.

Such a signal may be provided by a soluble factor secreted by DCs, like RELM α , which was shown to promote IL-10 and IL-13 secretion by lymph node cells following adoptive transfer of SEA-stimulated BMDCs (74). However, supernatants from SEA-primed moDCs do not skew towards Th2 (75), and SEA-stimulated BMDCs do not induce Th2 when separated from CD4⁺ T cells in transwells (76), indicating that an active polarizing signal in these studies is likely provided by surface molecules. Indeed, the Notch ligands Delta-4 and Jagged-2 have been linked to Th1 and Th2 polarization, respectively (77), and helminth antigens were shown to upregulate Jagged-2 on BMDCs (78;79) and to suppress Delta-4 expression in moDCs (80). However, Jagged-2-deficient BMDCs can still skew Th2 when challenged with SEA (78;79), suggesting that other molecules may be involved. For example, CD40 has been suggested to provide a polarizing signal, as its expression on SEA-stimulated BMDCs is required for the induction of a Th2 response (81), and mice lacking CD40 ligand suffer from impaired Th2 development during *S. mansoni* infection (82). Mechanistically, signaling through CD40 promotes OX40L expression, which is essential for optimal Th2 skewing by SEA-conditioned BMDCs (83) and moDCs (75), as well as TSLP-conditioned myeloid DCs (64). However, treatment with anti-OX40L does not significantly affect the Th2 response to *N. brasiliensis* infection (84), and it has been suggested that OX40L acts as a costimulatory molecule rather than a polarizing signal, since SEA-treated OX40L-knockout DCs induce Th2 cells, but fail to stimulate appropriate T cell expansion (83). Altogether, these studies suggest that there may not be one specific DC-associated molecule required for Th2 polarization, but rather a combination of signals that mediate both optimal T cell priming and expansion.

3.4.2 A role for the T cell receptor

Early reports have described that the antigen dose can determine the outcome of Th differentiation, with a high dose generally favoring Th1 development (85-87). These findings were confirmed in a recent report, which also indicated that Th1-inducing adjuvants promote a higher Ca²⁺ flux (representing T cell receptor (TCR)-signaling strength), and induce larger synapse size, than Th2-promoting molecules (88). In addition, it has been suggested that T cells activated by Th2-inducing ligands are less proliferative, as priming of splenic DCs with SEA reduces the frequency of CD4⁺ T cells progressing through the cell cycle, and drug-induced arrest of cell cycle progression promotes Th2 polarization (45). Together, these observations suggest that helminth molecules may reduce TCR triggering, impairing T cell proliferation in favor of Th2 differentiation. Indeed, treatment of splenic DCs with SEA results in shorter T cell-DC interaction times and lower TCR signaling when compared to a Th1-inducing adjuvant (88). Omega-1, a glycosylated identified as the major component in SEA (55), was also shown to reduce the capacity of BMDCs to form T cell-DC conjugates and to diminish the frequency of CD4⁺ T cells progressing through the cell cycle (76). Mechanistically, interaction between T cells and DCs was shown to depend at least in part on the co-stimulatory molecule CD80 (88). As discussed above, helminth products fail to induce upregulation of costimulatory molecules, which may also explain why DCs treated with helminth molecules are less capable of forming stable interactions with T cells.

4. IMPLICATIONS FOR METABOLIC DISORDERS

A growing body of literature indicates that obesity is associated with chronic low-grade inflammation of metabolic organs, in particular adipose tissue. In healthy adipose tissue, a wide variety of immune cell types play an important role in housekeeping, removal of apoptotic cells, and maintenance of homeostasis (89). However, fat accumulation results in chemokine secretion by adipocytes, attracting classically activated M1 macrophages that secrete pro-inflammatory cytokines like interleukin (IL)-1 β and tumor necrosis factor- α (TNF- α) (10;90;91). These cytokines interfere with insulin signaling (92;93) and induce lipolysis (94;95), thereby increasing circulating free fatty acids which promote peripheral insulin resistance (96). In addition to M1 macrophages, other pro-inflammatory immune cells have been associated with insulin resistance, including Th1 cells, Th17 cells, CD8⁺T cells and B lymphocytes (97) (**figure 2**).

By contrast, alternatively activated macrophages, also called M2 macrophages, prevail in lean white adipose tissue (WAT) and are involved in the maintenance of adipose tissue insulin sensitivity, partly through secretion of the anti-inflammatory cytokine IL-10 (10;98). The M2 phenotype is promoted by Th2-type cytokines IL-4, IL-5 and IL-13, which were shown to be secreted by WAT eosinophils (99) and ILC2s (100). In addition, various reports have shown that Th2-inducing conditions, such as *N. brasiliensis* infection (99;101), allergic inflammation (8), or SEA administration (102), improve insulin sensitivity and glucose tolerance in diet-induced obese mice. Furthermore, both *S. mansoni* infection (103) and SEA administration (104) reduce

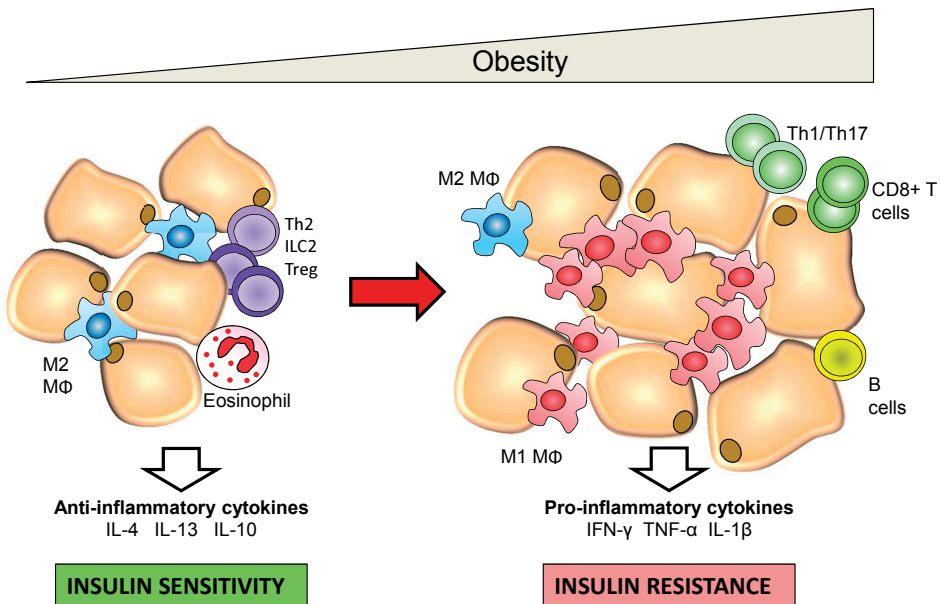


Figure 2. Obesity and inflammation of adipose tissue. As obesity develops, the expanding adipose tissue promotes the transition from an anti-inflammatory to a pro-inflammatory state.

the development of atherosclerotic lesions in mice, and adoptive transfer of CD4⁺T cells (mostly via Th2 cells) and IL-4 treatment can protect against diet-induced insulin resistance (8;105). Lastly, type 2-associated ILC2s (100;106) and eosinophils (99) were shown to play a crucial role in maintenance of whole-body metabolic homeostasis by sustaining adipose tissue alternatively activated M2 macrophages. These findings are in line with epidemiological studies indicating that infection with helminths inversely correlates with metabolic syndrome (107;108). These landmark studies identify the interplay between helminths and energy metabolism as an exciting new area that needs further dissection.

5. SCOPE OF THE THESIS

Over the last few decades, a wide array of studies have shed light on the possible mechanisms by which helminth molecules condition DCs for Th2 skewing. Nevertheless, due to the complex nature of many helminth-derived antigen preparations, it proved difficult to pinpoint specific receptors and/or mechanism involved. Therefore, the identification of omega-1, a glycosylated RNase, as the major immunomodulatory component in SEA has provided us with a powerful tool to further dissect the molecular mechanisms underlying Th2 polarization (55;76). The first part of this thesis centers on the following question:

How does omega-1 modulate dendritic cells for T helper 2 polarization?

Chapter 2 studies the molecule omega-1, and analyzes the requirement of glycosylation and RNase activity in the modulation of DCs for Th2 polarization, *in vitro* and *in vivo*.

In **chapter 3** we study the role of the mTOR pathway in the induction of Th2 responses by moDCs stimulated with SEA and omega-1.

Chapter 4 further characterizes moDCs primed for Th2 polarization by SEA or omega-1 using a mass spectrometry-based approach.

The second part of this thesis builds on landmark studies showing that type 2 inflammatory responses protect against metabolic disorders. These studies have identified the interplay between helminths and metabolic homeostasis as an exciting new area that needs further dissection. We focus on the following question:

*What are the effects of chronic *S. mansoni* infection and SEA administration on metabolic homeostasis?*

In **chapter 5**, we study the effects of chronic *Schistosoma mansoni* infection and SEA treatment on whole-body glucose homeostasis and insulin sensitivity in a mouse model of diet-induced

obesity. We perform in-depth metabolic profiling and analyze the immune cell composition of metabolic organs.

The MR is a marker for M2 macrophages, and was identified in Chapter 2 as the main receptor responsible for internalization of omega-1 by moDCs. In **chapter 6**, we therefore study the effect of HFD-feeding on metabolic homeostasis and immune cell polarization in mice deficient for the MR.

Chapter 7 summarizes the importance of our findings within the larger body of literature, and provides directions for future research towards understanding the link between schistosomes, Th2 polarization and metabolic disorders.

REFERENCES

1. Spellberg B, et al. Type 1/Type 2 immunity in infectious diseases. *Clin Infect Dis* 2001 Jan;32(1):76-102.
2. Gause WC, et al. Type 2 immunity and wound healing: evolutionary refinement of adaptive immunity by helminths. *Nat Rev Immunol* 2013 Aug;13(8):607-14.
3. Tong ZH, et al. Subpopulations of helper T lymphocytes in tuberculous pleurisy. *Tuberculosis (Edinb)* 2013 May;93(3):279-84.
4. Chen F, et al. An essential role for TH2-type responses in limiting acute tissue damage during experimental helminth infection. *Nat Med* 2012 Feb;18(2):260-6.
5. Monticelli LA, et al. Innate lymphoid cells promote lung-tissue homeostasis after infection with influenza virus. *Nat Immunol* 2011 Nov;12(11):1045-54.
6. Herbert DR, et al. Arginase I suppresses IL-12/IL-23p40-driven intestinal inflammation during acute schistosomiasis. *J Immunol* 2010 Jun 1;184(11):6438-46.
7. Pesce JT, et al. Arginase-1-expressing macrophages suppress Th2 cytokine-driven inflammation and fibrosis. *PLoS Pathog* 2009 Apr;5(4):e1000371.
8. Ricardo-Gonzalez RR, et al. IL-4/STAT6 immune axis regulates peripheral nutrient metabolism and insulin sensitivity. *Proc Natl Acad Sci USA* 2010 Dec 28;107(52):22617-22.
9. Donath MY, et al. Type 2 diabetes as an inflammatory disease. *Nat Rev Immunol* 2011 Feb;11(2):98-107.
10. Chawla A, et al. Macrophage-mediated inflammation in metabolic disease. *Nat Rev Immunol* 2011 Nov;11(11):738-49.
11. Pearce EJ, et al. The immunobiology of schistosomiasis. *Nat Rev Immunol* 2002 Jul;2(7):499-511.
12. Wilson MS, et al. Immunopathology of schistosomiasis. *Immunol Cell Biol* 2007 Feb;85(2):148-54.
13. Brunet LR, et al. IL-4 protects against TNF- α -mediated cachexia and death during acute schistosomiasis. *J Immunol* 1997 Jul 15;159(2):777-85.
14. Hoffmann KF, et al. IL-10 and the dangers of immune polarization: excessive type 1 and type 2 cytokine responses induce distinct forms of lethal immunopathology in murine schistosomiasis. *J Immunol* 2000 Jun 15;164(12):6406-16.
15. Wynn TA. Common and unique mechanisms regulate fibrosis in various fibroproliferative diseases. *J Clin Invest* 2007 Mar;117(3):524-9.
16. Chiamonte MG, et al. An IL-13 inhibitor blocks the development of hepatic fibrosis during a T-helper type 2-dominated inflammatory response. *J Clin Invest* 1999 Sep;104(6):777-85.
17. Fallon PG, et al. Schistosome infection of transgenic mice defines distinct and contrasting pathogenic roles for IL-4 and IL-13: IL-13 is a profibrotic agent. *J Immunol* 2000 Mar 1;164(5):2585-91.
18. Jankovic D, et al. Schistosome-infected IL-4 receptor knockout (KO) mice, in contrast to IL-4 KO mice, fail to develop granulomatous pathology while maintaining the same lymphokine expression profile. *J Immunol* 1999 Jul 1;163(1):337-42.
19. Baumgart M, et al. Naturally occurring CD4⁺Foxp3⁺ regulatory T cells are an essential, IL-10-independent part of the immunoregulatory network in *Schistosoma mansoni* egg-induced inflammation. *J Immunol* 2006 May 1;176(9):5374-87.
20. Hesse M, et al. The pathogenesis of schistosomiasis is controlled by cooperating IL-10-producing innate effector and regulatory T cells. *J Immunol* 2004 Mar 1;172(5):3157-66.
21. Maizels RM, et al. Regulation of pathogenesis and immunity in helminth infections. *J Exp Med* 2009 Sep 28;206(10):2059-66.
22. Husaarts L, et al. Regulatory B-cell induction by helminths: implications for allergic disease. *J Allergy Clin Immunol* 2011 Oct;128(4):733-9.
23. Steinman RM, et al. Identification of a novel cell type in peripheral lymphoid organs of mice. I. Morphology, quantitation, tissue distribution. *J Exp Med* 1973 May 1;137(5):1142-62.
24. Pulendran B, et al. Programming dendritic cells to induce T(H)2 and tolerogenic responses. *Nat Immunol* 2010 Aug;11(8):647-55.
25. Kapsenberg ML. Dendritic-cell control of pathogen-driven T-cell polarization. *Nat Rev Immunol* 2003 Dec;3(12):984-93.
26. Palucka K, et al. Cancer immunotherapy via dendritic cells. *Nat Rev Cancer* 2012 Apr;12(4):265-77.

27. Phytian-Adams AT, et al. CD11c depletion severely disrupts Th2 induction and development in vivo. *J Exp Med* 2010 Sep 27;207(10):2089-96.
28. Smith KA, et al. Type 2 innate immunity in helminth infection is induced redundantly and acts autonomously following CD11c(+) cell depletion. *Infect Immun* 2012 Oct;80(10):3481-9.
29. Smith KA, et al. Chronic helminth infection promotes immune regulation in vivo through dominance of CD11c^{lo}C. *J Immunol* 2011 Jun 15;186(12):7098-109.
30. Briseno CG, et al. Complementary diversification of dendritic cells and innate lymphoid cells. *Curr Opin Immunol* 2014 Aug;29:69-78.
31. Kumamoto Y, et al. CD301b(+) dermal dendritic cells drive T helper 2 cell-mediated immunity. *Immunity* 2013 Oct 17;39(4):733-43.
32. Gao Y, et al. Control of T helper 2 responses by transcription factor IRF4-dependent dendritic cells. *Immunity* 2013 Oct 17;39(4):722-32.
33. Connor LM, et al. Helminth-Conditioned Dendritic Cells Prime CD4+ T Cells to IL-4 Production In Vivo. *J Immunol* 2014 Sep 15;193(6):2709-17.
34. Leon B, et al. Regulation of T(H)2 development by CXCR5+ dendritic cells and lymphotoxin-expressing B cells. *Nat Immunol* 2012 Jul;13(7):681-90.
35. Tang H, et al. The T helper type 2 response to cysteine proteases requires dendritic cell-basophil cooperation via ROS-mediated signaling. *Nat Immunol* 2010 Jul;11(7):608-17.
36. Halim TY, et al. Group 2 innate lymphoid cells are critical for the initiation of adaptive T helper 2 cell-mediated allergic lung inflammation. *Immunity* 2014 Mar 20;40(3):425-35.
37. Kapsenberg ML. Dendritic-cell control of pathogen-driven T-cell polarization. *Nat Rev Immunol* 2003 Dec;3(12):984-93.
38. Iwasaki A, et al. Regulation of adaptive immunity by the innate immune system. *Science* 2010 Jan 15;327(5963):291-5.
39. Aksoy E, et al. Double-stranded RNAs from the helminth parasite *Schistosoma* activate TLR3 in dendritic cells. *J Biol Chem* 2005 Jan 7;280(1):277-83.
40. van der Kleij D, et al. A novel host-parasite lipid cross-talk. Schistosomal lysophosphatidylserine activates toll-like receptor 2 and affects immune polarization. *J Biol Chem* 2002 Dec 13;277(50):48122-9.
41. Goodridge HS, et al. Immunomodulation via novel use of TLR4 by the filarial nematode phosphorylcholine-containing secreted product, ES-62. *J Immunol* 2005 Jan 1;174(1):284-93.
42. Correale J, et al. Helminth antigens modulate immune responses in cells from multiple sclerosis patients through TLR2-dependent mechanisms. *J Immunol* 2009 Nov 1;183(9):5999-6012.
43. Thomas PG, et al. Maturation of dendritic cell 2 phenotype by a helminth glycan uses a Toll-like receptor 4-dependent mechanism. *J Immunol* 2003 Dec 1;171(11):5837-41.
44. Kane CM, et al. *Schistosoma mansoni* egg antigen-mediated modulation of Toll-like receptor (TLR)-induced activation occurs independently of TLR2, TLR4, and MyD88. *Infect Immun* 2008 Dec;76(12):5754-9.
45. Jankovic D, et al. Parasite-induced Th2 polarization is associated with down-regulated dendritic cell responsiveness to Th1 stimuli and a transient delay in T lymphocyte cycling. *J Immunol* 2004 Aug 15;173(4):2419-27.
46. van Liempt E, et al. *Schistosoma mansoni* soluble egg antigens are internalized by human dendritic cells through multiple C-type lectins and suppress TLR-induced dendritic cell activation. *Mol Immunol* 2007 Apr;44(10):2605-15.
47. Ritter M, et al. *Schistosoma mansoni* triggers Dectin-2, which activates the Nlrp3 inflammasome and alters adaptive immune responses. *Proc Natl Acad Sci U S A* 2010 Nov 23;107(47):20459-64.
48. van Dielel, et al. The dendritic cell-specific C-type lectin DC-SIGN is a receptor for *Schistosoma mansoni* egg antigens and recognizes the glycan antigen Lewis x. *Glycobiology* 2003 Jun;13(6):471-8.
49. Gringhuis SI, et al. Fucose-specific DC-SIGN signaling directs T helper cell type-2 responses via IKKepsilon- and CYLD-dependent Bcl3 activation. *Nat Commun* 2014;5:3898.
50. Terrazas CA, et al. Helminth-excreted/secreted products are recognized by multiple receptors on DCs to block the TLR response and bias Th2 polarization in a cRAF dependent pathway. *FASEB J* 2013 Nov;27(11):4547-60.
51. Terrazas CA, et al. Impaired pro-inflammatory cytokine production and increased Th2-

- biasing ability of dendritic cells exposed to *Taenia* excreted/secreted antigens: A critical role for carbohydrates but not for STAT6 signaling. *Int J Parasitol* 2010 Aug 1;40(9):1051-62.
52. Arthur JS, et al. Mitogen-activated protein kinases in innate immunity. *Nat Rev Immunol* 2013 Sep;13(9):679-92.
 53. Kane CM, et al. Helminth antigens modulate TLR-initiated dendritic cell activation. *J Immunol* 2004 Dec 15;173(12):7454-61.
 54. Cervi L, et al. Cutting edge: dendritic cells copulsed with microbial and helminth antigens undergo modified maturation, segregate the antigens to distinct intracellular compartments, and concurrently induce microbe-specific Th1 and helminth-specific Th2 responses. *J Immunol* 2004 Feb 15;172(4):2016-20.
 55. Everts B, et al. Omega-1, a glycoprotein secreted by *Schistosoma mansoni* eggs, drives Th2 responses. *J Exp Med* 2009 Aug 3;206(8):1673-80.
 56. Rigano R, et al. Echinococcus granulosus antigen B impairs human dendritic cell differentiation and polarizes immature dendritic cell maturation towards a Th2 cell response. *Infect Immun* 2007 Apr;75(4):1667-78.
 57. Balic A, et al. Selective maturation of dendritic cells by *Nippostrongylus brasiliensis*-secreted proteins drives Th2 immune responses. *Eur J Immunol* 2004 Nov;34(11):3047-59.
 58. Segura M, et al. Impairment of dendritic cell function by excretory-secretory products: a potential mechanism for nematode-induced immunosuppression. *Eur J Immunol* 2007 Jul;37(7):1887-904.
 59. Brannstrom K, et al. The *Schistosoma mansoni* protein Sm16/SmSLP/SmSPO-1 assembles into a nine-subunit oligomer with potential to inhibit Toll-like receptor signaling. *Infect Immun* 2009 Mar;77(3):1144-54.
 60. Everts B, et al. Helminths and dendritic cells: sensing and regulating via pattern recognition receptors, Th2 and Treg responses. *Eur J Immunol* 2010 Jun;40(6):1525-37.
 61. Agrawal S, et al. Cutting edge: different Toll-like receptor agonists instruct dendritic cells to induce distinct Th responses via differential modulation of extracellular signal-regulated kinase-mitogen-activated protein kinase and c-Fos. *J Immunol* 2003 Nov 15;171(10):4984-9.
 62. Arima K, et al. Distinct signal codes generate dendritic cell functional plasticity. *Sci Signal* 2010;3(105):ra4.
 63. Soumelis V, et al. Human epithelial cells trigger dendritic cell mediated allergic inflammation by producing TSLP. *Nat Immunol* 2002 Jul;3(7):673-80.
 64. Ito T, et al. TSLP-activated dendritic cells induce an inflammatory T helper type 2 cell response through OX40 ligand. *J Exp Med* 2005 Nov 7;202(9):1213-23.
 65. Artis D, et al. Dendritic cell-intrinsic expression of NF-kappa B1 is required to promote optimal Th2 cell differentiation. *J Immunol* 2005 Jun 1;174(11):7154-9.
 66. Thomas PG, et al. A helminth glycan induces APC maturation via alternative NF-kappa B activation independent of I kappa B alpha degradation. *J Immunol* 2005 Aug 15;175(4):2082-90.
 67. Bell BD, et al. The transcription factor STAT5 is critical in dendritic cells for the development of TH2 but not TH1 responses. *Nat Immunol* 2013 Apr;14(4):364-71.
 68. Hartmann S, et al. Modulation of host immune responses by nematode cystatins. *Int J Parasitol* 2003 Sep 30;33(11):1291-302.
 69. Dong C, et al. Cell fate decision: T-helper 1 and 2 subsets in immune responses. *Arthritis Res* 2000;2(3):179-88.
 70. Jankovic D, et al. Mechanisms underlying helminth-induced Th2 polarization: default, negative or positive pathways? *Chem Immunol Allergy* 2006;90:65-81.
 71. Oswald IP, et al. IL-12 inhibits Th2 cytokine responses induced by eggs of *Schistosoma mansoni*. *J Immunol* 1994 Aug 15;153(4):1707-13.
 72. Jankovic D, et al. In the absence of IL-12, CD4(+) T cell responses to intracellular pathogens fail to default to a Th2 pattern and are host protective in an IL-10(-/-) setting. *Immunity* 2002 Mar;16(3):429-39.
 73. Hussaarts L, et al. Rapamycin and omega-1: mTOR-dependent and -independent Th2 skewing by human dendritic cells. *Immunol Cell Biol* 2013 Aug;91(7):486-9.
 74. Cook PC, et al. Alternatively activated dendritic cells regulate CD4+ T-cell polarization in vitro and in vivo. *Proc Natl Acad Sci U S A* 2012 Jun 19;109(25):9977-82.
 75. de Jong EC, et al. Microbial compounds selectively induce Th1 cell-promoting or Th2

- cell-promoting dendritic cells in vitro with diverse th cell-polarizing signals. *J Immunol* 2002 Feb 15;168(4):1704-9.
76. Steinfeldt S, et al. The major component in schistosome eggs responsible for conditioning dendritic cells for Th2 polarization is a T2 ribonuclease (omega-1). *J Exp Med* 2009 Aug 3;206(8):1681-90.
 77. Amsen D, et al. Instruction of distinct CD4 T helper cell fates by different notch ligands on antigen-presenting cells. *Cell* 2004 May 14;117(4):515-26.
 78. Krawczyk CM, et al. Th2 differentiation is unaffected by Jagged2 expression on dendritic cells. *J Immunol* 2008 Jun 15;180(12):7931-7.
 79. Worsley AG, et al. Dendritic cell expression of the Notch ligand jagged2 is not essential for Th2 response induction in vivo. *Eur J Immunol* 2008 Apr;38(4):1043-9.
 80. van Riet E, et al. Combined TLR2 and TLR4 ligation in the context of bacterial or helminth extracts in human monocyte derived dendritic cells: molecular correlates for Th1/Th2 polarization. *BMC Immunol* 2009;10:9.
 81. MacDonald AS, et al. Cutting edge: Th2 response induction by dendritic cells: a role for CD40. *J Immunol* 2002 Jan 15;168(2):537-40.
 82. MacDonald AS, et al. Impaired Th2 development and increased mortality during *Schistosoma mansoni* infection in the absence of CD40/CD154 interaction. *J Immunol* 2002 May 1;168(9):4643-9.
 83. Jenkins SJ, et al. Dendritic cell expression of OX40 ligand acts as a costimulatory, not polarizing, signal for optimal Th2 priming and memory induction in vivo. *J Immunol* 2007 Sep 15;179(6):3515-23.
 84. Connor LM, et al. Helminth-Conditioned Dendritic Cells Prime CD4+ T Cells to IL-4 Production In Vivo. *J Immunol* 2014 Aug 8;
 85. Constant S, et al. Extent of T cell receptor ligation can determine the functional differentiation of naive CD4+ T cells. *J Exp Med* 1995 Nov 1;182(5):1591-6.
 86. Hosken NA, et al. The effect of antigen dose on CD4+ T helper cell phenotype development in a T cell receptor-alpha beta-transgenic model. *J Exp Med* 1995 Nov 1;182(5):1579-84.
 87. Boonstra A, et al. Flexibility of mouse classical and plasmacytoid-derived dendritic cells in directing T helper type 1 and 2 cell development: dependency on antigen dose and differential toll-like receptor ligation. *J Exp Med* 2003 Jan 6;197(1):101-9.
 88. van Panhuys N, et al. T-Cell-Receptor-Dependent Signal Intensity Dominantly Controls CD4(+) T Cell Polarization In Vivo. *Immunity* 2014 Jul 17;41(1):63-74.
 89. Schipper HS, et al. Adipose tissue-resident immune cells: key players in immunometabolism. *Trends Endocrinol Metab* 2012 Aug;23(8):407-15.
 90. Weisberg SP, et al. Obesity is associated with macrophage accumulation in adipose tissue. *J Clin Invest* 2003 Dec;112(12):1796-808.
 91. Xu H, et al. Chronic inflammation in fat plays a crucial role in the development of obesity-related insulin resistance. *J Clin Invest* 2003 Dec;112(12):1821-30.
 92. Hotamisligil GS, et al. IRS-1-mediated inhibition of insulin receptor tyrosine kinase activity in TNF-alpha- and obesity-induced insulin resistance. *Science* 1996 Feb 2;271(5249):665-8.
 93. Hotamisligil GS, et al. Adipose expression of tumor necrosis factor-alpha: direct role in obesity-linked insulin resistance. *Science* 1993 Jan 1;259(5091):87-91.
 94. Feingold KR, et al. Stimulation of lipolysis in cultured fat cells by tumor necrosis factor, interleukin-1, and the interferons is blocked by inhibition of prostaglandin synthesis. *Endocrinology* 1992 Jan;130(1):10-6.
 95. Green A, et al. Tumor necrosis factor increases the rate of lipolysis in primary cultures of adipocytes without altering levels of hormone-sensitive lipase. *Endocrinology* 1994 Jun;134(6):2581-8.
 96. Rosen ED, et al. Adipocytes as regulators of energy balance and glucose homeostasis. *Nature* 2006 Dec 14;444(7121):847-53.
 97. Mraz M, et al. The role of adipose tissue immune cells in obesity and low-grade inflammation. *J Endocrinol* 2014 Sep;222(3):R113-R127.
 98. Lumeng CN, et al. Obesity induces a phenotypic switch in adipose tissue macrophage polarization. *J Clin Invest* 2007 Jan;117(1):175-84.
 99. Wu D, et al. Eosinophils sustain adipose alternatively activated macrophages associated with glucose homeostasis. *Science* 2011 Apr 8;332(6026):243-7.

100. Molofsky AB, et al. Innate lymphoid type 2 cells sustain visceral adipose tissue eosinophils and alternatively activated macrophages. *J Exp Med* 2013 Mar 11;210(3):535-49.
101. Yang Z, et al. Parasitic nematode-induced modulation of body weight and associated metabolic dysfunction in mouse models of obesity. *Infect Immun* 2013 Jun;81(6):1905-14.
102. Bhargava P, et al. Immunomodulatory glycan LNFP III alleviates hepatosteatosis and insulin resistance through direct and indirect control of metabolic pathways. *Nat Med* 2012 Nov;18(11):1665-72.
103. Doenhoff MJ, et al. An anti-atherogenic effect of *Schistosoma mansoni* infections in mice associated with a parasite-induced lowering of blood total cholesterol. *Parasitology* 2002 Nov;125(Pt 5):415-21.
104. Wolfs IM, et al. Reprogramming macrophages to an anti-inflammatory phenotype by helminth antigens reduces murine atherosclerosis. *FASEB J* 2014 Jan;28(1):288-99.
105. Winer S, et al. Normalization of obesity-associated insulin resistance through immunotherapy. *Nat Med* 2009 Aug;15(8):921-9.
106. Hams E, et al. Cutting edge: IL-25 elicits innate lymphoid type 2 and type II NKT cells that regulate obesity in mice. *J Immunol* 2013 Dec 1;191(11):5349-53.
107. Aravindhan V, et al. Decreased prevalence of lymphatic filariasis among diabetic subjects associated with a diminished pro-inflammatory cytokine response (CURES 83). *PLoS Negl Trop Dis* 2010;4(6):e707.
108. Chen Y, et al. Association of previous schistosome infection with diabetes and metabolic syndrome: a cross-sectional study in rural China. *J Clin Endocrinol Metab* 2013 Feb;98(2):E283-E287.



**SCHISTOSOME-DERIVED OMEGA-1
DRIVES TH2 POLARIZATION BY
SUPPRESSING PROTEIN SYNTHESIS
FOLLOWING INTERNALIZATION BY
THE MANNOSE RECEPTOR**

Bart Everts, Leonie Husaarts,* Nicole N. Driessen,*
Moniek H.J. Meevissen, Gabriele Schramm,
Alwin J. van der Ham, Barbara van der Hoeven,
Thomas Scholzen, Sven Burgdorf, Markus Mohrs,
Edward J. Pearce, Cornelis H. Hokke, Helmut Haas,
Hermelijn H. Smits and Maria Yazdanbakhsh

*both authors contributed equally

© 2012 Everts et al. *Journal of Experimental Medicine*.
209:10 1753-1767. doi: 10.1084/jem.20111381

2

ABSTRACT

Omega-1, a glycosylated T2 ribonuclease (RNase) secreted by *Schistosoma mansoni* eggs and abundantly present in soluble egg antigen (SEA), has recently been shown to condition dendritic cells (DCs) to prime Th2 responses. However, the molecular mechanisms underlying this effect remain unknown. We show here by site-directed mutagenesis of omega-1 that both the glycosylation and the RNase activity are essential to condition DCs for Th2 polarization. Mechanistically, we demonstrate that omega-1 is bound and internalized via its glycans by the mannose receptor (MR) and subsequently impairs protein synthesis by degrading both ribosomal and messenger RNA. These studies reveal an unrecognized pathway, involving MR and interference with protein synthesis that conditions DCs for Th2 priming.

INTRODUCTION

Dendritic cells (DCs) play a central role in the development and maintenance of immune responses during infection, as they govern both the activation and polarization of adaptive T helper (Th) cells. Classically, upon recognition of invading pathogens, resting DCs undergo a process of activation, so-called maturation, that involves stable presentation of peptides in the context of major histocompatibility complex (MHC)-I and -II, up-regulation of co-stimulatory molecules, and production of polarizing cytokines, that collectively enable DCs to potently activate and direct CD4⁺ T cell responses (1).

This paradigm is largely based on observations of responses towards pathogens, like bacteria, viruses and fungi. These pathogens harbor pathogen-associated molecular patterns that lead to classic DC activation by engaging several classes of innate pattern recognition receptors, including the Toll-like receptors (TLRs). Binding of pathogen-associated molecular patterns to these receptors initiates signaling cascades that generally result in the conditioning of DCs for priming of Th1- or Th17-biased responses which are instrumental in combating prokaryotic and single cell eukaryotic pathogens (2). In contrast to this classical view of DC activation, components derived from parasitic helminths, when co cultured with DCs, fail to induce the traditional signs of DC maturation. However, although overt maturation is not observed, unlike immature DCs, helminth antigen-treated DCs are altered such that they prime Th2-polarized immune responses (3).

Despite this consistent picture, the pathways through which helminth antigens manipulate DC function and drive Th2 responses are still poorly understood (4). The majority of the studies have been conducted with a complex mixture of soluble egg antigens (SEA) from the trematode *Schistosoma mansoni*. SEA is regarded as one of the most potent helminth-derived antigenic extracts that instruct DCs to drive Th2 polarization (3;5). So far these studies have mainly suggested that carbohydrate structures play a role in DC modulation by SEA, given that chemical modification of glycans on proteins present in SEA is known to abolish their capacity to induce Th2 polarization (6). In this respect, another class of pattern recognition receptors expressed by DCs, the carbohydrate-binding C-type lectin receptors (CLRs), have been suggested to play a role in modulation of DC function by SEA (7). For instance, SEA contains carbohydrate structures, such as Lewis-x (Le^x), that can be recognized by DC SIGN (DC-specific intercellular adhesion molecule-3-grabbing non-integrin; 8-10). Engagement of this receptor by components from pathogens such as *Helicobacter pylori* has been shown to suppress IL-12 production and modulate TLR-induced DC activation and T cell polarization (8;11). In addition, more recently it has been shown that SEA can modulate cytokine responses through another CLR, dectin-2 (12). Finally, a number of studies have raised the possibility that TLRs are involved in SEA-mediated Th2 induction (13;14). However, direct evidence for involvement of specific receptors or downstream pathways in SEA-driven Th2 polarization has been missing.

The recent identification of omega-1, a glycosylated T2 RNase, as the major component in schistosome eggs that is responsible for conditioning DCs for Th2 polarization (15-17), has allowed us to dissect the molecular pathways involved in a precise manner. Through site-

directed mutagenesis we show that both the RNase activity and the glycosylation of omega-1 are essential for programming of DCs for Th2 induction. Furthermore, we provide evidence that MR is critical for omega-1-driven Th2 responses and that internalization via this receptor is needed for biological activity of omega-1, as it allows omega-1 to interfere with translation, by degrading rRNA and mRNA, and thereby to condition these cells to prime Th2 responses.

RESULTS

Omega-1 requires both its glycosylation and RNase activity to condition DCs for priming of Th2 responses

The RNase activity of omega-1 has been proposed to play a role in the conditioning of DCs to prime Th2 responses (16). However, this was based on a chemical inactivation of the RNase activity by diethylpyrocarbonate-treatment, which can result in off-target modification of histidines as well as other amino acids that could alter the function or structure of the protein (18). Therefore, we addressed the role of RNase activity in a more stringent and specific manner by creating a mutant of recombinant wildtype (WT) omega-1 lacking RNase activity by site-directed mutagenesis. Specifically, a histidine residue in its catalytic domain, known from other T2 RNases to be essential for the enzymatic activity (19), was replaced by phenylalanine (omega-1 H58F) (Fig. 1 A). Apart from RNase activity, glycosylation of omega-1 may also be important for its Th2-priming capacity, since chemical modification of glycans on proteins present in SEA is known to abolish the ability of SEA to induce Th2 polarization (6). Moreover, potentially Th2-polarizing Le^x glycan motifs have recently been described to be present in glycans on omega-1 (20). To address the role of glycosylation in Th2 priming by omega-1, a glycosylation mutant was generated by a single amino-acid replacement at each of the two N-linked glycosylation sites (omega-1-N71/176Q) (Fig. 1 A) (17;20). An RNase assay showed that the RNase mutant did not have any RNase activity, while the RNase activity of the glycosylation mutant was unaffected (Fig. 1 B). In addition, the banding patterns of recombinant WT omega-1 and the mutants on silver stained SDS-PAGE and anti-omega-1 Western blots were in line with the absence of carbohydrates on the glycosylation mutant as evident by a single band instead of the three glycoforms of the recombinant WT omega-1 and the RNase mutant (Fig. 1 C). With regard to the glycans present on recombinant WT omega-1 and the RNase mutant, mass spectrometric analysis of tryptic glycopeptides showed the presence of N-glycans on Asn₁₇₆ with the monosaccharide composition Hex₃HexNAc₆Fuc_{2/3} (Fig. 1 D). This composition is indicative of the presence of GalNAcβ1-4(Fucα1-3)GlcNAc (LDN-F) antennae, a glycan element previously found on a protein from HEK293 cells (21), the cell type in which recombinant omega-1 is expressed. LDN-F motifs frequently occur on helminth glycoproteins, and the characteristics of LDN-F with respect to binding to CLRs are similar to those of the Le^x element (9;10;20;22).

To assess the role of glycosylation and RNase activity in omega-1-driven Th2 polarization, a well-established *in vitro* culture system of human monocyte-derived DCs (moDCs) and naïve CD4⁺ T cells was used, which mimics *in vivo* DC-mediated Th cell polarization (1). Similar to

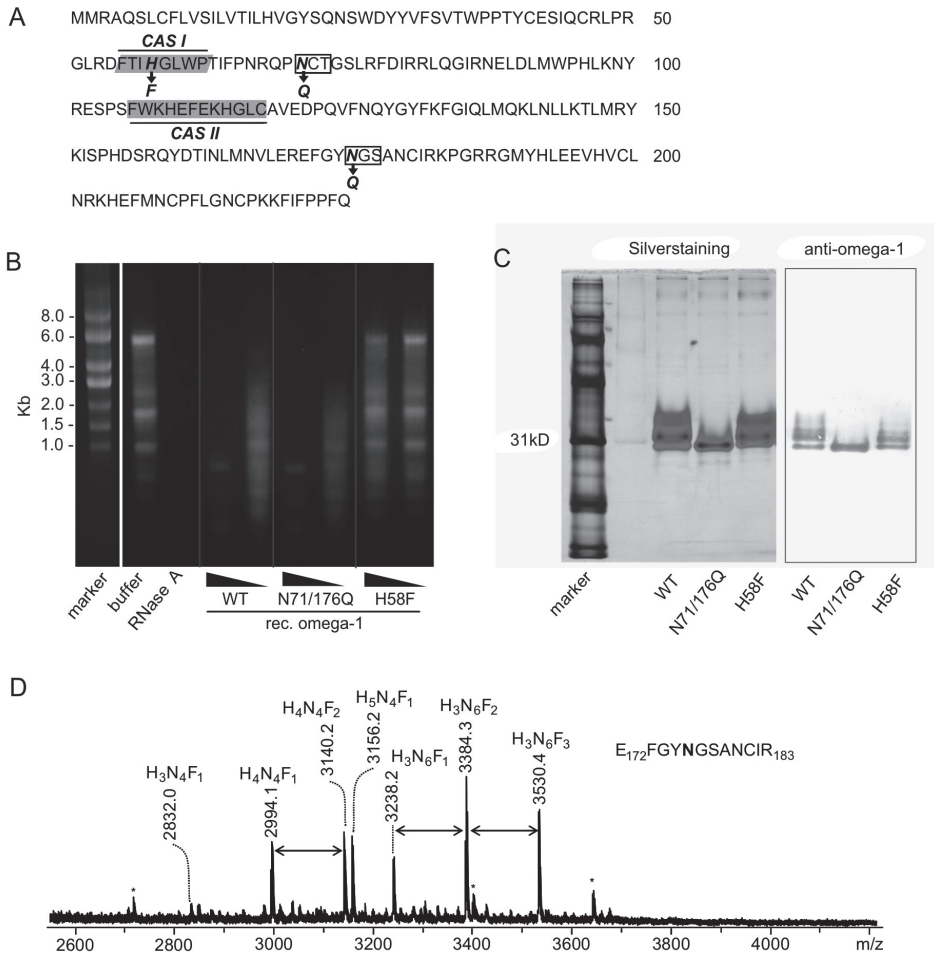


Figure 1. Generation and evaluation of glycosylation and RNase mutants of recombinant omega-1.

(A) The amino acid sequence of omega-1 (Acc.No. ABB73003.1) is shown in which the mutation sites are depicted. The two conserved amino acid sequence (CAS)-domains essential for catalytic activity are marked in grey and the two N-linked glycosylation sites are depicted in white boxes. (B) RNA from PBMCs was incubated for 1 h with the different omega-1 variants (500 ng/ml and 100ng/ml) and analyzed on a 2% agarose gel for breakdown. RNase A was used as a positive control. One of two experiments is shown. (C) The omega-1 mutants were run under non-reducing conditions by SDS-PAGE and silver stained. A Western Blot by staining with a specific anti-omega-1 monoclonal antibody was in line with the absence of glycosylation only on the omega-1 glycosylation mutant. (D) MALDI-TOF mass spectrum of glycopeptides from a tryptic digest of recombinant WT omega-1, covering the glycosylation site N176. Recombinant omega-1 was subjected to SDS-PAGE under reducing conditions and stained with Colloidal blue. Stained bands were excised, subjected to reduction and alkylation and digested with trypsin. The MALDI-TOF-MS spectrum derived from the upper band in the SDS-PAGE pattern is depicted. Signals ($[M+H]^+$) are labeled with monoisotopic masses. Composition of the glycan moieties are given in terms of hexose (H), N-acetylhexosamine (N) and fucose (F). Differences in fucose content are indicated by double-headed arrows. Signals that cannot be assigned to glycopeptides are marked with asterisks (*).

natural omega-1 (15), recombinant WT omega-1 consistently and significantly suppressed in a concentration dependent manner the lipopolysaccharide (LPS)-induced upregulation of the costimulatory molecule CD86 (Fig. 2 A), as well as the production of IL-12 p70 following CD40 ligation (Fig. 2 B), which is an important characteristic of Th2-priming DCs (3). However, both the glycosylation mutant and the RNase mutant failed to alter LPS-induced CD86 expression or IL-12 production of DCs at any of the concentrations tested. Importantly, in contrast to DCs primed with recombinant WT omega-1, those conditioned with either mutant did not prime a Th2 response (Fig. 2 C+D). Similar results were obtained with cultures in which DCs were conditioned by the omega-1 mutants in the absence of LPS (Fig. 2 E). These data show that the RNase activity and the glycosylation of omega-1 are both essential, but as single property not sufficient, for the induction of Th2 responses via DCs.

Omega-1 requires both its glycosylation and RNase activity to prime Th2 responses *in vivo*

To test whether the *in vivo* Th2-priming capacity of omega-1 is dependent on glycosylation and RNase activity, recombinant WT omega-1 or its mutants were administered to 4get/KN2 IL-4 dual-reporter mice (23). In these mice IL-4-competent cells are GFP⁺ and IL-4-producing cells additionally express huCD2, allowing the direct visualization of Th2 differentiation and IL-4 production. Following the s.c. injection of the antigens into the footpad, the draining popliteal lymph nodes (LNs) were harvested on day 7 and CD4⁺CD44^{high} effector T cells were analyzed for the expression of GFP and huCD2 directly ex vivo. Injection of SEA resulted in a significant increase of GFP⁺ and huCD2⁺ cells, reflecting the induction of Th2 differentiation and IL-4 production *in vivo* (Fig. 3). Importantly, while recombinant WT omega-1 induced a marked Th2 response and the production of IL-4, both mutants were significantly impaired to prime this response as evident from lower frequencies (Fig. 3 A and B) as well as total numbers of huCD2⁺ T cells (Fig. 3 C) in the draining LN. Taken together, these data show that the glycosylation and the RNase activity of omega-1 play a crucial role in Th2 polarization induced by omega-1 *in vivo*.

Omega-1 is internalized by DCs via the mannose receptor (MR)

To get a better understanding of how glycosylation is involved in omega-1-driven Th2 polarization, we tested whether recognition of omega-1 by human DCs was dependent on the glycans present on omega-1. While human DCs were capable of binding fluorescently-labeled recombinant WT omega-1 or the RNase mutant as determined by FACS analysis, DCs failed to bind the glycosylation mutant, demonstrating that glycans present on omega-1 are essential for recognition by DCs (Fig. 4 A). Given the importance of glycosylation of omega-1 for binding to DCs, we explored the involvement of carbohydrate-binding CLRs in the recognition and uptake of omega-1. While DCs readily bound fluorescently-labeled omega-1, binding of natural omega-1 was totally prevented when DCs were pre-incubated with the calcium-chelator EGTA, which abolishes CLR binding to carbohydrate ligands (Fig. 4 B). In contrast, treatment of DCs with EGTA after 1 h incubation with omega-1, could not reduce the fluorescent signal

of omega-1, indicating that by then all bound omega-1 had been internalized. This suggests that DCs recognize and rapidly internalize omega-1 in a CLR dependent manner. SEA has been reported to be recognized and endocytosed by human moDCs via the CLR DC-SIGN and MR (7) that have the capacity to bind fucose-residues such as those found in Le^x (9;10;24), a glycan motif present on natural omega-1 (20). To determine whether MR and DC-SIGN are involved in recognition and internalization of natural omega-1, DCs were pre-incubated with

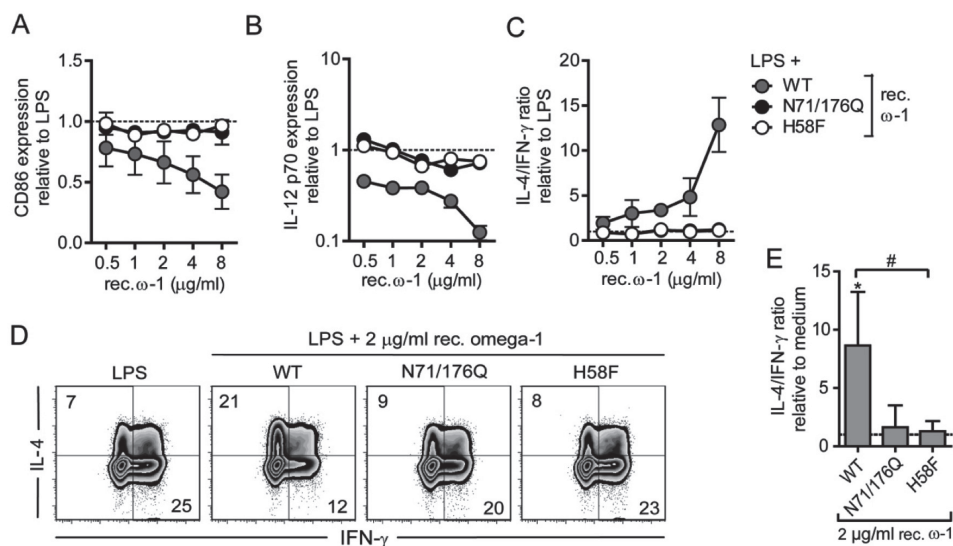


Figure 2. The glycosylation and RNase activity of omega-1 are essential for conditioning human DCs to prime Th2 responses. (A) Human moDCs were pulsed for 48 h with increasing concentrations of the mutant variants of recombinant omega-1 in combination with LPS (100 ng/ml) as a maturation factor and surface expression of CD86 was determined by FACS analysis. The expression levels, based on geometric mean fluorescence, are shown relative to the DCs stimulated with LPS alone, which is set to 1. Data are based on two independent experiments and shown as mean \pm SD. (B) Conditioned DCs were co-cultured for 24 h with a CD40-L expressing cell line, to mimic the interaction with T cells. IL-12p70 cytokine expression levels are shown relative to the DCs stimulated with LPS alone, which is set to 1. Data are representative of triplicate wells from one of 2 independent experiments and shown as mean \pm SD. (C) DCs conditioned as described in (A) were cultured with allogeneic naive CD4⁺ T cells for 12 days in the presence of staphylococcal enterotoxin B and IL-2. Intracellular cytokine production was assayed by FACS 6 h after the stimulation of primed T cells with phorbol 12-myristate 13-acetate (PMA) and ionomycin. Based on intracellular cytokine staining, the ratio of T cells single-positive for either IL-4 or IFN- γ was calculated relative to the control condition. Data are based on 2 independent experiments and shown as mean \pm SD. (D) An example of T cell polarization assay as described in (C) induced by the different recombinant omega-1 variants. The frequencies of each population are indicated as percentages in the plot. One representative result from 5 independent experiments is shown. (E) T cell polarization assay as described in (C) but in the absence of LPS. Data are representative of 3 independent experiments. Bars represent mean \pm SD. # $P < 0.05$, for significant differences compared to control conditions (*) or between test conditions (#) based on paired analysis (two-sided paired t -test). ω -1, omega-1; WT, wild type; H58F, RNase mutant; N71/176Q, glycosylation mutant.

mannan (a natural ligand that competes for binding to DC-SIGN and MR), or DC-SIGN- and MR-specific blocking antibodies, followed by a 1 h incubation with fluorescently-labeled SEA or natural omega-1. As reported previously (7), uptake of SEA by human moDCs could be reduced by mannan and either DC-SIGN or MR blocking antibodies in an additive manner (Fig. 4 C). With regard to omega-1, pre-treatment with mannan could fully block binding and uptake of omega-1 by DCs. Interestingly, binding and uptake of natural omega-1 were significantly reduced by MR but not by DC-SIGN blocking antibodies (Fig. 4 C). Pre-incubation with the combination of both blocking antibodies did not have any additional effect on the uptake of omega-1 as compared to pre-incubation with anti-MR antibody alone. In addition, we found that recombinant omega-1 was recognized and internalized by DCs in a similar MR-dependent fashion as natural omega-1 (Fig. 4 D). To further investigate the observations of selective recognition and uptake of omega-1 by MR, we made use of the K562 and 3T3 cell

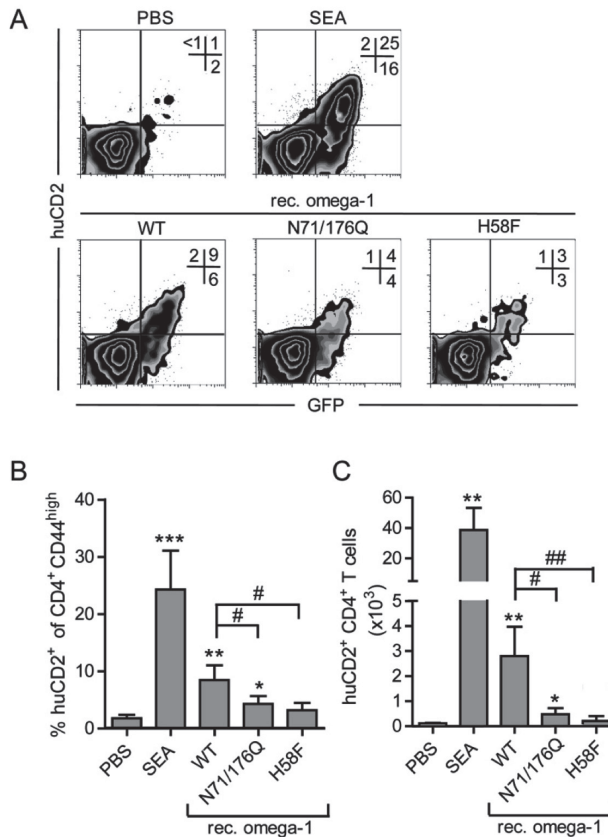


Figure 3. Glycosylation and RNase activity are essential for omega-1 to prime Th2 responses *in vivo*. 4get/KN2 IL-4 dual reporter mice were injected s.c. with SEA (20 µg) or 3 µg WT mutant recombinant omega-1 into the footpad. After 7 days the frequency of GFP⁺ and huCD2⁺ within the CD4⁺CD44^{high} effector T cell population was determined by flow cytometry in the draining popliteal lymph nodes. Depicted are (A) concatenated FACS plots, (B) frequencies of huCD2⁺ within the CD4⁺CD44^{high} population and (C) total huCD2⁺ T cell numbers in draining lymph nodes of combined data of 4 mice per group. (A) The frequencies of each population are indicated as percentages in the plots. One of 3 independent experiments is shown. Bars represent mean ± SD. *, # P < 0.05, ** P < 0.01, *** P < 0.001 for values significantly different from the PBS control (*) or between test conditions (#) based on two-sided t-test. WT, wild type; H58F, RNase mutant; N71/176Q, glycosylation mutant.

lines selectively expressing human DC-SIGN and MR, respectively. Fluorescently-labeled SEA was readily bound by both the DC-SIGN- and MR-expressing cells, which was not observed upon pre-incubation with EGTA or in parental control cell lines lacking CLR expression. In line with the DC-binding and uptake data, omega-1 binding could be observed in the cell line expressing MR (Fig. 4 E), but not in the cell line expressing DC-SIGN (Fig. 4 F). It should be noted that in these uptake experiments (Fig. 4 C+D), blocking with anti-MR antibody was not complete ($\pm 40\%$ reduction). However, given that blocking the binding of omega-1 to the cell

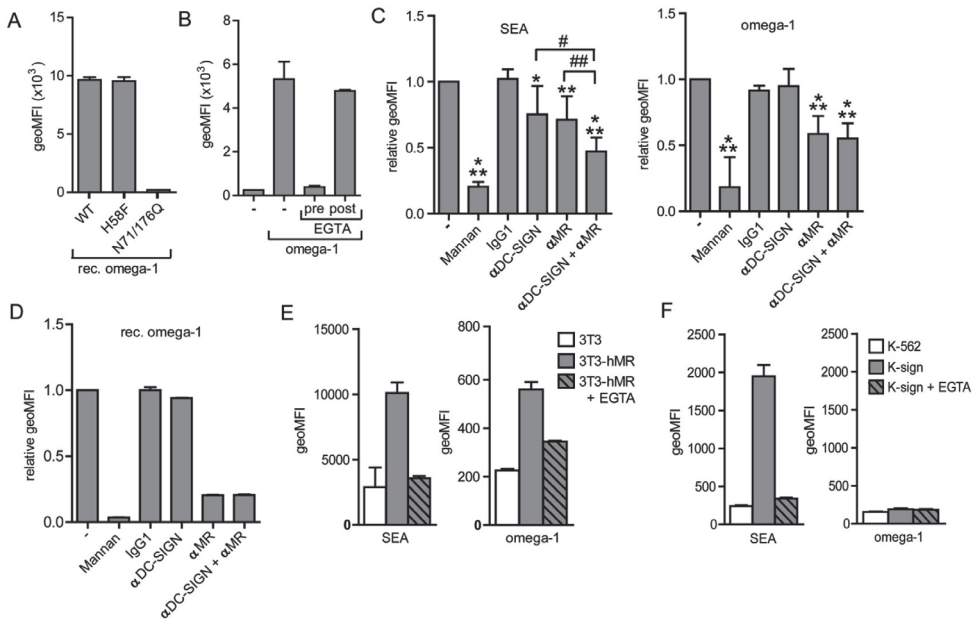


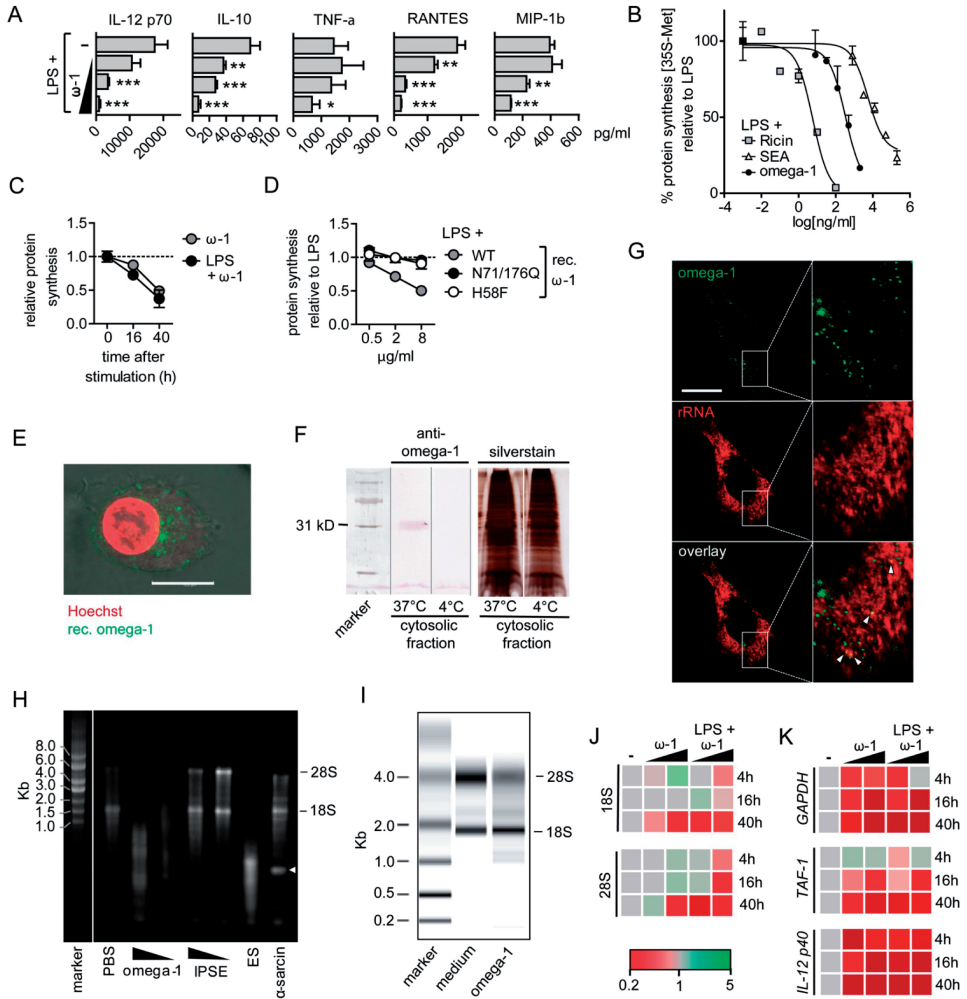
Figure 4. Mannose Receptor (MR) mediates recognition and internalization of omega-1 by human DCs. (A) Human moDCs were incubated for 1 h with PF-647-labeled recombinant WT omega-1, the glycosylation mutant or the RNase mutant and analyzed for uptake of antigens by FACS analysis. One representative experiment with duplicate samples out of 2 experiments is shown. Bars represent mean \pm SD. (B) Human moDCs were incubated for 1 h with PF-647-labeled omega-1 and, where indicated, either pre-incubated ('pre') with EGTA to prevent omega-1 binding to CLR*s a priori*, or treated afterwards with EGTA ('post') to remove any CLR-bound omega-1 from the cell surface. One of two independent experiments is shown and data represent mean \pm SD of duplicates. (C+D) A binding/internalization assay of natural (C) and recombinant omega-1 (D) by immature moDCs was performed analogous to (B) following pre-incubation with indicated reagents. Binding and internalization are shown relative to control pre-treatment. (C) Data are based on 5 experiments and are shown as mean \pm SD. (D) One of two independent experiments is shown and data represent mean \pm SD of duplicates. (E) 3T3 cell-line expressing MR and (F) K-SIGN expressing DC-SIGN or parental control cell lines (3T3 and K-562) were incubated with PF-647-labeled omega-1 and SEA in the presence or absence of EGTA to determine specificity. One representative experiment based on duplicate samples out of 2 is shown. Bars represent mean \pm SD. *,# $P < 0.05$, **,## $P < 0.01$, *** $P < 0.001$ for significant differences between control conditions (*) or between test conditions (#) based on two-sided *t*-test. WT, wild type; H58F, RNase mutant; N71/176Q, glycosylation mutant.

line selectively expressing MR with the anti-MR antibody was not complete either (data not shown), it is likely that a low affinity of the anti-MR antibody accounts for this finding rather than that other receptors are involved. Taken together, our data show that recognition and internalization of omega-1 by human DCs is dependent on its glycosylation and that MR is a major CLR involved in this process.

Omega-1 suppresses DC function by interfering with protein synthesis

Next we examined the molecular mechanism through which the RNase activity of omega-1 exerts its modulatory effects on human DCs. We noted that omega-1-stimulated DCs in response to CD40 ligation were not only impaired in their capacity to produce IL-12 p70, as reported previously (15), but also to secrete other cytokines and chemokines (Fig. 5 A). This suggested that the suppression may not be gene specific, but could be the result of general inhibition of protein synthesis. Indeed, following exposure of DCs to omega-1 or SEA, a dose-dependent reduction of protein synthesis could be observed, similar to what is found in DCs exposed to ricin, a well-known protein synthesis inhibitor (25) (Fig. 5 B). In addition, this inhibition by omega-1 was time-dependent and observed in both the presence and absence of LPS (Fig. 5 C). The capacity to inhibit protein synthesis was dependent on its RNase activity and uptake via its glycans, since the RNase as well as the glycosylation mutant failed to interfere with protein synthesis (Fig 5 D). As several fungal ribonucleolytic proteins, so-called ribotoxins, have been described to inhibit protein synthesis through cleavage of ribosomal RNA (rRNA) following translocation into the cytosol (26), we first evaluated the localization of omega-1 in human DCs following uptake. We found that omega-1 was efficiently internalized

Figure 5. Omega-1 suppresses protein synthesis through breakdown of rRNA and mRNA. (A) After human moDCs had been pulsed for 40 h with omega-1 (125, 250 and 500 ng/ml) in combination with LPS (100 ng/ml), the cells were co-cultured for 24 h with the J558 cell-line, expressing CD40-L, to mimic the interaction with T cells. Bars represent mean \pm SD of triplicate wells of one of two independent experiments. * $P < 0.05$, ** $P < 0.01$, *** $P < 0.001$ for values significantly different from the LPS control. (B) Following 16 h incubation of human DCs with a concentration range of indicated reagents in the presence of LPS (100 ng/ml), protein synthesis was assessed after a 2 h pulse with radioactively-labeled methionine. Ricin, as potent inhibitor of protein synthesis, was taken along as positive control (25). One of 2 experiments is shown. (C) As described in (B), protein synthesis by human DCs was followed over time after exposure to omega-1 (500 ng/ml) either in the presence or absence of LPS (100 ng/ml). Data are shown relative to unstimulated or LPS-stimulated controls as depicted by the dotted line. Data are representative of two independent experiments and are depicted as mean \pm SD. (D) Protein synthesis by human moDCs following exposure to increasing concentrations of the recombinant omega-1 variants was assessed as described in (B). Data are shown relative to LPS-stimulated DCs. Data are representative of two independent experiments and are depicted as mean \pm SD. (E) DCs were stimulated with FITC-labeled recombinant omega-1 for 1 h and uptake was visualized by confocal laser scanning microscopy. Nuclei were stained with Hoechst. One of three experiments is shown. Scale bar represents 10 μ m. See Fig. S1 for a video of Z-stacked images. (F) Cytoplasmic fractions of human DCs stimulated for 3 h with omega-1 were run under non-reducing conditions by SDS-PAGE and analyzed by Western Blot for presence of omega-1 or silver-stained to control for input. DCs incubated at 4°C were taken along as controls as these cells have surface-bound, but not internalized omega-1. One of two experiments is shown. (G) human DCs were stimulated with FITC-labeled omega-1 (1 μ g/ml) ►



- and after 2 h fixed and stained for rRNA. Subcellular localization of ω -1 was determined by confocal microscopy. One representative cell from three independent experiments is shown. Scale bar represents 10 μ m. (H) After rabbit reticulocyte lysate containing functional ribosomes was incubated for 1 h with ω -1 (1 and 5 μ g/ml), IPSE (1 and 5 μ g/ml) as negative control, or ES (schistosome egg excretory/secretory products) (25 μ g/ml), containing ω -1, isolated rRNA was analyzed for breakdown on a 2% agarose gel. The RNase α -sarcin was taken along as positive control as it should give a single rRNA cleavage product when incubated with functional ribosomes (white arrowhead) (28). One of three independent experiments is shown. (I) rRNA isolated from 24 h ω -1-stimulated human DCs and was visualized by running a lab-on-a-chip picogel. One of three experiments is shown. (J-K) rRNA or mRNA expression of indicated genes in DCs was assessed by real time-qPCR at different time points after stimulation with ω -1 (500 ng/ml and 2 μ g/ml) in the presence or absence of LPS (100 ng/ml). Data are shown relative to unstimulated or LPS-stimulated controls, which were set to 1. RNA expression was normalized based on a genomic real time-qPCR for *ccr5*. Data represent the mean of 3 independent experiments. ω -1, ω -1; WT, wild type; H58F, RNase mutant; N71/176Q, glycosylation mutant.

by DCs and present throughout the cell after 1 h (Fig. 5 E and Fig. S1). In addition, Western blots revealed the presence of omega-1 in the cytosolic fraction of omega-1-stimulated DCs after 3 h (Fig. 5 F). In line with this, co-localization experiments using immunofluorescence confocal microscopy by staining for rRNA, showed that 2 h after stimulation of DCs with omega-1, omega-1 partially co-localized with rRNA (Fig. 5 G). We next tested whether omega-1 could cleave rRNA in the context of functional ribosomes in a cell free assay. Omega-1 was able to break down rRNA, while IPSE, another *S. mansoni* egg-derived protein that lacks RNase activity but has identical glycans as omega-1 (27), did not induce any rRNA degradation (Fig. 5 H), indicating that omega-1 is able to interfere with ribosomal function by cleavage of rRNA. Analysis of the integrity of rRNA isolated from omega-1-exposed DCs by gel electrophoresis showed a preferential breakdown of 28S rRNA (Fig. 5 I). This was confirmed by real time-PCR, which additionally revealed breakdown of 18S at later time points (Fig. 5 J). Since the known T2 RNases have no sequence-specific RNase activity (19), we evaluated whether omega-1, which belongs to the T2 RNase family, may additionally impair protein synthesis by degrading not only rRNA but also mRNA transcripts in a generic manner. When DCs were stimulated with omega-1, both in the presence or absence of LPS, a concentration and time dependent loss in mRNA transcripts of housekeeping genes *TAF1* and *GAPDH* as well as *IL12B* could be observed (Fig. 5 K), suggesting that omega-1 targets mRNA transcripts in a general manner in DCs as well. Taken together, these data support the notion that the RNase activity enables omega-1 to modulate human DC function by interfering with protein synthesis through cleavage of rRNA and mRNA following translocation into the cytosol.

MR mediates omega-1-induced protein synthesis inhibition, DC modulation and Th2 polarization

To address the role of omega-1 binding by MR in mediating RNase-dependent DC modulation and Th2 priming by omega-1, we used blocking antibodies directed against MR or DC-SIGN. Blocking of MR during the stimulation of human DCs with omega-1 significantly prevented the inhibition of protein synthesis (Fig. 6 A), while blocking of DC-SIGN had no effect, showing that the interference with protein synthesis by omega-1 is dependent on MR. In line with these observations, blocking of MR significantly reduced the capacity of omega-1 to suppress LPS-induced CD86 expression (Fig. 6 B) and IL-12 production following CD40 ligation (Fig. 6 C) or to condition DCs to induce a Th2 response (Fig. 6 D). The importance of MR was further substantiated by the observations that in contrast to their WT counterparts, MR^{-/-} murine DCs, when conditioned with omega-1, failed to prime a Th2-skewed allogeneic T cell response *in vitro* (Fig. 6 E). These data establish that MR is essential for the omega-1-driven Th2 polarization via DCs *in vitro*.

Omega-1 requires MR to prime Th2 responses *in vivo*

Finally, to investigate the role of MR in Th2-priming by omega-1 *in vivo*, natural omega-1 or PBS were injected subcutaneously into the footpad of WT and MR^{-/-} mice. After 7 days

the draining popliteal LNs were harvested and restimulated *in vitro* with PBS, omega-1 or a polyclonal stimulus PHA and analyzed for cytokine production. Antigen-specific restimulation of omega-1-primed LNs from WT mice resulted in a Th2-polarized response as evidenced by elevated levels of Th2-associated cytokine IL-5 but not of Th1-associated cytokine IFN- γ , which was absent in LN cells derived from MR^{-/-} (Fig. 7 A). Furthermore, intracellular staining for IFN- γ and IL-4 following antigen-specific restimulation of CD4⁺ T cells from omega-1-primed LNs, showed a significant increase in IL-4-producing T cells from WT but not MR^{-/-} mice (Fig. 7 B). The failure of MR^{-/-} mice to prime a Th2-polarized response in response to omega-1 was not due to a general failure of MR^{-/-} cells to produce these cytokines as the responses to PHA were comparable in WT and MR^{-/-} mice (Fig. 7 A and B). Taken together, these data show that MR is essential for priming of Th2 responses by omega-1 *in vivo*.

DISCUSSION

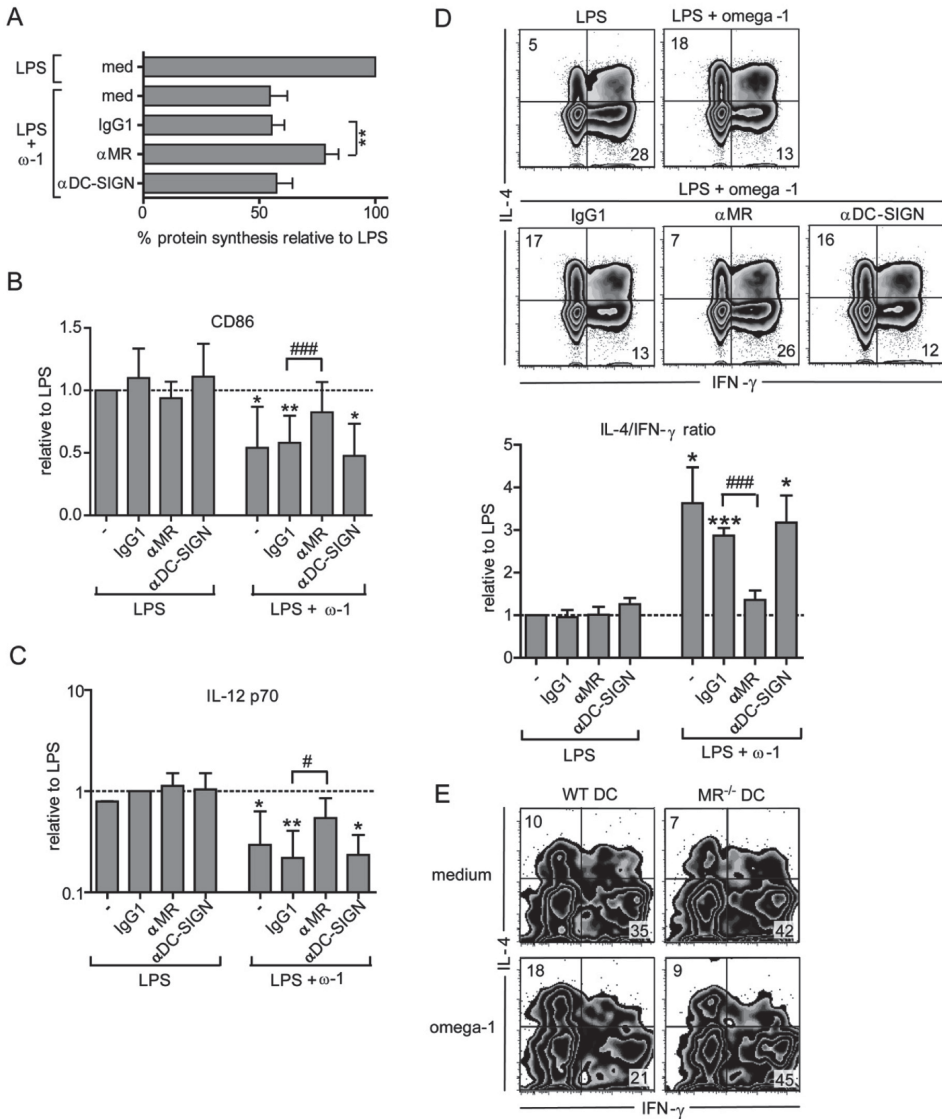
Using omega-1, a single glycosylated T2 RNase secreted by *Schistosoma mansoni* eggs, we studied the molecular mechanisms involved in conditioning dendritic cells to induce Th2 responses. By generating mutants of omega-1 we could show that both the glycosylation and the RNase activity of omega-1 are essential for its potent Th2-inducing activity both *in vitro* and *in vivo*. The glycan structures on omega-1 suggested that CLRs might play a role in its interaction with DCs. Although both MR and DC-SIGN have been shown to mediate binding and uptake of fucosylated antigens by DCs (29) and omega-1 harbors fucose-containing Le^x-glycan moieties, we observed that omega-1 significantly bound only to a MR-, but not to a DC-SIGN-expressing cell-line and that internalization by DCs was mainly MR-dependent and did not involve DC-SIGN. Lack of strong binding and uptake of omega-1 by DC-SIGN might be explained by the fact that in most DC-SIGN binding studies polyvalent Le^x-containing beads or conjugates have been used, which may be bound by DC-SIGN with a higher affinity than soluble glycoproteins, such as omega-1, that would present Le^x at a low valency (22). In line with this observation, DC-SIGN blocking experiments suggest that interaction with DC-SIGN does not play a major role in omega-1-driven Th2 polarization via DCs. On the other hand, the importance of MR in recognition and uptake of omega-1 was substantiated by the finding that conditioning of both human and murine DCs for Th2 polarization by omega-1 were significantly impaired when MR was blocked or when the DCs were deficient for MR, respectively. Furthermore, we confirmed and extended the importance of MR in Th2 polarization by omega-1 *in vivo* by showing that an antigen-specific Th2 response induced in MR^{-/-} mice following footpad injection of omega-1 was strongly reduced compared to the response elicited in WT mice. In this respect it is important to note that human and murine MR have a similar carbohydrate binding specificity (30). Thus, this establishes that omega-1 relies on MR to drive Th2 polarization. Apart from schistosome egg-derived antigens, it was recently shown that MR can also recognize glycosylated antigens derived from schistosome larvae in the skin (31), and that MR^{-/-} mice display a Th1-biased antigen-specific T cell response in the skin-draining LNs following infection with cercaria. This study along with our data, indicate

that MR may play a role in shaping of Th2-polarized immune responses during different stages of schistosome infection.

In vitro studies with DCs have shown that MR-crosslinking with antibodies (32) or by mannosylated antigens (33;34) can drive an anti-inflammatory cytokine program in DCs away from a Th1-promoting profile (32) and that allergen-driven Th2 polarization by DCs is in part dependent on MR (35;36). These studies suggest that engagement of MR may be sufficient to promote Th2 polarization, potentially via signaling events. However, our data demonstrate that MR binding alone is not sufficient for Th2 induction by omega-1, since glycans present on omega-1, in absence of RNase activity, fail to program DCs to induce Th2 responses. This is in line with the observation that IPSE/alpha-1, another major glycoprotein secreted by *S. mansoni* eggs with identical glycosylation as omega-1 (27), which can bind the cell line expressing MR (unpublished data) but lacks RNase activity, is unable to prime Th2 responses (15).

Apart from its glycosylation, omega-1 requires its RNase activity to induce a Th2 response via modulation of human DCs. It was observed that omega-1 in an RNase-dependent manner impaired protein synthesis and that DCs exposed to omega-1 displayed a progressive reduction in mRNA content of several unrelated genes as well as in rRNA levels. The drop in mRNA transcripts from both housekeeping genes (*TAF1* and *GAPDH*), inducible genes (*IL12B*), as well as rRNA (28S and 18S), suggests that omega-1 does not degrade specific transcripts, but targets the global RNA pool in DCs. While it currently remains to be determined what the relative contribution of each of these processes and their relative timing is to the impairment of protein synthesis, it is most likely that the observed inhibition in protein synthesis is a combined effect of degradation of mRNA transcripts and interference with ribosomal integrity due to rRNA cleavage. These data support the view that as a consequence of RNA breakdown, reduced protein synthesis is the mode of action through which the RNase activity enables omega-1 to condition DCs for priming of Th2 responses. Some RNases have been linked to Th2 polarization before. The major birch pollen allergen, Bet v 1 (37), was identified as an RNase. Furthermore, some fungal RNases that appear to selectively cleave rRNA, such as mitogillin and Asp f 1, are known to be allergens (38). Interestingly, for Asp f 1 it was found that its allergenicity was lost when its capacity to interfere with ribosomal function was abolished (39). In addition, a report has linked an endogenous RNase, the eosinophil-derived neurotoxin, to DC-mediated Th2 polarization (40). Although these studies have not specifically addressed the role of RNase activity in direct priming of Th2 responses, they do highlight the possibility

Figure 6. MR mediates omega-1-induced DC modulation and Th2 polarization *in vitro*. Following 1 h pre-incubation with blocking antibodies against MR, DC-SIGN or an isotype control (20 µg/ml), human moDCs were pulsed for 16 h (A) or 48 h (B-D) with natural omega-1 (500 ng/ml) in combination with LPS (100 ng/ml). (A) Protein synthesis was assessed as described in Fig. 5 B. One representative experiment based on duplicate samples out of 3 experiments is shown. Data are shown as mean ± SD. (B) The expression levels of CD86 on human DCs assessed by FACS are based on geometric mean fluorescence, relative to the DCs stimulated with LPS alone, which is set to 1 (dashed line). Data are based on 3 independent experiments and shown as mean ± SD. (C) Conditioned human DCs were co-cultured for 24 h with a CD40-L expressing cell line, to mimic the interaction with T cells. IL-12p70 cytokine ►



- expression levels are shown relative to the DCs stimulated with LPS alone, which is set to 1 (dashed line). Data are based on 3 independent experiments and shown as mean \pm SD. (D) Conditioned human moDCs were cultured with allogeneic naive CD4⁺ T cells for 12 days in the presence of staphylococcal enterotoxin B and IL-2, and T cell polarization was analyzed as described in figure 1. FACS plots of one representative experiment out of 6 is shown. Bar graphs are based on 6 independent experiments and represent mean \pm SD. (E) Murine splenic WT or MR^{-/-} DCs from a C57BL/6 background were co-cultured with naive Balb/c CD4⁺ T cells in the presence 2 μ g/ml omega-1. After an expansion with rIL-2 at d 3, T cells were restimulated on d 6 with PMA and ionomycin and analyzed for intracellular cytokines. 1 representative experiment out of 3 is shown. *,# P < 0.05, **,## P < 0.01, ***P < 0.001 for significant differences with the LPS control (*) or between test conditions (#) based on paired analysis (two-sided paired t-test). ω -1, omega-1.

that Th2 priming through interference with ribosomal function may not be a unique feature of *S. mansoni*-derived omega-1, but may be shared by other RNases as well. In this respect, it is interesting to note that RNase T2 homologs can be identified in the genomes of *S. japonicum* and *S. haematobium*, as well as of the nematodes *Brugia malayi*, *Loa loa* and *Ascaris suum* (41-43). However, it is currently unknown whether these parasites actually express these T2 RNases and if they do, whether they play any role in Th2 polarization in their host. Taken together, our data suggest that for an RNase to harbor a Th2-priming capacity, it needs to be recognized by DCs and routed to reach the cytosol where in turn its enzymatic activity would result in suppression of protein synthesis, yet without shutting down DC function altogether or inducing cell death before T cell priming has occurred.

It remains to be established how omega-1 would be able to reach the ribosomes present in the cytosol. Some ribosome-inactivating proteins have been shown to translocate from the ER into the cytosol after retrograde transport or by direct escape from endosomes into the cytosol (44). In this respect, since omega-1 is internalized via MR, it is interesting to note that cross-presentation of OVA by DCs, a process that requires translocation of the antigen from endosomes into the cytosol, has been shown to be dependent on MR (45;46). Mechanistically, it was demonstrated that binding of the MR to OVA leads to poly-ubiquitination of MR, resulting in the recruitment of the ATPase p97, a member of the ER-associated degradation machinery, towards the endosomal membrane. p97 in turn was found to provide the energy to pull out the MR ligand into the cytoplasm (47). This suggests that the MR itself can regulate the transport of its ligand, into the cytoplasm and provides a mechanism through which omega-1 could be translocated into the cytosol of DCs.

The suppression of protein synthesis in DCs by omega-1, would be in line with the documented inhibitory effects of omega-1 as well as SEA on DC activation and TLR-induced expression of co-stimulatory molecules and cytokines (15;16). In addition, this mode of action would also provide an explanation for the finding that omega-1 alters DC morphology as a result of cytoskeletal changes (16), since halting of translation and concomitant stress responses can affect actin rearrangements and thereby cell morphology (48). Importantly, during interactions with naïve T cells, omega-1-conditioned DCs will, in contrast to unconditioned DCs, be largely refractory to respond to CD40 ligation by T cells, as their protein synthesis machinery is impaired. As a consequence, T cells are primed in the absence of IL-12 and in the context of low antigen presentation, a situation that is known to favor the induction of Th2 responses (49;50). This mechanism would be different from a 'default hypothesis' for Th2 induction (51-53) as it represents a dominant and active suppression of signals during DC-T cell interactions. Such a model of active suppression of DC signals for Th2 polarization would be in line with recent data showing that SEA-pulsed DCs, although still capable of processing antigen to present it on MHC-II, are impaired in their upregulation of surface MHC-II and CD86 or expression of IL-12 in response to CD40 ligation (15;54), as well as with the observation that omega-1-primed DCs have a reduced capacity to form T cell-DC conjugates (16).

Taken together, based on our data we propose a model in which the glycans present on omega-1 do not play a dominant role in functional modulation of DC function for induction

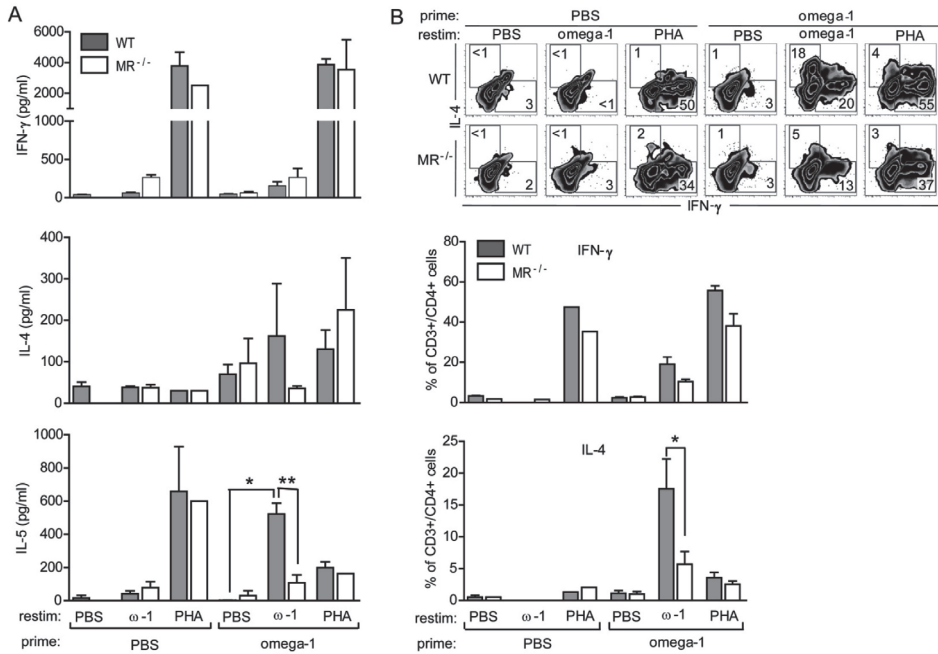


Figure 7. MR is essential for omega-1-driven Th2 polarization *in vivo*. MR^{-/-} and WT Bl/6 mice were injected s.c. with omega-1 (2 μg in 30 μl PBS) or PBS into the footpad. (A) After 7 days the cells from the draining lymph node (LNs) were restimulated *in vitro* for 4 days with PBS, omega-1 (2 μg/ml) or PHA (10 μg/ml), as polyclonal stimulus, after which cytokine production was determined by ELISA. (B) Intracellular cytokine production of the CD3⁺/CD4⁺ T cells from these LNs was assayed by FACS after an additional 6 h restimulation with PMA and ionomycin. FACS plots show concatenated data from 4 mice are shown. The bar graphs represent the percentage of T cells single-positive for either IL-4 or IFN-γ. One of 2 independent experiments is shown. Data are means ± s.e.m. of 4 mice per group based on pooled triplicate wells for each mouse. * P < 0.05, ** P < 0.01 for significant differences based on paired analysis (two-sided paired *t*-test). ω-1, omega-1.

of Th2 responses, but instead are essential for efficient recognition and internalization by DCs via the MR. Subsequently, following translocation into the cytosol, omega-1 programs DCs to drive Th2 polarization in an RNase-dependent manner by interfering with ribosomal function and protein synthesis. These studies have uncovered a novel mechanism through which DCs can be programmed to drive Th2 responses. It will be of great interest to study whether targeting of MR and the protein synthesis machinery to condition DCs for priming Th2 responses is unique to schistosome-driven Th2 polarization, or a mechanism that is also involved in the initiation of other Th2-polarized immune responses, found during other helminth infections or allergies. In addition, the insight may help the design of Th2-polarizing molecules, that could be used in the development of vaccines against parasitic worm infections or approaches to counterbalance unwanted Th1 responses in hyper-inflammatory diseases (55;56).

MATERIALS AND METHODS

Preparation and purification of *S. mansoni* egg-derived antigens

SEA, omega-1 and IPSE/alpha-1 were prepared and isolated as described previously (15;57). The purity of the preparations was controlled by SDS-PAGE and silverstaining. Protein concentrations were tested using the Bradford or BCA procedure. (58;59)

Generation and production of WT, glycosylation mutant and RNase mutant forms of recombinant omega-1

Site-directed mutagenesis was used to generate a glycosylation and RNase mutant by mutating the two putative N-linked glycosylation sites (N71/176Q) or by targeting a conserved amino-acid residue (H58F) that is known to be critical for enzymatic activity in homologous T2 RNases (17;19), respectively. H58F and N71/176Q mutants were created by polymerase chain reaction (PCR) using mutagenic primers on a DH5 α /pProExHtb plasmid (Invitrogen) containing the WT omega-1 sequence (Acc.No. ABB73003.1). Successful mutation was confirmed by DNA sequencing. Subsequently, using restriction enzymes Sfi I and ApaI the templates for WT and mutant omega-1 were subcloned into a pSecTag2 plasmid (Invitrogen) for stable transfection into HEK cells (15). Secreted recombinant omega-1 forms were sequentially purified from the HEK cell culture medium by immobilized metal affinity chromatography and size exclusion chromatography as described previously (15).

Human DC culture, stimulation and analysis

Monocytes were isolated from venous blood from healthy volunteers according to protocols approved by the Institutional Review Board of Leiden University Medical Center by density centrifugation on ficoll followed by CD14⁺ MACS isolation (Miltenyi) or a Percoll gradient as described (60) and were cultured in RPMI medium supplemented with 10% FCS, human rGM-CSF (50 ng/ml, Invitrogen) and human rIL-4 (25 units/ml) (R&D Systems). On day 3, culture medium including the supplements was replaced and on day 6 immature DCs were stimulated with the indicated reagents in the presence of ultrapure LPS (100 ng/ml) (*E. coli* 0111 B4 strain, InvivoGen). For CLR blocking indicated cells were pre-incubated with 20 μ g/ml anti-DC-SIGN (clone AZN-D1, Beckman Coulter) or 20 μ g/ml anti-MR (clone 15.2, Biolegend) for 60 min at 37 °C. As a Th1 control DCs were also pulsed with IFN- γ (1000 U/ml). After 48 h, DCs were harvested for co-culture with naïve T cells. In addition, 1 \times 10⁴ matured DCs were co-cultured with 1 \times 10⁴ CD40L-expressing J558 cells for 24 h to determine cytokine production by the DCs following activation by CD40L. IL-12p70 concentrations were determined by ELISA using mouse anti-human IL-12, clone 20C2 as capture antibody and biotinylated mouse-anti-human IL-12, clone C8.6 as detection antibody (both BD) Concentrations of IL-10, TNF- α , MIP-1 β and RANTES were determined by a multiplex LUMINEX assay according to the manufacturer's instruction (InvivoGen). The expression of CD86 on pulsed DCs was determined by FACS (FACSCanto) through staining with CD86-FITC (BD).

Murine T cell polarization assay

Splenic CD11c⁺MHCII⁺ DCs and CD62L⁺ CD4⁺ T cells were isolated by sorting from naive splenocytes derived from C57BL/6 and Balb/c mice, respectively. 2.5×10^5 CD4⁺ T cells were co-cultured with 1.25×10^5 splenic DCs and stimulated with 2 µg/ml omega-1. At d 3, T cells were expanded with 30 u/ml rIL-2 (R&D systems) and at d 6 restimulated with 50 ng/ml phorbol 12-myristate 13-acetate plus 2 µg/ml ionomycin for 5 h. 10 µg/ml brefeldin A was added during the last 2 h (all Sigma). The cells were stained with a combination of IL-4-PE and IFN-γ-APC antibodies (BD).

Human T cell culture and determination of T cell polarization

To determine T cell polarization, 5×10^3 48 h-pulsed DCs were co-cultured with 2×10^4 naïve T cells that were purified using a human CD4⁺/CD45RO⁻ column kit (R&D) in the presence of staphylococcal enterotoxin B (10 pg/ml; Sigma) in 96-well flat-bottom plates (Corning). On day 5, rhIL-2 (10 U/ml, R&D) was added and the cultures were expanded for another 7 days. For intracellular cytokine production, the primed CD4⁺ T cells were restimulated with 50 ng/ml phorbol 12-myristate 13-acetate plus 2 µg/ml ionomycin for 6 h. 10 µg/ml brefeldin A was added during the last 2 h (all Sigma). The cells were stained with a combination of IL-4-PE and IFN-γ-FITC antibodies (BD).

DC-SIGN- and MR-expressing cell line

K562 cell line stably expressing DC-SIGN (a gift from K. Figdor, Radboud University Nijmegen Medical Centre, Nijmegen, Netherlands; (61)) or 3T3 cell line stably expressing human MR (a gift from J.L. Miller, University of Oxford, Oxford, England, UK and G. Brown, University of Aberdeen, Aberdeen, Scotland, UK; (62)) and their respective parental control cell lines were seeded overnight in a 96-well plate at 10.000 cells/well. Where indicated, cells were pre-incubated with 10mM EGTA for 30 min at 37 °C. Subsequently, cells were incubated with 2 µg/ml PF-647-labeled SEA or 500 ng/ml PF-647-labeled omega-1 at 37 °C for 1 h and washed in ice cold PBS before analysis using flowcytometry.

Protein synthesis inhibition

Immature DCs were seeded overnight in 96-well flat bottom plates before stimulation with indicated reagents in the presence of LPS. At indicated time points after stimulation protein synthesis was determined by a 2 h pulse at 37 °C with 3µCi /0,05 ml [³⁵S]-methionine (EasyTag Express Protein labeling mix, Perkin Elmer) in serum-, cysteine and L-methionine free RPMI-1640. After a double washing step in PBS, cells were lysed for 5 min in AV-lysis buffer (20mM Tris HCl, pH7.6, 150 mM NaCl, 0.5% DOC, 1.0% NP40, 0.1% SDS) in the presence of protease inhibitors Leupeptin and Aprotinin 200ug/ml. Lysates were transferred on a filter (Perkin Elmer) and dried. After radioactive labeled proteins were precipitated on the filter with trichloroacetic acid, filters were washed with 96% ethanol and dried. Using a liquid scintillation cocktail for aqueous solution the radioactivity present on the filters was measured in a β-counter.

RNase activity assay

RNA was extracted from PBMC using the RNeasy kit (Qiagen). RNA was incubated for 1 h at 37 °C with indicated antigens in 0.01M Tris 0.02% Cu. Subsequently, RNA breakdown was visualized by running the samples on a 2% agarose gel containing ethidium bromide.

Ribosomal RNA breakdown

Rabbit Reticulocyte Lysate (Promega) was incubated with antigens as described by others (28). Briefly, following 1 h incubation at 37 °C in Tris-HCl (15 mM NaCl, 50 mM KCl, 2,5 mM EDTA), the reaction was stopped with 10% SDS and RNA was extracted from the ribosomes with phenol/chloroform. Next, isolated ribosomal RNA was denatured at 95°C and visualized by running the samples on a 2% agarose gel containing ethidium bromide.

Analysis of ribosomal RNA integrity in human DCs

mRNA was isolated from DCs conditioned by omega-1 for indicated time points using RNeasy mini Kit (Qiagen) according to the manufacturers recommendations. Integrity of rRNA was visualized using Agilent RNA 6000 Pico Kit in a 2100 Bioanalyzer (Agilent) according to the manufacturers recommendations.

RNA and DNA isolation, DNase treatment and cDNA synthesis

Total DNA and RNA was simultaneously extracted using Qiagen DNeasy blood and tissue kit as per manufacturer's instruction, except for that no RNase reaction was performed. DNase treatment was done using RQ1 RNase-Free DNase (Promega) as per manufacturer's instruction. cDNA synthesis was performed following standard procedures.

Analysis of gene expression levels

Primers and Taqman probes were provided as a Taqman gene expression kit (Applied Biosystems) or designed using Primer Express (Applied Biosystems) and synthesized by Bioglegio. Primers for DNA PCR for CCR5 was a generous gift from E. Boon (Leiden University Medical Centre, Leiden, Netherlands (63)). Real time qPCR was performed using ABI PRISM 7700 Sequence Detection System (SDS, Applied Biosystems). mRNA expression levels were normalized based on DNA input as determined by CCR5 PCR. Data were visualized as heatmaps using Tableau software (<http://www.tableausoftware.com>)

Antigen uptake by human DCs

SEA and omega-1 were fluorescently labeled with PF-647 using the Promofluor labeling kit (Promokine) and according to the manufacturers recommendations. 10.000 immature DCs/well were seeded in a 96 well plate. Where indicated cells were pre-incubated with 10mM EGTA, 100 µg/ml Mannan (Sigma-Aldrich), 20µg/ml anti-DC-SIGN (clone AZN-D1, Beckman Coulter) or 20 µg/ml anti-MR (clone 15.2, Biolegend) for 60 min at 37 °C. Subsequently, cells were incubated with 2 µg/ml PF-647-labeled SEA or 500 ng/ml PF-647-labeled omega-1 at 37 °C for 1 h and washed in ice cold PBS before analysis using flowcytometry.

Confocal microscopy

For live cell imaging, purified HEK-omega-1 was fluorescently labeled with N-hydroxysuccinimide (NHS)-fluorescein (Thermo-Scientific) according to the manufacturer's instructions. After protein labeling, nonreacted NHS-fluorescein was removed using Zeba desalt spin columns (Thermo-Scientific). Live cell imaging was performed with a TCS Sp5 inverse confocal laser scanning microscope (Leica) and analyzed with LAS AF software. In detail, 2.5×10^4 DCs were added to a channel of an IV0.4 μ -slide (Ibidi) and incubated for 2 h at 37°C and 6% CO₂ with 10 μ l fluorescein-labeled HEK-omega-1 (0.3 mg/ml). Nuclei of the cells were then counterstained with Hoechst 33342 (1:10,000) for 30 min. For confocal microscopy of fixed DCs, cells were allowed to adhere to Poly-D-Lysine coated cover slips overnight at a concentration of 80-100.000 cells/2 ml in 10% FCS/RPMI. DCs were incubated with omega-1 for 2 h at 37 °C (1 μ g/ml). Incubated cells were washed three times in 1% BSA/RPMI, fixed for 15 minutes with 4% paraformaldehyde (Sigma) in PBS, and washed twice in PBS. Next, cells were permeabilized with 0.1% Triton-X in PBS for 1 minute, washed twice in PBS and blocked for 15 minutes with 1% BSA/PBS. Cells were subsequently incubated with antibodies against rRNA (Abcam), followed by a secondary incubation step with a G α M-AF546 antibody (Invitrogen) in 1% BSA/PBS. Cells were washed in PBS and cover slips were mounted on glass slides with Vectashield and analyzed by confocal microscopy. Leica AOBSP2 confocal laser scanning microscope (CLSM) system was used, containing a DM-IRE2 microscope with glycerol objective lens (PL APO 63x/NA1.30) and images were acquired using Leica confocal software (version 2.61).

Cytoplasmic omega-1 Western blot

Cytoplasmic extracts of omega-1-incubated DCs were prepared using Nuclear Extraction Kit (Active Motif) as per manufacturer's instructions. Cytoplasmic extracts were concentrated 10-fold and subjected to 12% SDS-PAGE followed by silver staining or blotting onto nitrocellulose membrane. For silver staining 30 μ g/cm were applied, for Western blotting 100 μ g/cm. Omega-1 was then detected by the monoclonal anti-omega-1 antibody 140-3E11 and an alkaline phosphatase-labeled goat anti-mouse IgG (1:10,000) detection antibody (Dianova). Visualization was done by the substrate/chromogen mixture of 0.033% (w/v) nitro blue tetrazolium and 0.017% (w/v) 5-bromo-4-chloro-indolyl phosphate (Serva) in 0.1 M Tris-buffered saline, pH 9.5.

In vivo experiments

4get/KN2 (64) mice were bred and housed in the animal facility of the Trudeau Institute and used at 8-12 weeks of age. MR^{-/-} mice on a C57BL/6 background were provided by Dr. M. C. Nussenzweig (Rockefeller University, New York, NY) and were bred and housed in the animal facility of the Institutes of Molecular Medicine and Experimental Immunology at the University Hospital, Bonn. All experimental procedures were approved by the Institutional Animal Care and Use Committee of the Trudeau Institute, and Molecular Medicine and Experimental Immunology at the University Hospital of Bonn and by the Animal Studies Committee of Washington University School of Medicine. Mice were immunized s.c. into one

hind footpad with SEA (20 µg), omega-1 (3 µg), in a volume of 50 µl and the draining popliteal lymph nodes were analyzed one week later.

***In vitro* restimulation of lymph node cells**

1.5×10^6 popliteal LN cells/ml from individual animals were restimulated with 10 µg/ml SEA or 2 µg/ml omega-1. IL-5, IL-4 and IFN- γ were measured by ELISA in day 4 supernatants according to the manufacturer's recommendations (R&D). Following removal of the supernatants, cells were restimulated with 50 ng/ml phorbol 12-myristate 13-acetate plus 2 µg/ml ionomycin for 6 h. 10 µg/ml brefeldin A was added during the last 2 h (all Sigma). The cells were stained with a combination of IL-4-PE and IFN- γ -FITC antibodies (BD).

Statistical analysis

Data were analyzed for statistical significance using a two-sided paired Student's *t*-test or where indicated a two-sided unpaired Student's *t*-test. All *p*-values < 0.05 were considered significant.

Online supplemental material

Online supplemental material can be found at: <http://jem.rupress.org/content/209/10/1753/suppl/DC1>. Fig S1 shows a movie of z-stacked images of live DCs internalizing omega-1.

ACKNOWLEDGEMENTS

The authors thank Krystelle Nganou-Mkamdop for performing DC-antigen uptake experiments, and Heike Rohweder and Daniela Barths for their technical assistance in the mutagenesis and cloning studies of omega-1. Furthermore, we thank Dr. Buschow and Dr. Miller for providing the DC-SIGN- and MR-expressing cell-lines, respectively. This work was supported by the Netherlands Foundation for the Advancement of Tropical Research (WOTRO), Grant No W93-385 20077, the Dutch Organization for Scientific Research (NWO), Grant No ZONMW 912-03-048, ZONMW-VENI 016.066.093 NWO-CW 700.55.013 and the National Institutes of Health grant AI53825.

REFERENCES

1. Kapsenberg ML. Dendritic-cell control of pathogen-driven T-cell polarization. *Nat Rev Immunol* 2003 Dec;3(12):984-93.
2. Akira S, et al. Pathogen Recognition and Innate Immunity. *Cell* 2006 Feb 24;124(4):783-801.
3. Carvalho L, et al. Review series on helminths, immune modulation and the hygiene hypothesis: mechanisms underlying helminth modulation of dendritic cell function. *Immunology* 2009 Jan;126(1):28-34.
4. MacDonald AS, et al. Alarming dendritic cells for Th2 induction. *J Exp Med* 2008 Jan 21;205(1):13-7.
5. Phytian-Adams AT, et al. CD11c depletion severely disrupts Th2 induction and development in vivo. *J Exp Med* 2010 Sep 27;207(10):2089-96.
6. Okano M, et al. Induction of Th2 responses and IgE is largely due to carbohydrates functioning as adjuvants on *Schistosoma mansoni* egg antigens. *J Immunol* 1999 Dec 15;163(12):6712-7.
7. van Liempt E, et al. *Schistosoma mansoni* soluble egg antigens are internalized by human dendritic cells through multiple C-type lectins and suppress TLR-induced dendritic cell activation. *Mol Immunol* 2007 Apr;44(10):2605-15.
8. Gringhuis SI, et al. Carbohydrate-specific signaling through the DC-SIGN signalosome tailors immunity to *Mycobacterium tuberculosis*, HIV-1 and *Helicobacter pylori*. *Nat Immunol* 2009 Oct;10(10):1081-8.
9. van Liempt E, et al. Specificity of DC-SIGN for mannose- and fucose-containing glycans. *FEBS Lett* 2006 Nov 13;580(26):6123-31.
10. Van Diel, et al. The dendritic cell-specific C-type lectin DC-SIGN is a receptor for *Schistosoma mansoni* egg antigens and recognizes the glycan antigen Lewis x. *Glycobiology* 2003 Jun;13(6):471-8.
11. Bergman MP, et al. *Helicobacter pylori* modulates the T helper cell 1/T helper cell 2 balance through phase-variable interaction between lipopolysaccharide and DC-SIGN. *J Exp Med* 2004 Oct 18;200(8):979-90.
12. Ritter M, et al. *Schistosoma mansoni* triggers Dectin-2, which activates the Nlrp3 inflammasome and alters adaptive immune responses. *Proc Natl Acad Sci U S A* 2010 Nov 23;107(47):20459-64.
13. Correale J, et al. Helminth antigens modulate immune responses in cells from multiple sclerosis patients through TLR2-dependent mechanisms. *J Immunol* 2009 Nov 1;183(9):5999-6012.
14. Thomas PG, et al. Maturation of dendritic cell 2 phenotype by a helminth glycan uses a Toll-like receptor 4-dependent mechanism. *J Immunol* 2003 Dec 1;171(11):5837-41.
15. Everts B, et al. Omega-1, a glycoprotein secreted by *Schistosoma mansoni* eggs, drives Th2 responses. *J Exp Med* 2009 Aug 3;206(8):1673-80.
16. Steinfelder S, et al. The major component in schistosome eggs responsible for conditioning dendritic cells for Th2 polarization is a T2 ribonuclease (omega-1). *J Exp Med* 2009 Aug 3;206(8):1681-90.
17. Fitzsimmons CM, et al. Molecular characterization of omega-1: a hepatotoxic ribonuclease from *Schistosoma mansoni* eggs. *Mol Biochem Parasitol* 2005 Nov;144(1):123-7.
18. Wolf B, et al. A mechanism of the irreversible inactivation of bovine pancreatic ribonuclease by diethylpyrocarbonate. A general reaction of diethylpyrocarbonate. A general reaction of diethylpyrocarbonate with proteins. *Eur J Biochem* 1970 Apr;13(3):519-25.
19. Irie M, et al. Ribonuclease T2. *Methods Enzymol* 2001;341:42-55.
20. Meevissen MH, et al. Structural Characterization of Glycans on Omega-1, a Major *Schistosoma mansoni* Egg Glycoprotein That Drives Th2 Responses. *J Proteome Res* 2010 Mar 18;9(5):2630-42.
21. Yan SB, et al. Novel Asn-linked oligosaccharides terminating in GalNAc beta (1-->4)[Fuc alpha (1-->3)]GlcNAc beta (1-->) are present in recombinant human protein C expressed in human kidney 293 cells. *Glycobiology* 1993 Dec;3(6):597-608.
22. Meevissen MH, et al. *Schistosoma mansoni* egg glycoproteins and C-type lectins of host immune cells: Molecular partners that shape immune responses. *Exp Parasitol* 2011 May 15;
23. Mohrs M, et al. Analysis of type 2 immunity in vivo with a bicistronic IL-4 reporter. *Immunity* 2001 Aug;15(2):303-11.
24. Taylor ME, et al. Contribution to ligand binding by multiple carbohydrate-recognition domains in the macrophage mannose

- receptor. *J Biol Chem* 1992 Jan 25;267(3):1719-26.
25. Montanaro L, et al. Inhibition by ricin of protein synthesis in vitro. Ribosomes as the target of the toxin. *Biochem J* 1973 Nov;136(3):677-83.
 26. Lacadena J, et al. Fungal ribotoxins: molecular dissection of a family of natural killers. *FEMS Microbiol Rev* 2007 Mar;31(2):212-37.
 27. Wuhrer M, et al. IPSE/alpha-1, a major secretory glycoprotein antigen from schistosome eggs, expresses the Lewis X motif on core-difucosylated N-glycans. *FEBS J* 2006 May;273(10):2276-92.
 28. Kao R, et al. Mitogillin and related fungal ribotoxins. *Methods Enzymol* 2001;341:324-35.
 29. Frison N, et al. Oligoglycine-based oligosaccharide clusters: selective recognition and endocytosis by the mannose receptor and dendritic cell-specific intercellular adhesion molecule 3 (ICAM-3)-grabbing nonintegrin. *J Biol Chem* 2003 Jun 27;278(26):23922-9.
 30. East L, et al. The mannose receptor family. *Biochim Biophys Acta* 2002 Sep 19;1572(2-3):364-86.
 31. Paveley RA, et al. The Mannose Receptor (CD206) is an important pattern recognition receptor (PRR) in the detection of the infective stage of the helminth *Schistosoma mansoni* and modulates IFN γ production. *Int J Parasitol* 2011 Nov;41(13-14):1335-45.
 32. Chieppa M, et al. Cross-linking of the mannose receptor on monocyte-derived dendritic cells activates an anti-inflammatory immunosuppressive program. *J Immunol* 2003 Nov 1;171(9):4552-60.
 33. Op den Brouw ML, et al. The mannose receptor acts as hepatitis B virus surface antigen receptor mediating interaction with intrahepatic dendritic cells. *Virology* 2009 Oct 10;393(1):84-90.
 34. Yamamoto Y, et al. Involvement of mannose receptor in cytokine interleukin-1 β (IL-1 β), IL-6, and granulocyte-macrophage colony-stimulating factor responses, but not in chemokine macrophage inflammatory protein 1 β (MIP-1 β), MIP-2, and KC responses, caused by attachment of *Candida albicans* to macrophages. *Infect Immun* 1997 Mar;65(3):1077-82.
 35. Royer PJ, et al. The mannose receptor mediates the uptake of diverse native allergens by dendritic cells and determines allergen-induced T cell polarization through modulation of IDO activity. *J Immunol* 2010 Aug 1;185(3):1522-31.
 36. Li J, et al. The dendritic cell mannose receptor mediates allergen internalization and maturation involving notch 1 signalling. *Clin Exp Immunol* 2010 Nov;162(2):251-61.
 37. Bufe A, et al. The major birch pollen allergen, Bet v 1, shows ribonuclease activity. *Planta* 1996;199(3):413-5.
 38. Kao R, et al. Mitogillin and related fungal ribotoxins. *Methods Enzymol* 2001;341:324-35.
 39. Garcia-Ortega L, et al. Production and characterization of a noncytotoxic deletion variant of the *Aspergillus fumigatus* allergen Asp f1 displaying reduced IgE binding. *FEBS J* 2005 May;272(10):2536-44.
 40. Yang D, et al. Eosinophil-derived neurotoxin acts as an alarmin to activate the TLR2-MyD88 signal pathway in dendritic cells and enhances Th2 immune responses. *J Exp Med* 2008 Jan 21;205(1):79-90.
 41. The *Schistosoma japonicum* genome reveals features of host-parasite interplay. *Nature* 2009 Jul 16;460(7253):345-51.
 42. Young ND, et al. Whole-genome sequence of *Schistosoma haematobium*. *Nat Genet* 2012 Feb;44(2):221-5.
 43. Hillwig MS, et al. Zebrafish RNase T2 genes and the evolution of secretory ribonucleases in animals. *BMC Evol Biol* 2009;9:170.
 44. Sandvig K, et al. Delivery into cells: lessons learned from plant and bacterial toxins. *Gene Ther* 2005 Jun;12(11):865-72.
 45. Burgdorf S, et al. Spatial and mechanistic separation of cross-presentation and endogenous antigen presentation. *Nat Immunol* 2008 May;9(5):558-66.
 46. Burgdorf S, et al. Distinct pathways of antigen uptake and intracellular routing in CD4 and CD8 T cell activation. *Science* 2007 Apr 27;316(5824):612-6.
 47. Zehner M, Chasan AI, Scheutte V, Embgenbroich M, Quast T, Kolanus W, et al. Mannose Receptor poly-ubiquitination regulates endosomal recruitment of p97 and cytosolic antigen translocation for cross-presentation. *Proc Natl Acad Sci U S A*. In press 2011.
 48. Pelling AE, et al. Mechanical dynamics of single cells during early apoptosis. *Cell Motil Cytoskeleton* 2009 Jul;66(7):409-22.

49. Oswald IP, et al. IL-12 inhibits Th2 cytokine responses induced by eggs of *Schistosoma mansoni*. *J Immunol* 1994 Aug 15;153(4):1707-13.
50. Constant S, et al. Extent of T cell receptor ligation can determine the functional differentiation of naive CD4+ T cells. *J Exp Med* 1995 Nov 1;182(5):1591-6.
51. Wang ZE, et al. CD4+ effector cells default to the Th2 pathway in interferon gamma-deficient mice infected with *Leishmania major*. *J Exp Med* 1994 Apr 1;179(4):1367-71.
52. Yates A, et al. Cytokine-modulated regulation of helper T cell populations. *J Theor Biol* 2000 Oct 21;206(4):539-60.
53. Jankovic D, et al. Mechanisms underlying helminth-induced Th2 polarization: default, negative or positive pathways? *Chem Immunol Allergy* 2006;90:65-81.:65-81.
54. Marshall FA, et al. Uncoupling of induced protein processing from maturation in dendritic cells exposed to a highly antigenic preparation from a helminth parasite. *J Immunol* 2008 Dec 1;181(11):7562-70.
55. Ricardo-Gonzalez RR, et al. IL-4/STAT6 immune axis regulates peripheral nutrient metabolism and insulin sensitivity. *Proc Natl Acad Sci USA* 2010 Dec 28;107(52):22617-22.
56. Jager A, et al. Effector and regulatory T-cell subsets in autoimmunity and tissue inflammation. *Scand J Immunol* 2010 Sep;72(3):173-84.
57. de Jong EC, et al. Microbial compounds selectively induce Th1 cell-promoting or Th2 cell-promoting dendritic cells in vitro with diverse th cell-polarizing signals. *J Immunol* 2002 Feb 15;168(4):1704-9.
58. Woodward MP, et al. Detection of monoclonal antibodies specific for carbohydrate epitopes using periodate oxidation. *J Immunol Methods* 1985 Apr 8;78(1):143-53.
59. Hamilton JV, et al. Periodate-sensitive immunological cross-reactivity between keyhole limpet haemocyanin (KLH) and serodiagnostic *Schistosoma mansoni* egg antigens. *Parasitology* 1999 Jan;118 (Pt 1):83-9.
60. Sallusto F, et al. Efficient presentation of soluble antigen by cultured human dendritic cells is maintained by granulocyte/macrophage colony-stimulating factor plus interleukin 4 and downregulated by tumor necrosis factor alpha. *J Exp Med* 1994 Apr 1;179(4):1109-18.
61. Geijtenbeek TB, et al. Identification of DC-SIGN, a novel dendritic cell-specific ICAM-3 receptor that supports primary immune responses. *Cell* 2000 Mar 3;100(5):575-85.
62. Miller JL, et al. The mannose receptor mediates dengue virus infection of macrophages. *PLoS Pathog* 2008 Feb 8;4(2):e17.
63. Boon EM, et al. Y chromosome detection by Real Time PCR and pyrophosphorolysis-activated polymerisation using free fetal DNA isolated from maternal plasma. *Prenat Diagn* 2007 Oct;27(10):932-7.
64. Mohrs K, et al. A two-step process for cytokine production revealed by IL-4 dual-reporter mice. *Immunity* 2005 Oct;23(4):419-29.



**RAPAMYCIN AND OMEGA-1:
mTOR-DEPENDENT AND
-INDEPENDENT TH2 SKEWING BY
HUMAN DENDRITIC CELLS**

Leonie Hussaarts, Hermelijn H. Smits, Gabriele Schramm,
Alwin J. van der Ham, Gerard C. van der Zon, Helmut Haas,
Bruno Guigas and Maria Yazdanbakhsh

*Immunology and Cell Biology, August 2013,
Volume 91, 486-489*

3

ABSTRACT

Recent reports have attributed an immunoregulatory role to the mammalian target of rapamycin (mTOR), a key serine/threonine protein kinase integrating input from growth factors and nutrients to promote cell growth and differentiation. In the present study, we investigated the role of the mTOR pathway in Th2 induction by human monocyte-derived dendritic cells (moDCs). Using a co-culture system of human lipopolysaccharide (LPS)-matured moDCs and allogeneic naive CD4⁺ T cells, we show that inhibition of mTOR by the immunosuppressive drug rapamycin reduced moDC maturation and promoted Th2 skewing. Next, we investigated whether antigens from helminth parasites, the strongest natural inducers of Th2 responses, modulate moDCs via the mTOR pathway. In contrast to rapamycin, neither *Schistosoma mansoni*-soluble egg antigens (SEA) nor its major immunomodulatory component omega-1 affected the phosphorylation of S6 kinase (S6K) and 4E-binding protein 1 (4E-BP1), downstream targets of mTORC1. Finally, we found that the effects of rapamycin and SEA/omega-1 on Th2 skewing were additive, suggesting two distinct underlying molecular mechanisms. We conclude that conditioning human moDCs to skew immune responses towards Th2 can be achieved via an mTOR-dependent and -independent pathway triggered by rapamycin and helminth antigens, respectively.

INTRODUCTION

The interface of immunology and metabolism is an emerging field that focuses on the relation between cell-intrinsic metabolic processes and the responses of immune cells (1;2). The area has received increasing attention, as it is now recognized that the behavior of the cells of the immune system is at least partially controlled by various metabolic pathways (2). Among them, the mammalian target of rapamycin (mTOR) pathway was recently shown to have an important role in dendritic cell (DC)-mediated T helper cell differentiation (3;4). mTOR is a serine/threonine protein kinase constituting the catalytic subunit of two functionally distinct multiprotein complexes, designated mTORC1 and mTORC2. mTORC1 integrates input from growth factors and nutrient sensors, upon which it interacts with its downstream targets S6 kinase (S6K) and eukaryotic initiation factor 4E-binding protein 1 (4E-BP1) to promote or inhibit cell growth. mTORC2 mediates cytoskeletal organization, predominantly via interaction with protein kinase C family members and serum/glucocorticoid-regulated kinase 1 (5). The two complexes differ, among others, in that mTORC1 is highly sensitive to acute inhibition by the immunosuppressive drug rapamycin, while mTORC2 is not (6;7).

The role of the mTOR pathway in DC-mediated T-cell differentiation has mainly been studied in murine models. A decade ago, an early report showed that silencing of PI3K, which is located upstream of mTOR, increases DC IL-12 production and promotes protective Th1 responses against *Leishmania major* infection (8). More recent studies have demonstrated that differentiation of murine bone marrow-derived DCs with granulocyte-macrophage colony-stimulating factor (GM-CSF) and IL-4 in the presence of rapamycin generates DCs with low levels of co-stimulatory molecules (9;10) which are weak stimulators of CD4⁺ T cells and promote the expansion of regulatory T cells (10). In addition, upon exposure to lipopolysaccharide (LPS), rapamycin-treated bone marrow-derived DCs were shown to promote IL-4 secretion by T cells while decreasing IL-17 and IL-2 production (11), hinting towards a link between mTOR inhibition and Th2 induction.

In the present study, we therefore investigated the role of the mTOR pathway on Th2 polarization by human monocyte-derived DCs (moDCs). For this purpose, we compare the effects of rapamycin to those of *Schistosoma mansoni*-soluble egg antigens (SEA), the strongest natural inducer of Th2 responses (12), and omega-1, a single molecule recently identified to be the major SEA component involved in Th2 skewing (13-15).

RESULTS

In order to investigate the effect of mTOR inhibition on Th2 polarization by human DCs, we used a co-culture system of human LPS-matured moDCs and allogeneic naive CD4⁺ T cells, a well-characterized model reflecting the *in vivo* polarization of immune responses against pathogens and pathogen-derived compounds (13;16). Blocking the mTOR pathway in moDCs using rapamycin prior to Toll-like receptor-4 ligation reduced the LPS-driven upregulation of the maturation markers CD40, CD80 and CD86 (Figure 1a, Supplementary Figure S1). In addition, like SEA and omega-1, rapamycin modulated moDCs to instruct T cells towards a

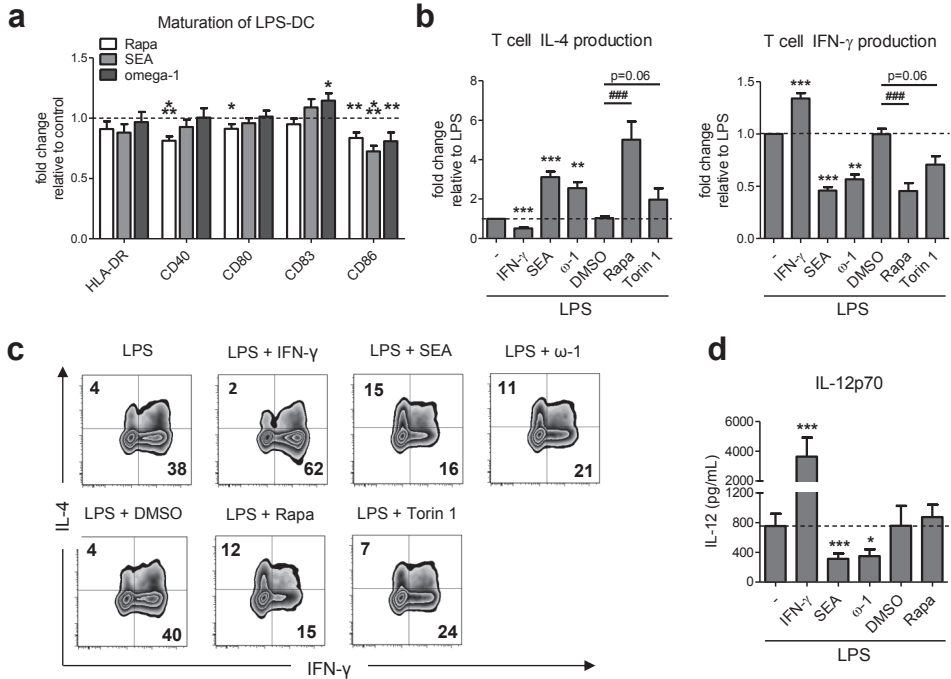


Figure 1. Rapamycin lowers DC maturation and primes for Th2 responses without affecting DC IL-12 production. (a) moDCs were either pulsed with SEA or omega-1 in the presence of LPS, or incubated for 90 min with rapamycin or its vehicle dimethyl sulfoxide (DMSO) prior to LPS stimulation. After 48 h, expression of maturation markers was analyzed by flow cytometry. The expression levels, based on the geometric mean fluorescence of at least nine independent experiments, are shown relative to the moDCs stimulated with LPS or LPS + DMSO alone, which were set to 1 for each marker (dashed line). (b) moDCs were either pulsed with SEA or omega-1 in combination with LPS, or incubated for 90 min with rapamycin, Torin1 or their vehicle DMSO prior to LPS stimulation. After 48 h of stimulation, moDCs were cultured with allogeneic naive CD4⁺ T cells for 11 days. Intracellular IL-4 and IFN- γ were analyzed by flow cytometry after a 6-h stimulation with phorbol myristate acetate and ionomycin. IFN- γ -stimulated moDCs were taken along as a Th1-inducing control. The percentages of T cells uniquely positive for either IL-4 or IFN- γ are expressed relative to the LPS condition. Data represent at least four independent experiments. (c) Representative FACS plots from one out of the four independent experiments are shown for conditions described for Figure 1b. (d) Following stimulation as described for Figure 1a, conditioned moDCs were co-cultured with a CD40L-expressing cell line. Supernatants were collected after 24 h and IL-12p70 concentrations were determined by ELISA. IFN- γ -stimulated moDCs were taken along as an IL-12 inducing control. Bars represent mean values + s.e.m.; * P <0.05; ** P <0.01; ***, ### P <0.001 for significant differences with the control (*; either LPS or LPS + DMSO) or between test conditions (#), based on one-sided Wilcoxon-signed rank testing. ω -1, omega-1; Rapa, rapamycin.

Th2 response characterized by increased expression of IL-4 and decreased interferon (IFN)- γ production (Figures 1b and c, Supplementary Figure S2). Interestingly, in contrast to SEA and omega-1, rapamycin skewed Th2 responses without affecting the pro-inflammatory cytokine IL-12 (Figure 1d). Of note, Torin1, a second-generation highly selective inhibitor of both mTORC1 and mTORC2 (17), also induced skewing towards Th2 when added to moDCs (Figures 1b and c,

Supplementary Figure S2). However, Torin1 was a less potent Th2-inducer than rapamycin, even though blocking of mTORC1 by Torin1 and rapamycin was equally effective (data not shown). This difference in potency may reflect the complex and distinct molecular mechanisms by which the two drugs operate (18), which for rapamycin has even been described to differ between cell types (7).

As both helminth antigens and rapamycin reduce CD86 on moDCs and prime for Th2 skewing, we hypothesized the existence of a common underlying mechanism involving inhibition of mTOR activity. We therefore addressed the question whether SEA and omega-1, like rapamycin, inhibit the mTOR pathway and thereby modulate moDCs for Th2 polarization. To this end, moDCs were stimulated with LPS in the presence of helminth antigens or rapamycin for 6 and 48 h, and the phosphorylation states of mTOR and the mTORC1 downstream targets S6K and 4E-BP1 were determined. Although rapamycin strongly inhibited LPS-induced mTORC1 activity at 6 and 48 h, as shown by reduced phosphorylation of both S6K and 4E-BP1, no such effects were observed with either SEA or omega-1 (Figures 2a and b). A similar trend was observed when phosphorylation of mTOR was analyzed (Figure 2a). Interestingly, co-stimulation with rapamycin and SEA or omega-1 promoted a stronger Th2 response than stimulation with rapamycin, SEA or omega-1 alone (Figures 2c and d, Supplementary Figure S3), suggesting the existence of both mTOR-dependent and -independent mechanisms for Th2 skewing.

DISCUSSION

Recent studies have indicated that signaling pathways involved in the regulation of metabolism can control immune-cell fate and functions (2). Although much is known about the control of Th1 and Th17 differentiation, the mechanisms by which DCs skew Th2 remain largely unknown to date (19). In this study, we analyzed the role of the mTOR pathway in the induction of Th2 responses by human moDCs. To our knowledge, the present study is the first one reporting that inhibition of the mTOR pathway using the immunosuppressive drug rapamycin primes human moDCs to induce strong Th2 responses characterized by increased IL-4 and decreased IFN- γ production. This finding apparently differs from the one reported by Turnquist et al. (11), showing that rapamycin-conditioned human moDCs promote the expansion of both IL-4 and IFN- γ -producing T cells. However, it is important to note that in the study by Turnquist et al. (11), moDCs were differentiated using IL-4 and GM-CSF in the presence of rapamycin. It has been described that GM-CSF activates the mTOR pathway, and differentiation of moDCs in the presence of rapamycin hampers the survival and the immunostimulatory capacity of moDCs (20). In contrast, in our model, moDCs were exposed to rapamycin after differentiation. Our findings are therefore complementary to the study by Turnquist et al. (11), and highlight that the effect of rapamycin on moDC-mediated T-cell polarization critically depends on the timing and the duration of exposure to rapamycin.

In addition to the effect of rapamycin on T-cell skewing, we found that exposure to the drug reduces moDC maturation. These effects are similar to those induced by the helminth

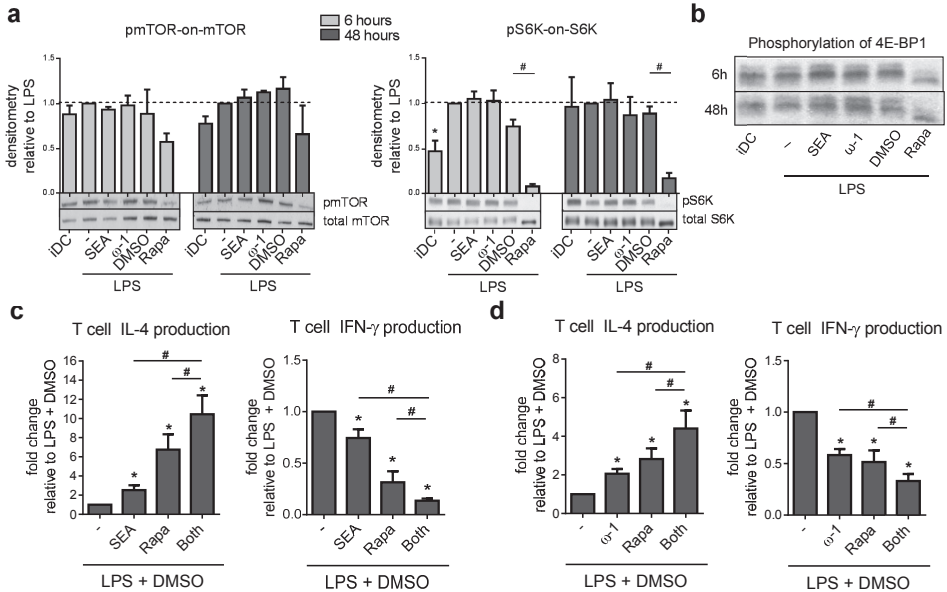


Figure 2. Unlike rapamycin, SEA and omega-1 do not affect the mTOR pathway to condition DCs for Th2 priming. MoDCs were stimulated as described in the legend of Figure 1. (a,b) moDC lysates were collected after 6 and 48 h of stimulation. Proteins were visualized by western blotting using antibodies against S6K and S6K phosphorylation at Thr421, and mTOR and mTOR phosphorylation at Ser2448. Western blot results were quantified using ImageJ software. The pS6K-on-S6K and pmTOR-on-mTOR ratios were calculated relative to the LPS condition. Representative blots from one out of five (6 h) or four (48 h) independent experiments are shown. (b) moDC lysates were collected after 6 and 48 h of stimulation. 4E-BP1 phosphorylation at Thr37/46 was assessed by western blotting. (c,d) moDCs stimulated for 48 h were cultured with allogeneic naive CD4⁺ T cells for 11 days and T-cell cytokine production was analyzed as described in the legend of Figure 1. Data represent at least five independent experiments. Bars represent mean values \pm s.e.m.; *, #P<0.05 for significant differences with the control (*, either LPS or LPS + DMSO) or between test conditions (#) based on one-sided Wilcoxon-signed rank testing. iDC, immature (nonstimulated) moDC; ω -1, omega-1; Rapa, rapamycin; Both, rapamycin and SEA or omega-1.

antigens, SEA and omega-1, which suppress DC maturation and are the strongest natural inducers of Th2 responses (12;13;15). Importantly, we demonstrate that SEA and omega-1, unlike rapamycin, do not affect the phosphorylation of mTOR and the mTORC1 downstream targets S6K and 4E-BP1. The finding that rapamycin and helminth antigens affect moDCs in a distinct manner is further supported by the differential effect of rapamycin and SEA or omega-1 on moDC IL-12 production.

Although both SEA and omega-1 reduce IL-12 levels, as reported previously (13), rapamycin does not. Secretion of IL-12 by antigen-presenting cells has classically been associated with Th1 differentiation (21), and the mere absence of IL-12 and other Th1-inducing molecules was suggested to promote a Th2 response (22). As rapamycin, unlike SEA and omega-1, does not attenuate moDC IL-12 secretion, this so-called default hypothesis for Th2 polarization fails to

explain the dominant Th2 response induced by rapamycin. Our results suggest the existence of mTOR-dependent and -independent mechanisms for Th2 skewing, which is further supported by experiments that show an additive effect on Th2 priming by moDCs co-stimulated with both rapamycin and helminth antigens. Needless to say, we do not exclude the possibility that rapamycin and helminth antigens target other common downstream pathways. Whether rapamycin may have similar effects on T-cell polarization by different DC subsets, remains an intriguing area of research, as it has been demonstrated that rapamycin differentially affects moDCs and myeloid DCs (20).

In summary, our observations suggest that conditioning human DCs to skew immune responses towards Th2 can be achieved by an mTOR-dependent and an mTOR-independent mechanism by rapamycin and helminth antigens, respectively. These findings are important when considering the increasing interest in DC-based immune therapy for cancer (23), transplantation and autoimmunity (24). This requires in-depth understanding of the different modes and mechanisms, whereby DCs can be accurately modulated for clinical use.

METHODS

Preparation and purification of *S. mansoni*-derived antigens

SEA and omega-1 from *S. mansoni* were prepared as described previously (25;26). The purity of the preparations was controlled by SDS-PAGE and silver staining. The protein concentrations were determined using the Bradford or BCA procedure.

Human DC culture, stimulation and analysis

Peripheral blood mononuclear cells were isolated from venous blood of healthy volunteers diluted in an equivalent volume of HBSS, by means of a Ficoll density gradient. Monocytes were isolated by positive magnetic cell sorting using CD14-beads (Miltenyi Biotec, Bergisch Gladbach, Germany) and cultured in RPMI supplemented with 10% FCS, human rGM-CSF (20 ng/ml; BioSource/Invitrogen, Carlsbad, CA, USA) and human rIL-4 (0.86 ng/mL, R&D Systems, Minneapolis, MN, USA). The culture medium including supplements was replaced on day 2 or 3. Immature moDCs were stimulated on day 6. Indicated conditions were preincubated with rapamycin (100 nM; Sigma-Aldrich, Zwijndrecht, The Netherlands) or Torin1 (100 nM; a kind gift from Dr. Thomas Weichhart) or their vehicle dimethyl sulfoxide for 90min prior to stimulation with ultrapure LPS (100 ng/mL; *Escherichia coli* 0111 B4 strain, InvivoGen, San Diego, CA, USA) supplemented with human rGM-CSF. Alternatively, moDCs were pulsed with SEA (50 µg/mL), omega-1 (500 ng/mL) or IFN-γ (1000 U/mL) in the presence of ultrapure LPS (100 ng/mL) and human rGM-CSF. After 48 h of stimulation, surface expression of co-stimulatory molecules was determined by FACS (FACS-Canto, BD Biosciences, Breda, The Netherlands) using the following antibodies: CD86 FITC, CD40 APC, CD80 Horizon V450 (all BD Biosciences), HLA-DR APC-eFluor 780 (eBioscience, San Diego, CA, USA) and CD83 PE (Beckman-Coulter, Fullerton, CA, USA). Only live cells, which were negative for 7AAD (eBioscience), were included in the analysis. In addition, 1×10^4 matured moDCs were co-

cultured with 1×10^4 CD40L-expressing J558 cells. Supernatants were collected after 24 h and IL-12p70 concentrations were determined by ELISA using mouse anti-human IL-12 (clone 20C2) as a capture antibody and biotinylated mouse-anti-human IL-12 (clone C8.6) as a detection antibody (BD Biosciences).

Human T-cell culture and analysis of T-cell polarization

For analysis of T-cell polarization, 48-h-pulsed moDCs were cultured with allogeneic naive CD4⁺ T cells for 11 days in the presence of staphylococcal enterotoxin B (10 pg/mL). On days 6 and 8, rhIL-2 (10 U/mL, R&D Systems) was added and the T cells were expanded until day 11. Intracellular cytokine production was analyzed after restimulation with 100 ng/mL phorbol myristate acetate plus 2 µg/mL ionomycin for 6 h; 10 µg/ml brefeldin A was added during the last 4 h and the cells were fixed with 3.7% paraformaldehyde (all Sigma-Aldrich). The cells were permeabilized with 0.2% saponin (Sigma-Aldrich) and stained with PE- and FITC-labelled antibodies against IL-4 and IFN- γ , respectively, (BD Biosciences).

Western blot analysis

moDC lysates were collected after 6 and 48 h of stimulation. Western blotting was performed as described previously,(27) the primary antibodies used were: mTOR; mTOR-Ser2448; S6K-Thr421; p4E-BP1-Thr37/46 (Cell Signaling Technology, Danvers, MA, USA) and S6K (Santa Cruz Biotechnology, Dallas, TX, USA). Western blot results were quantified using ImageJ software (NIH, Bethesda, MD, USA) and the phosphorylations of S6K (pS6K) and mTOR (pmTOR) were expressed relative to their total proteins as the pS6K-on-S6K ratio and the pmTOR-on-mTOR ratio, respectively.

Statistical analysis

Statistical analysis was performed using GraphPad Prism version 5.00 (GraphPad Software, La Jolla, CA, USA) for Windows.

ACKNOWLEDGEMENTS

This research was supported by the EU-funded project, *Immunological Interplay between Poverty Related Diseases and Helminth infections: An African-European Research Initiative 'IDEA'* (HEALTH-F3-2009-241642).

REFERENCES

1. Finlay D, et al. Metabolism, migration and memory in cytotoxic T cells. *Nat Rev Immunol* 2011 Feb;11(2):109-17.
2. Mathis D, et al. Immunometabolism: an emerging frontier. *Nat Rev Immunol* 2011 Feb;11(2):81.
3. Salmond RJ, et al. The influence of mTOR on T helper cell differentiation and dendritic cell function. *Eur J Immunol* 2011 Aug;41(8):2137-41.
4. Thomson AW, et al. Immunoregulatory functions of mTOR inhibition. *Nat Rev Immunol* 2009 May;9(5):324-37.
5. Laplante M, et al. mTOR signaling in growth control and disease. *Cell* 2012 Apr 13;149(2):274-93.
6. Ye L, et al. Rapamycin has a biphasic effect on insulin sensitivity in C2C12 myotubes due to sequential disruption of mTORC1 and mTORC2. *Front Genet* 2012;3:177.
7. Sarbassov DD, et al. Prolonged rapamycin treatment inhibits mTORC2 assembly and Akt/PKB. *Mol Cell* 2006 Apr 21;22(2):159-68.
8. Fukao T, et al. PI3K-mediated negative feedback regulation of IL-12 production in DCs. *Nat Immunol* 2002 Sep;3(9):875-81.
9. Hackstein H, et al. Rapamycin inhibits IL-4--induced dendritic cell maturation in vitro and dendritic cell mobilization and function in vivo. *Blood* 2003 Jun 1;101(11):4457-63.
10. Turnquist HR, et al. Rapamycin-conditioned dendritic cells are poor stimulators of allogeneic CD4+ T cells, but enrich for antigen-specific Foxp3+ T regulatory cells and promote organ transplant tolerance. *J Immunol* 2007 Jun 1;178(11):7018-31.
11. Turnquist HR, et al. mTOR and GSK-3 shape the CD4+ T-cell stimulatory and differentiation capacity of myeloid DCs after exposure to LPS. *Blood* 2010 Jun 10;115(23):4758-69.
12. Allen JE, et al. Evolution of Th2 immunity: a rapid repair response to tissue destructive pathogens. *PLoS Pathog* 2011 May;7(5):e1002003.
13. Everts B, et al. Omega-1, a glycoprotein secreted by *Schistosoma mansoni* eggs, drives Th2 responses. *J Exp Med* 2009 Aug 3;206(8):1673-80.
14. Everts B, et al. Schistosoma-derived omega-1 drives Th2 polarization by suppressing protein synthesis following internalization by the mannose receptor. *J Exp Med* 2012 Sep 24;209(10):1753-67, S1.
15. Steinfeld S, et al. The major component in schistosome eggs responsible for conditioning dendritic cells for Th2 polarization is a T2 ribonuclease (omega-1). *J Exp Med* 2009 Aug 3;206(8):1681-90.
16. Kapsenberg ML. Dendritic-cell control of pathogen-driven T-cell polarization. *Nat Rev Immunol* 2003 Dec;3(12):984-93.
17. Guertin DA, et al. The pharmacology of mTOR inhibition. *Sci Signal* 2009;2(67):e24.
18. Benjamin D, et al. Rapamycin passes the torch: a new generation of mTOR inhibitors. *Nat Rev Drug Discov* 2011 Nov;10(11):868-80.
19. Pulendran B, et al. Programming dendritic cells to induce T(H)2 and tolerogenic responses. *Nat Immunol* 2010 Aug;11(8):647-55.
20. Haidinger M, et al. A versatile role of mammalian target of rapamycin in human dendritic cell function and differentiation. *J Immunol* 2010 Oct 1;185(7):3919-31.
21. Trinchieri G. Interleukin-12: a cytokine produced by antigen-presenting cells with immunoregulatory functions in the generation of T-helper cells type 1 and cytotoxic lymphocytes. *Blood* 1994 Dec 15;84(12):4008-27.
22. Jankovic D, et al. Th1- and Th2-cell commitment during infectious disease: asymmetry in divergent pathways. *Trends Immunol* 2001 Aug;22(8):450-7.
23. Palucka K, et al. Cancer immunotherapy via dendritic cells. *Nat Rev Cancer* 2012 Apr;12(4):265-77.
24. Thomson AW, et al. Tolerogenic dendritic cells for autoimmune disease and transplantation. *Ann Rheum Dis* 2008 Dec;67 Suppl 3:iii90-iii96.
25. Grogan JL, et al. Elevated proliferation and interleukin-4 release from CD4+ cells after chemotherapy in human *Schistosoma haematobium* infection. *Eur J Immunol* 1996 Jun;26(6):1365-70.
26. Dunne DW, et al. The purification, characterization, serological activity and hepatotoxic properties of two cationic glycoproteins (alpha 1 and omega 1) from *Schistosoma mansoni* eggs. *Parasitology* 1991 Oct;103 Pt 2:225-36.
27. Linszen MM, et al. Prednisolone-induced beta cell dysfunction is associated with impaired endoplasmic reticulum homeostasis in INS-1E cells. *Cell Signal* 2011 Nov;23(11):1708-15.

SUPPLEMENTAL DATA

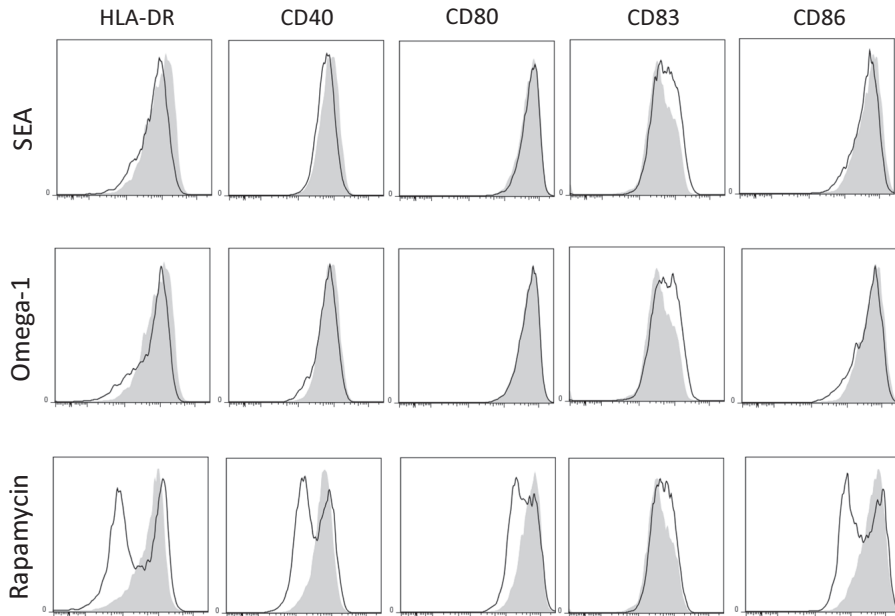


Figure S1. Rapamycin lowers LPS-induced DC maturation. moDCs were either pulsed with SEA or omega-1 in the presence of LPS, or incubated for 90 minutes with rapamycin or its vehicle DMSO prior to LPS stimulation. After 48 hours, expression of maturation markers was analyzed by flow cytometry. Representative histograms from 1 out of 9 independent experiments are shown. Filled histograms represent control conditions (either LPS or LPS + DMSO).

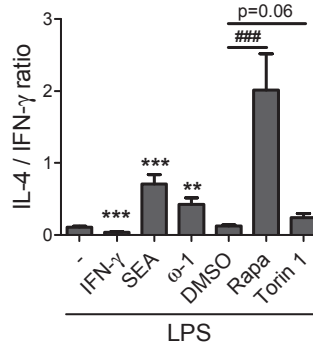


Figure S2. Rapamycin primes DCs for Th2 responses. moDCs were either pulsed with SEA or omega-1 in combination with LPS, or incubated for 90 minutes with rapamycin, Torin1 or their vehicle DMSO prior to LPS stimulation. After 48 hours of stimulation, moDCs were cultured with allogeneic naive CD4⁺ T cells for 11 days. Intracellular IL-4 and IFN-γ were analyzed by flow cytometry after 6h stimulation with PMA and ionomycin. IFN-γ-stimulated moDCs were taken along as a Th1-inducing control. The ratio of T cells uniquely positive for either IL-4 or IFN-γ was calculated. Data represent at least 4 independent experiments. Bars represent mean values + s.e.m.; ** $P < 0.01$; ***, ### $P < 0.001$ for significant differences with the LPS control (*) or between test conditions (#) based on one-sided Wilcoxon signed rank testing. ω-1, omega-1; Rapa, rapamycin.

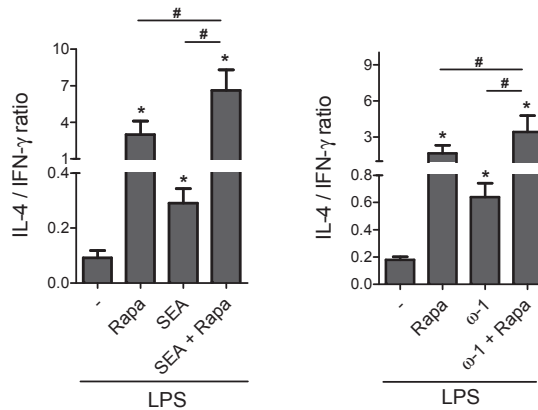
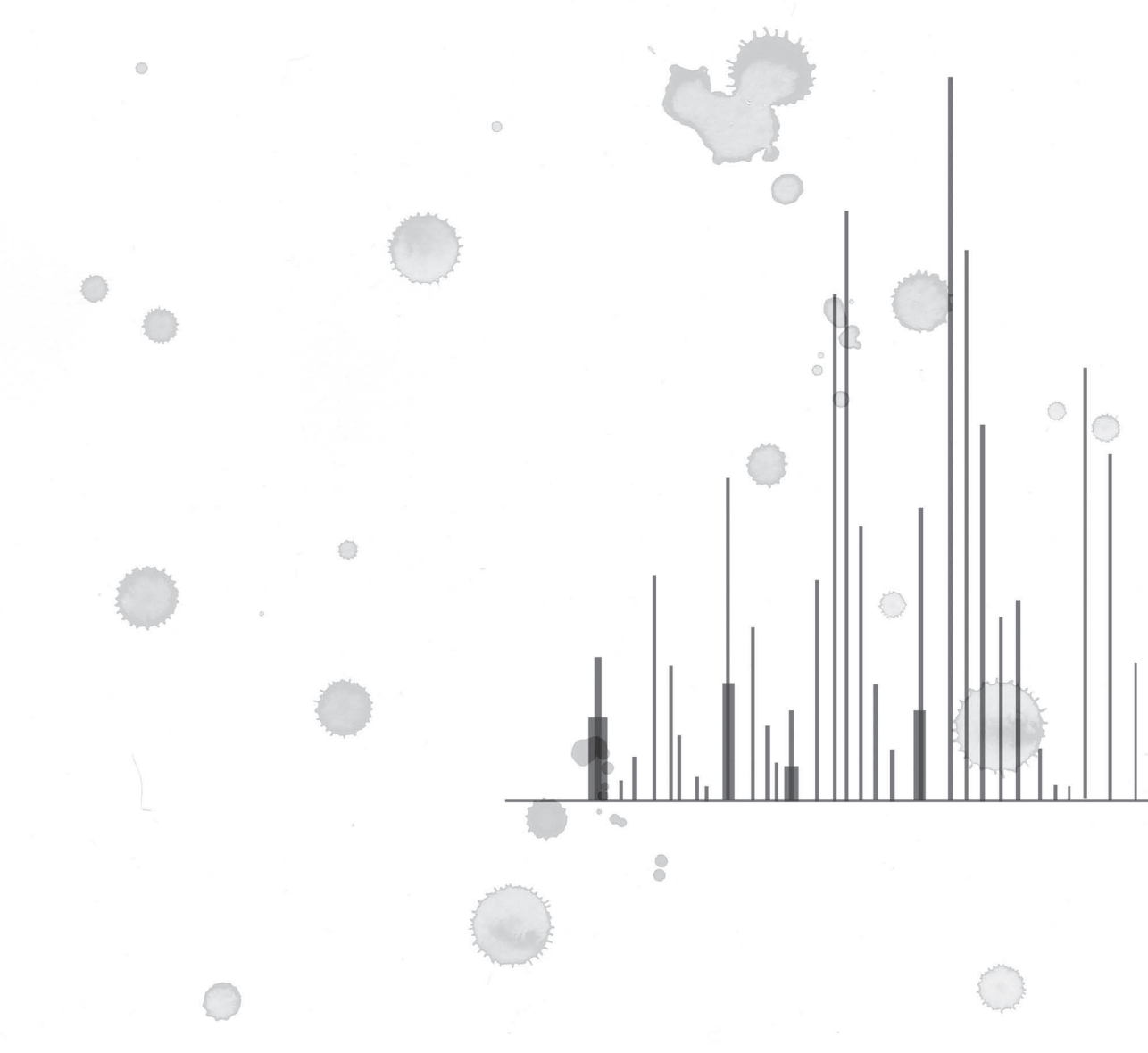


Figure S3. Co-stimulation with rapamycin and SEA or omega-1 primes a stronger Th2 response than stimulation with rapamycin, SEA or omega-1 alone. moDCs were either pulsed with SEA or omega-1 in combination with LPS, and / or incubated for 90 minutes with rapamycin, or its vehicle DMSO prior to stimulation. T cell responses were analysed as described for Supplementary figure 2. Bars represent mean values + s.e.m.; *, # $P < 0.05$; for significant differences with the LPS control (*) or between test conditions (#) based on one-sided Wilcoxon signed rank testing. ω-1, omega-1; Rapa, rapamycin.



ANALYSIS OF HUMAN DENDRITIC
CELL MATURATION AND
POLARIZATION USING LABEL-FREE
QUANTITATIVE PROTEOMICS

Leonie Husaarts, Maria Kaisar, Arzu Tugce Guler,
Hans Dalebout, André M. Deelder, Magnus Palmblad
and Maria Yazdanbakhsh

Manuscript in preparation

4

ABSTRACT

Dendritic cells (DC) are the sentinels of the immune system. Upon recognition of a pathogen, they undergo maturation and migrate to the lymph node to polarize T helper (Th) subsets. Although it is known that helminths and helminth-derived molecules condition dendritic cells to polarize T cells towards Th2, the underlying mechanism remains unknown. We chose to conduct a proteome analysis of the dendritic cells, in order to gain more insight into the cellular processes associated with their ability to polarize cellular immune responses. We analyzed DC maturation and polarization in nine different donors and at three different time points, using liquid chromatography and high-resolution Fourier transform ion cyclotron resonance mass spectrometry (LC-FTICRMS) for relative quantitation. We report that lipopolysaccharide-induced maturation had the strongest effect on the DC proteome, and promoted expression of proteins related to metabolic, cellular and immune system processes or transport. LPS-DCs additionally stimulated with IFN- γ , a Th1-inducing stimulus, differentially expressed cytoskeletal proteins and proteins involved in immune regulation, after 6h of stimulation, suggesting that they undergo accelerated maturation. Stimulation of LPS-DCs with omega-1 and SEA strongly increased 60S acidic ribosomal protein P2 (RPLP2). In addition, both SEA and omega-1 decreased expression of proteins related to antigen processing and presentation. In conclusion, our data support the hypothesis that reduced interaction between T cells and DCs at the level of the immunological synapse may promote Th2 polarization, and provide novel leads for the identification of molecular mechanisms for Th2 polarization.

INTRODUCTION

Dendritic cells (DCs) (1) are professional antigen-presenting cells located in peripheral tissues, that continuously sample the environment to capture antigens from invading microbes. Upon recognition of pathogens-associated molecules, DCs undergo maturation and migrate to the draining lymph nodes where they present antigen to antigen-specific T helper (Th) cells. Different classes of pathogens polarize DCs for the induction of different types of Th cell responses. In general, rapidly replicating intracellular microorganisms such as viruses and certain bacteria activate Th1 cells. The principal regulators of anti-helminth immunity are Th2 cells, and fungi and extracellular bacteria give Th17 responses (2-4).

While much is known about the regulation of Th1 and Th17 responses, the mechanisms that control Th2 activation are still not fully understood (5). Although helminths are strong inducers of Th2 responses, it proved difficult to pinpoint the specific mechanisms involved due to the complex nature of many helminth-derived antigen preparations. For example, *Schistosoma mansoni* soluble egg antigen (SEA), among the most widely used preparations for studying immune responses to helminth antigens, contains more than 600 different proteins (6). The identification of omega-1 as the major immunomodulatory component in SEA therefore provided an opportunity to further dissect the molecular mechanisms underlying Th2 skewing (7;8). We have previously shown that omega-1 is a glycosylated T2 RNase that conditions DCs for Th2 induction by suppressing protein synthesis (9). However, it remains unclear which mechanisms subsequently enable Th2 skewing.

Maturation of DCs is largely controlled at the posttranscriptional and posttranslational level (10;11). Therefore, as a representative indicator of cell function and phenotype, various groups have studied the proteome of pro-Th2 DCs. Using semi-quantitative gel-based techniques, three cytoplasmic proteins were found to be exclusive to the Th2-inducing proteome of human monocyte-derived DCs (12). In mouse bone marrow-derived DCs (BMDCs), four proteins were significantly affected by stimulation with helminth antigens (13). A third study on pro-Th2 BMDCs used iTRAQ labeling for relative quantitation of plasma membrane proteins, and showed that pro-Th2 BMDCs upregulated proteins related to cell metabolism and downregulated proteins associated with the cytoskeleton (14). Although these studies provide valuable directions for future research, the use of 2-DE and iTRAQ does not allow for high-throughput analysis and direct comparison of a large number of biological replicates. This is especially relevant when donor-to-donor variation is expected, for example when working with DCs from human donors, and may explain why only very few proteins were found in common between different gel-based studies on lipopolysaccharide (LPS)-matured human DCs (15-18).

As such, the introduction of a high-resolution label-free and gel-free method for quantitative analysis of DC proteomes would be highly beneficial. In this study, we analyzed DC maturation and polarization using liquid chromatography Fourier transform ion cyclotron resonance mass spectrometry (LC-FTICRMS) for accurate mass measurement and relative quantitation (19;20). This method allowed us to include a total of nine DC donors and four

different stimuli. We included an early (6h) and a late (32h) time point in addition to baseline (0h), to reflect maturation stages associated with migration and antigen presentation. Using SEA, a complex antigen preparation, and omega-1, a single molecule for Th2 polarization, we focus on the identification of proteins associated with the pro-Th2 DC proteome.

RESULTS

Functional characterization of human DCs

Immature DCs (iDCs) generated from nine donors were matured with LPS, in the presence or absence of IFN- γ as a Th1-inducing stimulus, and SEA or omega-1 as Th2-inducing conditions. To functionally characterize these DCs, a co-culture system of human LPS-matured DCs and allogeneic naïve CD4⁺ T cells was used. DCs expressed high levels of CD1a and no CD14, as expected (Fig. 1A), and strongly upregulated CD86 expression upon LPS stimulation (Fig. 1B). Additional stimulation with IFN- γ did not affect LPS-induced CD86 expression but strongly induced IL-12p70 production (Fig. 1C), while SEA and ω -1 decreased expression of both CD86 and IL-12p70, as described previously (9). Analysis of T cell cytokine production confirmed that omega-1 and SEA induced a Th2 response, characterized by a high frequency of IL-4-producing T cells (Fig. 1D), while stimulation of DCs with IFN- γ promoted a Th1 response (Fig. 1E).

Protein Identifications

To establish the effect of maturation and polarization on the DC proteome, iDCs and LPS-matured DCs stimulated with IFN- γ , SEA or omega-1, were collected from each of the nine

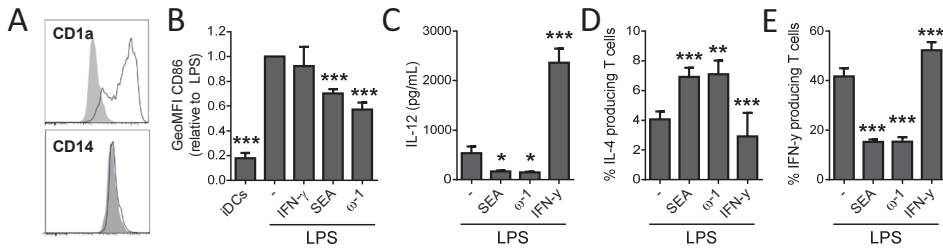


Figure 1. Functional characterization of pro-Th1 and pro-Th2 DCs. Monocyte-derived DCs were either left untreated or pulsed with LPS in the presence or absence of IFN- γ , SEA, or omega-1. After 48h, expression of surface markers was analyzed by flow cytometry. (A) Representative histograms for expression of CD1a and CD14 are shown. Filled histograms represent unstained controls. (B) Expression levels of CD86, based on the geometric mean fluorescence, are shown relative to LPS, which was set to 1. (C) Following stimulation, moDCs were co-cultured with a CD40L-expressing cell line. Supernatants were collected after 24 h and IL-12p70 concentrations were determined by ELISA. (D) 48h-matured DCs were cultured with allogeneic naïve CD4⁺ T cells for 11 days. Intracellular cytokine production as analyzed by flow cytometry after 6h of stimulation with phorbol myristate acetate and ionomycin. The percentages of T cells uniquely positive for either IL-4 or (E) IFN- γ are shown. Bars represent mean values + s.e.m.; *P<0.05; **P<0.01; ***<0.001 for significant differences with the LPS control based on a paired Student's t-test. ω -1, omega-1.

donors at three different time points: before stimulation (0h), six hours after stimulation (6h) and 32 hours after stimulation (32h). Proteins were digested after which peptides were identified using LC-MS/MS in an ion trap, resulting in the identification of 1159 unique peptides from 439 unique proteins with a false-discovery rate (FDR) of 1.0%. These were used for matching with and querying the LC-FTICRMS data for label-free quantitation (19;20). In total, 208 proteins were quantified with multiple peptides in each biological replicate and at each time point.

Effects of maturation on the human DC proteome

To identify proteins that were differentially expressed due to stimulation, the stimulus-induced fold change in abundance was determined for each protein, by calculating the mean fold change of the nine donors. Corresponding p-values were obtained from a paired Student's t-test after log-transformation. Proteins were considered differentially expressed when $P < 0.05$ and the stimulus-induced fold change was more than 1.5-fold decreased or increased (i.e. fold change < 0.67 or > 1.5). LPS-induced maturation displayed a pronounced effect on the DC proteome. Compared to iDCs, LPS promoted differential expression of ten proteins after 6h (**Table 1**). Analysis of protein classification according to Gene Ontology terms indicated that the eight upregulated proteins are mostly involved in transport or cell communication. The two downregulated proteins were both cytoskeletal proteins. After 32 hours, LPS promoted differential expression of 22 proteins (**Table 1**). The majority of proteins was upregulated and related to different metabolic, cellular and immune system processes or transport. The protein most strongly upregulated by LPS stimulation was TNF receptor-associated factor 1 (TRAF1), an adapter molecule that regulates activation of NF- κ B and JNK. In addition, actin cross-linking proteins Fascin and Myristoylated alanine-rich C-kinase substrate (MARCS) were profoundly induced, as well as the MHC class I molecule HLA-B, involved in antigen presentation. Among the four downregulated proteins, Macrophage mannose receptor 1 is involved in antigen uptake, cathepsins play a role in antigen processing, and Ganglioside GM2 activator (GM2A) mediates presentation of lipids (21-23).

Effects of polarizing stimuli on the human DC proteome

LPS-matured DCs additionally stimulated with IFN- γ , a Th1-inducing stimulus, differentially expressed ten proteins after 6h of stimulation compared to stimulation with LPS alone (**Table 2**). Five proteins were downregulated, of which three were members of the cytoskeleton. The proteins most strongly upregulated were Heat Shock Protein HSP 90-alpha (HSP90AA1), which mediates inflammatory responses, and cytoplasmic tryptophan--tRNA ligase (WARS), also known as Interferon-induced protein 53. After 32h, four proteins were downregulated (**Table 2**), including a tyrosine-protein kinase involved in regulation of immune responses (FGR), and Peptidyl-prolyl cis-trans isomerase A (PPIA), also known as Cyclophilin A, which plays an important role in protein folding, trafficking, and immune cell activation (24).

Following 6h of stimulation with Th2-inducing SEA, five proteins were upregulated compared to stimulation with LPS alone (**Table 2**). Interestingly, in contrast to 32h of

Table 1. Differentially expressed proteins in LPS-DCs versus iDCs.

Accession	Protein	6 hours		32 hours	
		Fold	P-val	Fold	P-val
LPS-induced, 6 hours					
P45880	Voltage-dependent anion-selective channel protein 2	2.74	0.04	1.81	0.57
P30040	Endoplasmic reticulum resident protein 29	2.59	0.00	1.67	0.64
Q13077	TNF receptor-associated factor 1	2.25	0.01	14.95	0.00
P61604	10 kDa heat shock protein. mitochondrial	2.23	0.03	1.68	0.76
P05362	Intercellular adhesion molecule 1	1.89	0.00	3.60	0.01
P30464*	HLA class I histocompatibility antigen, B-15 alpha chain	1.83	0.02	7.89	0.00
P29966	Myristoylated alanine-rich C-kinase substrate	1.77	0.02	10.76	0.00
Q9BQE5	Apolipoprotein L2	1.64	0.05	2.95	0.00
Q71U36	Tubulin alpha-1A chain	0.63	0.03	1.58	0.82
P06396	Gelsolin	0.62	0.00	1.96	0.48
LPS-induced, 32 hours					
Q13077	TNF receptor-associated factor 1	2.25	0.01	14.95	0.00
P29966	Myristoylated alanine-rich C-kinase substrate	1.77	0.02	10.76	0.00
P30464*	HLA class I histocompatibility antigen, B-15 alpha chain	1.83	0.02	7.89	0.00
Q16658	Fascin	1.26	0.61	5.48	0.00
P04179	Superoxide dismutase [Mn], mitochondrial	1.20	0.68	4.66	0.00
P23381	Tryptophan--tRNA ligase, cytoplasmic	0.98	0.55	3.77	0.00
Q9UL46	Proteasome activator complex subunit 2	0.92	0.25	3.68	0.00
P05362	Intercellular adhesion molecule 1	1.89	0.00	3.60	0.01
P80723	Brain acid soluble protein 1	1.21	0.54	3.46	0.00
P27348	14-3-3 protein theta	0.96	0.40	3.00	0.00
Q9BQE5	Apolipoprotein L2	1.64	0.05	2.95	0.00
P19971	Thymidine phosphorylase	1.00	0.76	2.79	0.04
Q14974	Importin subunit beta-1	0.98	0.38	2.39	0.02
P02786	Transferrin receptor protein 1	1.14	0.77	2.20	0.00
P08107	Heat shock 70 kDa protein 1A/1B	1.19	0.41	1.93	0.02
P20700	Lamin-B1	1.34	0.40	1.85	0.04
P34931	Heat shock 70 kDa protein 1-like	1.16	0.52	1.55	0.04
Q9BZQ8	Protein Niban	1.14	0.32	1.54	0.01
P07339	Cathepsin D	1.68	0.76	0.63	0.03
P22897	Macrophage mannose receptor 1	0.98	0.36	0.63	0.02
P17900	Ganglioside GM2 activator	1.40	0.19	0.58	0.02
Q9UBR2	Cathepsin Z	1.30	0.01	0.56	0.00

*HLA serotypes originate from the same gene and share common peptides. The serotype attributed to the identification may therefore not be accurate.

stimulation with IFN- γ , SEA induced strong upregulation of PPIA. SEA also increased expression of Eukaryotic initiation factor 4A-I, involved in translation initiation, Endoplasmic reticulum chaperone proteins (HSP90B1), HSP90AA1, and Fascin. After 32h, SEA promoted differential expression of six proteins (**Table 2**). Among those, four proteins were downregulated, including WARS which was induced by IFN- γ , and HLA-B and CD44 which are involved in antigen presentation and T cell activation (25). The protein most strongly upregulated by 32h of SEA stimulation was 60S acidic ribosomal protein P2 (RPLP2), which plays an important role in the elongation step of protein synthesis.

Omega-1 induced upregulation of five proteins after 6h, and seven proteins after 32 hours (**Table 2**), most of which were ribosomal proteins, chaperones or enzymes. Among those, several proteins were highly upregulated, including mitochondrial Thioredoxin-dependent peroxidoreductase (6h), a protein involved in redox regulation of the cell, RPLP2 (32h), and the chaperone Calnexin (32h). After 32h of omega-1 stimulation, seven proteins were downregulated. In particular, omega-1 strongly decreased expression of HLA-B, HLA-C and CD44, as well as MARCS.

Analysis of proteins exclusive to the Th2-inducing proteome

The identification of proteins uniquely associated with the Th2-inducing DC proteome could provide valuable leads for understanding initiation of Th2 responses by DCs. We therefore analyzed proteins affected by stimulation with SEA as well as omega-1, by looking at protein expression dynamics and individual donor responses. As can be appreciated from **Table 2**, omega-1 and SEA did not share differentially expressed proteins after 6h of stimulation. After 32h, however, they shared five differentially expressed proteins. Among those five, Transferrin receptor protein 1 is seemingly downregulated by omega-1 and SEA, but also by IFN- γ ($P=0.051$), suggesting that this may not be a Th2-exclusive protein.

Analysis of protein expression dynamics of the four remaining Th2-associated proteins showed that RPLP2 was strongly upregulated by 32h of stimulation with SEA and omega-1 in at least eight out of nine donors (**Fig. 2A**). Synaptic vesicle membrane protein VAT-1 homolog (VAT1) was upregulated by SEA and omega-1 in at least seven donors after 32h of stimulation (**Fig. 2B**), but was also mildly increased by IFN- γ stimulation in the majority of donors. CD44 was significantly downregulated by SEA in seven donors, and by omega-1 nine donors (**Fig. 2C**). Lastly, LPS-induced upregulation of HLA-B was inhibited by SEA and omega-1 in eight donors (**Fig. 2D**). These findings suggest that in particular upregulation of RPLP2, and downregulation of CD44 and HLA-B, are characteristics of pro-Th2 DCs.

Further exploration of the data by association analysis

To explore whether there are specific networks and functional classifications significantly affected by Th2-inducing stimuli, we analyzed our data using GeneMANIA software. For hypothesis-generating purposes, less stringent thresholds were applied. First, all proteins significantly affected by stimulation (i.e. fold change $P<0.05$); and second, those proteins with $P<0.1$ and a fold change of <0.67 or >1.5 , were included. For a complete list of all accessions (with

Table 2. Differentially expressed proteins in pro-Th1 and pro-Th2 DCs versus LPS-DCs.

Accession	Protein	IFN- γ		SEA		Omega-1	
		Fold	P-val	Fold	P-val	Fold	P-val
IFN-γ-induced, 6 hours							
P07900	Heat shock protein HSP 90-alpha	2.42	0.02	2.98	0.02	2.42	0.14
P23381	Tryptophan-tRNA ligase, cytoplasmic	2.13	0.04	1.20	0.43	1.07	0.61
P13639	Elongation factor 2	1.82	0.01	1.64	0.12	1.34	0.33
P30508*	HLA class I histocompatibility antigen, Cw-12 alpha chain	1.78	0.03	1.61	0.41	1.29	0.97
P09467	Fructose-1,6-bisphosphatase 1	1.69	0.02	1.54	0.07	1.53	0.25
P26038	Moesin	0.66	0.04	0.86	0.16	1.12	0.58
P67936	Tropomyosin alpha-4 chain	0.66	0.02	0.90	0.18	1.08	0.36
P02545	Prelamin-A/C	0.64	0.00	0.95	0.21	1.09	0.73
P16070	CD44 antigen	0.63	0.01	1.01	0.40	0.89	0.21
P10599	Thioredoxin	0.52	0.02	2.31	0.33	1.10	0.07
IFN-γ-induced, 32 hours							
P40926	Malate dehydrogenase, mitochondrial	0.59	0.00	0.99	0.29	0.97	0.38
P62937	Peptidyl-prolyl cis-trans isomerase A	0.58	0.02	2.38	0.44	3.71	0.59
P04908	Histone H2A type 1-B/E	0.55	0.00	1.07	0.15	1.31	0.20
P09769	Tyrosine-protein kinase Fgr	0.65	0.03	0.68	0.01	0.95	0.40
SEA-induced, 6 hours							
P62937	Peptidyl-prolyl cis-trans isomerase A	4.02	0.45	11.27	0.01	1.62	0.54
Q9BZQ8**	Protein Niban	1.10	0.85	9.78	0.00	1.03	0.89
P14625	Endoplasmic	1.47	0.58	4.14	0.04	2.31	0.88
P60842	Eukaryotic initiation factor 4A-I	1.83	0.32	3.21	0.04	1.17	0.47
P07900	Heat shock protein HSP 90-alpha	2.42	0.02	2.98	0.02	2.42	0.14
Q16658	Fascin	1.15	0.92	1.74	0.04	1.40	0.32
SEA-induced, 32 hours							
P05387	60S acidic ribosomal protein P2	1.68	0.17	2.27	0.01	4.63	0.01
Q9BZQ8**	Protein Niban	1.19	0.20	2.20	0.01	1.20	0.73
Q99536	Synaptic vesicle membrane protein VAT-1 homolog	1.29	0.20	1.59	0.03	1.53	0.02
P16070	CD44 antigen	1.47	0.81	0.63	0.02	0.47	0.00
P23381	Tryptophan-tRNA ligase, cytoplasmic	1.45	0.34	0.60	0.00	0.92	0.19
P02786	Transferrin receptor protein 1	0.75	0.05	0.56	0.00	0.49	0.00
P30464*	HLA class I histocompatibility antigen, B-15 alpha chain	1.27	0.79	0.45	0.00	0.40	0.00
Omega-1-induced, 6 hours							
P30048	Thioredoxin-dependent peroxide reductase, mitochondrial	7.06	0.14	2.56	0.64	4.03	0.04
P05388	60S acidic ribosomal protein P0	1.47	0.06	1.31	0.64	1.86	0.02
P30041	Peroxiredoxin-6	1.33	0.63	1.44	0.33	1.77	0.02
Q01813	6-phosphofructokinase type C	1.39	0.02	1.13	0.43	1.65	0.01
P61158	Actin-related protein 3	1.47	0.50	2.11	0.67	1.61	0.04

Table 2. Differentially expressed proteins in pro-Th1 and pro-Th2 DCs versus LPS-DCs. (Continued)

Accession	Protein	IFN- γ		SEA		Omega-1	
		Fold	P-val	Fold	P-val	Fold	P-val
Omega-1-induced, 32 hours							
P05387	60S acidic ribosomal protein P2	1.68	0.17	2.27	0.01	4.63	0.01
P27824	Calnexin	1.32	0.93	1.76	0.51	2.64	0.05
P55084	Trifunctional enzyme subunit beta, mitochondrial	1.72	0.14	1.48	0.13	2.52	0.05
P63104	14-3-3 protein zeta/delta	1.60	0.55	1.51	0.18	2.33	0.04
P50502	Hsc70-interacting protein	1.29	0.48	1.45	0.06	2.05	0.02
P30041	Peroxiredoxin-6	0.94	0.32	1.46	0.32	2.02	0.02
Q99536	Synaptic vesicle membrane protein VAT-1 homolog	1.29	0.20	1.59	0.03	1.53	0.02
P17900	Ganglioside GM2 activator	1.04	0.20	1.26	0.68	0.65	0.03
P30508	HLA class I histocompatibility antigen, Cw-12 alpha chain	1.02	0.29	1.01	0.05	0.63	0.01
P29966	Myristoylated alanine-rich C-kinase substrate	1.19	0.78	0.73	0.06	0.58	0.01
P04179	Superoxide dismutase [Mn], mitochondrial	1.30	0.85	1.24	0.37	0.52	0.01
P02786	Transferrin receptor protein 1	0.75	0.05	0.56	0.00	0.49	0.00
P16070	CD44 antigen	1.47	0.81	0.63	0.02	0.47	0.00
P30504*	HLA class I histocompatibility antigen, Cw-4 alpha chain	0.72	0.10	1.88	0.21	0.47	0.02
P30464*	HLA class I histocompatibility antigen, B-15 alpha chain	1.27	0.79	0.45	0.00	0.40	0.00

*HLA serotypes originate from the same gene and share common peptides. The serotype attributed to the identification may therefore not be accurate. **The signal attributed to the VLTSEDEYNLLSDR peptide in NIBAN is likely coming from the $^{13}\text{C}_6$ -peak of the YCLQLYDETYER peptide from the SEA-derived protein Interleukin-4-inducing protein (IPSE). Protein Niban was removed from further analysis.

corresponding gene names) included for GeneMANIA analysis, see **Table S1**. In addition to the genes of the differentially expressed proteins, we allowed for display of ten associated genes.

After 6h of stimulation, SEA promoted differential expression of proteins in a network enriched for mitochondrial matrix proteins (FDR = 0.055) and MHC class II protein complex binding (FDR = 0.002) (**Fig. S1**). The two SEA-responsive proteins involved in MHC class II protein complex binding were the MHC class II molecule HLA-DRA and Heat Shock Protein HSP90AA1, which were increased by SEA treatment (**Table S1**). By contrast, after 32h of treatment, SEA decreased expression of HLA-DRB1, another MHC class II molecule, in line with previous studies on long-term SEA treatment of DCs (26). GeneMANIA analysis indicated that 32h of SEA treatment affected proteins in a network enriched for antigen processing and presentation (FDR = 0.001) (**Fig. S2**). Examination of the three SEA-responsive proteins within this functional classification indicated that all three proteins (HLA-B, HLA-DRB1 and CD74) were downregulated.

Stimulation with omega-1 induced differential expression of proteins in a network enriched for phagocytosis (FDR = 0.000, proteins were both up- and downregulated) and glycolysis (FDR = 0.039) (**Fig. S3**). Related to glycolysis, omega-1 increased expression of 6-phosphofructokinase

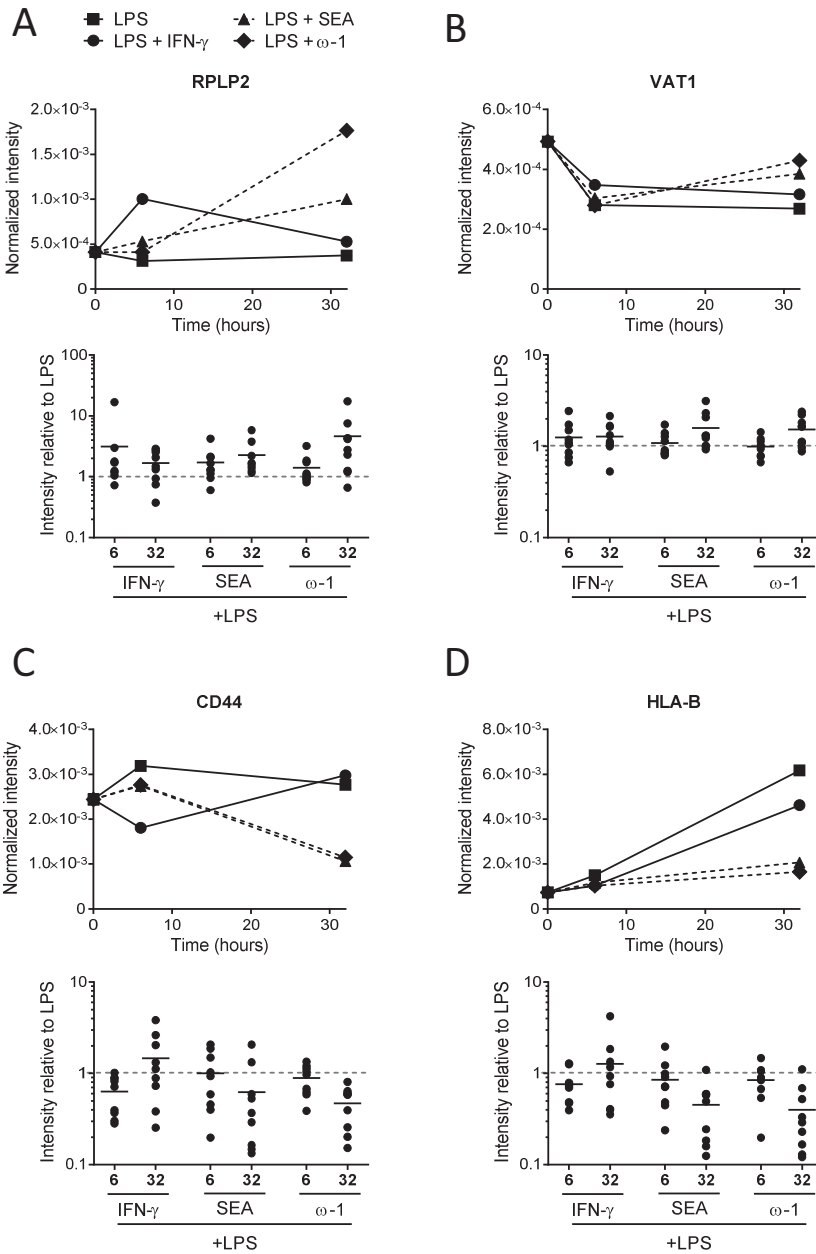


Figure 2. Protein expression dynamics of Th2-associated differentially expressed proteins. Monocyte-derived DCs were stimulated as described in the legend of figure 1. Protein expression was analyzed by LC-FTICRMS. Differentially expressed proteins shared between 32h of stimulation of with omega-1 and SEA are shown. The top panel of each figure shows the protein expression dynamics, the bottom panel shows the normalized intensity relative to LPS, which was set to 1 at 6h and at 32h (dashed line). (A) 60S acidic ribosomal protein P2. (B) Synaptic vesicle membrane protein VAT-1 homolog. (C) CD44 antigen. (D) HLA-B.

type C (PFKP), which catalyzes the third step of glycolysis, while expression of Glyceraldehyde 3-phosphate dehydrogenase (GAPDH) that catalyzes the sixth step was decreased (Table S1). Like SEA, 32h of omega-1 treatment affected proteins in a network enriched for antigen processing and presentation (FDR = 0.000; Fig. 3). Out of the four omega-1-responsive proteins within this functional classification, three were downregulated (HLA-B, HLA-C and Cathepsin D). In addition, 32h of omega-1 stimulation affected proteins in a network significantly enriched for translational elongation (FDR = 0.001). Within this functional classification, RPLP2 and Elongation factor 1-delta (EEF1D) were upregulated, while Ubiquitin-60S ribosomal protein L40 (UBA52) was downregulated.

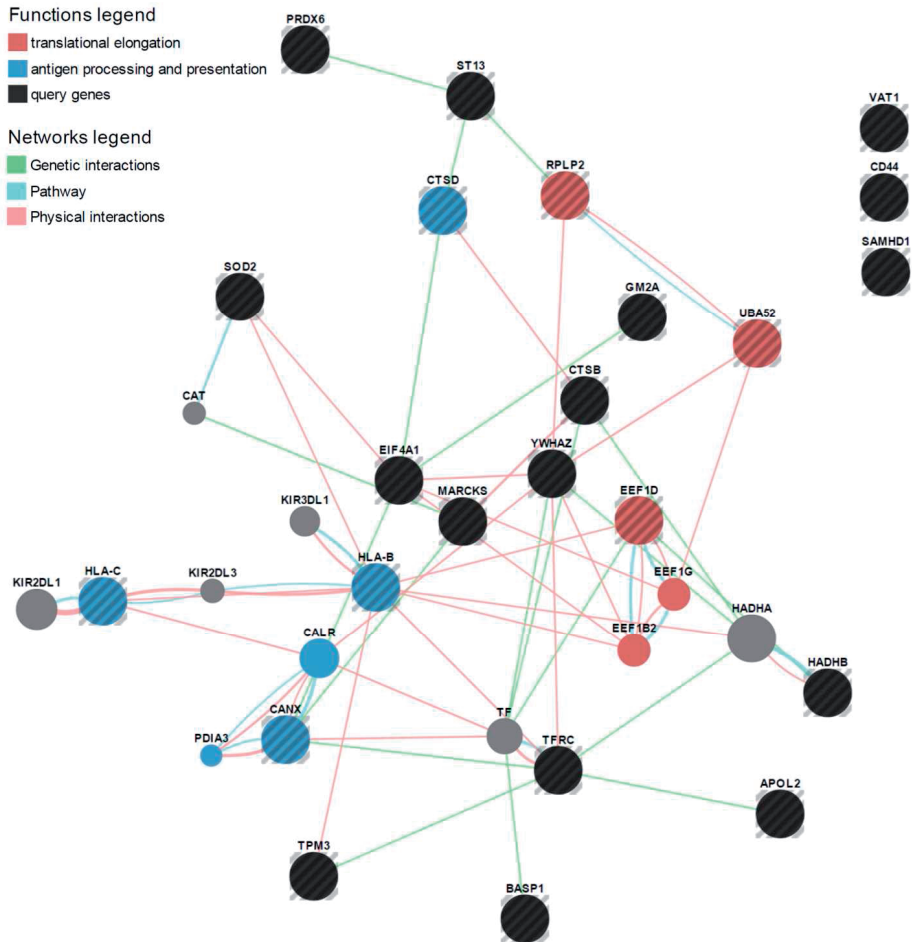


Figure 3. Network analysis of 32h omega-1-response proteins. Monocyte-derived DCs were stimulated as described for the legend of figure 1, and protein expression was analyzed by LC-FTICRMS. For GeneMANIA analysis, all 32h omega-1-responsive proteins with $P < 0.05$, and those proteins with $P < 0.1$ and a fold change of < 0.67 or > 1.5 , were included. Black and/or striped nodes represent genes of which the proteins were differentially expressed (query genes); grey nodes represent associated genes added by GeneMANIA. Colored nodes highlight significantly enriched Gene Ontologies.

DISCUSSION

Over the past decade, studies on the proteome of matured or polarized DCs relied on label- and gel-based techniques. Such approaches do not allow for high-throughput analysis of many different conditions or biological replicates, which might explain why only few proteins were found in common between different reports (15-18;27). Here, we used ion traps for tandem mass spectrometry and LC-FTICRMS for label- and gel-free quantitation (19), which had previously been used for the analysis of the plasma proteome (20). This approach allowed us to analyze the proteomes of LPS-matured and pro-Th1 versus pro-Th2 DCs from nine different human donors.

As expected, LPS-induced maturation displayed the most pronounced effect on the DC proteome. After 6h of maturation, proteins involved in intracellular transport and cell communication were upregulated, and cytoskeletal proteins were either up- or downregulated. These processes may reflect that the DCs are preparing for migration, which requires profound alterations in cell morphology and motility (28). The strongest effect on the DC proteome was observed after 32h of LPS-induced maturation, when many proteins were upregulated at least 3-fold. Among the proteins most strongly induced was mitochondrial Superoxide dismutase (SODM). Indeed, DCs are known to upregulate reactive oxygen species in response to stimulation with LPS (29;30), and subsequent upregulation of superoxide dismutases has also been reported (31). In addition, stimulation with LPS induced Fascin, an actin cross-linking that plays a critical role in migration of mature DCs into lymph nodes. Specifically, actin bundling by Fascin was shown to promote membrane protrusions and mediates disassembly of podosomes, which are specialized structures for cell-matrix adhesion (32). A second actin cross-linking protein, MARCS, was also profoundly induced, in line with a previous report (33). The other two proteins most strongly affected by LPS stimulation were MHC class I molecule HLA-B, involved in antigen presentation, and TRAF1, an adapter molecule that regulates activation of NF- κ B and JNK. Indeed, NF- κ B activation was previously shown to be required for DC maturation (34). The proteins downregulated after 32h of LPS stimulation were involved in antigen uptake, processing and presentation of lipids. Together, these findings reflect that after 32h of stimulation, LPS-DCs have become specialized for entering lymph nodes and presenting antigen to naïve T cells, which identifies the FTICR-ion trap cluster as an appropriate method to for high-throughput quantitative analysis of dendritic cell lysates.

Importantly, we find many differentially expressed proteins in common with a proteomics study by Ferreira *et al.* (35), which further validates our method. In our and their study, maturation reduces expression of cathepsins and GM2A, and increases expression of Apolipoprotein L2, Fascin, Proteasome activator complex subunit 2, and SODM. Furthermore, in line with another report (11), we observe an increase in Heat shock protein (Hsp) expression. Unique to our study, the FTICR method allowed us to perform statistical analysis on protein expression data from nine biological replicates. In addition, multiple time points were included, which provides information about protein expression dynamics. Our study therefore strengthens and expands previous reports on maturation of human DCs.

Using the cytokine IFN- γ , we polarized LPS-DCs for Th1 skewing, and observed that pro-Th1 DCs differentially expressed cytoskeletal proteins and proteins involved in inflammatory processes after 6h of stimulation, compared to LPS-DCs. Among those proteins, HSP90AA1 and WARS were most strongly upregulated. Indeed, under inflammatory conditions, heat shock proteins (HSPs) can act as chaperones to facilitate antigen presentation and enhance the immune response (36). In line with our results, Ferreira *et al.* also described upregulation of WARS in DCs following LPS + IFN- γ treatment (35). It has been demonstrated that transcription of WARS is responsive to IFN- γ treatment in non-lymphoid cell lines (37), and tryptophan catabolism was shown to promote DC-mediated T cell tolerance (38), but role of WARS in DC-mediated T cell activation remains to be determined. After 32h of IFN- γ stimulation, the effect on the DC proteome was less pronounced, as only 4 proteins were downregulated, including FGR and PPIA involved in immune regulation and activation. These findings may suggest that IFN- γ treatment induces strong effects early after treatment, reminiscent of accelerated maturation.

Interestingly, in contrast to 32h of treatment with IFN- γ , short-term (6h) stimulation of DCs with Th2-inducing SEA induced strong expression of PPIA, also known as Cyclophilin A, which is the primary binding protein of Cyclosporin A, an immunosuppressive drug that antagonizes calcium-dependent T cell activation (39). How the expression of Cyclophilin A affects the polarizing capacity of DCs remains to be investigated.

Since only few proteins were differentially expressed by 6h SEA or omega-1 treatment, we also performed association analysis using GeneMANIA, applying less stringent thresholds for hypothesis generation. SEA induced differential expression of proteins in a network enriched for mitochondrial matrix proteins, and omega-1 affected proteins in a network enriched for glycolysis. Although the differentially expressed proteins within those functional classifications were both up- and down-regulated, these findings may suggest that 6h after stimulation, SEA and omega-1 may affect cellular metabolism. In line with these findings, recent studies have indicated that modulation of metabolic pathways within dendritic cells can regulate DC function and the outcome of the immune response (40;41). Whether omega-1 and SEA indeed modulate cellular metabolism, and whether this contributes to Th2 polarization, requires further studies.

The most profound effect of Th2-inducing stimuli was observed after 32h of stimulation, when SEA and omega-1 both strongly increased expression of ribosomal protein RPLP2. Since the presence of ribosomal P proteins may enhance ribosomal performance (42), we speculate that the increase in RPLP2 may represent a feedback mechanism secondary to SEA- and omega-1-induced ribosome degradation. In addition, SEA and omega-1 decreased expression of CD44 and suppressed LPS-induced upregulation of HLA-B. Interestingly, CD44 expression by DCs was shown to promote CD4 T cell proliferation (25). Together, these findings may suggest that Th2-inducing conditions interfere with efficient antigen presentation to T cells. Indeed, GeneMANIA analysis indicated that SEA and omega-1 both decreased expression of proteins in a protein network enriched for antigen processing and presentation. It has been suggested that T cells are polarized towards Th2 if the interaction between DCs and T cells is weak (43-45).

In addition, it was demonstrated that omega-1 reduces the capacity of bone marrow-derived DCs to form T cell-DC conjugates (8). Taken together, these studies suggest that reduced interaction between T cells and DCs at the level of the immunological synapse may promote Th2 polarization by helminth antigens.

In conclusion, our work has identified the FTICR-ion trap cluster as an appropriate method for quantitative high-throughput analysis of cell lysates. Our data on DC polarization suggest that pro-Th1 DCs undergo accelerated maturation compared to LPS-DCs, and indicate that pro-Th2 DCs may affect cellular metabolism and decrease expression of proteins involved in antigen processing and presentation. Future research should therefore focus on studying the contribution of metabolic pathways, TCR signaling, and the possible relation between the two, to further dissect the mechanisms of helminth-induced T helper 2 polarization via dendritic cells. Such investigations will not only improve our fundamental understanding of DC biology, but may also provide leads for the development of DC-based immunotherapies.

METHODS

Human DC culture, stimulation, and analysis

Monocytes isolated from venous blood of 9 healthy volunteers were differentiated as described previously (46). On day 6 the immature DCs (iDCs) were stimulated with SEA (50 mg/mL), omega-1 (250 ng/mL) or IFN- γ (1000 U/mL) in the presence of 100ng/mL ultrapure LPS (*E. coli* 0111 B4 strain, InvivoGen) and human rGM-CSF (20 ng/mL; Life Technologies). At the indicated time points, samples were collected for protein extraction and digestion as described below. Alternatively, after 48 hours of stimulation, expression of surface molecules was determined by flow cytometry (FACSCanto, BD Biosciences) using the following antibodies: CD14 PerCP, CD86 FITC (both BD Biosciences), and CD1a PE (Beckman-Coulter). In addition, 1×10^4 48h-matured DCs were co-cultured with 1×10^4 CD40L-expressing J558 cells. Supernatants were collected after 24h and IL-12p70 concentrations were determined by ELISA using mouse anti-human IL-12 (clone 20C2) as a capture antibody and biotinylated mouse anti-human IL-12 (clone C8.6) as a detection antibody (BD Biosciences). Volunteers signed informed consent forms and the samples were handled according to the guidelines described by the Dutch Federation of Medical Scientific Societies in the Code of Conduct for the responsible use of human tissue for medical research (47).

Human T cell culture and analysis of T cell polarization

For analysis of T cell polarization, 5×10^3 matured DCs were cultured with 2×10^4 allogeneic naïve CD4⁺ T cells that were isolated from buffy coat (Sanquin) peripheral blood mononuclear cells using a CD4⁺/45RO⁻ Naive T Cell Enrichment Column (R&D Systems). Co-cultures were performed in the presence of staphylococcal enterotoxin B (10 pg/mL). On days 6 and 8, rhIL-2 (10 U/mL, R&D Systems) was added and the T cells were expanded until day 11. Intracellular cytokine production was analyzed after restimulation with 100 ng/mL phorbol myristate acetate plus 1 μ g/mL ionomycin for 6h; 10 μ g/mL brefeldin A was added during the last 4h and the cells were fixed with 3.7% paraformaldehyde (all Sigma-Aldrich). The cells were permeabilized with

0.5% saponin (Sigma-Aldrich) and stained with PE- and FITC-labelled antibodies against IL-4 and IFN- γ , respectively (BD Biosciences).

Protein extraction and in-solution digestion

Cells were harvested with PBS at the indicated time points and centrifuged at 522 *g* for 8 minutes at 4°C, after which they were transferred with 1 mL PBS to a microcentrifuge tube and centrifuged for 5 minutes at 5,000 *g*, 4°C. The supernatant was removed and pellets were snap-frozen in liquid nitrogen and stored at -80°C. Samples were thawed in 30 μ L lysis buffer consisting of 1% SDS, 125 U/mL benzonase nuclease (Sigma), 2 mM MgCl₂, and protease inhibitors (cOmplete ULTRA tablets, mini, EDTA-free, Roche) in 50 mM ammonium bicarbonate (ABC). Samples were placed at 95°C for 5 minutes and following centrifugation at 16 000 *g* for 30 min, the supernatant was collected. A BCA assay (Pierce Biotechnology) was conducted to determine the protein concentration. An equivalent of 10 μ g protein was dissolved in 25 μ L ABC and reduced using 10 mM DTT (Sigma) for 5 minutes at 95°C, followed by 1 hour alkylation using 40 mM iodoacetamide (Sigma) at room temperature. Using 3 kDa spin filters, the remainder of the lysis buffer was exchanged for ABC according to manufacturer's protocol (Millipore), and samples were digested for 17 hours with sequencing-grade trypsin (Promega) at an enzyme to protein ratio of 1:50. The digestion was quenched with 2% trifluoroacetic acid to lower the pH. Peptide samples were stored at -35°C until analysis.

Liquid chromatography - mass spectrometry

All samples were analyzed using a splitless NanoLC-Ultra 2D plus (Eksigent) system for parallel liquid chromatography (LC) with additional trap columns for desalting. The LC systems were configured with 300 μ m-i.d. 5-mm PepMap C18 trap columns (Thermo Fisher Scientific) and 15-cm 300 μ m-i.d. ChromXP C18 columns (Eksigent). Peptides were separated by a 90-minute linear gradient from 4 to 33% acetonitrile in 0.05% formic acid with the 4 μ L/min flow rate. The LC systems were coupled on-line to amaZon speed ETD high-capacity 3D ion traps and a 12 T solariX FTICR system (all from Bruker Daltonics) in an FTICR-ion trap cluster (19). For peptide identification in the ion traps, we generated three sample pools. Pool 1 contained a fraction of each sample that was stimulated for 32h with LPS or LPS + IFN- γ . Pool 2 contained a fraction of each 0h and 6h iDC sample. Pool 3 contained a fraction of each uneven sample (all samples received a random number). These sample pools were run in triplicate on the ion traps. Up to ten abundant multiply charged precursors in *m/z* 300-1300 were selected for MS/MS in each MS scan in a data-dependent manner. After having been selected twice, each precursor was excluded for one minute. The LC systems were controlled using the HyStar 3.4 (Bruker) with a plug-in from Eksigent, the amaZon ion trap by trapControl 7.0, and the solariX FTICR system by solariXcontrol 1.3 (both Bruker).

Data analysis

The raw datasets from ion trap LC-MS/MS and LC-FTICRMS were converted to mzXML (48). The mzXML files were analysed using a scientific workflow called "Label-free proteomics using

LC-MSⁿ (<http://www.myexperiment.org/workflows/4552.html>). The workflow was designed using the Taverna workflow management system (49).

The LC-MS/MS data was used for identification. The TANDEM application (50) from the X!Tandem provided in Trans Proteomics Pipeline V4.7.7 was run to match the spectra with tryptic peptide sequences derived from UniProt *Homo sapiens* reference proteome database retrieved on 25.07.2014, for each pooled sample. The k-score plug-in was selected for the search with a minimum ion count of 1, and 2 maximum missed cleavage sites. The allowed parent monoisotopic mass error was ± 5.0 Da, and the allowed fragment monoisotopic mass error was 0.4 Da. After peptide assignments to MS/MS spectra, the results were converted to pepXML format, an XML-based format that is used in peptide-level analysis (51), using the Tandem2XML application.

To use the high-resolution MS profiles for more precise quantification, each pepXML file was aligned with one master LC-FTICRMS data file. The alignment was done with pepAlign (52), which uses a genetic algorithm to align the two chromatographic time scales with a partial linear function. The output from pepAlign was the breakpoints of this function. The alignment was based on the X! Tandem expect scores and allowed a mass measurement error of ± 50 ppm. The retention times in each pepXML file were changed according to the chromatographic alignment function by the pepWarp program. The accuracy of the peptide assignments to tandem mass spectra was assessed by PeptideProphet using the xinteract application provided in Trans Proteomics Pipeline V4.6.3 (53). This application also combined the input datasets, so that all identifications with assigned probabilities were contained in a single output file. This validated pepXML was then aligned with each individual LC-FTICRMS dataset. For quantitation of identified peptides, we used only peptides with PeptideProphet probabilities higher than 0.9369, giving a peptide-spectrum match false discovery rate of 1.0%. Modified peptides were not included.

The monoisotopic mass was calculated for each peptide of interest and the maximum intensity corresponding to this mass was extracted from a window ± 60 seconds relative to the aligned retention time and ± 25 ppm relative to the calculated mass. As the final output of the workflow, all peptide quantifications were combined into a single table where each row represents a peptide sequence and each column contains the intensity of that peptide in each sample. Missing values were imputed from a normal distribution representing the background signal removed during acquisition. A final matrix was created with proteins identified by more than two peptides, where the abundance of each protein was calculated as the median intensity of its peptides and normalized to the total signal intensity of all proteins in the entire LC-MS dataset. Fold changes in protein abundance between conditions were calculated in R based on the mean fold change of the nine different donors, and corresponding p-values were obtained from paired Student's t-testing of log-transformed protein intensities for each treatment and time point. Analysis of Gene Ontology terms was performed using Protein Annotation THrough Evolutionary Relationship (PANTHER) (54;55), and association analysis was performed using GeneMANIA (56). Associations were analyzed based on genetic interactions, pathways, and physical interactions. In addition to the differentially expressed proteins, we allowed for display of 10 related proteins and 10 related attributes, and Gene Ontology network weighting was based on biological processes.

ACKNOWLEDGEMENTS

This project was supported by the EU (HEALTH-F3-2009-241642). The authors thank Susan Coort (Maastricht University) for assistance with data analysis.

REFERENCES

- Steinman RM, et al. Identification of a novel cell type in peripheral lymphoid organs of mice. I. Morphology, quantitation, tissue distribution. *J Exp Med* 1973 May 1;137(5):1142-62.
- Kapsenberg ML. Dendritic-cell control of pathogen-driven T-cell polarization. *Nat Rev Immunol* 2003 Dec;3(12):984-93.
- Zelante T, et al. IL-17/Th17 in anti-fungal immunity: what's new? *Eur J Immunol* 2009 Mar;39(3):645-8.
- Tato CM, et al. Immunology: what does it mean to be just 17? *Nature* 2006 May 11;441(7090):166-8.
- Hussaarts L, et al. Priming dendritic cells for th2 polarization: lessons learned from helminths and implications for metabolic disorders. *Front Immunol* 2014;5:499.
- Mathieson W, et al. A comparative proteomic study of the undeveloped and developed *Schistosoma mansoni* egg and its contents: the miracidium, hatch fluid and secretions. *Int J Parasitol* 2010 Apr;40(5):617-28.
- Everts B, et al. Omega-1, a glycoprotein secreted by *Schistosoma mansoni* eggs, drives Th2 responses. *J Exp Med* 2009 Aug 3;206(8):1673-80.
- Steinfeldt S, et al. The major component in schistosome eggs responsible for conditioning dendritic cells for Th2 polarization is a T2 ribonuclease (omega-1). *J Exp Med* 2009 Aug 3;206(8):1681-90.
- Everts B, et al. Schistosome-derived omega-1 drives Th2 polarization by suppressing protein synthesis following internalization by the mannose receptor. *J Exp Med* 2012 Sep 24;209(10):1753-67, S1.
- Le NF, et al. Profiling changes in gene expression during differentiation and maturation of monocyte-derived dendritic cells using both oligonucleotide microarrays and proteomics. *J Biol Chem* 2001 May 25;276(21):17920-31.
- Richards J, et al. Integrated genomic and proteomic analysis of signaling pathways in dendritic cell differentiation and maturation. *Ann NY Acad Sci* 2002 Dec;975:91-100.
- Gundacker NC, et al. Cytoplasmic proteome and secretome profiles of differently stimulated human dendritic cells. *J Proteome Res* 2009 Jun;8(6):2799-811.
- Ferret-Bernard S, et al. Proteomic profiling reveals that Th2-inducing dendritic cells stimulated with helminth antigens have a 'limited maturation' phenotype. *Proteomics* 2008 Mar;8(5):980-93.
- Ferret-Bernard S, et al. Plasma membrane proteomes of differentially matured dendritic cells identified by LC-MS/MS combined with iTRAQ labelling. *J Proteomics* 2012 Jan 4;75(3):938-48.
- Ferreira GB, et al. Protein-induced changes during the maturation process of human dendritic cells: A 2-D DIGE approach. *Proteomics Clin Appl* 2008 Sep;2(9):1349-60.
- Pereira SR, et al. Changes in the proteomic profile during differentiation and maturation of human monocyte-derived dendritic cells stimulated with granulocyte macrophage colony stimulating factor/interleukin-4 and lipopolysaccharide. *Proteomics* 2005 Apr;5(5):1186-98.
- Richards J, et al. Integrated genomic and proteomic analysis of signaling pathways in dendritic cell differentiation and maturation. *Ann NY Acad Sci* 2002 Dec;975:91-100.
- Gundacker NC, et al. Cytoplasmic proteome and secretome profiles of differently stimulated human dendritic cells. *J Proteome Res* 2009 Jun;8(6):2799-811.
- Palmblad M, et al. A novel mass spectrometry cluster for high-throughput quantitative proteomics. *J Am Soc Mass Spectrom* 2010 Jun;21(6):1002-11.
- Johansson A, et al. Identification of genetic variants influencing the human plasma proteome. *Proc Natl Acad Sci U S A* 2013 Mar 19;110(12):4673-8.
- Martinez-Pomares L. The mannose receptor. *J Leukoc Biol* 2012 Dec;92(6):1177-86.

22. Kolter T, et al. Principles of lysosomal membrane digestion: stimulation of sphingolipid degradation by sphingolipid activator proteins and anionic lysosomal lipids. *Annu Rev Cell Dev Biol* 2005;21:81-103.
23. Katunuma N, et al. Insights into the roles of cathepsins in antigen processing and presentation revealed by specific inhibitors. *Biol Chem* 2003 Jun;384(6):883-90.
24. Nigro P, et al. Cyclophilin A: a key player for human disease. *Cell Death Dis* 2013;4:e888.
25. Termeer C, et al. Targeting dendritic cells with CD44 monoclonal antibodies selectively inhibits the proliferation of naive CD4+ T-helper cells by induction of FAS-independent T-cell apoptosis. *Immunology* 2003 May;109(1):32-40.
26. Everts B, et al. Helminths and dendritic cells: sensing and regulating via pattern recognition receptors, Th2 and Treg responses. *Eur J Immunol* 2010 Jun;40(6):1525-37.
27. Ferreira GB, et al. Understanding dendritic cell biology and its role in immunological disorders through proteomic profiling. *Proteomics Clin Appl* 2010 Feb;4(2):190-203.
28. Alvarez D, et al. Mechanisms and consequences of dendritic cell migration. *Immunity* 2008 Sep 19;29(3):325-42.
29. Matsue H, et al. Generation and function of reactive oxygen species in dendritic cells during antigen presentation. *J Immunol* 2003 Sep 15;171(6):3010-8.
30. Yamada H, et al. LPS-induced ROS generation and changes in glutathione level and their relation to the maturation of human monocyte-derived dendritic cells. *Life Sci* 2006 Jan 25;78(9):926-33.
31. Rivollier A, et al. High expression of antioxidant proteins in dendritic cells: possible implications in atherosclerosis. *Mol Cell Proteomics* 2006 Apr;5(4):726-36.
32. Yamakita Y, et al. Fascin1 promotes cell migration of mature dendritic cells. *J Immunol* 2011 Mar 1;186(5):2850-9.
33. Buhligen J, et al. Lysophosphatidylcholine-mediated functional inactivation of syndecan-4 results in decreased adhesion and motility of dendritic cells. *J Cell Physiol* 2010 Nov;225(3):905-14.
34. Rescigno M, et al. Dendritic cell survival and maturation are regulated by different signaling pathways. *J Exp Med* 1998 Dec 7;188(11):2175-80.
35. Ferreira GB, et al. Protein-induced changes during the maturation process of human dendritic cells: A 2-D DIGE approach. *Proteomics Clin Appl* 2008 Sep;2(9):1349-60.
36. Srivastava P. Roles of heat-shock proteins in innate and adaptive immunity. *Nat Rev Immunol* 2002 Mar;2(3):185-94.
37. Fleckner J, et al. Differential regulation of the human, interferon inducible tryptophanyl-tRNA synthetase by various cytokines in cell lines. *Cytokine* 1995 Jan;7(1):70-7.
38. Mellor AL, et al. IDO expression by dendritic cells: tolerance and tryptophan catabolism. *Nat Rev Immunol* 2004 Oct;4(10):762-74.
39. Almawi WY, et al. Clinical and mechanistic differences between FK506 (tacrolimus) and cyclosporin A. *Nephrol Dial Transplant* 2000 Dec;15(12):1916-8.
40. Pearce EL, et al. Metabolic pathways in immune cell activation and quiescence. *Immunity* 2013 Apr 18;38(4):633-43.
41. Pearce EJ, et al. Dendritic cell metabolism. *Nat Rev Immunol* 2014 Dec 23;15(1):18-29.
42. Tchorzewski M. The acidic ribosomal P proteins. *Int J Biochem Cell Biol* 2002 Aug;34(8):911-5.
43. Constant S, et al. Extent of T cell receptor ligation can determine the functional differentiation of naive CD4+ T cells. *J Exp Med* 1995 Nov 1;182(5):1591-6.
44. Hosken NA, et al. The effect of antigen dose on CD4+ T helper cell phenotype development in a T cell receptor-alpha beta-transgenic model. *J Exp Med* 1995 Nov 1;182(5):1579-84.
45. van Panhuys N, et al. T-Cell-Receptor-Dependent Signal Intensity Dominantly Controls CD4(+) T Cell Polarization In Vivo. *Immunity* 2014 Jul 17;41(1):63-74.
46. Hussaarts L, et al. Rapamycin and omega-1: mTOR-dependent and -independent Th2 skewing by human dendritic cells. *Immunol Cell Biol* 2013 Aug;91(7):486-9.
47. Dutch Federation of Medical Scientific Societies. Dutch Federation of Medical Scientific Societies. www.fedra.org 2013 [cited 2013 Sep 17]; Available from: URL: www.fedra.org
48. Pedrioli PG, et al. A common open representation of mass spectrometry data

- and its application to proteomics research. *Nat Biotechnol* 2004 Nov;22(11):1459-66.
49. Wolstencroft K, et al. The Taverna workflow suite: designing and executing workflows of Web Services on the desktop, web or in the cloud. *Nucleic Acids Res* 2013 Jul;41(Web Server issue):W557-W561.
 50. Craig R, et al. TANDEM: matching proteins with tandem mass spectra. *Bioinformatics* 2004 Jun 12;20(9):1466-7.
 51. Keller A, et al. A uniform proteomics MS/MS analysis platform utilizing open XML file formats. *Mol Syst Biol* 2005;1:2005.
 52. Palmblad M, et al. Chromatographicalignment of LC-MS and LC-MS/MS datasets by genetic algorithm feature extraction. *J Am Soc Mass Spectrom* 2007 Oct;18(10):1835-43.
 53. Keller A, et al. Empirical statistical model to estimate the accuracy of peptide identifications made by MS/MS and database search. *Anal Chem* 2002 Oct 15;74(20):5383-92.
 54. Mi H, et al. PANTHER in 2013: modeling the evolution of gene function, and other gene attributes, in the context of phylogenetic trees. *Nucleic Acids Res* 2013 Jan;41(Database issue):D377-D386.
 55. Mi H, et al. Large-scale gene function analysis with the PANTHER classification system. *Nat Protoc* 2013 Aug;8(8):1551-66.
 56. Warde-Farley D, et al. The GeneMANIA prediction server: biological network integration for gene prioritization and predicting gene function. *Nucleic Acids Res* 2010 Jul;38(Web Server issue):W214-W220.

SUPPLEMENTAL DATA

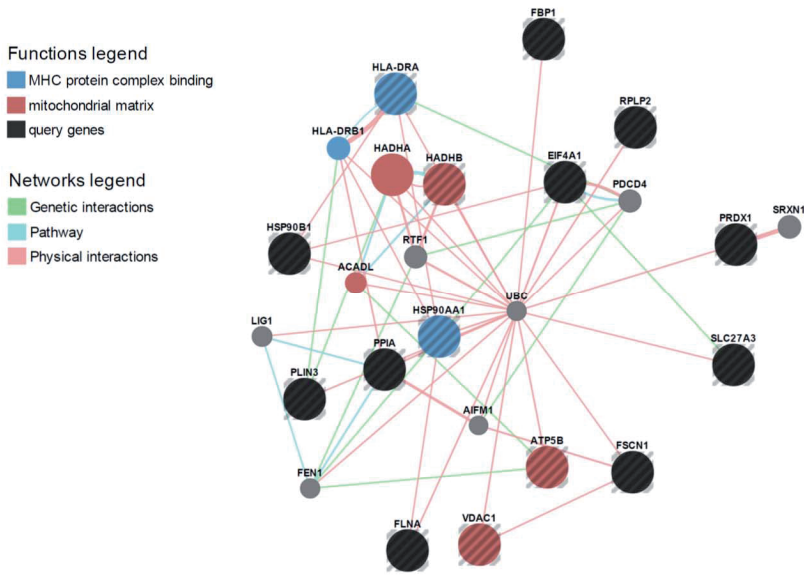
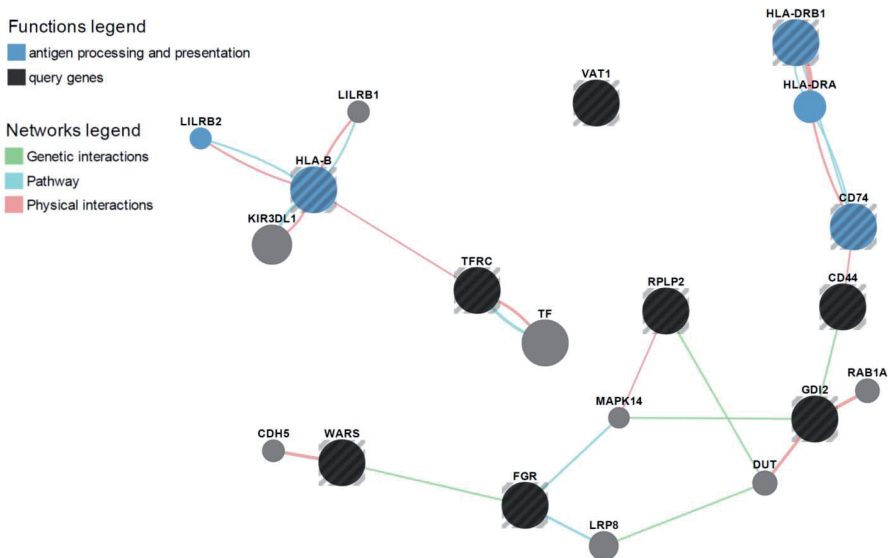


Figure S1. Network analysis of 6h SEA-response proteins. Monocyte-derived DCs were pulsed with LPS in the presence of SEA or omega-1, and protein expression was analyzed by LC-FTICRMS. For GeneMANIA analysis, all 6h SEA-responsive proteins with $P < 0.05$, and those proteins with $P < 0.1$ and a fold change of < 0.67 or > 1.5 , were included. Black and/or striped nodes represent genes of which the proteins were differentially expressed (query genes); grey nodes represent associated genes added by GeneMANIA. Colored nodes highlight significantly enriched Gene Ontologies.



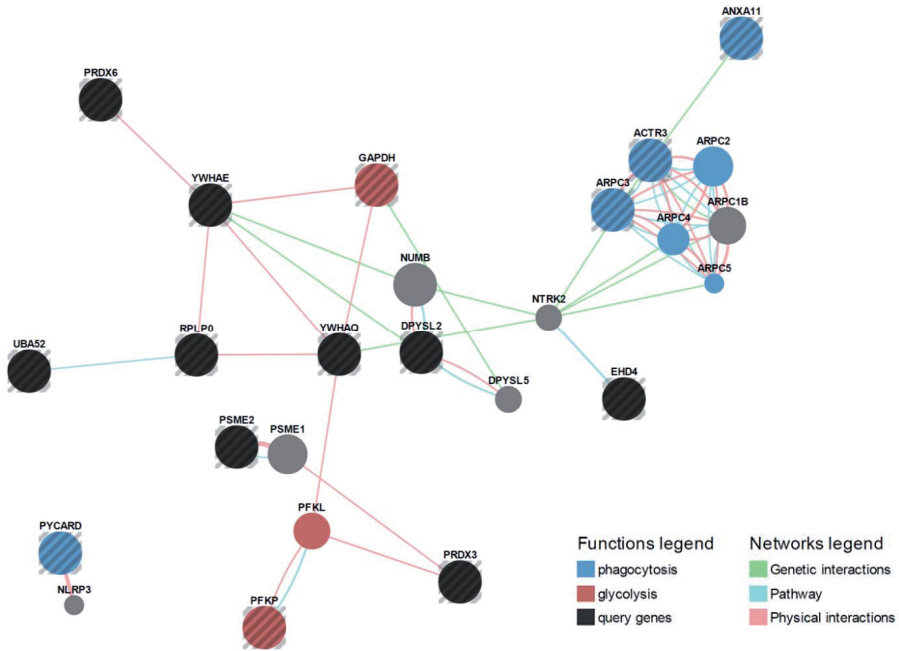


Figure S3. Network analysis of 6h omega-1-response proteins. Monocyte-derived DCs were pulsed and analyzed as describe for figure S1. For GeneMANIA analysis, all 6h omega-1-responsive proteins with $P < 0.05$, and those proteins with $P < 0.1$ and a fold change of < 0.67 or > 1.5 , were included. Black and/or striped nodes represent genes of which the proteins were differentially expressed (query genes); grey nodes represent associated genes added by GeneMANIA. Colored nodes highlight significantly enriched Gene Ontologies.

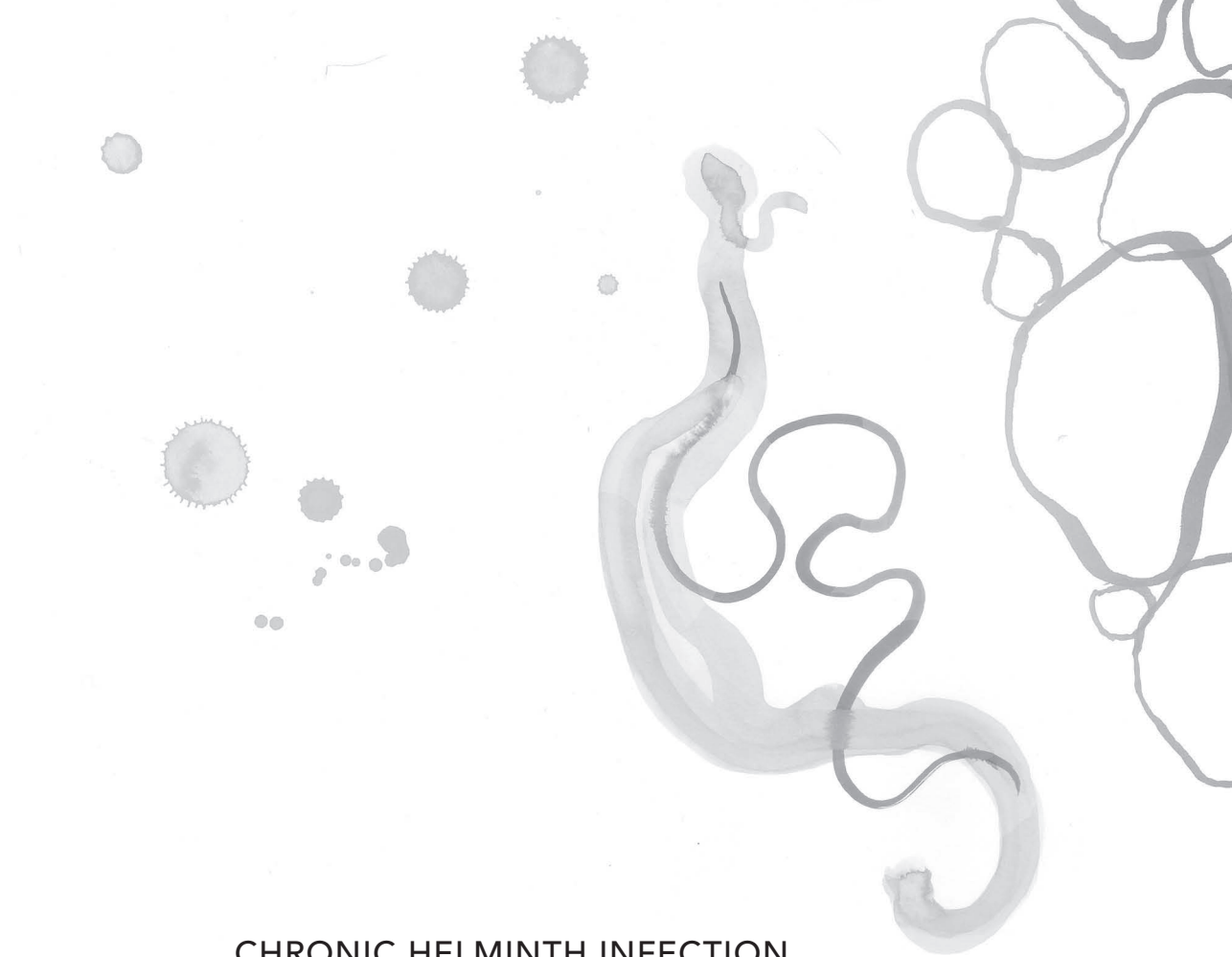
◀ **Figure S2. Network analysis of 32h SEA-response proteins.** Monocyte-derived DCs were pulsed and analyzed as describe for figure S1. For GeneMANIA analysis, all 32h SEA-responsive proteins with $P < 0.05$, and those proteins with $P < 0.1$ and a fold change of < 0.67 or > 1.5 , were included. Black and/or striped nodes represent genes of which the proteins were differentially expressed (query genes); grey nodes represent associated genes added by GeneMANIA. Colored nodes highlight significantly enriched Gene Ontologies.

Table S1. Differentially expressed proteins included for GeneMANIA analysis.

Accession	Gene Name	Fold Change	P-value
SEA-induced, 6 hours			
P62937	PPIA	11.27	0.012
P14625	HSP90B1	4.14	0.039
P06576	ATP5B	3.44	0.075
P60842	EIF4A1	3.21	0.042
P07900	HSP90AA1	2.98	0.019
P01903	HLA-DRA	2.39	0.056
P21333	FLNA	2.07	0.091
Q06830	PRDX1	1.90	0.062
P55084	HADHB	1.79	0.093
Q16658	FSCN1	1.74	0.041
P05387	RPLP2	1.71	0.066
P09467	FBP1	1.54	0.074
O60664	PLIN3	1.36	0.035
P21796	VDAC1	0.78	0.048
Q5K4L6	SLC27A3	0.77	0.005
SEA-induced, 32 hours			
P05387	RPLP2	2,27	0,006
P50395	GDI2	1,60	0,093
Q99536	VAT1	1,59	0,028
P04229	HLA-DRB1	0,70	0,018
P04233	CD74	0,69	0,020
P09769	FGR	0,68	0,009
P16070	CD44	0,63	0,023
P23381	WARS	0,60	0,004
P02786	TFRC	0,56	0,002
P30464	HLA-B	0,45	0,003
Omega-1-induced, 6 hours			
P30048	PRDX3	4.03	0.036
Q9ULZ3	PYCARD	2.08	0.074
P05388	RPLP0	1.86	0.021
O15145	ARPC3	1.80	0.052
P30041	PRDX6	1.77	0.020
Q01813	PFKP	1.65	0.006
P61158	ACTR3	1.61	0.038
P27348	YWHAQ	1.46	0.014
Q9UL46	PSME2	1.43	0.005
Q9H223	EHD4	1.42	0.020

Table S1. Differentially expressed proteins included for GeneMANIA analysis. (Continued)

Accession	Gene Name	Fold Change	P-value
Q16555	DPYSL2	1.24	0.022
P62258	YWHAE	1.16	0.010
P62987	UBA52	0.83	0.041
P04406	GAPDH	0.72	0.043
P50995	ANXA11	0.72	0.043
Omega-1-induced, 32 hours			
P55084	HADHB	2.52	0.045
P63104	YWHAZ	2.33	0.035
P60842	EIF4A1	2.30	0.086
P50502	ST13	2.05	0.024
P30041	PRDX6	2.02	0.020
Q99536	VAT1	1.53	0.016
P06753	TPM3	1.43	0.049
P29692	EEF1D	1.35	0.001
P29966	MARCKS	0.58	0.015
P04179	SOD2	0.52	0.006
P02786	TFRC	0.49	0.002
P30504	HLA-C	0.47	0.019
P16070	CD44	0.47	0.002
P30464	HLA-B	0.40	0.002
Q9Y3Z3	SAMHD1	1.70	0.070
P27824	CANX	2.64	0.047
P05387	RPLP2	4.63	0.013
P30508	HLA-C	0.63	0.012
P17900	GM2A	0.65	0.026
P62987	UBA52	0.70	0.025
P07339	CTSD	0.73	0.036
P07858	CTSB	0.74	0.029
Q9BQE5	APOL2	0.76	0.031
P80723	BASP1	0.76	0.042



CHRONIC HELMINTH INFECTION
AND HELMINTH-DERIVED EGG
ANTIGENS PROMOTE ADIPOSE
TISSUE M2 MACROPHAGES AND
IMPROVE INSULIN SENSITIVITY
IN OBESE MICE

Leonie Hussaarts, Noemí García-Tardón,
Lianne van Beek, Mattijs M. Heemskerk, Simone Haeberlein,
Gerard C. van der Zon, Arifa Ozir-Fazalalikhan,
Jimmy F. P. Berbée, Ko Willems van Dijk,
Vanessa van Harmelen, Maria Yazdanbakhsh
and Bruno Guigas

*The FASEB Journal, published online ahead of print
in April 2015. doi:10.1096/fj.14-262329*

5

ABSTRACT

Chronic low-grade inflammation associated with obesity contributes to insulin resistance and type 2 diabetes. Helminth parasites are the strongest natural inducers of type 2 immune responses, and short-lived infection with rodent nematodes was reported to improve glucose tolerance in obese mice. Here, we investigated the effects of chronic infection (12 weeks) with *Schistosoma mansoni*, a helminth that infects millions of humans worldwide, on whole-body metabolic homeostasis and white adipose tissue (WAT) immune cell composition in high-fat diet-induced obese C57BL/6 male mice. Our data indicate that chronic helminth infection reduced body weight gain (-62%), fat mass gain (-89%) and adipocyte size; lowered whole-body insulin resistance (-23%) and glucose intolerance (-16%); and improved peripheral glucose uptake (+25%) and WAT insulin sensitivity. Analysis of immune cell composition by flow cytometry and quantitative PCR revealed that *S. mansoni* promoted strong increases in WAT eosinophils and alternatively activated M2 macrophages. Importantly, injections with *S. mansoni* soluble egg antigens recapitulated the beneficial effect of parasite infection on whole-body metabolic homeostasis and induced type 2 immune responses in WAT and liver. Taken together, we provide novel data suggesting that chronic helminth infection and helminth-derived molecules protect against metabolic disorders by promoting a T helper 2 response, eosinophilia and WAT M2 polarization.

INTRODUCTION

The obesity epidemic represents a growing threat to public health, not only in industrialized countries but also in urban centers of developing countries. Obesity significantly increases the risk for the development of type 2 diabetes, cardiovascular diseases, and eventually cancer (1;2) and is often associated with a state of chronic, low-grade inflammation, which contributes to tissue-specific insulin resistance and whole-body metabolic dysfunction (3). Among the underlying molecular mechanisms, classically activated (M1) macrophages were shown to accumulate in white adipose tissue (WAT) from obese mice, where they secrete pro-inflammatory cytokines such as interleukin (IL)-1 β and tumor necrosis factor- α (TNF- α) (4-6). These cytokines interfere with insulin signaling (7;8) and induce lipolysis (9;10), thereby increasing circulating free fatty acids which promote peripheral insulin resistance (11). Other immune cell types, including neutrophils (12), mast cells (13), B cells (14;15) and CD8⁺ T cells (16), have also been shown to mediate insulin resistance.

By contrast, alternatively activated (M2) macrophages prevail in lean WAT and are involved in the maintenance of adipose tissue insulin sensitivity, partly through secretion of the anti-inflammatory cytokine IL-10 (6;17). The M2 phenotype is promoted by T helper 2 (Th2)-type cytokines like IL-4, secreted by WAT eosinophils (18), and IL-5 and IL-13, released from WAT innate lymphoid type 2 cells (ILC2s) (19). In addition, Th2 and regulatory T cell responses, as well as administration of IL-4, have been associated with protection against insulin resistance (20-22). Together, these studies illustrate that type 2 and anti-inflammatory responses are beneficial for the expanding adipose tissue environment and the maintenance of tissue-specific insulin sensitivity and whole-body glucose homeostasis.

Helminth parasites are the strongest natural inducers of type 2 inflammatory responses, and epidemiological studies in India and rural China revealed that helminth infections inversely correlate with metabolic syndrome (23-25). In addition, seminal papers recently reported that the rodent nematode *Nippostrongylus brasiliensis*, which is spontaneously cleared within two weeks of infection, improves glucose tolerance in diet-induced obese mice (18;26), associated with WAT eosinophilia (18) or increased M2 gene expression (26). Furthermore, *Schistosoma mansoni* soluble egg antigens could protect against atherosclerosis in hyperlipidemic LDLR knockout mice (27). These studies suggest that manipulation of the immune system by helminths or their molecules might be beneficial for metabolic homeostasis. However, it remains unclear which aspects of whole-body energy metabolism are affected by the worms, and the immunological changes that take place in WAT have not yet been characterized at the cellular level.

Furthermore, as most helminth infections in humans are chronic in nature, it would be important to test whether the beneficial effect on metabolic homeostasis also occurs in a model of chronic infection. Of the various helminth species, schistosomes are among the most prevalent and chronically infect millions of people worldwide (28). While infection with *N. brasiliensis* induces a strong Th2 response that mediates parasite rejection within two weeks after infection, the Th2 response in schistosomiasis emerges after 5-6 weeks of infection,

with the onset of egg production that also triggers the development of M2 macrophages (29). In most individuals, infection often reaches a chronic stage, characterized by a decline in Th2 inflammation and the presence of regulatory B and T cells (30;31). In the present study, we therefore investigated the impact of *S. mansoni* infection for 12 weeks on whole-body metabolic homeostasis, WAT insulin sensitivity, and WAT immune cell composition in mice fed either low- or high-fat diet (HFD). Next, to study the impact of helminth-derived molecules on metabolic disorders in a pathogen-free setting, we treated HFD-fed mice with *S. mansoni* soluble egg antigens (SEA) for 4 weeks and assessed whole-body glucose tolerance and insulin sensitivity, and the immune cell composition of WAT and liver.

MATERIALS AND METHODS

Animals, diet and *S. mansoni* infection

All mouse experiments were performed in accordance with the Guide for the Care and Use of Laboratory Animals of the Institute for Laboratory Animal Research and have received approval from the university Ethical Review Boards (Leiden University Medical Center, Leiden, The Netherlands; DEC2189). Male C57BL/6J mice (8-10 weeks old; Charles River, L'Arbresle Cedex, France) were housed in a temperature-controlled room with a 12-hour light-dark cycle. Throughout the experiment, food and tap water were available *ad libitum*. Mice were fed a high-fat diet (45% energy derived from fat, D12451, Research Diets, Wijk bij Duurstede, The Netherlands) or a low-fat diet (10% energy derived from fat, D12450B, Research Diets), which were similar in composition in all respects apart from the total fat content. After 6 weeks, mice were randomized according to body weight and fasting plasma glucose and insulin levels and percutaneously infected with 36 *S. mansoni* cercariae, as previously described (32). Mice were monitored for 12 additional weeks. The effects of chronic infection were assessed in 2 independent experiments. Before SEA injections, mice were fed a LFD or HFD for 12 weeks after which they were randomized according to body weight, fasting plasma glucose and insulin levels, and fat mass. SEA (50 µg) was injected intraperitoneally once every 3 days for a period of 4 weeks. The effects of SEA treatment were assessed in 2 independent experiments.

Plasma analysis

Blood samples were collected from the tail tip of 4-hour-fasted mice (food removed at 9 am) by use of chilled capillaries. Blood glucose level was determined by use of a glucometer (Accu-Check, Roche Diagnostics Almere, The Netherlands) and plasma insulin level was measured by use of a commercial kit according to the instructions of the manufacturer (Millipore, The Netherlands).

Glucose and insulin tolerance tests

The effect of chronic *S. mansoni* infection on glucose tolerance was assessed by intravenous glucose tolerance test (ivGTT) at week 5 and 11 postinfection. Mice were fasted for 6 hours, and the tests were carried out at 2 pm. After an initial blood collection ($t=0$), a glucose

load (2g D-Glucose/kg total body weight of which 50% of the glucose was [6,6-²H₂]glucose (Sigma-Aldrich, Zwijndrecht, The Netherlands) was administered in conscious mice via injection in the tail vein. Blood sampling was performed by tail bleeding at 2.5, 15, 30, 60, 90 and 120 minutes: 5-10 μ L whole blood was spotted on sample carrier paper (Sartorius Stedim, Goettingen, Germany) and an additional drop was used to measure glucose using a glucometer (Accu-Check, Roche Diagnostics). To analyze peripheral glucose uptake, blood spot glucose enrichment was measured by extracting glucose from the filter paper with 75 μ L water (B. Braun, Oss, Netherlands) and 1 mL methanol. The extracted glucose was derivatized to aldonitrile penta-acetate and reconstituted in 100 μ L ethyl acetate, of which 1 μ L was injected for gas chromatography (HP6890II) mass spectrometry (HP5973, Hewlett-Packard Co., Palo Alto, CA, USA), as described previously (33). Mass-over-charge ratios of 187, 188 and 189 were monitored in selective ion monitoring mode, from which the percentage of unlabeled and labeled glucose was calculated based on theoretical isotopic distribution. Concentrations of labeled glucose were calculated based on the plasma glucose levels, and values were natural log-transformed after which a decay curve was fitted. Individual decay curves were calculated, of which the slope represents the peripheral glucose uptake. The effect of SEA treatment on glucose tolerance was assessed by an i.p. glucose tolerance test (2 g D-Glucose/kg total body weight) in 6-hour fasted mice at week 3 postinjections.

Whole-body insulin sensitivity was determined by an intraperitoneal insulin tolerance test (ITT) at 5 and 11 weeks postinfection or at week 3 post-SEA treatment. Mice were fasted for 4 hours, and the tests were carried out at 1 pm. After an initial blood collection ($t=0$), an intraperitoneal bolus of insulin (1 U/kg lean body mass; NOVORAPID, Novo Nordisk, Alphen aan den Rijn, Netherlands) was administered to the mice. Blood glucose was measured by tail bleeding at 15, 30, 60, and 120 minutes after insulin administration by use of a glucometer.

Body composition and indirect calorimetry

Body composition was measured by MRI using an EchoMRI (Echo Medical Systems, Houston, TX, USA). Groups of 8 mice with free access to food and water were subjected to individual indirect calorimetric measurements at week 11 postinfection for a period of 7 consecutive days using a Comprehensive Laboratory Animal Monitoring System (Columbus Instruments, Columbus, OH, USA). Before the start of the measurements, the animals were acclimated to the cages and the single housing for a period of 48 hours. Feeding behavior was assessed by real-time food intake. Spontaneous locomotor activity was determined by the measurement of beam breaks. Oxygen consumption and carbon dioxide production were measured at 15-minute intervals and normalized for body surface area ($\text{kg}^{0.75}$). Respiratory exchange ratio and energy expenditure were calculated as described previously (34).

Isolation of adipocytes and stromal vascular fraction (SVF) from adipose tissue

Gonadal (epididymal), visceral (mesenteric) and subcutaneous (flank) adipose tissues were collected from infected and uninfected mice, minced, and digested for 1 h at 37°C in HEPES buffer (pH 7.4) containing 0.5g/l type 1 collagenase from *Clostridium histolyticum* (Sigma-Aldrich)

and 2% (w/v) dialyzed bovine serum albumin (Fraction V; Sigma-Aldrich). The disaggregated adipose tissue was filtered through a 236 μm nylon mesh. Mature adipocytes were isolated from the surface of the filtrate and washed several times with PBS. Cell size was determined using an imaging technique implemented in MATLAB which automatically determines size of isolated adipocytes from microscopic pictures (~1000 cells/fat tissue sample). The adipocyte size distribution, mean adipocyte diameter and volume, and adipocyte number per fat pad were calculated, as described previously (35). The residue of the gonadal and visceral adipose tissue filtrate was used for the isolation of stromal vascular cells for flow cytometry. In brief, after centrifugation (350 g , 10 minutes, room temperature), the supernatant was discarded and the pellet was treated with erythrocyte lysis buffer. The cells were washed twice with PBS and counted manually or using an automated cell counter (TC10, Bio-Rad, Hercules, CA, USA). Following SEA injections, stromal vascular cells from gonadal adipose tissue were isolated as described above, with the exception that the disaggregated adipose tissue was passed through a 100 μm cell strainer that was washed with PBS supplemented with 2.5 mM EDTA and 5% fetal calf serum (FCS).

Isolation of CD45⁺ cells from liver tissue

Livers were minced and digested for 45 minutes at 37°C in RPMI 1640 + Glutamax (Life Technologies, Bleiswijk, The Netherlands) containing 1 mg/mL collagenase type IV from *Clostridium histolyticum*, 2000 U/mL DNase (both Sigma-Aldrich), and 1 mM CaCl_2 . The digested liver tissues were passed through 100 μm cell strainers that were washed with PBS supplemented with 2.5 mM EDTA and 5% FCS. Following centrifugation (530 g , 10 minutes, 4°C), the supernatant of the filtrate was discarded, after which the pellet was resuspended in PBS + 2.5 mM EDTA and 5% FCS and centrifuged at 50 g to remove hepatocytes (3 minutes, 4 degrees). Next, supernatants were collected and pelleted (530 g , 10 minutes, 4°C). The pellet was treated with erythrocyte lysis buffer, and the cells were washed once more with PBS + 2.5 mM EDTA and 5% FCS. CD45⁺ cells were isolated by use of LS columns and CD45 MicroBeads (35 μL /liver; Miltenyi Biotec, Bergisch Galdbach, Germany) according to manufacturer's protocol. Isolated CD45⁺ cells were counted and processed as described for the SVF.

Processing of isolated cells for flow cytometry

For analysis of macrophage and lymphocyte subsets, isolated stromal vascular cells and CD45⁺ cells from liver were stained with the live/dead marker Aqua (Invitrogen), after which they were fixed with 1.9% paraformaldehyde (Sigma-Aldrich) and stored in FACS buffer (PBS, 0.02% sodium azide, 0.5% FCS) at 4°C in the dark until subsequent analysis. For analysis of cytokine production, isolated cells were cultured for 4 hours in culture medium in the presence of 100 ng/mL phorbol myristate acetate (PMA), 1 μg /mL ionomycin and 10 μg /mL Brefeldin A (all Sigma-Aldrich). After culture, cells were washed with PBS, stained with Aqua, and fixed as described above.

Flow cytometry

For analysis of lymphocyte subsets, SVF cells were stained with antibodies against CD4 (GK1.5), CD3 (17A2), B220 (RA3-6B2) or CD19 (1D3; all eBioscience, San Diego, CA, USA), CD8 (53-6.7), CD45 (104; both BioLegend, San Diego, CA, USA) and NK1.1 (PK136, eBioscience or BD Biosciences, San Jose, CA, USA). Following SEA injections, when ILC2s were analyzed, additional antibodies were included against Thy1.2 (52-2.1), CD11b (M1/7; both eBioscience), CD11c (HL3) and GR-1 (RB6-8C5; both BD Biosciences), to gate on lineage-negative Thy1.2⁺ cells. For analysis of macrophages and eosinophils, cells were permeabilized with 0.5% saponin (Sigma-Aldrich) in which they were also stained. Cells were incubated with an antibody against Ym1 conjugated to biotin (R&D Systems, Minneapolis, MN, USA), washed, and stained with streptavidin-PerCP (BD Biosciences) and antibodies directed against CD45, CD11b, CD11c, F4/80 (BM8; eBioscience), Siglec-F (E50-2440; BD Biosciences), and following SEA injections, Ly6C (HK1.4; BioLegend). Cytokine production of Th2 cells and ILC2s was analyzed following permeabilization, as described above, using antibodies against CD11b, CD11c, GR-1, B220, NK1.1, CD3, CD45, CD4, Thy1.2, IL-4 (11B11; eBioscience), IL-13 (eBio13A; eBioscience) and IL-5 (TRFK5; BioLegend). Flow cytometry was performed using a FACSCanto (BD Biosciences), and gates were set according to Fluorescence Minus One (FMO) controls. Representative gating schemes are shown in Supplemental Fig. 1.

In vivo insulin signaling

Mice were food-deprived for 4 hours and subjected to an i.p. injection of human recombinant insulin (1 U/kg body weight; NOVORAPID, Novo Nordisk) at 1 pm. Mice were sacrificed after 15 minutes and gonadal and visceral adipose tissues were isolated and immediately snap-frozen. Subsequently, the tissue samples (~30 mg) were lysed in ice-cold buffer containing 50 mM Hepes (pH 7.6), 50 mM NaF, 50 mM KCl, 5 mM NaPPi, 1 mM EDTA, 1 mM EGTA, 1 mM DTT, 5 mM β -glycerophosphate, 1 mM sodium vanadate, 1% NP40 and protease inhibitor cocktail (Complete, Roche Diagnostics). Western blots were performed using phospho-specific (Thr308-PKB, Cell Signaling Technology, Leiden, The Netherlands) or total primary antibodies (tubulin from Cell Signalling; insulin receptor β (IR β) from Santa Cruz Biotechnology, Dallas, TX, USA), as described previously (36). Bands were visualized by enhanced chemiluminescence and quantified by use of ImageJ (NIH, Bethesda, MD, USA).

RNA purification and qRT-PCR

RNA was extracted from snap-frozen tissue samples (~20 mg) using Tripure RNA Isolation reagent (Roche Diagnostics). Total RNA (1 μ g) was reverse transcribed and quantitative real-time PCR was then performed with SYBR Green Core Kit on a MyIQ thermal cycler (Bio-Rad) using specific primers sets: 5'-GCCACCAACCTTCTGGCTG-3' (Itgax-R), 5'-TTGGACTCTGCTGTGCAGTTG-3' (Itgax-F), 5'-GTCCCCAAGGGATGAGAAG-3' (Tnfa-R), 5'-CACTTGGTGGTTTGCTACGA-3' (Tnfa-F), 5'-TCCTGGACATTACGACCCCT-3' (Nos2-R), 5'-CTCTGAGGGCTGACACAAGG-3' (Nos2-F), 5'-TCAGCCAGATGCAGTTAACGCCC-3' (Ccl2-R), 5'-GCTTCTTTGGACACCTGCTGCT-3' (Ccl2-F), 5'-CCTGCCCTGCTGGGATGACT-3' (Retnla-R), 5'-GGGCAGTGGTCCAGTCAACGA-3' (Retnla-F),

5'-ACAATTAGTACTGGCCACCAGGAA-3' (Chil3-R), 5'-TCCTTGAGCCACTGAGCCTTCA-3' (Chil3-F), 5'-GACCACGGGGACCTGGCCTT-3' (Arg1-R), 5'-ACTGCCAGACTGTGGTCTCCACC-3' (Arg1-F), 5'-CCTCACAGCAACGAAGAACA-3' (Il4-R), 5'-ATCGAAAAGCCCCGAAAGAGT-3' (Il4-F), 5'-TGGGGGTACTGTGGAATGC-3' (Il5-R), 5'-CCACACTTCTTTTTTGGCGG-3' (Il5-F), 5'-CCCTGGATTCCCTGACCAAC-3' (Il13-R), 5'-GGAGGCTGGAGACCGTAGT-3' (Il13-F), 5'-CTTTGGCTATGGGCTCCAGTC-3' (Emr1-R), 5'-GCAAGGAGGACAGAGTTTATCGTG-3' (Emr1-F), 5'-ACTGAAGTACCAAATGGACAATGTTAGT-3' (Clec4f-R), 5'-GTCAGCATTACATCCTCCAGA-3' (Clec4f-F). mRNA expression was normalized to RplP0 mRNA content and expressed as fold change compared to noninfected LFD-fed mice using the $\Delta\Delta$ CT method.

Statistical analysis

All data are presented as means \pm SEM. Statistical analysis was performed using GraphPad Prism version 6.00 for Windows (GraphPad Software, La Jolla, CA, USA) with 2-tailed unpaired Student's *t* test. Differences between groups were considered statistically significant at $P < 0.05$. For repeated measurements, data were analyzed assuming the same scatter to increase power.

RESULTS

Chronic *S. mansoni* infection reduces fat mass in HFD-induced obese mice

To study the effect of chronic helminth infection on whole-body energy homeostasis, C57BL/6 male mice were fed a LFD or HFD for 6 weeks, before infection with *S. mansoni* for 12 additional weeks. HFD induced a time-dependent increase in body weight (Fig. 1A), fat mass (Fig. 1B,C), and mean adipocyte volume (Fig. 1D) when compared with LFD-fed mice. In response to *S. mansoni* infection, HFD-fed mice gained significantly less weight (Fig. 1A), an effect exclusively resulting from a reduction in body fat mass without affecting lean body mass (Fig. 1B,C). Morphometric analysis of various WATs revealed that chronic *S. mansoni* infection reduced HFD-induced adipocyte hypertrophy (Fig. 1D), while cell numbers remained unaffected (data not shown). In LFD-fed animals, *S. mansoni* induced a small but significant decrease in gonadal adipocyte mean volume, but did not affect body weight and fat mass. Next, by use of metabolic cages, we found that food intake and spontaneous locomotor activity were not affected by chronic infection (Fig. 1E,F), and indirect calorimetry also revealed that infection did not affect the respiratory exchange ratio (Fig. 1G) or energy expenditure (Fig. 1H) in HFD-fed animals.

Chronic *S. mansoni* infection improves whole-body glucose tolerance and insulin sensitivity in HFD-induced obese mice

We next investigated the effect of chronic *S. mansoni* infection on whole-body metabolic homeostasis in lean and HFD-induced obese mice. As expected, HFD increased fasting plasma glucose and insulin levels (Fig. 2A), and HOMA-IR (HOMeostatis Model Assessment of Insulin Resistance; Fig. 2B). In addition, HFD impaired whole-body glucose tolerance (Fig. 2C,D), peripheral glucose uptake (Fig. 2E,F), and insulin sensitivity (Fig. 2G,H). Chronic *S. mansoni* infection restored fasting blood glucose and insulin levels in mice on HFD (Fig. 2A), resulting

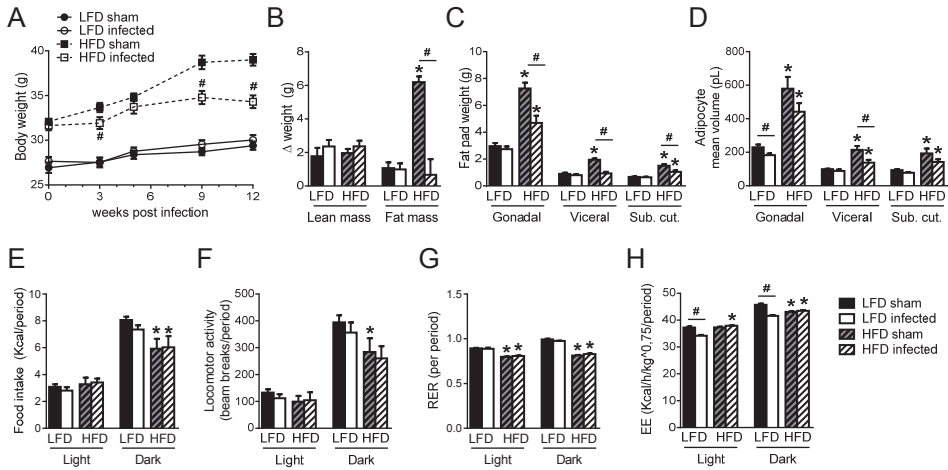


Figure 1. Chronic *S. mansoni* infection reduces body weight gain, fat mass and adipocyte size in diet-induced obese mice. Mice were fed a LFD or HFD for 6 weeks before infection with *S. mansoni* cercariae or sham-infection for 12 weeks. Body weight was monitored throughout the experimental period (A). The change in body composition from the start of infection (B), weight of different fat pads (C) and adipocyte mean volume (D) were measured at week 12 postinfection. Food intake (E), spontaneous locomotor activity (F), respiratory exchange ratio (RER; G) and energy expenditure (EE; H) were assessed using fully automated single-housed metabolic cages during week 11. Results are expressed as means \pm SEM. * $P < 0.05$ HFD vs LFD, # $P < 0.05$ helminth- vs sham-infected group ($n = 4-11$ animals per group in B, D-H, and 12-19 animals per group in A, C).

in a time-dependent reduction in HOMA-IR (Fig. 2B). Furthermore, chronic infection restored HFD-induced whole-body glucose tolerance (Fig. 2C,D), improved peripheral glucose uptake (Fig. 2E,F) and promoted whole-body insulin sensitivity (Fig. 2G,H). Of note, except for a slight but significant decrease in fasting plasma insulin level, *S. mansoni* infection did not affect any metabolic parameters in LFD-fed mice. Overall, these data indicate that *S. mansoni* improves whole-body glucose tolerance and insulin resistance in diet-induced obese mice.

Chronic *S. mansoni* infection improves adipose tissue insulin sensitivity in HFD-induced obese mice

To study the effect of chronic *S. mansoni* infection on WAT-specific insulin sensitivity, mice were subjected to an acute intraperitoneal insulin injection. The expression of IR β and insulin-induced phosphorylation of protein kinase B (PKB) were assessed by Western Blot in both gonadal and visceral WAT. As expected, HFD reduced IR β protein expression (Fig. 2I,K) and impaired PKB phosphorylation in response to insulin (Fig. 2J,K) in both gonadal and visceral WAT, indicating tissue-specific insulin resistance. Chronic *S. mansoni* infection restored IR β protein expression and insulin-induced PKB phosphorylation in WAT of HFD-fed mice (Fig. 2I-K), suggesting that the beneficial effect of helminths observed at the systemic level might be secondary to improved tissue-specific insulin sensitivity.

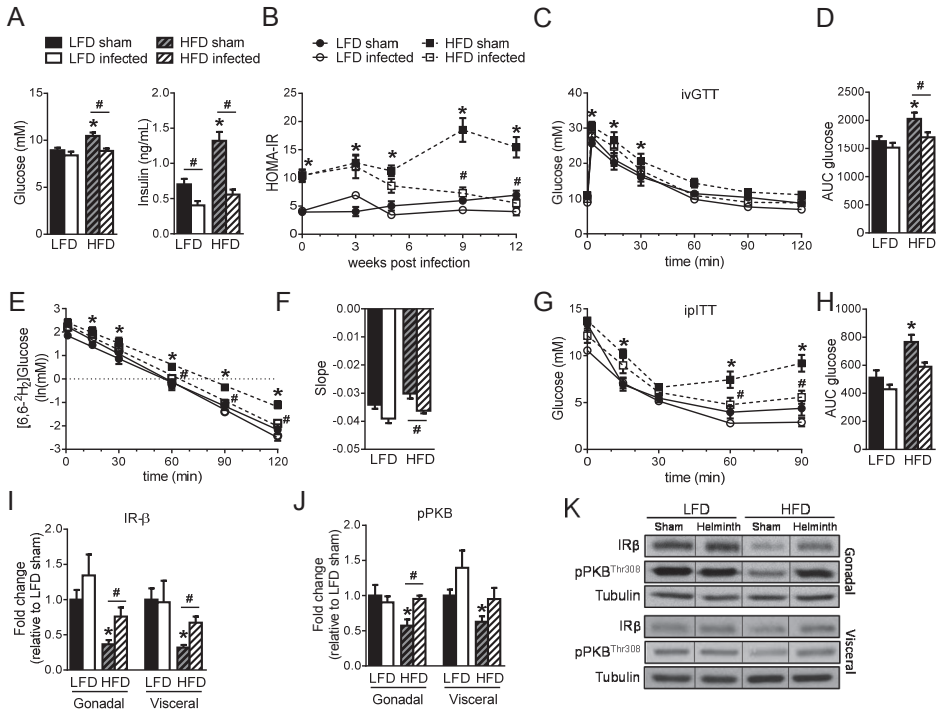


Figure 2. Chronic *S. mansoni* infection improves whole-body glucose tolerance and insulin sensitivity in diet-induced obese mice. Mice were fed a LFD or HFD and were infected with *S. mansoni* as described in the legend of Fig. 1. Plasma glucose and insulin levels (A) were determined in 4h-fasted mice at week 12 postinfection. HOMA-IR was calculated throughout the experimental period (B). An intravenous glucose tolerance test (2g D-glucose with 50% [6,6-²H₂]glucose / kg body weight) was performed in 6h-fasted mice at week 11. Blood glucose levels were measured at the indicated time points (C) and the area under the curve (AUC) of the glucose excursion curve was calculated as a measure for glucose tolerance (D). Blood was also collected for determination of the time-dependent change in [6,6-²H₂]glucose concentration by gas chromatography mass spectrometry (E). For each mouse, a decay curve was fitted of which the slope represents peripheral glucose uptake (F). An i.p. insulin tolerance test (1U/kg lean body mass) was performed in 4h-fasted mice at week 11. Blood glucose levels were measured at the indicated time points (G) and the AUC of the glucose excursion curve was calculated as a measure for insulin resistance (H). After 12 weeks of infection, 4h-fasted mice received an intravenous injection of insulin (1 U/kg lean body mass) and were sacrificed by cervical dislocation after 15 minutes. Gonadal and visceral adipose tissues were collected and immediately snap-frozen. The protein expression of IR β (I) and the phosphorylation state of PKB-Thr308 (J) were assessed by Western blot and quantified by densitometry analysis. Tubulin expression was used as internal housekeeping protein. Representative Western blots are shown (K) Results are expressed as means \pm SEM. *P<0.05 HFD vs LFD, #P<0.05 helminth- vs sham-infected group. Figures C, E and G: statistical significance of HFD sham vs LFD sham and HFD infected vs HFD sham is shown (n = 12-19 animals per group in A and B and 3-11 animals per group in C-J).

Chronic *S. mansoni* infection increases adipose tissue eosinophils and alternatively activated M2 macrophages

The immune cell composition of WAT, specifically the eosinophil content and the balance between M1 and M2 macrophages, has been shown to play a crucial role in the maintenance of adipocyte insulin sensitivity and whole-body metabolic homeostasis (6). To investigate whether chronic *S. mansoni* infection affects the immune cell composition in WAT, the stromal vascular fraction (SVF) was isolated from gonadal and visceral WAT of sham- and helminth-infected mice, and the immune cell composition was analyzed by flow cytometry (see Supplemental Fig. 1 for gating strategy). We found that HFD significantly reduced B cell, NK cell, and NKT cell numbers per gram of gonadal WAT (Supplemental Fig. 2A). *S. mansoni* promoted infiltration of leukocytes into gonadal WAT, resulting in increased numbers of all lymphocyte subsets studied in both LFD- and HFD-fed mice (Supplemental Fig. 2A). No major effect of diet or infection was observed on lymphocytes in visceral WAT (Supplemental Fig. 2B).

Subsequent analysis of eosinophils, identified by CD45 and Siglec-F expression, revealed a trend for a decrease in WAT eosinophil numbers in HFD-fed mice (Fig. 3A,B), in line with a previous report (18). Chronic *S. mansoni* infection induced a strong increase in eosinophil infiltration into gonadal and visceral WATs from both LFD- and HFD-fed mice (Fig. 3A,B).

Finally, the expression of CD11c and Ym1 in CD11b⁺F4/80⁺ cells allowed us to discriminate between M1 and M2 macrophages, respectively (17) (Fig. 3C). HFD promoted a significant increase in M1 macrophages in gonadal WAT (Fig. 3D) and a decrease in M2 macrophages in visceral WAT (Fig. 3E). Analysis of adipose tissue gene expression confirmed that M1 markers were increased in HFD-fed mice, an effect particularly clear in gonadal WAT, although M2-associated genes were not down-regulated significantly (Fig. 3G,H). Chronic *S. mansoni* infection had a marginal effect on WAT M1 macrophage counts as determined by flow cytometry analysis, but strongly increased M2 macrophage numbers in both gonadal and visceral WAT from LFD- and HFD-fed mice (Fig. 3D,E), shifting the M2/M1 ratio toward M2 (Fig. 3F). In line with these results, infection induced a strong up-regulation of M2-associated genes in both gonadal and visceral WAT from LFD- and HFD-fed mice, whereas the expression of M1-related genes was barely affected (Fig. 3G,H). Lastly, mRNA expression of the type 2-associated cytokines IL-4 and IL-5 were also significantly up-regulated in WAT from helminth-infected mice (Fig. 3G,H). Taken together, these results suggest that chronic *S. mansoni* infection promotes WAT type 2 inflammation characterized by adipose tissue eosinophilia and accumulation of M2 macrophages.

***S. mansoni* soluble egg antigens improve whole-body metabolic homeostasis and promote a type 2 immune response in WAT and liver from obese mice**

To exclude that the beneficial effects of helminth infection on metabolic homeostasis are simply a result of parasitism, we next investigated whether *S. mansoni*-derived molecules can alleviate diet-induced metabolic disorders. For this purpose, HFD-fed mice were subjected to repetitive i.p. injections with SEA, which was shown to promote a strong Th2 response *in vitro* (37) and *in vivo* (38). Importantly, treatment with SEA for 4 weeks did neither affect body

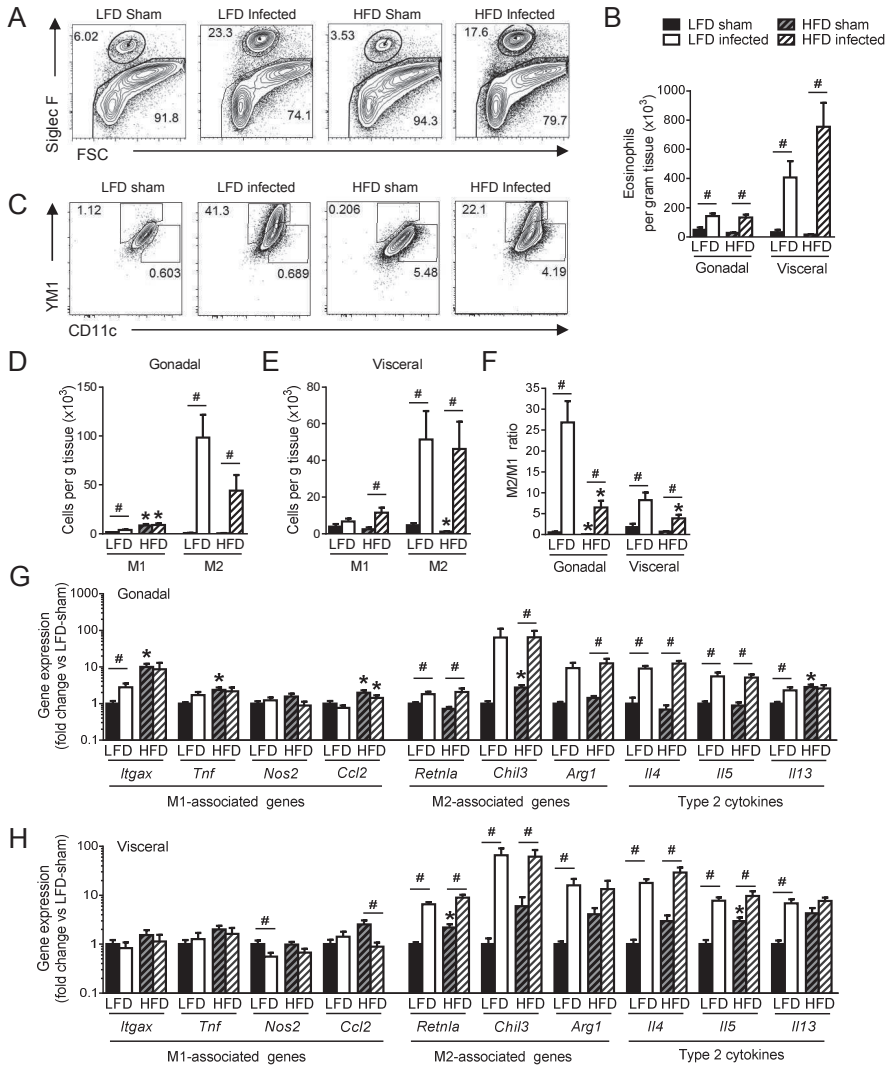


Figure 3. Chronic *S. mansoni* infection increases adipose tissue eosinophils and alternatively-activated M2 macrophages. Mice were fed a LFD or HFD and infected with *S. mansoni* as described in the legend of Fig. 1. At sacrifice (week 12), various adipose tissues were collected. Small tissue pieces were snap-frozen for qPCR analysis and the remaining tissue pieces were used for SVF isolation. Following fixation and permeabilization, SVF cells were stained and analyzed by flow cytometry. The complete gating scheme is shown in Supplemental Fig. 1. Representative flow cytometry plots from gonadal adipose tissue show the percentage of eosinophils based on Siglec-F expression in Aqua⁺CD45⁺ cells (A). The numbers of eosinophils per gram tissue were determined (B). Macrophages were identified as Aqua⁺CD45⁺Siglec-F⁺CD11b⁺F4/80⁺ cells. Representative flow cytometry plots from gonadal adipose tissue show the percentage of CD11c⁺ (M1) and Ym1⁺ (M2) macrophages (C). The numbers of M1 and M2 macrophages per gram tissue in gonadal (D) and visceral (E) WAT were determined and the M2/M1 ratios were calculated (F). mRNA expression of the indicated genes in gonadal (G) and visceral (H) adipose tissues were quantified by RT-PCR relative to RplP0 gene and expressed as fold difference compared with the non-infected LFD-fed mice. *Itgax* encodes CD11c; *Retnla* encodes Fizz1; *Chil3* encodes Ym1. Results are expressed as means \pm SEM. *P<0.05 HFD vs LFD, #P<0.05 helminth- vs sham-infected group (n = 8-16 animals per group).

weight nor lean or fat body mass (Fig. 4A), but improved fasting plasma glucose and insulin levels (Fig. 4B,C), HOMA-IR (Fig. 4C), and whole-body glucose tolerance (Fig. 4E) and insulin sensitivity (Fig. 4F).

Like the chronic parasite infection, SEA exposure promoted WAT eosinophilia (Fig. 5A), associated with accumulation of M2 macrophages (Fig. 5B), leading to a shift in the M2/M1 ratio toward M2 polarization (Fig. 5C). As we showed that helminth infection promoted gene expression of type 2-associated cytokines in WAT (Fig. 3), we next determined the numbers of CD4⁺ T cells and ILCs (lineage-negative Thy1.2⁺) in gonadal WAT (see Supplemental Fig. 1 for gating strategy), and analyzed cytokine expression by these lymphocyte subsets following stimulation with PMA and ionomycin (gating strategy shown in fig. 5E). Compared to LFD, HFD decreased the total number of CD4⁺ T cells and ILCs (Fig. 5D), and the percentage of CD4⁺ T cells expressing IL-4, but not IL-5 or IL-13 (Fig. 5F), and did not significantly affect cytokine production by ILCs (Fig. 5G). Treatment of HFD-fed mice with SEA strongly enhanced the percentage of IL-4-, IL-5- and IL-13-expressing CD4⁺ T cells in gonadal WAT (Fig. 5F), and slightly increased IL-5 production by ILCs (Fig. 5G). These findings were confirmed by quantitative PCR (qPCR), which showed that SEA promotes gene expression of M2-associated markers and type 2 cytokines (Fig. 5H).

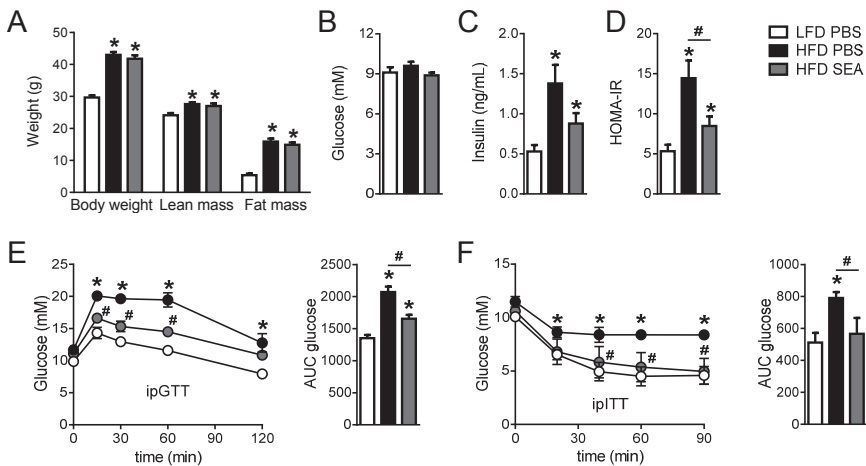


Figure 4. SEA improves whole-body metabolic homeostasis in HFD-induced obese animals. Mice were fed a LFD or HFD for 12 weeks, after which they were treated i.p. with PBS or 50 μ g SEA once every 3 days for a period of 4 weeks. Body weight and body composition were analyzed after 4 weeks of treatment (A). Plasma glucose (B) and insulin (C) levels were determined in 4h-fasted mice after 4 weeks of treatment and HOMA-IR was calculated (D). An i.p. glucose tolerance test (2 g/kg body weight) was performed in 6h-fasted mice at week 3. Blood glucose levels were measured at the indicated time points and the area under the curve (AUC) of the glucose excursion curve was calculated as a measure for glucose tolerance (E). An i.p. insulin tolerance test (1U/kg lean body mass) was performed in 4h-fasted mice at week 3. Blood glucose levels were measured at the indicated time-points, and the AUC of the glucose excursion curve was calculated as a measure for insulin resistance (F). Results are expressed as means \pm SEM. * $P < 0.05$ HFD vs LFD, # $P < 0.05$ PBS vs SEA (n = 11-13 animals per group in A-E and 3-6 animals per group in F).

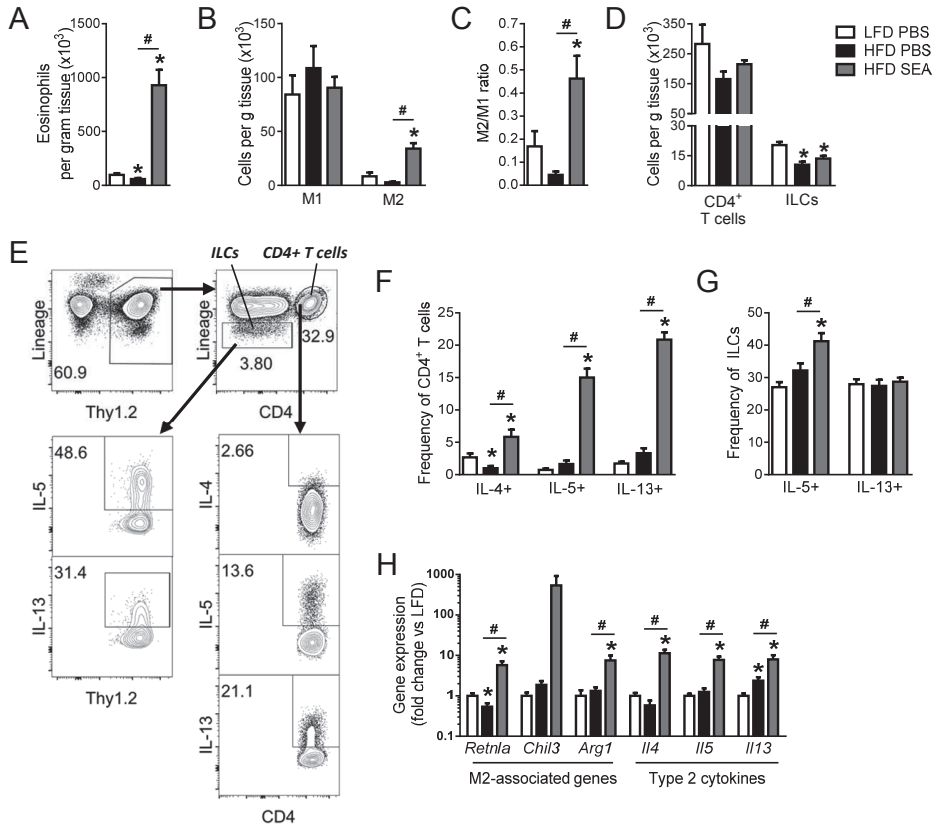


Figure 5. SEA treatment promotes adipose tissue Th2 polarization, and accumulation of eosinophils and alternatively-activated M2 macrophages. Mice were fed a LFD or HFD for 12 weeks, after which they were treated i.p. with PBS or 50 μ g SEA once every 3 days for a period of 4 weeks. At sacrifice (week 4), gonadal adipose tissue was collected and processed as described in the legend of Fig. 3. Following fixation, SVF cells were stained and analyzed by flow cytometry. Gating schemes for *ex vivo* analysis of lymphocyte subsets are shown in Supplemental Fig. 1. The numbers of eosinophils (A) and M1 and M2 macrophages (B) per gram tissue were determined, and the M2/M1 ratio was calculated (C). The numbers of CD4⁺ T cells and ILCs were determined (D). Intracellular cytokine production was analyzed after 4h stimulation with PMA and ionomycin in the presence of brefeldin A. Following gating on Aqua⁺CD45⁺ cells, lymphocyte subsets were analyzed by selecting for Thy1.2⁺ cells to enrich for T cells and ILCs. CD4⁺ T cells were subsequently identified as Lineage⁻CD4⁺ cells, in which the lineage cocktail included antibodies against CD3, CD11b, CD11c, B220, GR-1 and NK1.1. ILCs were identified as Lineage⁺CD4⁻ cells. Representative flow cytometry plots show the gating strategy for analysis of cytokine-expressing CD4⁺ T cells and ILCs (E). The frequencies of cytokine-expressing T cells (F) and ILCs (G) were determined. mRNA expression of the indicated genes was analyzed as described in the legend of Fig. 3 (H). *Retnla* encodes Fizz1; *Chil3* encodes Ym1. Results are expressed as means \pm SEM. * $P < 0.05$ HFD vs LFD, # $P < 0.05$ PBS vs SEA (n = 9-13 animals per group for all measurements except for intracellular analysis of IL-5 (n = 3-7)).

As classical activation of liver macrophages has also been observed in diet-induced obesity (39), we determined the effect of SEA treatment on the hepatic immune cell composition. Analysis of myeloid cells showed that HFD did not affect liver eosinophil numbers (Fig. 6A). Assessment of CD45⁺Siglec-F⁺CD11b^{lo}F4/80^{hi} macrophages (Fig. 6B), which were identified previously as Kupffer cells (40), showed that HFD promoted CD11c expression in these cells with no effect on Ym1 expression (Fig. 6C), thereby strongly decreasing the Ym1/CD11c ratio (Fig. 6D). HFD also decreased the numbers of CD4⁺T cells and ILCs (Fig. 6E), although analysis of cytokine production (Fig. 6F) showed that HFD did not affect expression of Th2 cytokines by T cells (Fig. 6G). HFD reduced the frequency of IL-5- and IL-13-expressing ILCs (Fig. 6G). SEA injections promoted eosinophil infiltration (Fig. 6A), but did not affect macrophage polarization (Fig. 6B,C), which was also confirmed by qPCR analysis (Fig. 6I). In line with our findings in WAT, SEA strongly increased expression of IL-4, IL-5 and IL-13 by CD4⁺ T cells in the liver (Fig. 6G), without a pronounced effect on the expression of type 2 cytokines by ILCs (Fig. 6H). Taken together, these findings indicate that helminth-derived molecules improve metabolic homeostasis, associated with the induction of eosinophils and Th2 cells in WAT and liver, and M2 macrophage polarization in WAT.

DISCUSSION

Over the past decade, it has become increasingly clear that multiple facets of the Th2-associated immune response promote metabolic homeostasis (6). Landmark studies have shown that infection of diet-induced obese mice with the rodent nematode *N. brasiliensis* ameliorates whole-body insulin sensitivity and glucose tolerance (18;26). In the present study, we analyzed which aspects of whole-body energy metabolism and WAT immune cell composition are affected by helminths, using a model of chronic *S. mansoni* infection. Unlike *N. brasiliensis*, which gives a strong Th2 response that mediates parasite clearance within two weeks, *S. mansoni* establishes a chronic infection, characterized by the presence of Th2 cells, alternatively activated macrophages, and a regulatory network (29). To study the effect of Th2-inducing conditions in a pathogen-free setting, we next exposed mice on a HFD to repetitive injections with *S. mansoni* soluble egg antigens.

We report that chronic exposure to *S. mansoni* induces a type 2 immune response in adipose tissue and improves both insulin sensitivity and glucose tolerance. These findings indicate that the beneficial effect of chronic *S. mansoni* infection on whole-body metabolic homeostasis, as reported previously for short-lived infection with *N. brasiliensis* (18;26), is a hallmark of helminth infection. Unique to our study, we have performed in-depth metabolic profiling, which showed that helminth infection specifically reduced fat mass and dampened HFD-induced adipocyte hypertrophy. However, we surprisingly did not find any changes in food intake or energy expenditure in our experimental conditions, leading us to speculate that chronic *S. mansoni* infection may affect nutrient efficiency by impairing intestinal lipid absorption. Another possibility is that dietary fat could be incorporated into eggs by the worms and next excreted through the feces. Further studies are required to clarify this specific

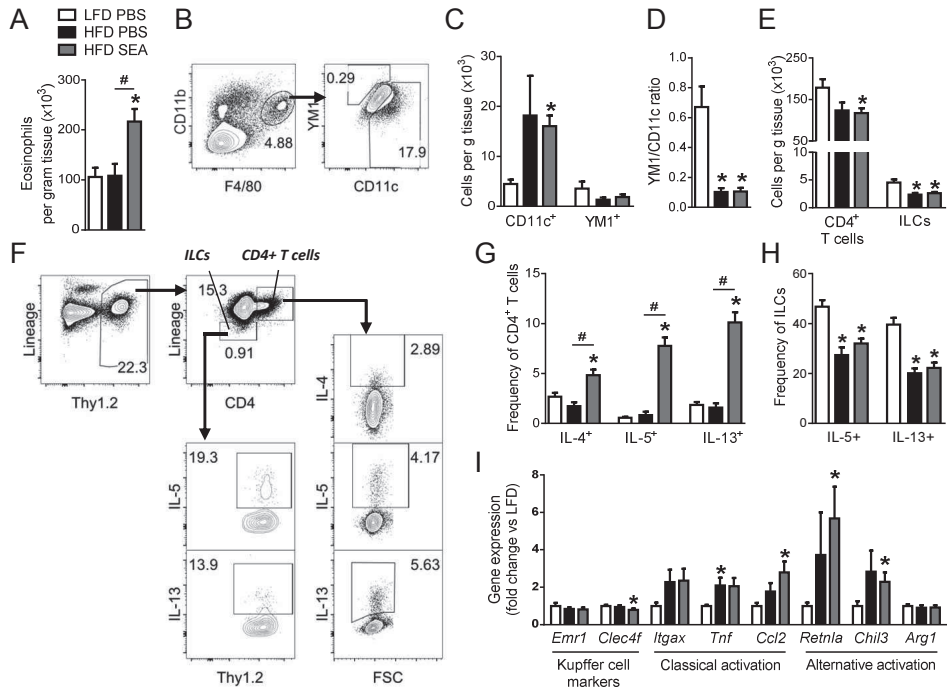


Figure 6. SEA treatment promotes accumulation of eosinophils and Th2 polarization in liver. Mice were fed a LFD or HFD for 12 weeks, after which they were treated i.p. with PBS or 50 μ g SEA once every 3 days for a period of 4 weeks. At sacrifice, livers were collected and a small piece was snap-frozen for qPCR analysis. From the remaining liver tissue, CD45⁺ cells were isolated and analyzed by flow cytometry. Gating schemes for *ex vivo* analysis of lymphocyte subsets are shown in Supplemental Fig. 1. The numbers of eosinophils (A) were determined. Kupffer cells were gated based on CD11b and F4/80 expression in Aqua CD45⁺Siglec-F⁺ cells (B). The number of CD11c⁺ and Ym1⁺ Kupffer cells (C) per gram liver were determined, and the Ym1⁺/CD11c⁺ ratio was calculated (D). The numbers of CD4⁺T cells and ILCs were determined (E). Intracellular cytokine expression was analyzed as described in the legend of Fig. 5. The gating strategy for analysis of cytokine-expressing CD4⁺T cells and ILCs is shown (F). The frequencies of cytokine-expressing CD4⁺T cells (G) and ILCs (H) were determined. mRNA expression of the indicated genes was analyzed as described in the legend of Fig. 3 (I). *Emr1* encodes F4/80; *Itgax* encodes CD11c; *Retnla* encodes Fizz1; *Chil3* encodes Ym1. Results are expressed as means \pm SEM. * P <0.05 HFD vs LFD, # P <0.05 WT vs Mrc1 (n = 11-13 animals per group).

point. Remarkably, infection improved fasting plasma glucose and insulin levels, whole-body glucose tolerance and insulin sensitivity in HFD-fed mice. Among the possible underlying mechanisms, we found that *S. mansoni* reversed HFD-induced inhibition of peripheral glucose uptake, which may be secondary to tissue-specific improvement of insulin sensitivity, as *S. mansoni*-infected HFD-fed mice exhibited higher insulin-induced PKB phosphorylation in WAT than uninfected controls.

Except for small effects on adipocyte volume, fasting insulin and energy expenditure, none of the metabolic parameters analyzed were affected by *S. mansoni* infection in mice on LFD, suggesting that helminths improve metabolic homeostasis independently of putative

S. mansoni-induced pathologies. We cannot exclude the possibility that part of the effect may be secondary to body weight loss or increased glucose/lipid metabolism by the helminths themselves. However, sustained exposure to SEA did not significantly affect body weight, but improved HOMA-IR, whole-body glucose tolerance and insulin sensitivity, in line with a previous report (41). Taken together, these findings suggest that the beneficial effects of helminths on metabolic homeostasis are not secondary to parasitism on host metabolism, but likely due to a direct effect on metabolic tissues or immune cells.

We demonstrate that *S. mansoni* infection reduced diet-induced body weight gain and improved HOMA-IR, once infection was established beyond 6 weeks. Glucose tolerance and peripheral glucose uptake were also improved after 11 but not 5 weeks of infection (Supplemental Fig. 3). Since egg production by adult worms triggers the development of a type 2 response ~6 weeks after infection (42), it is therefore likely that the beneficial effect of helminths on metabolic homeostasis may be mediated by the presence of eggs. This is further supported by our data showing that *S. mansoni* egg-derived soluble molecules improve glucose tolerance and insulin sensitivity in HFD-fed mice. Interestingly, improvements in metabolic homeostasis were also found in obese mice treated with the Lewis^x-containing glycan LNFPIII (41). Of note, we have demonstrated previously that omega-1, a Lewis^x-containing immunomodulatory RNase isolated from SEA, skews strong Th2 responses (43;44). Whether omega-1 contributes to the beneficial effect of helminth infection or SEA injection on energy homeostasis requires further study.

It is well-established that adipocyte hypertrophy in response to HFD induces cell necrosis, leading to the infiltration of M1 macrophages which later form crown-like structures around the necrotic cells (45;46). Chronic *S. mansoni* infection did not reduce M1 gene expression or cell numbers, suggesting that M1 macrophages continue to reside in WAT, even though glucose homeostasis improves. In line with this, SEA injections did not affect M1 cell numbers. These findings differ from a study by Fujisaka *et al.* (47) in which the anti-diabetic drug pioglitazone reduced expression of the CD11c-encoding gene, and lowered M1 cell numbers in gonadal WAT in HFD-fed mice. In addition, both infection with *N. brasiliensis* and pioglitazone treatment reduced total WAT macrophages (18;47), whereas chronic *S. mansoni* infection or SEA administration increased WAT macrophage numbers, as a result of an increase in M2 numbers. Taken together, these findings indicate that the M2/M1 ratio, rather than an increase or decrease in a particular macrophage subset, might be critical for metabolic homeostasis.

Mechanistically, the rise in WAT M2 macrophage numbers following chronic *S. mansoni* infection or repeated SEA administration may be a result of local macrophage proliferation, which has been reported in the pleural cavity upon infection with the filarial helminth *Litomosoides sigmodontis* in response to IL-4 (48). An alternative explanation could be that *S. mansoni* or SEA induce WAT monocyte infiltration and differentiation into M2 macrophages, which is plausible since we observed a significant increase in blood CD11b⁺Ly6C⁺ inflammatory Ym1-expressing monocytes during chronic infection (data not shown). Of note, it is rather unlikely that helminth-derived molecules trigger M2 polarization by directly interacting with

macrophages, as it has been described that SEA treatment does not induce expression of *Chil3* (encoding *Ym1*), *Mrc1* and *Arg1* by bone marrow-derived macrophages *in vitro* (27).

Importantly, it was demonstrated recently that maintenance of M2 macrophages in WAT depends on the presence of IL-4-secreting eosinophils (18), which are sustained by IL-5- and IL-13-producing ILC2s (19). In our study, we showed that chronic *S. mansoni* infection and SEA treatment promoted eosinophil accumulation in WAT, consistent with a previous reports on *N. brasiliensis* infection (18;19), and increased the mRNA levels of the type 2 cytokines IL-4 and IL-5. By analyzing intracellular IL-4, IL-5 and IL-13 cytokine production by lymphocytes isolated from gonadal WAT of SEA-treated mice, we found that CD4⁺ T cells, but not ILCs, produced increased levels of these type 2 cytokines. Recent literature described that IL-13 production by ILC2s in response to *S. mansoni* egg challenge peaks after 7 days of challenge and is reduced to baseline by day 21 (49). Since we analyze cytokine responses after 4 weeks of SEA administration, we speculate that ILC2 cytokine production has already diminished. Therefore, it is still possible that *S. mansoni*-induced ILC2s may be the first trigger for eosinophilia and accumulation of M2 macrophages in WAT. Then, at a later stage of infection or after long-term helminth antigen exposure, Th2-derived cytokines such as IL-4 may mediate M2 proliferation (48). Of note, we analyzed expression of a variety of eosinophil-attracting chemokines and eotaxins in WAT, but found no effect of SEA treatment (data not shown). Taken together, the interaction between the different cell types involved, as well as their relative contribution to the beneficial effect of helminths on WAT insulin sensitivity and whole-body metabolic homeostasis, requires further studies.

In addition to profound effects of SEA treatment on immune cells in WAT, we also observed increased eosinophilia and Th2 cytokine expression in the liver, suggesting that the adipose tissue is not an exclusive target of *S. mansoni*-derived antigens. Interestingly, it has been reported that both IL-4 and IL-13 may contribute to glucose homeostasis by directly regulating hepatic insulin sensitivity and glucose production, respectively (21;50). Helminth molecules may indeed work as a double-edged sword, acting on inflammatory and metabolic pathways in WAT and liver. The exact contribution of the liver to the whole-body metabolic beneficial phenotype observed in response to SEA treatment remains to be clarified.

In conclusion, our work has revealed that chronic infection with *S. mansoni*, as well as SEA treatment, protects against metabolic disorders in a mouse model of HFD-induced obesity. We have established that *S. mansoni* reduces adipocyte size and promotes peripheral glucose uptake and WAT-specific insulin sensitivity. Through analysis of immune cell composition at the cellular level, we show that SEA injections strongly increase eosinophils and Th2 cells in both WAT and liver, although they only promote M2 macrophage polarization in WAT. Collectively, our data identify *S. mansoni*-derived egg antigens as attractive agents for therapeutic manipulation of the immune system in the context of metabolic disorders. Several clinical trials are currently registered to assess the safety or efficacy of helminth therapy for the treatment of various inflammatory diseases in humans. As helminth infections can induce pathological conditions, studies are now focusing on helminth-derived molecules (51;52). The identification of single active molecules and the mechanisms by which they improve whole-body metabolic

homeostasis may offer new insights toward the development of novel therapeutics for the treatment of metabolic syndrome.

ACKNOWLEDGEMENTS

The authors also thank Bart Everts (LUMC, Leiden, The Netherlands) for critically reading the manuscript. This work was supported by an EFSD/Lilly Research Grant Fellowship from the European Federation for the Study of Diabetes (to BG), a Scientific Programme Indonesia-Netherlands-The Royal Netherlands Academy of Sciences Grant (SPIN-KNAW; KNAW-57-SPIN3-JRP; to MY and BG), the EU-funded project IDEA (HEALTH-F3-2009-241642; to MY), a ZonMW TOP Grant from the Dutch Organization for Scientific Research (91214131; to MY and BG), and a grant from the Board of Directors of the Leiden University Medical Center (to VvH).

REFERENCES

1. Calle EE, et al. Overweight, obesity, and mortality from cancer in a prospectively studied cohort of U.S. adults. *N Engl J Med* 2003 Apr 24;348(17):1625-38.
2. Herman WH, et al. Type 2 diabetes: an epidemic requiring global attention and urgent action. *Diabetes Care* 2012 May;35(5):943-4.
3. Ouchi N, et al. Adipokines in inflammation and metabolic disease. *Nat Rev Immunol* 2011 Feb;11(2):85-97.
4. Weisberg SP, et al. Obesity is associated with macrophage accumulation in adipose tissue. *J Clin Invest* 2003 Dec;112(12):1796-808.
5. Xu H, et al. Chronic inflammation in fat plays a crucial role in the development of obesity-related insulin resistance. *J Clin Invest* 2003 Dec;112(12):1821-30.
6. Chawla A, et al. Macrophage-mediated inflammation in metabolic disease. *Nat Rev Immunol* 2011 Nov;11(11):738-49.
7. Hotamisligil GS, et al. IRS-1-mediated inhibition of insulin receptor tyrosine kinase activity in TNF- α - and obesity-induced insulin resistance. *Science* 1996 Feb 2;271(5249):665-8.
8. Hotamisligil GS, et al. Adipose expression of tumor necrosis factor- α : direct role in obesity-linked insulin resistance. *Science* 1993 Jan 1;259(5091):87-91.
9. Feingold KR, et al. Stimulation of lipolysis in cultured fat cells by tumor necrosis factor, interleukin-1, and the interferons is blocked by inhibition of prostaglandin synthesis. *Endocrinology* 1992 Jan;130(1):10-6.
10. Green A, et al. Tumor necrosis factor increases the rate of lipolysis in primary cultures of adipocytes without altering levels of hormone-sensitive lipase. *Endocrinology* 1994 Jun;134(6):2581-8.
11. Rosen ED, et al. Adipocytes as regulators of energy balance and glucose homeostasis. *Nature* 2006 Dec 14;444(7121):847-53.
12. Talukdar S, et al. Neutrophils mediate insulin resistance in mice fed a high-fat diet through secreted elastase. *Nat Med* 2012 Sep;18(9):1407-12.
13. Liu J, et al. Genetic deficiency and pharmacological stabilization of mast cells reduce diet-induced obesity and diabetes in mice. *Nat Med* 2009 Aug;15(8):940-5.
14. Winer DA, et al. B cells promote insulin resistance through modulation of T cells and production of pathogenic IgG antibodies. *Nat Med* 2011 May;17(5):610-7.
15. DeFuria J, et al. B cells promote inflammation in obesity and type 2 diabetes through regulation of T-cell function and an inflammatory cytokine profile. *Proc Natl Acad Sci USA* 2013 Mar 26;110(13):5133-8.
16. Nishimura S, et al. CD8+ effector T cells contribute to macrophage recruitment and adipose tissue inflammation in obesity. *Nat Med* 2009 Aug;15(8):914-20.
17. Lumeng CN, et al. Obesity induces a phenotypic switch in adipose tissue macrophage polarization. *J Clin Invest* 2007 Jan;117(1):175-84.
18. Wu D, et al. Eosinophils sustain adipose alternatively activated macrophages associated with glucose homeostasis. *Science* 2011 Apr 8;332(6026):243-7.
19. Molofsky AB, et al. Innate lymphoid type 2 cells sustain visceral adipose tissue eosinophils and alternatively activated macrophages. *J Exp Med* 2013 Mar 11;210(3):535-49.
20. Winer S, et al. Normalization of obesity-associated insulin resistance through immunotherapy. *Nat Med* 2009 Aug;15(8):921-9.
21. Ricardo-Gonzalez RR, et al. IL-4/STAT6 immune axis regulates peripheral nutrient metabolism and insulin sensitivity. *Proc Natl Acad Sci USA* 2010 Dec 28;107(52):22617-22.
22. Feuerer M, et al. Lean, but not obese, fat is enriched for a unique population of regulatory T cells that affect metabolic parameters. *Nat Med* 2009 Aug;15(8):930-9.
23. Chen Y, et al. Association of previous schistosome infection with diabetes and metabolic syndrome: a cross-sectional study in rural China. *J Clin Endocrinol Metab* 2013 Feb;98(2):E283-E287.
24. Aravindhan V, et al. Decreased prevalence of lymphatic filariasis among diabetic subjects associated with a diminished pro-inflammatory cytokine response (CURES 83). *PLoS Negl Trop Dis* 2010;4(6):e707.
25. Wiria AE, et al. Helminth infections, type-2 immune response, and metabolic syndrome. *PLoS Pathog* 2014 Jul;10(7):e1004140.
26. Yang Z, et al. Parasitic nematode-induced modulation of body weight and associated metabolic dysfunction in mouse models of obesity. *Infect Immun* 2013 Jun;81(6):1905-14.

27. Wolfs IM, et al. Reprogramming macrophages to an anti-inflammatory phenotype by helminth antigens reduces murine atherosclerosis. *FASEB J* 2014 Jan;28(1):288-99.
28. World Health Organization. Schistosomiasis. <http://www.who.int/schistosomiasis/en/> 2013 Available from: URL: <http://www.who.int/schistosomiasis/en/>
29. Dunne DW, et al. A worm's eye view of the immune system: consequences for evolution of human autoimmune disease. *Nat Rev Immunol* 2005 May;5(5):420-6.
30. Maizels RM, et al. Immune regulation by helminth parasites: cellular and molecular mechanisms. *Nat Rev Immunol* 2003 Sep;3(9):733-44.
31. Hussaarts L, et al. Regulatory B-cell induction by helminths: implications for allergic disease. *J Allergy Clin Immunol* 2011 Oct;128(4):733-9.
32. Smits HH, et al. Protective effect of Schistosoma mansoni infection on allergic airway inflammation depends on the intensity and chronicity of infection. *J Allergy Clin Immunol* 2007 Oct;120(4):932-40.
33. Ackermans MT, et al. The quantification of gluconeogenesis in healthy men by (2)H₂O and [2-(13)C]glycerol yields different results: rates of gluconeogenesis in healthy men measured with (2)H₂O are higher than those measured with [2-(13)C]glycerol. *J Clin Endocrinol Metab* 2001 May;86(5):2220-6.
34. van den Berg SA, et al. High levels of dietary stearate promote adiposity and deteriorate hepatic insulin sensitivity. *Nutr Metab (Lond)* 2010;7:24.
35. Jo J, et al. Hypertrophy and/or Hyperplasia: Dynamics of Adipose Tissue Growth. *PLoS Comput Biol* 2009 Mar;5(3):e1000324.
36. Geerling JJ, et al. Metformin Lowers Plasma Triglycerides by Promoting VLDL-Triglyceride Clearance by Brown Adipose Tissue in Mice. *Diabetes* 2014 Mar;63(3):880-91.
37. de Jong EC, et al. Microbial compounds selectively induce Th1 cell-promoting or Th2 cell-promoting dendritic cells in vitro with diverse th cell-polarizing signals. *J Immunol* 2002 Feb 15;168(4):1704-9.
38. Okano M, et al. Induction of Th2 responses and IgE is largely due to carbohydrates functioning as adjuvants on Schistosoma mansoni egg antigens. *J Immunol* 1999 Dec 15;163(12):6712-7.
39. Morinaga H, et al. Characterization of Distinct Subpopulations of Hepatic Macrophages in HFD/Obese Mice. *Diabetes* 2014 Oct 14;
40. Movita D, et al. Kupffer cells express a unique combination of phenotypic and functional characteristics compared with splenic and peritoneal macrophages. *J Leukoc Biol* 2012 Oct;92(4):723-33.
41. Bhargava P, et al. Immunomodulatory glycan LNFP III alleviates hepatosteatosis and insulin resistance through direct and indirect control of metabolic pathways. *Nat Med* 2012 Nov;18(11):1665-72.
42. Pearce EJ, et al. The immunobiology of schistosomiasis. *Nat Rev Immunol* 2002 Jul;2(7):499-511.
43. Everts B, et al. Omega-1, a glycoprotein secreted by Schistosoma mansoni eggs, drives Th2 responses. *J Exp Med* 2009 Aug 3;206(8):1673-80.
44. Everts B, et al. Schistosome-derived omega-1 drives Th2 polarization by suppressing protein synthesis following internalization by the mannose receptor. *J Exp Med* 2012 Sep 24;209(10):1753-67, S1.
45. Pajvani UB, et al. Fat apoptosis through targeted activation of caspase 8: a new mouse model of inducible and reversible lipodystrophy. *Nat Med* 2005 Jul;11(7):797-803.
46. Cinti S, et al. Adipocyte death defines macrophage localization and function in adipose tissue of obese mice and humans. *J Lipid Res* 2005 Nov;46(11):2347-55.
47. Fujisaka S, et al. Regulatory mechanisms for adipose tissue M1 and M2 macrophages in diet-induced obese mice. *Diabetes* 2009 Nov;58(11):2574-82.
48. Jenkins SJ, et al. Local macrophage proliferation, rather than recruitment from the blood, is a signature of TH2 inflammation. *Science* 2011 Jun 10;332(6035):1284-8.
49. Hams E, et al. IL-25 and type 2 innate lymphoid cells induce pulmonary fibrosis. *Proc Natl Acad Sci USA* 2014 Jan 7;111(1):367-72.
50. Stanya KJ, et al. Direct control of hepatic glucose production by interleukin-13 in mice. *J Clin Invest* 2013 Jan 2;123(1):261-71.
51. Harnett W, et al. Helminth-derived immunomodulators: can understanding the worm produce the pill? *Nat Rev Immunol* 2010 Apr;10(4):278-84.
52. Wammes LJ, et al. Helminth therapy or elimination: epidemiological, immunological, and clinical considerations. *Lancet Infect Dis* 2014 Nov;14(11):1150-62.

SUPPLEMENTAL DATA

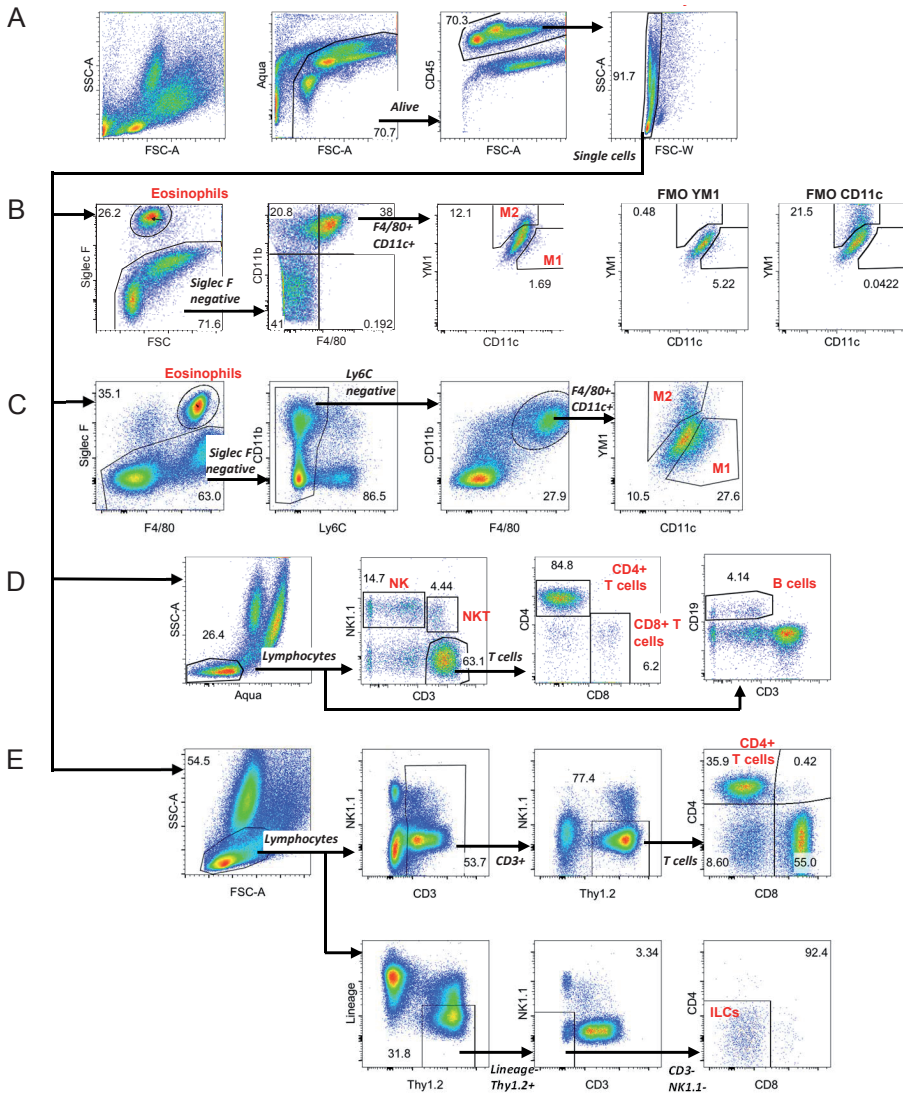


Figure S1. Gating strategies. Isolated cells were pre-gated on Aqua CD45⁺ single cells (A). The gating strategy for analysis of eosinophils, CD11c⁻ M1 macrophages and Ym1⁺ M2 macrophages is shown, including Fluorescence Minus One (FMO) controls for Ym1 and CD11c, in a representative sample from the chronic infection study (B) and the i.p. injection study (C). The gating strategy is shown for NK cells, NKT cells, CD4⁺ T cells, CD8⁺ T cells and B cells in a representative sample from the chronic infection study (D), and for CD4⁺ T cells and innate lymphoid cells (ILCs) in a representative sample from the i.p. study (E). For *ex vivo* analysis of CD4⁺ T cells and ILCs, the lineage cocktail included antibodies against CD11b, CD11c, B220 and GR-1. Note: Gating on CD4⁺ T and ILCs with CD3 in the lineage channel gave similar results. Representative samples were chosen from gonadal adipose tissue; gating strategies were similar for the analysis of myeloid and lymphoid subsets in visceral adipose tissue and liver.

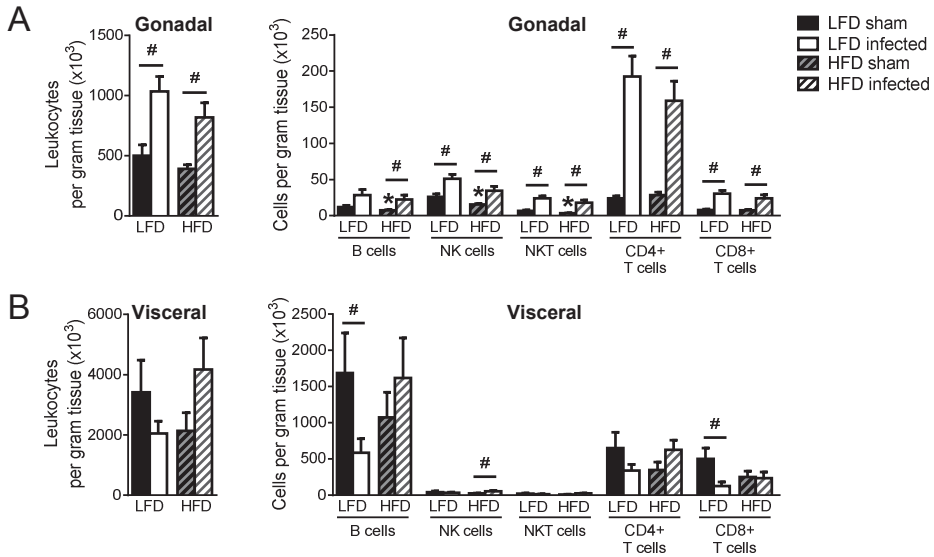


Figure S2. Lymphocyte composition of WAT. Mice were fed a LFD or a HFD for 6 weeks before infection with *S. mansoni* cercariae or sham-infection for 12 weeks. At sacrifice (week 12), various adipose tissues were collected and their stromal vascular fractions (SVF) were isolated. Following fixation, SVF cells were stained and analyzed by flow cytometry. The gating strategy is shown in figure S1D. The numbers of CD45⁺ leukocytes and indicated lymphocyte populations per gram tissue for gonadal (A) and visceral (B) WAT were determined. Results are expressed as means \pm SEM. * $P < 0.05$ vs LFD, # $P < 0.05$ vs sham-infected group (n = 12-18 animals per group in A, and 5-13 animals per group in B).

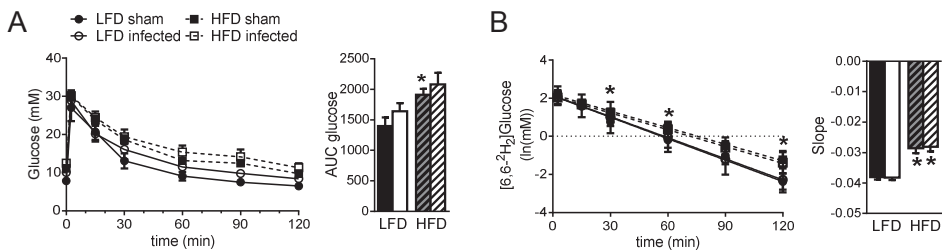
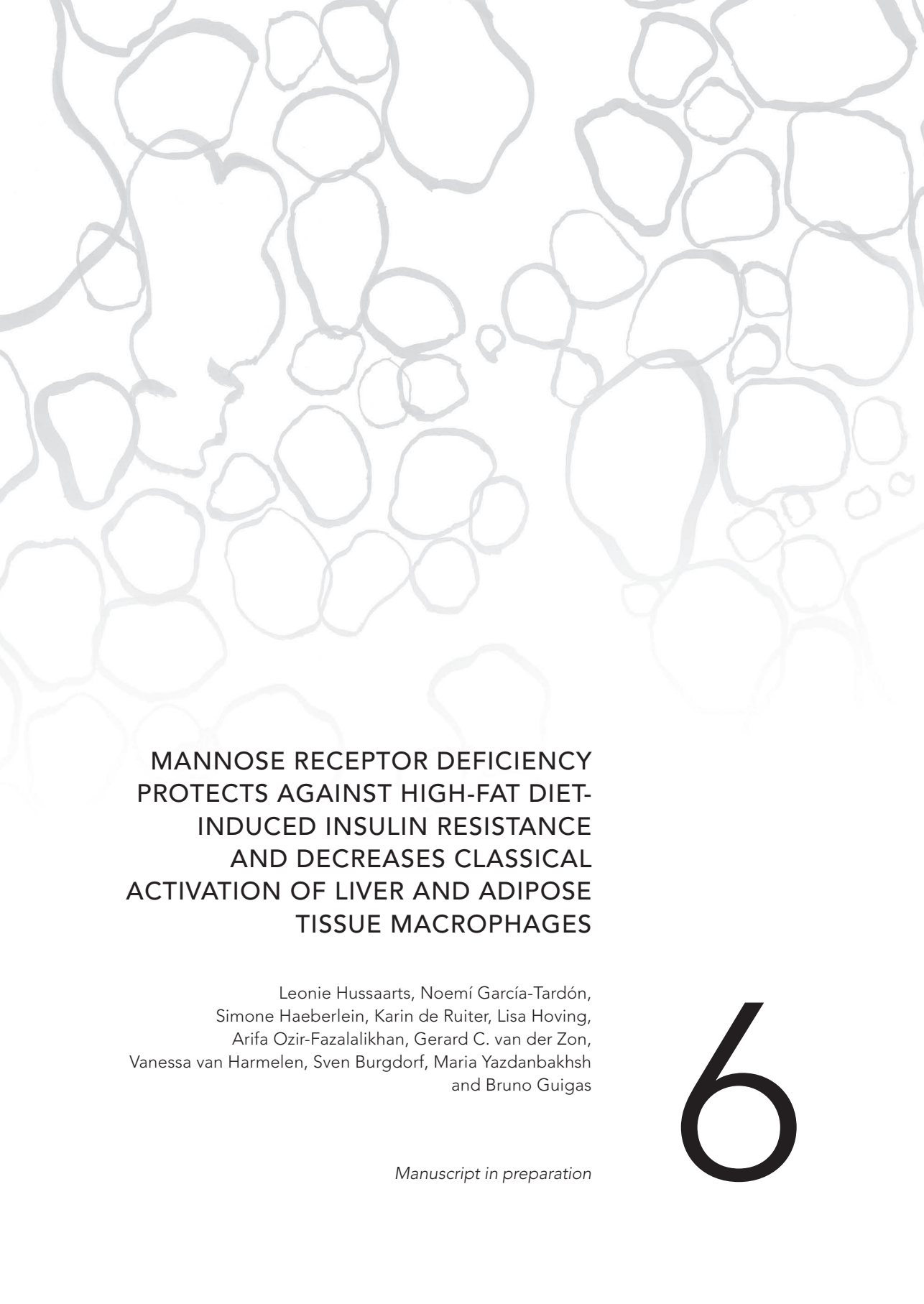


Figure S3. *S. mansoni* infection does not affect glucose tolerance or uptake after 5 weeks of infection. Mice were fed a LFD or a HFD and were infected with *S. mansoni* as described in the legend of Fig. S2. An intravenous glucose tolerance test (2g D-glucose with 50% [6,6-²H₂]glucose / kg BW) was performed in 6h-fasted mice at week 5. Blood glucose levels were measured at the indicated time points and the area under the curve (AUC) of the glucose excursion curve was calculated (A). Blood was also collected for determination of the time-dependent change in [6,6-²H₂]glucose concentration by gas chromatography mass spectrometry. For each mouse, a decay curve was fitted of which the slope represents peripheral glucose uptake (B). Results are expressed as means \pm SEM. * $P < 0.05$ vs LFD (n = 4-11 animals per group).



**MANNOSE RECEPTOR DEFICIENCY
PROTECTS AGAINST HIGH-FAT DIET-
INDUCED INSULIN RESISTANCE
AND DECREASES CLASSICAL
ACTIVATION OF LIVER AND ADIPOSE
TISSUE MACROPHAGES**

Leonie Hussaarts, Noemí García-Tardón,
Simone Haeberlein, Karin de Ruiter, Lisa Hoving,
Arifa Ozir-Fazalalikhhan, Gerard C. van der Zon,
Vanessa van Harmelen, Sven Burgdorf, Maria Yazdanbakhsh
and Bruno Guigas

Manuscript in preparation

6

ABSTRACT

Chronic low-grade inflammation associated with obesity is one of the major contributors to insulin resistance, enhancing the risk for type 2 diabetes and cardiovascular diseases. The mannose receptor (MR) is an endocytic C-type lectin receptor predominantly expressed by dendritic cells and macrophages, including alternatively activated M2 macrophages that protect against insulin resistance. To investigate the role of MR on whole-body metabolic homeostasis, wild-type (WT) and MR knockout (MR^{-/-}) mice were studied following 18 weeks of low-fat diet (LFD) or high-fat diet (HFD). Although no metabolic phenotype was observed in LFD-fed MR^{-/-} mice, on HFD we found significant reductions in total body weight (-8.3%), fat mass gain (-25.6%), and liver weight (-16.6%) compared to WT mice. Furthermore, MR deficiency lowered HFD-induced alterations in both whole-body glucose tolerance and insulin sensitivity (-22.9% and -17.1%, respectively), as assessed by intraperitoneal glucose and insulin tests. This effect was associated with enhanced locomotor activity, food intake and energy expenditure in MR^{-/-} mice when compared to WT. Remarkably, analysis of the immune cell composition of metabolic organs indicated that HFD decreased white adipose tissue (WAT) eosinophil numbers in WT but not MR^{-/-} mice. In addition, MR^{-/-} mice were less susceptible to HFD-induced classical activation of macrophages, in both WAT and liver. In conclusion, we show that whole-body MR deficiency lowers HFD-induced chronic low grade inflammation of metabolic tissues and protects against insulin resistance in obese mice, suggesting that MR might play an unexpected role in the development of metabolic disorders.

INTRODUCTION

The mannose receptor (MR, CD206) is an endocytic C-type lectin receptor implicated in binding of glycoproteins from endogenous and microbial origin, and in antigen presentation (1). Over the past decade, it has become clear that the MR may play a pivotal role in regulating type 2 inflammatory responses. For example, MR is required for Th2 polarization by human monocyte-derived dendritic cells stimulated with helminth antigens (2) and Der p 1 allergen (3). In line with these findings, lack of MR was shown to promote Th1 cytokine production following *Schistosoma mansoni* infection (4), and to reduce IgE production in response to allergen sensitization (5). Furthermore, MR-deficient mice exhibit defective clearance of endogenous serum glycoproteins (6), and it was recently described that MR expression by macrophages mediates collagen uptake (7), suggesting that the receptor may also contribute to tissue repair and remodeling.

MR is predominantly expressed by subpopulations of dendritic cells and macrophages, including microglial cells (8;9), although its expression is not only restricted to leukocytes. For example, in mice, MR is also expressed by hepatic, splenic, lymphatic and dermal microvascular endothelia, and by glomerular kidney mesangial cells, tracheal smooth muscle cells, and retinal pigment epithelium (1;9;10). Macrophage subpopulations are traditionally classified along a linear scale, on which pro-inflammatory M1 macrophages represent one extreme, and alternatively activated M2 macrophages the other (11). While classical activation of macrophages depends on T helper 1-associated cytokines like IFN- γ (12;13), M2-like activation is mediated by type 2 cytokines, like IL-4 and IL-13, which concomitantly promote upregulation of MR expression (14;15).

While accumulation of TNF- α -secreting M1 macrophages has been reported in both liver and white adipose tissue (WAT) of obese mice, M2 macrophages prevail in lean adipose tissue and liver (16-19), where they can mediate energy homeostasis via multiple routes. WAT M2 macrophages were shown to secrete IL-10, which can act directly on adipocytes to potentiate insulin signaling and therefore inhibit TNF- α -induced insulin resistance (18;20). In addition, M2 macrophages mediate tissue repair (reviewed in (21)) and regulate thermogenesis by promoting biogenesis of beige fat in response to cold (22;23). In liver, M2-like Kupffer cells were suggested to directly modulate hepatic metabolism in favor of β -oxidation and mitochondrial oxidative phosphorylation (16). The M2 phenotype is sustained by cells that secrete type 2 cytokines, like eosinophils (24) and type 2 innate lymphoid cells (25), which thereby also contribute to metabolic homeostasis.

Although expression of MR is a hallmark of the M2 phenotype (14), and a close link has been described between MR and type 2 inflammation, the role of the MR in metabolic homeostasis remains unclear. In the present study, we therefore studied whole-body insulin sensitivity and glucose homeostasis, and immune cell polarization in metabolic organs from wild-type (WT) and MR-deficient mice (MR^{-/-}) fed a low-fat diet (LFD) or high-fat diet (HFD). We report that MR^{-/-} mice are less susceptible to HFD-induced obesity, insulin resistance and inflammation of metabolic tissues than WT mice, suggesting that the MR plays an unexpected role in the development of HFD-induced metabolic disorders.

RESULTS

MR deficiency protects against HFD-induced obesity

Before being put on LFD or HFD, three-month-old WT and MR^{-/-} mice were similar in terms of body weight, lean mass, fat mass, and fasting plasma glucose and triglyceride levels (Table S1). However, MR^{-/-} mice had slightly higher fasting plasma cholesterol levels, and a trend for lower insulin levels (Table S1). To investigate the impact of MR deficiency on whole-body energy and metabolic homeostasis, C57BL/6 WT and MR^{-/-} mice were fed a LFD or HFD for 18 weeks. As expected, HFD induced an increase in body weight (Fig. 1A) and fat mass (Fig. 1B)

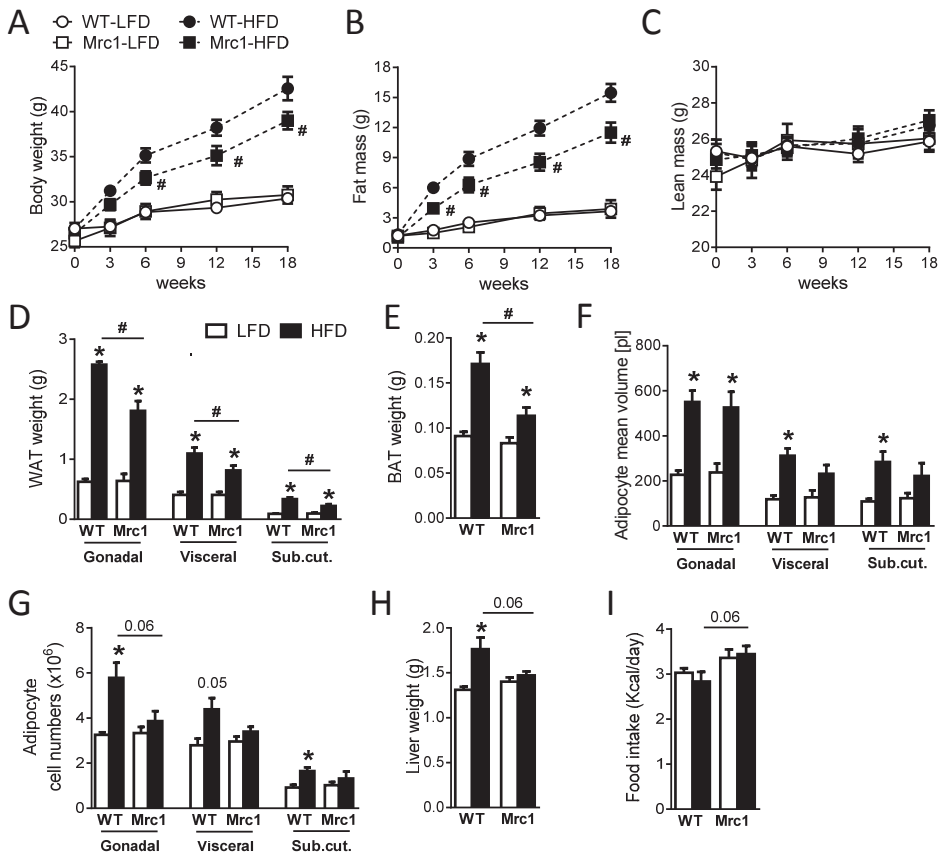


Figure 1. MR deficiency protects against HFD-induced weight gain, fat mass gain and adipocyte hyperplasia. Wild-type (WT) and MR-deficient (Mrc1) mice were fed a LFD or a HFD for 18 weeks. Throughout the experimental period, body weight (A) and body composition were monitored, and fat mass (B) and lean mass (C) were determined. At sacrifice, the weight of the different white fat pads (D) and of the subcutaneous brown fat (E) were measured, as well as the adipocyte mean volume (F) and the number of adipocytes (G). Liver weight was determined at sacrifice (H), and food intake was assessed using fully automated single-housed metabolic cages at week 16 (I). Results are expressed as means \pm SEM. * $P < 0.05$ HFD vs LFD, # $P < 0.05$ WT vs Mrc1 ($n = 10-15$ animals per group in A-E, H, and 4-8 animals per group in F, G, I).

without affecting lean mass (Fig. 1C) in both WT and MR^{-/-} mice. However, MR^{-/-} mice gained significantly less body weight than WT mice (Fig. 1A), secondary to a decrease in fat mass gain (Fig. 1B). Analysis of the individual fat pads showed that MR deficiency impaired HFD-induced weight gain of WAT (Fig. 1D) and brown adipose tissue (Fig. 1E). White adipocyte volume was not significantly different between genotypes (Fig. 1F), but the number of adipocyte cells was lower in HFD-fed MR^{-/-} when compared to WT mice (Fig. 1G). MR deficiency also impaired HFD-induced gain of liver mass (Fig. 1H), suggesting a reduction in hepatic steatosis. Importantly, the effects of MR deficiency on body composition were not due to a decrease in food consumption, since lack of MR was rather accompanied by a mild increase in caloric intake (Fig. 1I).

Furthermore, HFD reduced locomotor activity (Fig. 2A) and energy expenditure (EE; Fig. 2B) in WT mice, but not in MR^{-/-} mice. In both genotypes, HFD reduced carbohydrate oxidation (CHO; Fig. 2C) and increased fatty acid oxidation (FAO; Fig. 2D), although MR^{-/-} mice were found to oxidize slightly more carbohydrates (Fig. 2C). Taken together, these findings show that MR^{-/-} mice are partly protected against HFD-induced obesity, an effect associated with increased locomotor activity, food intake and energy expenditure.

MR deficiency improves whole-body glucose tolerance and insulin sensitivity in HFD-fed mice

We next investigated the effect of MR deficiency on fasting plasma parameters in LFD- and HFD-fed mice. In both genotypes, HFD increased plasma glucose (Fig. 3A) and insulin levels (Fig. 3B), HOMA-IR (Fig. 3C), and total cholesterol (Fig. 3D), without affecting triglyceride levels (Fig. 3E). However, lack of MR significantly decreased the HFD-induced rise in plasma insulin levels (Fig. 3B) and improved HOMA-IR (Fig. 3C), suggesting a lower insulin resistance than WT mice. In line with these findings, HFD-fed MR^{-/-} mice exhibited a better glucose tolerance, as assessed by an intraperitoneal glucose tolerance test (ipGTT Fig. 3F), without a change in insulin levels (Fig. 3G), indicating improvement in whole-body insulin sensitivity. This was confirmed by an intraperitoneal insulin tolerance test (ipITT) showing that acute injection of insulin lowered glucose levels to a larger extent in MR^{-/-} mice compared to WT mice (Fig. 3H). Taken together, these findings suggest that MR^{-/-} mice are less susceptible to HFD-induced metabolic dysfunctions than WT mice.

MR deficiency attenuates HFD-induced inflammation in adipose tissue

Based on the finding that M2 macrophages protect against insulin resistance (26), and the association between the MR and the M2 phenotype (14), we next investigated whether MR deficiency affects adipose tissue inflammation. We isolated the stromal vascular fraction (SVF) from gonadal WAT and analyzed the immune cell composition by flow cytometry. Analysis of myeloid cells (Fig. 4A) indicated that HFD reduced the numbers of eosinophils (Fig. 4B) and neutrophils (Fig. 4C) only in WT mice and not in MR^{-/-} mice. Furthermore, HFD increased the number of M1 macrophages in WT mice (Fig. 4D), thereby decreasing the M2/M1 ratio (Fig. 4E), as expected. Remarkably, while total macrophage numbers were not affected by diet

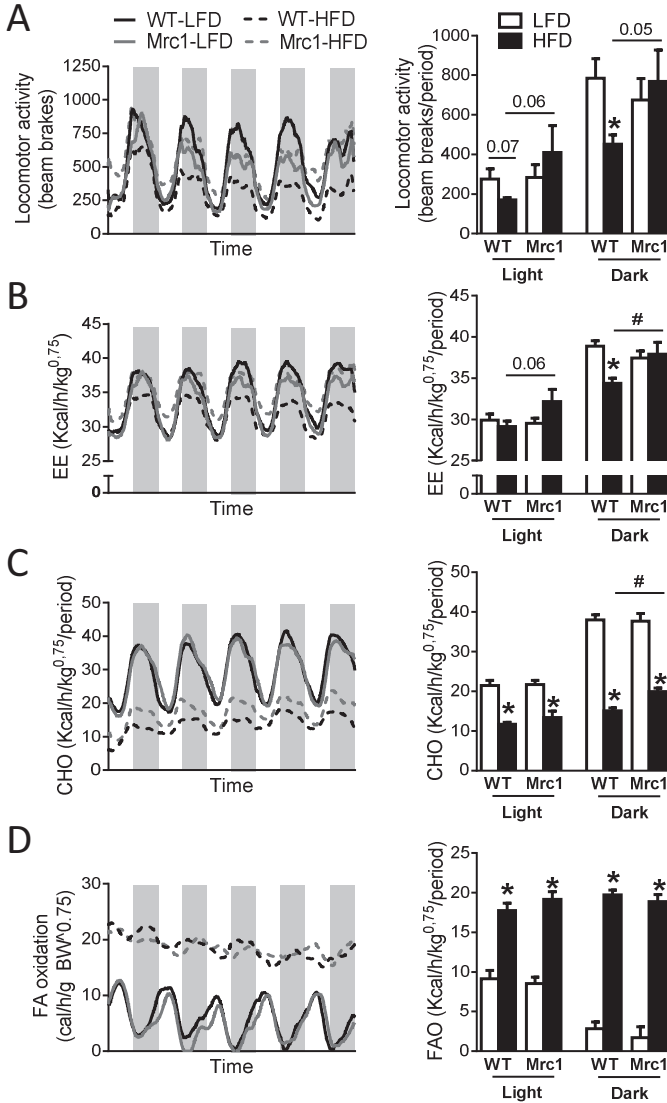


Figure 2. HFD does not affect locomotor activity and energy expenditure in MR^{-/-} mice. Wild-type (WT) and MR-deficient (Mrc1) mice were fed a LFD or a HFD for 18 weeks. At week 16, mice with free access to food and water were subjected to individual indirect calorimetric measurements using fully automated metabolic cages. Spontaneous locomotor activity (A), energy expenditure (EE; B), carbohydrate oxidation (CHO; C) and fatty acid oxidation (FAO; D) were determined. Results are expressed as means ± SEM. * P<0.05 HFD vs LFD, # P<0.05 WT vs Mrc1 (n = 6-8 animals per group).

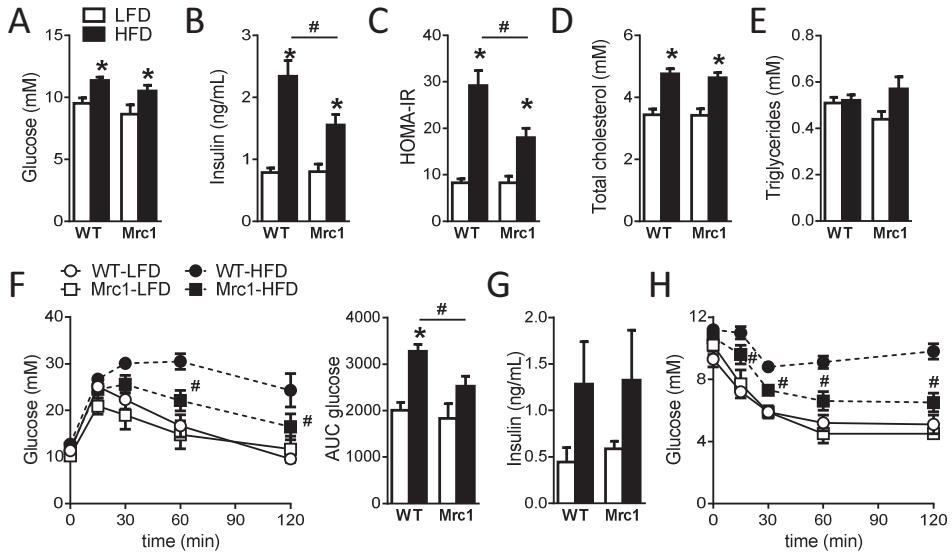


Figure 3. MR deficiency improves whole-body glucose tolerance and insulin sensitivity in HFD-fed animals. Wild-type (WT) and MR-deficient (*Mrc1*) mice were fed a LFD or a HFD for 18 weeks. At week 18, mice were fasted for 4h and plasma was collected to determine glucose (A) and insulin levels (B), HOMA-IR (C), and total cholesterol (D) and triglyceride levels (E). An intravenous glucose tolerance test (2g D-glucose/kg body weight) was performed in 6h-fasted mice at week 17. Blood glucose levels were measured at the indicated time points and the area under the curve (AUC) of the glucose excursion curve was calculated as a measure for glucose tolerance (F). 15 minutes after the i.p. bolus of glucose, blood was also collected for analysis of plasma insulin levels (G). An i.p. insulin tolerance test (1U/kg lean body mass) was performed in 4h-fasted mice at week 15. Blood glucose levels were measured at the indicated time points (H). Results are expressed as means \pm SEM. * $P < 0.05$ HFD vs LFD, # $P < 0.05$ WT vs *Mrc1*. Figures F, and H: only statistical significance of HFD WT vs HFD *Mrc1* is shown (n = 10-15 animals per group in A-E, and 3-10 animals per group in F-H).

or genotype (Fig. 4E), MR-deficient mice had higher numbers of M2 macrophages, and were partly protected against HFD-induced M1 polarization (Fig. 4F). As a consequence, HFD did not alter the M2/M1 ratio in MR^{-/-} mice (Fig. 4G). These findings were confirmed by quantitative PCR (qPCR), which indicated that lack of MR reversed HFD-induced increases in gene expression levels of *Itgax* (encoding CD11c), and the chemokine receptor *Ccr2* (Fig. S1A). Interestingly, neither diet nor genotype affected the numbers of eosinophils, neutrophils and inflammatory monocytes in the blood (Fig. S2), suggesting that the observed changes in myeloid immune cell composition are adipose tissue-specific.

Cells that secrete type 2 cytokines were shown to promote alternative activation of macrophages (13). Therefore, T cell and ILC responses in WAT of HFD-fed mice were analyzed next (Fig. 4G). MR deficiency significantly increased the frequency of ILCs, but not CD4⁺ T cells (Fig. 4H). Analysis of cytokine expression following *ex vivo* stimulation with phorbol myristate acetate (PMA) and ionomycin showed that IL-13 expression by WAT CD4⁺ T cells and ILCs was not significantly different between genotypes (Fig. 4I). We confirmed these findings by qPCR,

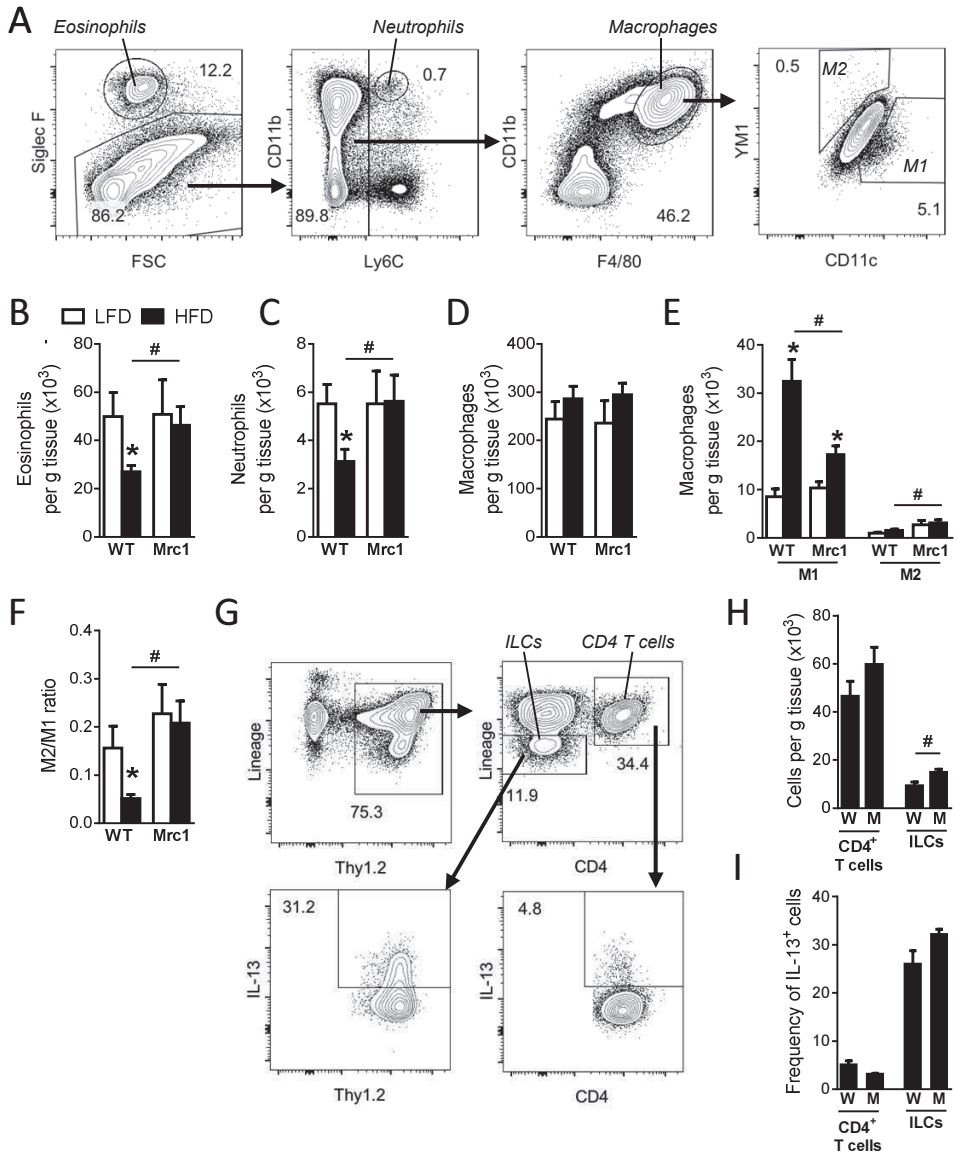


Figure 4. MR-deficient mice are less sensitive to HFD-induced inflammation in adipose tissue. Wild-type (WT) and MR-deficient (*Mrc1*) mice were fed a LFD or a HFD for 18 weeks. At sacrifice, gonadal adipose tissue was collected and the stromal vascular fraction (SVF) was isolated. Following fixation and permeabilization, SVF cells were stained and analyzed by flow cytometry. Cells were pre-gated for Aqua-CD45⁺ single cells. The gating strategy is shown for eosinophils, neutrophils, CD11c⁺ M1 macrophages and YM1⁺ M2 macrophages (A). The numbers of eosinophils (B), neutrophils (C), total macrophages (D) and M1 and M2 macrophages (E) per gram WAT were determined and the M2/M1 ratio was calculated (F). Following gating on Aqua-CD45⁺ single cells, lymphocyte subsets were analyzed by selecting for Thy1.2⁺ cells to enrich for T cells and ILCs. T cells were subsequently identified as Lineage⁻CD4⁺ cells, in which the lineage cocktail included antibodies against CD3, CD11b, CD11c, B220, GR-1, and NK1.1. ILCs were identified

which indicated that expression of pro- and anti-inflammatory cytokines was largely similar between groups (Fig. S1A).

MR deficiency attenuates HFD-induced activation of Kupffer cells

Obesity has also been associated with classical activation of liver macrophages (19). Therefore, CD45⁺ cells were isolated from liver and the hepatic immune cell composition was studied. Analysis of myeloid cells (Fig. 5A) showed that neither HFD nor genotype affected the numbers of eosinophils (Fig. 5B), neutrophils (Fig. 5C), monocytes (not shown), or CD45⁺SiglecF⁺CD11b^{lo}F4/80^{hi} macrophages (Fig. 5D), which were previously identified as Kupffer cells (27). Although we did not observe an effect of diet or genotype on YM1 expression by Kupffer cells, HFD significantly increased the expression of CD11c by these cells in WT mice, as expected (19). Remarkably, CD11c expression by Kupffer cells from MR^{-/-} mice was not affected by HFD-feeding (Fig. 5E). These findings were confirmed and expanded by qPCR analysis, which showed that HFD-feeding induced expression of *Itgax*, *Nos2*, *Ccl2* and *Ccr2* in WT but not MR^{-/-} mice (Fig. S1B).

Analysis of cytokine responses (Fig. 5F) indicated that HFD reduced the frequency of type 2 cytokine-expressing CD4⁺ T cells (Fig. 5G) and ILCs (Fig. 5H) in the livers of WT mice. Furthermore, expression of the ILC2-associated marker ICOS was decreased as a consequence of HFD (Fig. 5I). Although not significant, similar trends were observed for MR^{-/-} mice fed a HFD. These findings were confirmed by qPCR (Fig. S1B). Taken together, the results indicate that MR deficiency reduces susceptibility to HFD-induced classical activation of macrophages, in both WAT and liver.

DISCUSSION

Alternatively activated M2 macrophages prevail in lean adipose tissue and protect against diet-induced metabolic disorders (26). Because the MR is highly expressed by M2 macrophages (14), we explored the role the MR in the context of diet-induced obesity using MR^{-/-} mice. We report that lack of MR did not affect whole-body glucose tolerance and insulin sensitivity in mice fed a LFD, but counterintuitively improved metabolic homeostasis in mice fed a HFD despite considerable weight gain. Specifically, MR^{-/-} mice on HFD were less susceptible to fat mass gain and adipocyte hyperplasia, had a higher locomotor activity, and showed better insulin sensitivity and glucose tolerance than WT mice on HFD. Immune profiling indicated that in line with their metabolic phenotype, MR-deficient mice were less sensitive to HFD-induced classical activation of M1-like macrophages, in both liver and adipose tissue. Furthermore, in WAT, HFD reduced eosinophil and neutrophil numbers in WT but not MR^{-/-} mice. Contrary to expectations,

- ▶ as Lineage⁻CD4⁺ cells (G). The numbers of CD4⁺ T cells and ILCs per gram WAT were determined (H). Intracellular IL-13 expression was analyzed after 4h stimulation with PMA and ionomycin in the presence of Brefeldin A, the frequencies of IL-13⁺ CD4⁺ T cells and the frequencies of IL-13⁺ ILCs are shown (I). Results are expressed as means ± SEM. * P<0.05 HFD vs LFD, # P<0.05 WT vs Mrc1 (n = 10-15 animals per group in A-F, and 5-10 animals per group in G-I).

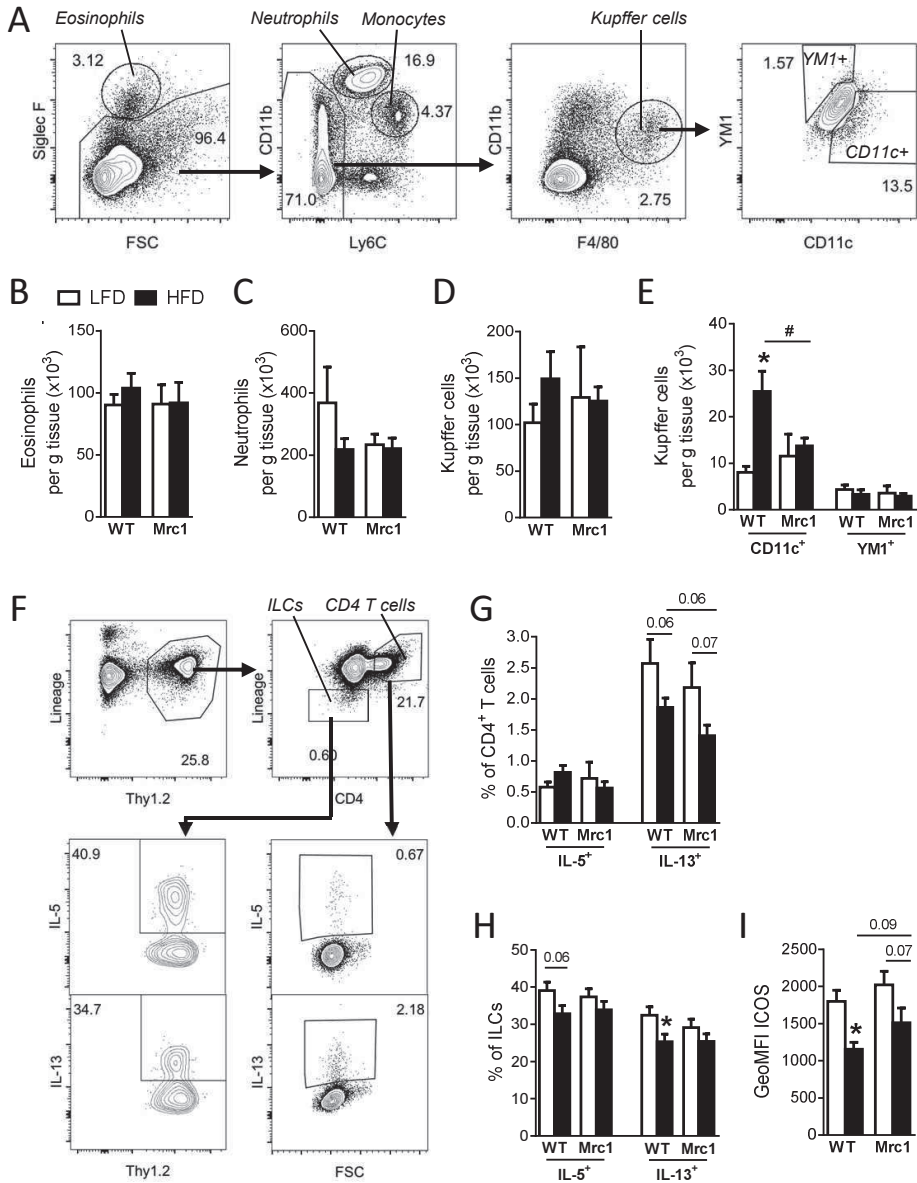


Figure 5. MR-deficient mice are less sensitive to HFD-induced activation of Kupffer cells. Wild-type (WT) and MR-deficient (*Mrc1*) mice were fed a LFD or a HFD for 18 weeks. At sacrifice, CD45⁺ liver cells were isolated and analyzed by flow cytometry as described in the legend of Figure 4. The gating strategy is shown for eosinophils, neutrophils, CD11c⁺ Kupffer cells and YM1⁺ Kupffer cells (A). The numbers of eosinophils (B), neutrophils (C), Kupffer cells (D), and CD11c⁺ and YM1⁺ Kupffer cells (E) per gram of liver tissue were determined. Intracellular cytokine expression was analyzed after 4h stimulation with PMA and ionomycin in the presence of Brefeldin A, as described in the legend of Figure 4, is shown for CD4⁺ T cells and ILCs (F). The frequencies of IL-5⁺ and IL-13⁺ CD4⁺ T cells (G) and IL-5⁺ and IL-13⁺ ILCs (H) are shown, and the expression of ICOS by ILCs was analyzed (I). Results are expressed as means \pm SEM. * $P < 0.05$ HFD vs LFD, # $P < 0.05$ WT vs *Mrc1* ($n = 10$ -15 animals per group).

M2-like activation and type 2-associated cytokine expression by T helper cells and ILC2s were not as strongly affected by genotype. These effects were surprising, given the association between MR and the M2 phenotype (14), and the pivotal role MR plays in the initiation of type 2 immune responses (2-5). The question whether immune- on non-immune-mediated mechanisms promote metabolic health in MR-deficient obese mice needs to be addressed.

We observed that MR-deficient mice are less susceptible to HFD-induced classical activation of macrophages. A possible immune-based explanation may be provided by our finding that M1 macrophages can also express MR, albeit to a much lower extent than M2 macrophages (unpublished data). In this context, it is worth mentioning that macrophage-associated scavenger receptors have been described to promote either pro- or anti-inflammatory responses depending on the co-receptor they form complexes with (28), and it has been suggested that the MR can form complexes with other receptors (29). Taken together, these observations may indicate that the MR can deliver a signal directly into the MR-bearing macrophage, which may result in polarization of either pro- or anti-inflammatory macrophages, depending on the nature of the co-receptors. Future studies are needed to elucidate whether MR expression by macrophages indeed mediates a pro-inflammatory phenotype under HFD conditions.

It is important to consider that MR^{-/-} mice lack whole-body expression of the *Mrc1* gene. In the mouse adult brain, MR is expressed by microglia and astrocytes, although its activities and involvement in brain functions are largely unknown (30). Of note, hypothalamic inflammation has been described to contribute to HFD-induced weight gain by promoting accumulation of microglia and astrocytes in various regions of the hypothalamus that coordinate the regulation of peripheral nutrient metabolism and energy expenditure (31;32). To study whether neuroinflammation differs between WT and MR^{-/-} mice, we performed qPCR analysis on whole hypothalamus. Although we observed the classical HFD-induced increase in some markers of inflammation, we did not find significant effects of genotype on expression of inflammatory genes (not shown). Recent literature suggested that the brain can also regulate metabolic homeostasis through the cholinergic anti-inflammatory reflex. In this reflex, molecular products of inflammation promote the release of acetylcholine by the *vagus* nerve, which reduces inflammation (33). It was recently demonstrated that neuronal deletion of *Pten*, a negative regulator of the PI3K pathway, activates the anti-inflammatory reflex, which promotes WAT M2 polarization and protects against insulin resistance in mice on HFD (34). The question whether MR deficiency affects HFD-induced neuroinflammation and/or activation of the anti-inflammatory reflex, and the possible consequences for metabolic disorders, remains an intriguing area of research.

MR expression is not only restricted to leukocytes (1), and the beneficial effect of MR deficiency on metabolic homeostasis might therefore be due to effects beyond the immune system or the brain. For example, high-fat diet-feeding increases LPS translocation from the gut (35), and it has been suggested that this so-called metabolic endotoxemia can contribute to M1 polarization in WAT (36). It would therefore be important to establish whether lack of MR affects LPS translocation and its circulating plasma level in response to HFD. Furthermore, MR on lymphatics is required for lymphocyte trafficking from the periphery into the draining

lymph nodes (37). MR deficiency may therefore prevent the induction of a strong immune response to HFD-feeding. Lastly, MR can also be expressed by cells in metabolic organs where it can play a functional role. Expression of MR by liver sinusoidal endothelial cells has been associated with clearance of lysosomal enzymes and collagen (6;38;39), and it was suggested that MR is required for the growth of skeletal muscle myofibers (40). We did not observe a metabolic phenotype in the LFD-fed MR^{-/-} animals, but we cannot exclude the possibility that expression of MR in metabolic tissues may mediate insulin resistance when the system is triggered by HFD-feeding.

In conclusion, our work has revealed an unexpected role for the MR in the development of obesity-induced metabolic disorders. Contrary to expectations, we have established that MR^{-/-} mice are less susceptible to HFD-induced weight gain, insulin resistance and glucose intolerance. These effects were associated with increased locomotor activity and energy expenditure, and decreased classical activation of WAT and liver macrophages. Whether the protective effect of MR deficiency can be attributed to MR expression by immune or non-immune cells remains an important area of research. Understanding these processes may offer valuable insights towards the development of targeted therapeutics for the treatment of metabolic syndrome.

MATERIALS AND METHODS

Animals and diet

All experiments were performed in accordance with the Guide for the Care and Use of Laboratory Animals of the Institute for Laboratory Animal Research and have received approval from the university Ethical Review Boards (Leiden University Medical Center, Leiden, The Netherlands). Male MR^{-/-} mice on a CD57BL/6 background, generated as described previously (6), were provided by Dr. Sven Burgdorf (University of Bonn, Germany). MR^{-/-} mice and age-matched C57BL/6 WT mice from the same breeding facility were housed in a temperature-controlled room with a 12 hour light-dark cycle. Throughout the experiment, food and tap water were available *ad libitum*. 8 – 10 week old mice were randomized according to total body weight, lean and fat mass, and fasting plasma glucose, insulin, TC and TG levels, after which they were fed a high-fat diet (HFD, 45% energy derived from fat, D12451, Research Diets) or a low-fat diet (LFD, 10% energy derived from fat, D12450B, Research Diets) for 18 weeks. Diets were similar in composition in all respects apart from the total fat content.

Plasma analysis

Blood samples were collected at 1:00 pm using chilled paraoxon-coated capillaries from the tail tip of 4h-fasted mice 18 weeks after the start of LFD- or HFD-feeding. Blood glucose level was determined using a Glucometer (Accu-Check, Roche Diagnostics). Using commercially available kits and standards according to the instructions of the manufacturer, we determined total cholesterol and triglycerides (Instruchemie) and plasma insulin (Chrystal Chem).

Glucose and insulin tolerance tests

Glucose tolerance was assessed by an ipGTT 17 weeks after the start of LFD- or HFD-feeding. Mice were fasted for 6h, and the tests were carried out at 2:00 pm. After an initial blood collection ($t=0$), an i.p. injection of glucose (2g D-Glucose/kg total body weight, Sigma-Aldrich) was administered in conscious mice. Blood glucose was measured by tail bleeding at 15, 30, 60, 90 and 120 minutes after glucose administration using a Glucometer (Accu-Check, Roche Diagnostics). At 15 minutes, blood was also collected for analysis of plasma insulin levels as described above.

Whole-body insulin sensitivity was assessed by an ipITT at 15 weeks post-infection. Mice were fasted for 4h, and the tests were carried out at 1:30 P.M. After an initial blood collection ($t=0$), an i.p. bolus of insulin (1 U/kg lean body mass; NOVORAPID, Novo Nordisk) was administered to the mice. Blood glucose was measured by tail bleeding at 15, 30, 60, and 90 min after insulin administration using a Glucometer.

Body composition and indirect calorimetry

Body composition was measured by MRI using an EchoMRI (Echo Medical Systems). Groups of eight mice with free access to food and water were subjected to individual indirect calorimetric measurements at 16 weeks after the start of the experiment for a period of 5 consecutive days using a Comprehensive Laboratory Animal Monitoring System (Columbus Instruments). Before the start of the measurements, the animals were acclimated to the cages and the single housing for a period of 48 h. Feeding behavior was assessed by real-time food intake. Spontaneous locomotor activity was determined by the measurement of beam breaks. Oxygen consumption and carbon dioxide production were measured at 15-min intervals. Energy expenditure and carbohydrate and fatty acid oxidation were calculated and normalized for body surface area ($\text{kg}^{0.75}$), as previously described (41).

Isolation of adipocytes and SVF from adipose tissue

Adipose tissues from the gonadal regions were collected. Two small fractions were taken for determination of adipocyte morphology and qPCR analysis, while the remainder was used for immune cell profiling by flow cytometry. For determination of adipocyte morphology, adipocytes were treated as described previously (Chapter 5, this thesis). The adipocyte size distribution, mean adipocyte diameter and volume, and adipocyte number per fat pad were calculated (42). For immune cell profiling by flow cytometry, adipose tissues were minced and digested for 1 h at 37°C in HEPES buffer (pH 7.4) containing 0.5g/l type 1 collagenase from *Clostridium histolyticum* (Sigma-Aldrich), 2% (w/v) dialyzed bovine serum albumin (BSA, fraction V, Sigma-Aldrich) and 6 mM glucose. Disaggregated adipose tissues were passed through 100 μm cell strainers which were washed with PBS supplemented with 2.5 mM EDTA and 5% FCS. After centrifugation (350 g , 10 minutes, room temperature), the supernatant of the filtrate was discarded and the pellet was treated with erythrocyte lysis buffer. The cells were washed once more and counted manually. Isolated SVF cells were split in two and either processed directly for the analysis of myeloid cells, or cultured for 4 hours in culture medium

in the presence of 100 ng/mL PMA, 1 µg/mL ionomycin and 10 µg/mL Brefeldin A (all Sigma-Aldrich). Following staining with the live/dead marker Aqua (Invitrogen), cells were fixed with 1.9% paraformaldehyde (Sigma-Aldrich) and stored in FACS buffer (PBS, 0.02% sodium azide, 0.5% FCS) at 4°C in the dark until subsequent analysis.

Isolation of CD45⁺ cells from liver tissue

Livers were minced and digested for 45 minutes at 37°C in RPMI 1640 + Glutamax (Life Technologies) containing 1 mg/mL collagenase type IV from *Clostridium histolyticum*, 2000 U/mL DNase (both Sigma-Aldrich) and 1 mM CaCl₂. The digested liver tissues were passed through 100 µm cell strainers which were washed with PBS supplemented with 2.5 mM EDTA and 5% FCS. Following centrifugation (530 g, 10 minutes, 4 degrees), the supernatant of the filtrate was discarded, after which the pellet was resuspended in PBS + 2.5 mM EDTA and 5% FCS and centrifuged at 50 g to remove hepatocytes (3 minutes, 4 degrees). Next, supernatants were collected and pelleted (530 g, 10 minutes, 4 degrees). The pellet was treated with erythrocyte lysis buffer, and the cells were washed once more with PBS + 2.5 mM EDTA and 5% FCS. CD45⁺ cells were isolated using LS columns and CD45 MicroBeads (35 µL per liver, Miltenyi Biotec) according to manufacturer's protocol. Isolated CD45⁺ cells were counted and processed as described for the SVF.

Flow cytometry

For analysis of myeloid subsets, cells were permeabilized with 0.5% saponin (Sigma-Aldrich) in which they were also stained. Cells were incubated with an antibody against YM1 conjugated to biotin, washed, and stained with streptavidin-PerCP (BD Biosciences) and antibodies directed against CD45 (FITC), CD11b (PE-Cy7), CD11c (HV450), F4/80 (APC), Siglec-F (PE) and Ly6C (APC-Cy7). Analysis of lymphocyte subsets in CD45⁺ cells isolated from liver was done using antibodies against CD45 (FITC), NK1.1 (PE), CD3 (APC), CD4 (PE-Cy7), CD8 (APC-Cy7), and B220 (eFluor450) diluted in FACS buffer. Finally, in PMA/ionomycin-stimulated samples, cytokine production of Th2 cells and ILCs was analysed following permeabilization as described above, using antibodies against CD11b (FITC), CD11c (FITC), GR-1 (FITC), B220 (FITC), NK1.1 (FITC), CD3 (FITC), CD4 (PerCP-eF710 or PE-Cy7), Thy1.2 (APC-eFluor780), and IL-13 (eFluor450). The stimulated CD45⁺ cells isolated from liver were also stained for ICOS (PE-Cy7) and IL-5 (PE), while the stimulated SVF was additionally stained for CD45 (PE). Flow cytometry was performed using a FACSCanto (BD Biosciences), and gates were set according to Fluorescence Minus One (FMO) controls. Antibody information is provided in Table S2.

RNA purification and qRT-PCR

RNA was extracted from snap-frozen adipose tissue samples (~20 mg) using Tripure RNA Isolation reagent (Roche Diagnostics). Total RNA (1 µg) was reverse transcribed and quantitative real-time PCR was then performed with SYBR Green Core Kit on a MyIQ thermal cycler (Bio-Rad) using specific primers sets (available upon request). mRNA expression was normalized to Rplp0 mRNA content and expressed as fold change compared to non-infected LFD-fed mice using the $\Delta\Delta\text{CT}$ method.

Statistical analysis

All data are presented as mean \pm standard error of the mean (SEM). Statistical analysis was performed using GraphPad Prism version 6.00 for Windows (GraphPad Software, La Jolla, CA, USA) with two-tailed unpaired Student's t tests. Differences between groups were considered statistically significant at $P < 0.05$. For repeated measurements, data were analysed assuming the same scatter to increase power.

ACKNOWLEDGEMENTS

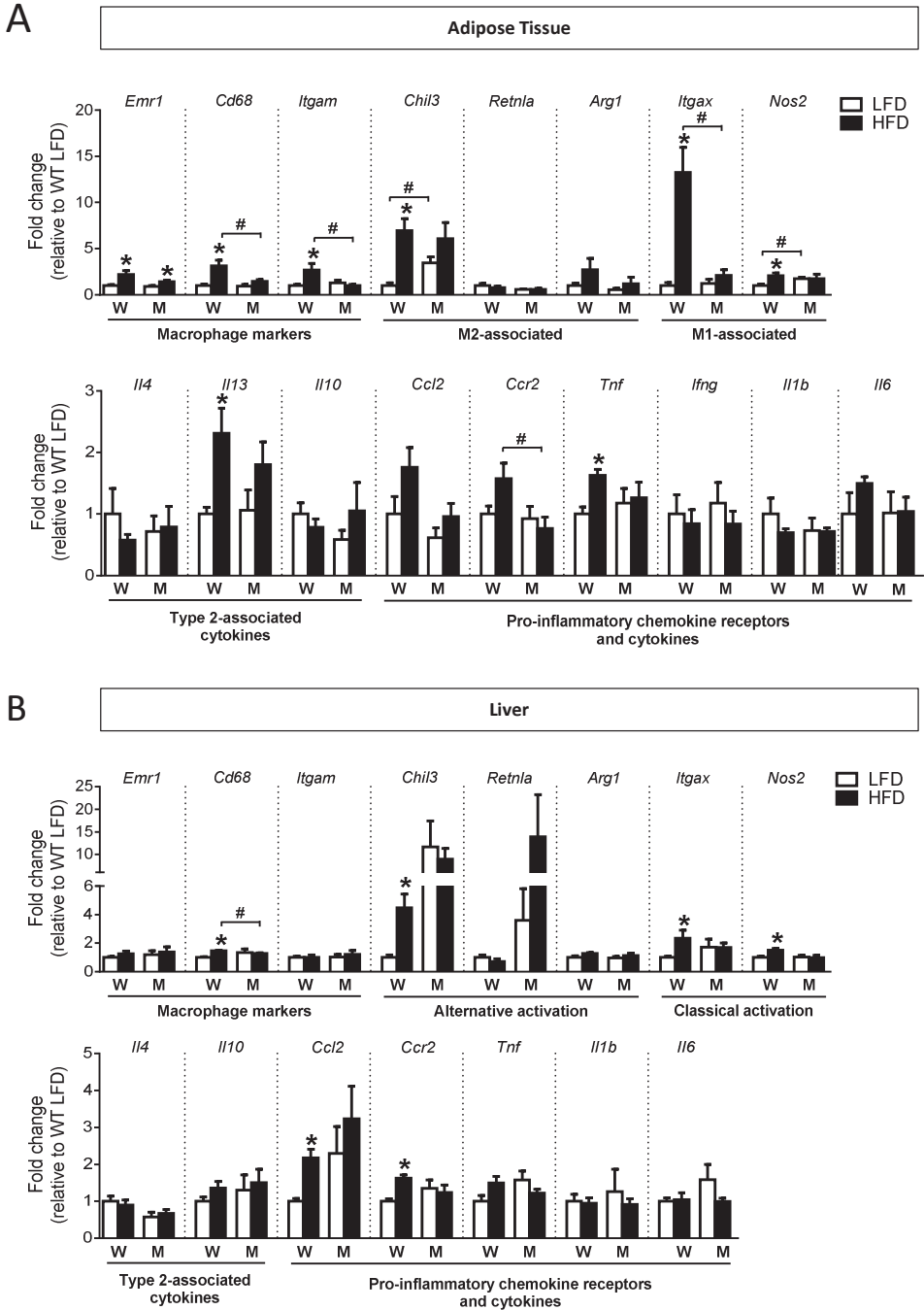
The authors thank Sander Kooijman, Patrick Rensen and Ko Willems van Dijk (LUMC) for facilitating experiments with automated metabolic cages.

REFERENCES

1. Martinez-Pomares L. The mannose receptor. *J Leukoc Biol* 2012 Dec;92(6):1177-86.
2. Everts B, et al. Schistosome-derived omega-1 drives Th2 polarization by suppressing protein synthesis following internalization by the mannose receptor. *J Exp Med* 2012 Sep 24;209(10):1753-67, S1.
3. Royer PJ, et al. The mannose receptor mediates the uptake of diverse native allergens by dendritic cells and determines allergen-induced T cell polarization through modulation of IDO activity. *J Immunol* 2010 Aug 1;185(3):1522-31.
4. Paveley RA, et al. The Mannose Receptor (CD206) is an important pattern recognition receptor (PRR) in the detection of the infective stage of the helminth *Schistosoma mansoni* and modulates IFN γ production. *Int J Parasitol* 2011 Nov;41(13-14):1335-45.
5. Emará M, et al. Recognition of the major cat allergen Fel d 1 through the cysteine-rich domain of the mannose receptor determines its allergenicity. *J Biol Chem* 2011 Apr 15;286(15):13033-40.
6. Lee SJ, et al. Mannose receptor-mediated regulation of serum glycoprotein homeostasis. *Science* 2002 Mar 8;295(5561):1898-901.
7. Madsen DH, et al. M2-like macrophages are responsible for collagen degradation through a mannose receptor-mediated pathway. *J Cell Biol* 2013 Sep 16;202(6):951-66.
8. McKenzie EJ, et al. Mannose receptor expression and function define a new population of murine dendritic cells. *J Immunol* 2007 Apr 15;178(8):4975-83.
9. Linehan SA, et al. Mannose receptor and its putative ligands in normal murine lymphoid and nonlymphoid organs: In situ expression of mannose receptor by selected macrophages, endothelial cells, perivascular microglia, and mesangial cells, but not dendritic cells. *J Exp Med* 1999 Jun 21;189(12):1961-72.
10. Taylor PR, et al. The mannose receptor: linking homeostasis and immunity through sugar recognition. *Trends Immunol* 2005 Feb;26(2):104-10.
11. Mosser DM, et al. Exploring the full spectrum of macrophage activation. *Nat Rev Immunol* 2008 Dec;8(12):958-69.
12. Dalton DK, et al. Multiple defects of immune cell function in mice with disrupted interferon-gamma genes. *Science* 1993 Mar 19;259(5102):1739-42.
13. Gordon S. Alternative activation of macrophages. *Nat Rev Immunol* 2003 Jan;3(1):23-35.
14. Stein M, et al. Interleukin 4 potently enhances murine macrophage mannose receptor activity: a marker of alternative immunologic macrophage activation. *J Exp Med* 1992 Jul 1;176(1):287-92.
15. Coste A, et al. PPAR γ promotes mannose receptor gene expression in murine macrophages and contributes to the induction of this receptor by IL-13. *Immunity* 2003 Sep;19(3):329-39.
16. Odegaard JI, et al. Alternative M2 activation of Kupffer cells by PPAR δ ameliorates obesity-induced insulin resistance. *Cell Metab* 2008 Jun;7(6):496-507.
17. Chawla A, et al. Macrophage-mediated inflammation in metabolic disease. *Nat Rev Immunol* 2011 Nov;11(11):738-49.
18. Lumeng CN, et al. Obesity induces a phenotypic switch in adipose tissue macrophage polarization. *J Clin Invest* 2007 Jan;117(1):175-84.
19. Morinaga H, et al. Characterization of Distinct Subpopulations of Hepatic Macrophages in HFD/Obese Mice. *Diabetes* 2014 Oct 14;
20. Feuerer M, et al. Lean, but not obese, fat is enriched for a unique population of regulatory T cells that affect metabolic parameters. *Nat Med* 2009 Aug;15(8):930-9.
21. Mantovani A, et al. Macrophage plasticity and polarization in tissue repair and remodelling. *J Pathol* 2013 Jan;229(2):176-85.
22. Nguyen KD, et al. Alternatively activated macrophages produce catecholamines to sustain adaptive thermogenesis. *Nature* 2011 Dec 1;480(7375):104-8.
23. Qiu Y, et al. Eosinophils and type 2 cytokine signaling in macrophages orchestrate development of functional beige fat. *Cell* 2014 Jun 5;157(6):1292-308.
24. Wu D, et al. Eosinophils sustain adipose alternatively activated macrophages associated with glucose homeostasis. *Science* 2011 Apr 8;332(6026):243-7.
25. Molofsky AB, et al. Innate lymphoid type 2 cells sustain visceral adipose tissue eosinophils and

- alternatively activated macrophages. *J Exp Med* 2013 Mar 11;210(3):535-49.
26. Odegaard JI, et al. Alternative macrophage activation and metabolism. *Annu Rev Pathol* 2011;6:275-97.
 27. Movita D, et al. Kupffer cells express a unique combination of phenotypic and functional characteristics compared with splenic and peritoneal macrophages. *J Leukoc Biol* 2012 Oct;92(4):723-33.
 28. Canton J, et al. Scavenger receptors in homeostasis and immunity. *Nat Rev Immunol* 2013 Sep;13(9):621-34.
 29. Gazi U, et al. Influence of the mannose receptor in host immune responses. *Immunobiology* 2009;214(7):554-61.
 30. Regnier-Vigouroux A. The mannose receptor in the brain. *Int Rev Cytol* 2003;226:321-42.
 31. Thaler JP, et al. Minireview: Inflammation and obesity pathogenesis: the hypothalamus heats up. *Endocrinology* 2010 Sep;151(9):4109-15.
 32. Thaler JP, et al. Obesity is associated with hypothalamic injury in rodents and humans. *J Clin Invest* 2012 Jan 3;122(1):153-62.
 33. Andersson U, et al. Neural reflexes in inflammation and immunity. *J Exp Med* 2012 Jun 4;209(6):1057-68.
 34. Wang L, et al. Pten deletion in RIP-Cre neurons protects against type 2 diabetes by activating the anti-inflammatory reflex. *Nat Med* 2014 May;20(5):484-92.
 35. Cani PD, et al. Metabolic endotoxemia initiates obesity and insulin resistance. *Diabetes* 2007 Jul;56(7):1761-72.
 36. Schipper HS, et al. Adipose tissue-resident immune cells: key players in immunometabolism. *Trends Endocrinol Metab* 2012 Aug;23(8):407-15.
 37. Marttila-Ichihara F, et al. Macrophage mannose receptor on lymphatics controls cell trafficking. *Blood* 2008 Jul 1;112(1):64-72.
 38. Elvevold K, et al. Liver sinusoidal endothelial cells depend on mannose receptor-mediated recruitment of lysosomal enzymes for normal degradation capacity. *Hepatology* 2008 Dec;48(6):2007-15.
 39. Malovic I, et al. The mannose receptor on murine liver sinusoidal endothelial cells is the main denatured collagen clearance receptor. *Hepatology* 2007 Jun;45(6):1454-61.
 40. Jansen KM, et al. Mannose receptor regulates myoblast motility and muscle growth. *J Cell Biol* 2006 Jul 31;174(3):403-13.
 41. van den Berg SA, et al. High levels of dietary stearate promote adiposity and deteriorate hepatic insulin sensitivity. *Nutr Metab (Lond)* 2010;7:24.
 42. Jo J, et al. Hypertrophy and/or Hyperplasia: Dynamics of Adipose Tissue Growth. *PLoS Comput Biol* 2009 Mar;5(3):e1000324.

SUPPLEMENTAL DATA



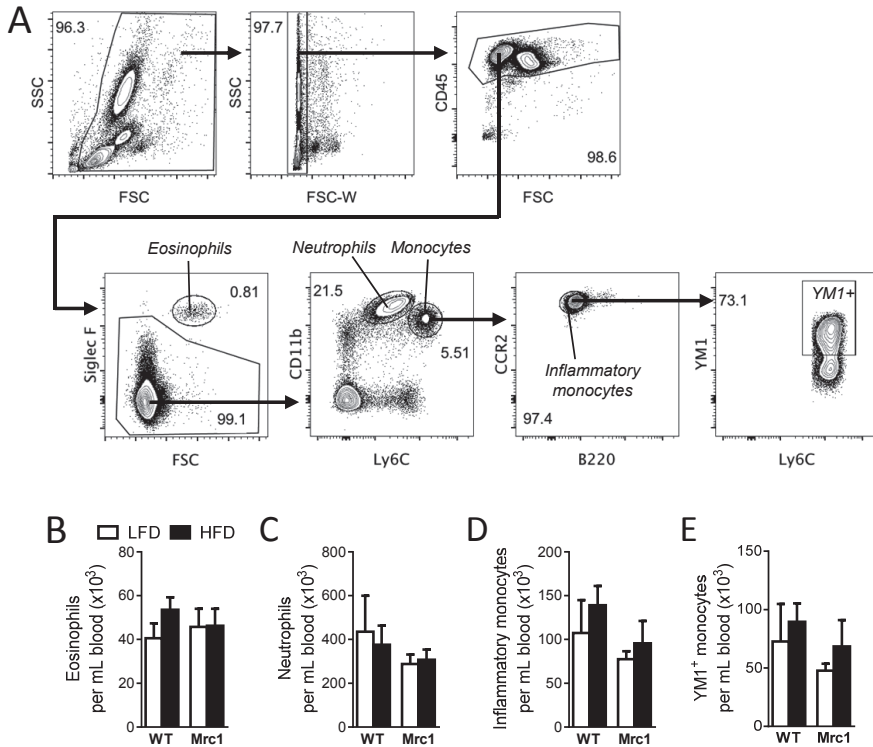


Figure S2. Diet and genotype do not affect myeloid cells in blood. Wild-type (WT) and MR-deficient (*Mrc1*) mice were fed a LFD or HFD for 18 weeks. At sacrifice, blood was collected and fixed using Lyse/Fix buffer (BD Biosciences). Blood cells were counted, stained and analyzed by flow cytometry. The gating strategy is shown for eosinophils, neutrophils, monocytes, inflammatory monocytes, and YM1⁺ inflammatory monocytes (A). The numbers of eosinophils (B), neutrophils (C), inflammatory monocytes (D) and YM1⁺ inflammatory monocytes (E) per mL blood were determined. Results are expressed as means \pm SEM. * $P < 0.05$ HFD vs LFD, # $P < 0.05$ WT vs *Mrc1* ($n = 10-15$ animals per group).

◀ **Figure S1. Analysis of inflammatory markers in adipose tissue and liver by qPCR.** Wild-type (WT) and MR-deficient (*Mrc1*) mice were fed a LFD or HFD for 18 weeks. At sacrifice gonadal WAT and liver tissues were collected and immediately snap-frozen. mRNA expression of the indicated genes in gonadal WAT (A) and liver (B) was quantified by RT-PCR relative to Rplp0 gene and expressed as fold difference compared to the LFD-fed mice. Primer sequences are provided on request. Results are expressed as means \pm SEM. * $P < 0.05$ HFD vs LFD, # $P < 0.05$ WT vs *Mrc1* ($n = 4-6$ animals per group). Genes encode the following proteins: F4/80 (*Emr1*); CD68 (*CD68*); CD11b (*Itgam*); YM1 (*Chil3*); FIZZ1 (*Retnla*); Arginase-1 (*Arg1*); CD11c (*Itgax*); iNOS (*Nos2*); IL-4 (*Il4*); IL-13 (*Il13*); IL-10 (*Il10*); MCP-1 (*Ccl2*); CCR-2 (*Ccr2*); TNF- α (*Tnf*); IFN- γ (*Ifng*); IL-1 β (*Il1b*); IL-6 (*Il6*).

Table S1. Baseline characteristics of WT and MR-deficient mice.

	WT	Mrc1	P-value
Body weight	27.04 ± 0.39	26.12 ± 0.43	0.12
Lean mass	25.27 ± 0.39	24.43 ± 0.42	0.15
Fat mass	1.28 ± 0.10	1.11 ± 0.08	0.18
Glucose	8.78 ± 0.20	8.45 ± 0.27	0.33
Insulin	0.49 ± 0.04	0.38 ± 0.04	0.07
Total Cholesterol	2.56 ± 0.06	2.79 ± 0.07	0.03
Triglycerides	0.54 ± 0.02	0.50 ± 0.02	0.21

Baseline characteristics of wild-type (WT) and MR-deficient (Mrc1) mice were determined at the start of the experiment. Body weight and body composition are shown, and plasma glucose, insulin, total cholesterol and triglyceride levels in 4h-fasted mice. Results are expressed as means ± SEM (n = 25 for WT and 22 for Mrc1).

Table S2. Antibody information.

Target	Clone	Conjugate	Manufacturer
B220	RA3-6B2	eFluor450	eBioscience
B220	RA3-6B2	FITC	eBioscience
CD3	17A2	APC	eBioscience
CD3	17A2	FITC	eBioscience
CD4	GK1.5	PE-Cy7	eBioscience
CD4	GK1.5	PerCP-eF710	eBioscience
CD8a	53-6.7	APC-Cy7	Biolegend
CD11b	M1/70	PE-Cy7	eBioscience
CD11b	M1/70	FITC	eBioscience
CD11c	HL3	Horizon V450	BD Biosciences
CD11c	HL3	FITC	BD Biosciences
CD45.2	104	FITC	Biolegend
CD45.2	104	PE	Biolegend
F4/80	BM8	APC	eBioscience
GR-1	RB6-8C5	FITC	BD Biosciences
IL-5	TRFK5	PE	Biolegend
IL-13	eBio13A	eFluor450	eBioscience
ICOS	C398.4A	PE-Cy7	Biolegend
Ly-6C	HK1.4	APC-Cy7	Biolegend
NK1.1	PK136	PE	BD Biosciences
NK1.1	PK136	FITC	eBioscience
Siglec-F	E50-2440	PE	BD Biosciences
Thy1.2	52-2.1	APC-eFluor780	eBioscience

The background of the page features a light gray, semi-transparent illustration of biological cells. On the right side, there is a dense cluster of cells with irregular, rounded outlines. On the left side, there are several smaller, spiky spherical particles of varying sizes, some of which appear to be interacting with or entering the cells. The overall aesthetic is clean and scientific.

SUMMARIZING DISCUSSION

7

WHAT WAS ALREADY KNOWN ABOUT TH2 POLARIZATION, HELMINTHS, AND METABOLIC DISORDERS?

Helminths are the strongest natural inducers of type 2 immune responses, and many advances in dissecting the mechanisms underlying Th2 polarization have been made using either models of helminth infection or helminth-derived products. It is now recognized that helminth molecules can interact with a variety of receptors on dendritic cells (DCs), including TLRs and CLRs, which either bind or internalize antigens to condition DCs for Th2 skewing via different mechanisms. For example, various reports have indicated that signaling through members of the NF- κ B and ERK pathways seem to play a role in Th2 polarization. In addition, filarial-derived cystatins were suggested to regulate immune cell polarization via signaling-independent mechanisms, by interfering with antigen processing. In terms of DC-derived polarizing signals, up- or downregulation of various soluble factors and/or surface molecules was shown to contribute to Th2 skewing. Furthermore, various reports have described a role for T cell-DC interactions and the T cell receptor (TCR) in T cell skewing. Specifically, Th1-inducing antigens were shown to promote stronger T cell-DC interactions than Th2-inducing antigens (reviewed in (1)).

Over the past five years, the mechanisms underlying Th2 polarization have received accelerating interest, since it is now recognized that multiple facets of the Th2-associated immune response are involved in metabolic regulation (2). For example, IL-4 can regulate the balance between fatty acid and glucose oxidation in hepatocytes (3), and a negative association between metabolic syndrome and helminth infection has been reported (reviewed in (4)). Furthermore, using mouse models of *Nippostrongylus brasiliensis* infection, a rodent nematode spontaneously cleared within two weeks, it has been demonstrated that infected mice on a high-fat diet (HFD) are protected from glucose intolerance, associated with increased white adipose tissue (WAT) eosinophilia and the expression of M2-related genes (5;6). In a follow-up

Summary of what was already known

- Helminth-derived molecules can bind a variety of receptors on DCs, including TLRs and CLRs
- Helminth-derived molecules can modulate DCs for Th2 polarization via signaling-dependent and -independent mechanisms
- Th2 skewing by DCs seems to require upregulation of Th2-polarizing signals and / or downmodulation of Th1-polarizing signals
- Th1-inducing antigens promote stronger T cell-DC interactions than Th2-inducing antigens
- *N. brasiliensis* infection protects mice against HFD-induced insulin resistance and glucose intolerance, increases adipose tissue ILC2s and eosinophils, and promotes the expression of M2-related genes in WAT

study, *N. brasiliensis* was shown to promote accumulation of adipose tissue eosinophils via the induction of group 2 innate lymphoid cells in mice on a chow diet (7). These landmark studies are a major contribution to the field, and highlight the interplay between helminths and metabolic disorders as an exciting area that needs further dissection.

HOW DID OUR STUDIES ADVANCE THE FIELD?

Mechanisms of Th2 polarization: lessons from studying omega-1

Using *Schistosoma mansoni* soluble egg antigens (SEA), it had been described that schistosome antigens can modulate DCs for Th2 polarization by signaling through p42/p44 MAPK (ERK1/2), which lowers IL-12 production and suppresses Th1 polarization (8). Likewise, it was recently suggested that nuclear accumulation of the atypical NF- κ B family member Bcl3 is required for SEA-induced Th2 polarization by downregulating IL-12 mRNA (9). By studying omega-1 in **chapter 2**, we describe a signaling-independent mechanism through which schistosomes can suppress Th1-polarizing signals. Omega-1, a glycosylated T2 ribonuclease (RNase) secreted by *S. mansoni* eggs, was previously identified as the major immunomodulatory component in SEA (10;11). Using recombinant mutants of omega-1 and a co-culture model of human monocyte-derived DCs and allogeneic naïve T cells, we demonstrate that omega-1 requires both its glycosylation and its RNase activity to condition DCs for Th2 polarization. Mechanistically, omega-1 is bound by its glycans and subsequently internalized via the mannose receptor (MR), after which the molecule impairs protein synthesis by degrading both ribosomal and messenger RNA. Interestingly, various Th2-inducing allergens are also RNases (12;13), as well as the endogenous eosinophil-derived neurotoxin that can amplify DC-mediated Th2 polarization (14). Together, these reports suggest that any RNase that ends up in the cytosol of DCs may harbor Th2-priming capacities, through cleavage of ribosomal and/or messenger RNA (1). By doing so, RNases may inhibit the production of IL-12 and other Th1-inducing molecules like Delta-4 (15).

It has been proposed that the mere absence of IL-12 and other Th1-inducing molecules promotes a Th2 response (16), but the results presented in **chapter 3** argue against this hypothesis. In this chapter, we studied the role of the mTOR pathway in T helper polarization by moDCs, building on various reports that suggest involvement of mTOR in T helper cell differentiation (17;18). We show that omega-1 and SEA skew Th2 independent of the mTOR pathway, and additionally demonstrate that blocking the mTOR pathway in LPS-matured moDCs using rapamycin induces a profound Th2 response. These data, together with our finding that co-stimulation of moDCs with rapamycin and helminth antigens results in an additive effect on Th2 cytokine production, led us to conclude that there are mTOR-dependent and -independent mechanisms for Th2 skewing. Interestingly, we also show that rapamycin, unlike SEA and omega-1, skews a very potent Th2 response without affecting LPS-induced IL-12. These data complement early findings showing that mice lacking IL-12 do not develop a Th2 response to microbial pathogens (19), and suggest that there are active signals involved in Th2 differentiation.

In **chapter 4**, we therefore searched for Th2-associated polarizing signals in the DC proteome, since maturation of DCs is largely controlled at the posttranscriptional and posttranslational level (20;21). We employed LC-FTICRMS, a high-throughput gel-free technique for accurate mass measurement and relative quantitation (22), to analyze proteomes of monocyte-derived DCs from nine different donors. We found that SEA and omega-1 strongly increase relative expression of 60S acidic ribosomal protein P2 (RPLP2), which we speculate represent a feedback mechanism secondary to SEA- and omega-1-induced ribosome degradation. In addition, SEA and omega-1 decreased expression of HLA-B, involved in MHC class I-dependent antigen presentation, and CD44, a surface molecule that was previously shown to promote CD4 T cell proliferation by mediation calcium signaling (23). Decreases in HLA-B and CD44 may suggest that Th2-inducing conditions interfere with efficient antigen presentation to T cells. Indeed, both SEA and omega-1 decreased expression of proteins in a protein network enriched for antigen processing and presentation, which supports the hypothesis that weak interaction between T cells and DCs at the level of the immunological synapse may contribute to Th2 polarization by helminth antigens. We also performed GeneMANIA analysis (24), which predicts associations of input genes and related genes, with less stringent thresholds. Analysis of 6h-stimulated samples suggests that SEA and omega-1 may affect cellular glucose metabolism. However, these results are speculative and need experimental confirmation.

Of note, at the start of the LC-FTICRMS project, we hoped to identify novel Th2-associated protein networks. However, we confidently identified only few Th2-associated differentially expressed proteins, which mostly confirmed previously established hypotheses. Because of time and money investments required for an LC-FTICRMS study, we therefore propose that this method is most suitable for screening of samples in which strong effects on proteomes are expected.

In conclusion, our work on DCs and T cell polarization has shed light on the requirements for Th2 skewing by omega-1, which needs both its glycosylation and its RNase activity. We further show that omega-1 does not engage the mTOR pathway to skew T cells, even though blocking mTOR using rapamycin enables DCs to polarize a very potent Th2 response. Lastly, our proteomics study revealed that omega-1 promotes an increase in relative expression of RPLP2, a ribosomal protein, while downregulating proteins involved in antigen presentation. Together, these results highlight that there may be multiple routes for Th2 skewing, involving both signaling-dependent and -independent mechanisms. Follow-up studies will guide design of drugs that reprogram the innate immune system to induce a type 2-associated immune response, which would be desirable in the context of active type 1-mediated metabolic disorders such as obesity and type 2 diabetes.

Helminths and high-fat diet-induced metabolic disorders

Chapter 5 builds on landmark studies showing that conditions that induce type 2 inflammatory responses improve metabolic disorders. We demonstrate that chronic infection with *S. mansoni* protects against high fat diet-induced weight gain, insulin resistance and glucose intolerance in mice. We further show that infection does not affect energy expenditure, but enhances

peripheral glucose uptake and adipose tissue insulin signaling. These effects were associated with the induction of white adipose tissue (WAT) eosinophilia and M2 polarization. Before our study, the effect of helminths on metabolic homeostasis had only been reported in the context of infection with *N. brasiliensis*, a natural nematode of rodents, and little was studied beyond whole-body glucose tolerance and insulin sensitivity (5;6). Our study on chronic infection with *S. mansoni* thus strengthens and complements these findings, and advances the field by providing data on a wide array of metabolic parameters in the context of a helminth that chronically infects millions of people worldwide (25).

In addition, **chapter 5** describes that the beneficial effect of *S. mansoni* infection can be recapitulated in a pathogen-free setting, through repetitive injections with SEA. Specifically, SEA protected against HFD-induced insulin resistance and glucose intolerance without affecting body weight. Although the beneficial effect of SEA injections on glucose and insulin tolerance had been described previously (26), we are the first to have performed in-depth metabolic characterization of SEA-injected mice. In addition, we studied immune cell polarization at the cellular level, and describe that SEA induces a Th2 response, eosinophilia and M2 polarization in WAT. In liver, SEA also promoted eosinophilia and a Th2 response, which may contribute to glucose homeostasis by directly regulating hepatic insulin sensitivity and glucose production via IL-4 and IL-13, respectively (3;27).

Among the different type-2-associated immune cells, the M2 macrophage probably plays the most central role in the maintenance of glucose homeostasis (2;28). A hallmark of the M2 phenotype is enhanced expression of the MR (29), which we showed in **chapter 2** to be required for internalization of omega-1 and subsequent Th2 polarization. Although the MR is widely used as an M2 marker, its role in metabolic homeostasis was not yet studied. In **chapter 6**, we explored the role the MR in the context of diet-induced obesity using whole-body MR^{-/-} mice, and describe that MR deficiency protects against high-fat diet-induced metabolic disorders. Specifically, in mice fed a HFD, lack of MR strongly reduced fat mass gain, adipocyte hyperplasia, glucose intolerance and insulin resistance, and restored locomotor activity and energy expenditure. Thus, despite considerable weight gain, the MR^{-/-} mice were more healthy than WT obese mice. In line with the metabolic phenotype, lack of MR protected mice from HFD-induced classical activation of macrophages in adipose tissue and liver.

The protective effect of MR deficiency on HFD-induced metabolic disorders was surprising, given the association between MR and the M2 phenotype (29), and the pivotal role MR plays in the initiation of type 2 immune responses (30-33). Since we also observed low expression of MR by M1 macrophages, we speculate that MR can deliver signals directly into MR-bearing macrophages through interaction with co-receptors, which might result in a pro-inflammatory phenotype under HFD conditions. It is also important to consider that MR^{-/-} mice lack whole-body expression of the *Mrc1* gene, and that MR expression is not restricted to leukocytes (34). For example, MR is expressed by microglia and astrocytes in the brain (35). Interestingly, hypothalamic inflammation has been described to contribute to HFD-induced weight gain (36), and activation of the cholinergic anti-inflammatory reflex was recently demonstrated to promote metabolic homeostasis (37). Whether the beneficial effect of MR deficiency on

metabolic homeostasis can be attributed to immune cell signaling, altered neuroinflammation, defects in the anti-inflammatory reflex, or effects beyond the immune system or the brain, remains to be determined.

In sum, our work on helminths and high-fat diet-induced metabolic disorders has provided valuable insights into the effects of helminths and their molecules on metabolic homeostasis. Of particular interest may be the finding that chronic helminth infection enhances peripheral glucose uptake and insulin action in WAT, an effect that may be secondary to the induction of a type 2-associated immune response. Furthermore, our findings on the beneficial effect of SEA on metabolic homeostasis identify helminth molecules as attractive agents for therapeutic manipulation of the immune system in the context of metabolic disorders. Lastly, our data on the unexpected role of MR in the development of metabolic homeostasis provide a novel lead for studying the etiology of diet-induced metabolic disorders.

Summary of the new findings

In this thesis, we studied the *S. mansoni* egg-derived molecule omega-1, a T2 RNase with strong Th2-polarizing capacities. We investigated how this molecule modulates dendritic cells for Th2 skewing at the molecular level. Furthermore, we analyzed the effect of high-fat diet-feeding in mice chronically infected with *S. mansoni* or chronically exposed to SEA. Lastly, we performed in-depth metabolic and immune cell profiling of MR-deficient mice fed a HFD. The main findings are:

- Omega-1 requires both its glycosylation and its RNase activity to condition DCs for Th2 polarization (**Chapter 2**)
- Omega-1 is bound and internalized via its glycans by the MR, and impairs protein synthesis by degrading both ribosomal and messenger RNA (**Chapter 2**)
- SEA and omega-1 skew Th2 without affecting the mTOR pathway (**Chapter 3**)
- Blocking the mTOR pathway using rapamycin primes DCs for Th2 skewing without affecting IL-12 production (**Chapter 3**)
- SEA and omega-1 alter the DC proteome, with the most pronounced effect on 60S acidic ribosomal protein P2 and proteins involved in antigen presentation (**Chapter 4**)
- Chronic *S. mansoni* infection and SEA treatment protect against metabolic disorders in HFD-induced obesity, and strongly increase adipose tissue eosinophilia and M2 polarization (**Chapter 5**)
- Chronic *S. mansoni* infection reduces adipocyte size and increases peripheral glucose uptake and WAT insulin sensitivity in HFD-fed mice (**Chapter 5**)
- Chronic administration of SEA promotes a Th2 response in WAT and liver of HFD-induced obese mice (**Chapter 5**)
- MR deficiency protects against HFD-induced insulin resistance and glucose intolerance and decreases HFD-induced classical activation of liver and WAT macrophages (**Chapter 6**)

DIRECTIONS FOR FUTURE RESEARCH¹

The studies presented in this thesis shed new light on the mechanisms of DC-mediated Th2 polarization by helminth antigens. They further demonstrate that chronic *S. mansoni* infection and SEA administration protect against diet-induced metabolic disorders, and propose that the MR plays an unexpected role in the development of diet-induced insulin resistance. As this thesis progressed, so did the field, and our findings together with several exciting (new) areas of research fuel directions for future studies.

DC metabolism and Th2 polarization

Recent studies indicate that modulation of metabolic pathways within immune cells can regulate their function and, thereby, the outcome of the immune response (38). For example, BMDCs switch their core metabolism from mitochondrial oxidative phosphorylation to glycolysis upon TLR-ligation, and inhibition of this switch interferes with maturation, IL-12 expression, and the ability to induce CD4⁺ T cell proliferation (39;40). The question whether helminths or their products affect glycolytic reprogramming in DCs, and how this relates to Th2 polarization, constitutes an exciting new area of research.

The T cell receptor

It has been suggested that T cells are polarized towards Th2 if the interaction between DCs and T cells is weak (41-43). Interestingly, others have demonstrated that omega-1 reduces the capacity of BMDCs to form T cell–DC conjugates and diminishes the frequency of CD4⁺ T cells progressing through the cell cycle (11). Novel techniques allow for the analysis of DC-T cell interactions *in vivo*, through intravital dynamic 2-photon microscopy (43). Future studies could therefore explore the strength of TCR signaling in the context of helminth-induced Th2 polarization *in vitro* and *in vivo*.

DCs and the microenvironment

Accumulating evidence points towards a crucial role for the microenvironment in which DCs are primed for T cell polarization. For example, epithelial-derived cytokine alarmins like thymic stromal lymphopoietin (TSLP) and IL-33 condition DCs to skew Th2 (44-46), IL-33 treatment improves Th2 cytokine production and expulsion of *Trichuris muris* (47), and mice deficient for the IL-33 receptor T1/ST2 fail to develop a Th2 response to *S. mansoni* eggs (48). Importantly, T1/ST2 is not only present on DCs but also on lymphocyte subsets including ILC2s, which were shown to potentiate Th2 responses by promoting DC migration and interacting with T cells via MHC-II (49;50). In addition, it has been suggested that DCs require B cells for the initiation of a Th2 response since B cells enable proper localization in the lymph node (51). Together, these studies highlight the importance of studying polarizing alarmins and accessory cells in the search for mechanisms of Th2 polarization.

¹ Parts of this section are based on the review "Priming dendritic cells for Th2 polarization: lessons learned from helminths and implications for metabolic disorders" (1).

Helminths, immune cells, and protection against metabolic disorders

It has been demonstrated that maintenance of M2 macrophages in WAT depends on the presence of IL-4-secreting eosinophils (5), which are sustained by IL-5 and IL-13-producing ILC2s (7) in non-infected mice. In our study, we observe an increase in cytokine-producing Th2 cells and eosinophils following chronic exposure to *S. mansoni* or SEA, but the relative contribution of each cell type to the beneficial effect on WAT insulin sensitivity and whole-body metabolic homeostasis remains unknown. Future studies are needed using mice deficient in different immune cell types or their effector cytokines, in order to understand how helminths promote metabolic homeostasis.

Furthermore, in relation to the role of the MR in the development of diet-induced metabolic disorders (chapter 6), the use of conditional knockout mice or adoptive transfer experiments should elucidate whether the protective effect of MR deficiency on high-fat diet-induced insulin resistance can be attributed to MR expression by immune or non-immune cells.

Helminth molecules and direct interaction with metabolic cells

A recent landmark study demonstrated that SEA can directly suppress lipogenesis in primary hepatocytes (26), which led us to hypothesize that helminth molecules may protect against metabolic disorders by acting as a double-edged sword (Figure 1). Helminth antigens may regulate glucose homeostasis directly by modulating metabolic pathways, or indirectly by polarizing a type 2 immune response. Future studies should therefore focus on the identification of the cellular targets of helminth antigens, as well as the specific helminth-derived molecules involved.

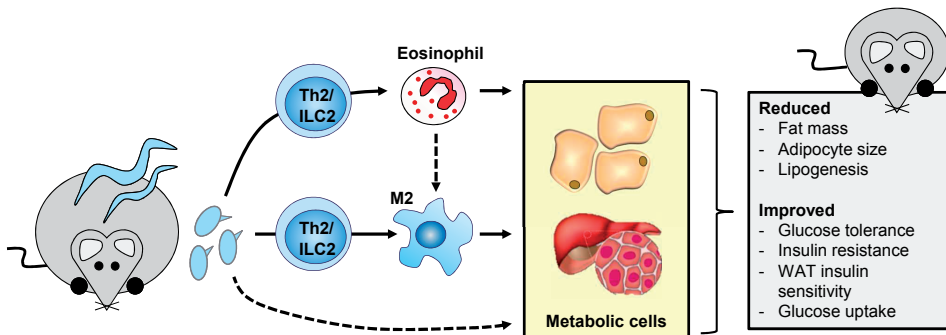


Figure 1. *S. mansoni* and protection against metabolic disorders: A double-edged sword? *S. mansoni* egg-derived molecules may protect against metabolic disorders by skewing a type 2 immune response, or through direct interaction with metabolic cells, like adipocytes or hepatocytes.

Remaining questions

- Do helminth antigens affect DC metabolism and does this contribute to the initiation of a Th2 response?
- Does the strength of TCR signaling play a role in Th2 polarization by helminth antigens?
- What is the role of the microenvironment in DC-mediated for Th2 polarization?
- What is the contribution of different immune cells to the beneficial effect of helminth antigens on diet-induced metabolic disorders, and how do these immune cells interact?
- Do helminth molecules act on non-immune cells to promote metabolic homeostasis?
- Which helminth-derived single molecules contribute to metabolic homeostasis?
- Can the protective effect of MR deficiency on diet-induced obesity be attributed to immune or non-immune cells?

CONCLUDING REMARKS

To date, the mechanisms that govern Th2 polarization are still not fully understood. Future studies should focus on pinpointing the requirements that qualify DCs for Th2 skewing, bearing in mind that DCs operate in a microenvironment that may influence priming. It is now recognized that type 2 immune responses can also regulate energy metabolism, and studying how helminths generate Th2 responses and contribute to metabolic homeostasis will therefore not only shed light on the mechanisms that promote control of parasite infection, but may provide valuable leads for the development of pharmaceutical agents for the treatment of metabolic disorders.

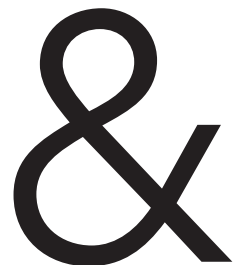
REFERENCES

1. Husaarts L, et al. Priming dendritic cells for th2 polarization: lessons learned from helminths and implications for metabolic disorders. *Front Immunol* 2014;5:499.
2. Chawla A, et al. Macrophage-mediated inflammation in metabolic disease. *Nat Rev Immunol* 2011 Nov;11(11):738-49.
3. Ricardo-Gonzalez RR, et al. IL-4/STAT6 immune axis regulates peripheral nutrient metabolism and insulin sensitivity. *Proc Natl Acad Sci U S A* 2010 Dec 28;107(52):22617-22.
4. Wiria AE, et al. Helminth infections, type-2 immune response, and metabolic syndrome. *PLoS Pathog* 2014 Jul;10(7):e1004140.
5. Wu D, et al. Eosinophils sustain adipose alternatively activated macrophages associated with glucose homeostasis. *Science* 2011 Apr 8;332(6026):243-7.
6. Yang Z, et al. Parasitic nematode-induced modulation of body weight and associated metabolic dysfunction in mouse models of obesity. *Infect Immun* 2013 Jun;81(6):1905-14.
7. Molofsky AB, et al. Innately lymphoid type 2 cells sustain visceral adipose tissue eosinophils and alternatively activated macrophages. *J Exp Med* 2013 Mar 11;210(3):535-49.
8. Agrawal S, et al. Cutting edge: different Toll-like receptor agonists instruct dendritic cells to induce distinct Th responses via differential modulation of extracellular signal-regulated kinase-mitogen-activated protein kinase and c-Fos. *J Immunol* 2003 Nov 15;171(10):4984-9.
9. Gringhuis SI, et al. Fucose-specific DC-SIGN signalling directs T helper cell type-2 responses via I K K epsilon- and CYLD-dependent Bcl3 activation. *Nat Commun* 2014;5:3898.
10. Everts B, et al. Omega-1, a glycoprotein secreted by *Schistosoma mansoni* eggs, drives Th2 responses. *J Exp Med* 2009 Aug 3;206(8):1673-80.
11. Steinfeldt S, et al. The major component in schistosome eggs responsible for conditioning dendritic cells for Th2 polarization is a T2 ribonuclease (omega-1). *J Exp Med* 2009 Aug 3;206(8):1681-90.
12. Bufe A, et al. The major birch pollen allergen, Bet v 1, shows ribonuclease activity. *Planta* 1996;199(3):413-5.
13. Kao R, et al. Mitogillin and related fungal ribotoxins. *Methods Enzymol* 2001;341:324-35.
14. Yang D, et al. Eosinophil-derived neurotoxin acts as an alarmin to activate the TLR2-MyD88 signal pathway in dendritic cells and enhances Th2 immune responses. *J Exp Med* 2008 Jan 21;205(1):79-90.
15. van Riet E, et al. Combined TLR2 and TLR4 ligation in the context of bacterial or helminth extracts in human monocyte derived dendritic cells: molecular correlates for Th1/Th2 polarization. *BMC Immunol* 2009;10:9.
16. Jankovic D, et al. Th1- and Th2-cell commitment during infectious disease: asymmetry in divergent pathways. *Trends Immunol* 2001 Aug;22(8):450-7.
17. Salmond RJ, et al. The influence of mTOR on T helper cell differentiation and dendritic cell function. *Eur J Immunol* 2011 Aug;41(8):2137-41.
18. Thomson AW, et al. Immunoregulatory functions of mTOR inhibition. *Nat Rev Immunol* 2009 May;9(5):324-37.
19. Jankovic D, et al. In the absence of IL-12, CD4(+) T cell responses to intracellular pathogens fail to default to a Th2 pattern and are host protective in an IL-10(-/-) setting. *Immunity* 2002 Mar;16(3):429-39.
20. Le NF, et al. Profiling changes in gene expression during differentiation and maturation of monocyte-derived dendritic cells using both oligonucleotide microarrays and proteomics. *J Biol Chem* 2001 May 25;276(21):17920-31.
21. Richards J, et al. Integrated genomic and proteomic analysis of signaling pathways in dendritic cell differentiation and maturation. *Ann NY Acad Sci* 2002 Dec;975:91-100.
22. Johansson A, et al. Identification of genetic variants influencing the human plasma proteome. *Proc Natl Acad Sci U S A* 2013 Mar 19;110(12):4673-8.
23. Termeer C, et al. Targeting dendritic cells with CD44 monoclonal antibodies selectively inhibits the proliferation of naive CD4+ T-helper cells by induction of FAS-independent T-cell apoptosis. *Immunology* 2003 May;109(1):32-40.
24. Warde-Farley D, et al. The GeneMANIA prediction server: biological network integration for gene prioritization and predicting gene function. *Nucleic Acids Res* 2010 Jul;38(Web Server issue):W214-W220.
25. Pearce EJ, et al. The immunobiology of schistosomiasis. *Nat Rev Immunol* 2002 Jul;2(7):499-511.

26. Bhargava P, et al. Immunomodulatory glycan LNFPIII alleviates hepatosteatosis and insulin resistance through direct and indirect control of metabolic pathways. *Nat Med* 2012 Nov;18(11):1665-72.
27. Stanya KJ, et al. Direct control of hepatic glucose production by interleukin-13 in mice. *J Clin Invest* 2013 Jan 2;123(1):261-71.
28. Odegaard JI, et al. Alternative macrophage activation and metabolism. *Annu Rev Pathol* 2011;6:275-97.
29. Stein M, et al. Interleukin 4 potently enhances murine macrophage mannose receptor activity: a marker of alternative immunologic macrophage activation. *J Exp Med* 1992 Jul 1;176(1):287-92.
30. Everts B, et al. Schistosome-derived omega-1 drives Th2 polarization by suppressing protein synthesis following internalization by the mannose receptor. *J Exp Med* 2012 Sep 24;209(10):1753-67, S1.
31. Royer PJ, et al. The mannose receptor mediates the uptake of diverse native allergens by dendritic cells and determines allergen-induced T cell polarization through modulation of IDO activity. *J Immunol* 2010 Aug 1;185(3):1522-31.
32. Paveley RA, et al. The Mannose Receptor (CD206) is an important pattern recognition receptor (PRR) in the detection of the infective stage of the helminth *Schistosoma mansoni* and modulates IFN γ production. *Int J Parasitol* 2011 Nov;41(13-14):1335-45.
33. Emará M, et al. Recognition of the major cat allergen Fel d 1 through the cysteine-rich domain of the mannose receptor determines its allergenicity. *J Biol Chem* 2011 Apr 15;286(15):13033-40.
34. Martínez-Pomares L. The mannose receptor. *J Leukoc Biol* 2012 Dec;92(6):1177-86.
35. Regnier-Vigouroux A. The mannose receptor in the brain. *Int Rev Cytol* 2003;226:321-42.
36. Thaler JP, et al. Minireview: Inflammation and obesity pathogenesis: the hypothalamus heats up. *Endocrinology* 2010 Sep;151(9):4109-15.
37. Wang L, et al. Pten deletion in RIP-Cre neurons protects against type 2 diabetes by activating the anti-inflammatory reflex. *Nat Med* 2014 May;20(5):484-92.
38. Pearce EL, et al. Metabolic pathways in immune cell activation and quiescence. *Immunity* 2013 Apr 18;38(4):633-43.
39. Krawczyk CM, et al. Toll-like receptor-induced changes in glycolytic metabolism regulate dendritic cell activation. *Blood* 2010 Jun 10;115(23):4742-9.
40. Everts B, et al. TLR-driven early glycolytic reprogramming via the kinases TBK1-IKK ϵ supports the anabolic demands of dendritic cell activation. *Nat Immunol* 2014 Apr;15(4):323-32.
41. Constant S, et al. Extent of T cell receptor ligation can determine the functional differentiation of naive CD4+ T cells. *J Exp Med* 1995 Nov 1;182(5):1591-6.
42. Hosken NA, et al. The effect of antigen dose on CD4+ T helper cell phenotype development in a T cell receptor-alpha beta-transgenic model. *J Exp Med* 1995 Nov 1;182(5):1579-84.
43. van Panhuys N, et al. T-Cell-Receptor-Dependent Signal Intensity Dominantly Controls CD4(+) T Cell Polarization In Vivo. *Immunity* 2014 Jul 17;41(1):63-74.
44. Soumelis V, et al. Human epithelial cells trigger dendritic cell mediated allergic inflammation by producing TSLP. *Nat Immunol* 2002 Jul;3(7):673-80.
45. Besnard AG, et al. IL-33-activated dendritic cells are critical for allergic airway inflammation. *Eur J Immunol* 2011 Jun;41(6):1675-86.
46. Eiwegger T, et al. IL-33 links tissue cells, dendritic cells and Th2 cell development in a mouse model of asthma. *Eur J Immunol* 2011 Jun;41(6):1535-8.
47. Humphreys NE, et al. IL-33, a potent inducer of adaptive immunity to intestinal nematodes. *J Immunol* 2008 Feb 15;180(4):2443-9.
48. Townsend MJ, et al. T1/ST2-deficient mice demonstrate the importance of T1/ST2 in developing primary T helper cell type 2 responses. *J Exp Med* 2000 Mar 20;191(6):1069-76.
49. Halim TY, et al. Group 2 innate lymphoid cells are critical for the initiation of adaptive T helper 2 cell-mediated allergic lung inflammation. *Immunity* 2014 Mar 20;40(3):425-35.
50. Oliphant CJ, et al. MHCII-mediated dialog between group 2 innate lymphoid cells and CD4(+) T cells potentiates type 2 immunity and promotes parasitic helminth expulsion. *Immunity* 2014 Aug 21;41(2):283-95.
51. Leon B, et al. Regulation of T(H)2 development by CXCR5+ dendritic cells and lymphotoxin-expressing B cells. *Nat Immunol* 2012 Jul;13(7):681-90.

ADDENDUM

Nederlandse samenvatting
Dankwoord / Acknowledgements
Curriculum vitae
List of publications



NEDERLANDSE SAMENVATTING

Het immuunsysteem

Het afweersysteem, ook wel het immuunsysteem genoemd, beschermt ons tegen pathogene ziekteverwekkers zoals virussen, bacteriën en parasitaire wormen. Het immuunsysteem kan grofweg worden onderverdeeld in twee takken: de aspecifieke afweer en de specifieke afweer, die samenwerken als er een infectie optreedt. Pathogenen die door de huid of de slijmvliezen het lichaam weten binnen te dringen, stuiten als eerste op de witte bloedcellen van de aspecifieke afweer. Onderdeel van de aspecifieke afweer zijn de dendritische cellen (DCs), die in staat zijn om de specifieke afweer te activeren. Zodra een DC een pathogeen tegenkomt, presenteert de DC delen van het pathogeen (antigenen) op zijn buitenzijde en migreert naar een lymfeklier. Daar bevinden zich de T-helpercellen, onderdeel van de specifieke afweer. Komt de DC een T-helpercel tegen die gericht is tegen het gepresenteerde antigen, dan wordt de T-helpercel geactiveerd. De T-helpercel geeft vervolgens specifieke signalen af, die helpen bij het activeren van andere witte bloedcellen die de ziekteverwekker opruimen.

Niet alle ziekteverwekkers worden bestreden met hetzelfde type afweerreactie, binnen de T-helpercellen worden dan ook verschillende soorten onderscheiden. Zo activeren virale of bacteriële infecties veelal T-helper-1 (Th1)-cellen, die helpen bij het initiëren een type 1 afweerreactie. Parasitaire wormen wekken daarentegen een type 2-afweerreactie op, waarin de Th2-cellen centraal staan. De activatie van verschillende typen T-helpercellen wordt T-helpercel-differentiatie genoemd. Dit proces wordt aangestuurd door de DCs die in staat zijn verschillende antigenen van elkaar te onderscheiden: op basis van het type antigeen geven de DCs signalen af die de T-helpercel-differentiatie beïnvloeden. Een DC heeft in zijn interactie met het specifieke afweersysteem dus twee belangrijke taken: het presenteren van de antigenen die vereist zijn voor T-cel-activatie, en het afgeven van signalen die de differentiatie van T cellen sturen.

Naast het afweren van pathogenen heeft het immuunsysteem ook andere functies. Zo helpen bepaalde type 2-afweercellen (de M2-macrofagen) bijvoorbeeld bij het opruimen van dode lichaamscellen. Helaas kan het immuunsysteem zich ook tegen ons keren: als verschillende componenten van het immuunsysteem uit balans zijn, kunnen er allergieën en auto-immuunziekten ontstaan. Recent onderzoek heeft aangetoond dat het immuunsysteem ook ontregeld is bij mensen met overtollig vetweefsel, wat de kans op diabetes type 2 vergroot.

Afweerreacties en diabetes type 2

Patiënten met diabetes type 2, beter bekend als ouderdomsdiabetes, zijn minder gevoelig voor het hormoon insuline. Insuline zorgt ervoor dat glucose uit het bloed kan worden opgenomen door alle cellen in het lichaam, die dit gebruiken om energie van te maken. Als de cellen in het lichaam echter niet meer reageren op insuline, oftewel insulineresistent zijn geworden, blijven de bloedsuikerspiegels hoog wat op lange termijn zenuwen en bloedvaten kan beschadigen.

Vetweefsel van muizen op een normaal dieet bevat vooral type 2-afweercellen, die het vetweefsel gezond houden en de werking van insuline bevorderen. In vetweefsel van muizen



met overgewicht ontstaat echter een chronische ontsteking, gekenmerkt door een groot aantal type 1-afweercellen die de werking van insuline belemmeren. Om diabetes type 2 te kunnen behandelen, is het dus essentieel dat de type 1-afweercellen in het vetweefsel weer plaats maken voor type 2-afweercellen.

Zoals hierboven beschreven zijn type 2-afweercellen bij uitstek aanwezig tijdens infecties met parasitaire wormen. Daarnaast is aangetoond dat een infectie met de parasitaire worm *Nippostrongylus brasiliensis* een positief effect heeft op de insulinegevoeligheid in muizen met overgewicht. Door te onderzoeken hoe parasitaire wormen een type 2-afweerreactie bewerkstelligen, kunnen we dus ook meer leren over hoe diabetes type 2 bestreden zou kunnen worden.

Leren van wormen

Naar schatting een kwart van de wereldbevolking is geïnfecteerd met parasitaire wormen, vooral in tropische landen. Er zijn veel verschillende soorten parasitaire wormen, waaronder de *Schistosoma*-platwormen die vaak worden gebruikt in onderzoek naar type 2-afweerreacties. Dit komt doordat de antigenen van *Schistosoma*-eitjes (SEA) sterke Th2-sturende capaciteiten bezitten, zowel *in vivo* (in de muis) als *in vitro* (in het laboratorium).

Om uit te kunnen zoeken hoe het komt dat SEA DCs aanzet tot Th2-differentiatie, wordt vaak gebruik gemaakt van een *in vitro* DC-model. Dat houdt in dat DCs in het laboratorium worden blootgesteld aan SEA, waarna de DCs worden gekweekt met T-helpercellen om de differentiatie te bestuderen. Met behulp van dit model is ontdekt dat een klein eiwit in SEA, genaamd *omega-1*, sterke Th2-sturende capaciteiten heeft. Door het effect van *omega-1* op DCs te bestuderen, proberen we te ontrafelen welke mechanismen ten grondslag liggen aan Th2-differentiatie.

Onderzoek beschreven in dit proefschrift

Hoofdstuk 2 beschrijft onderzoek met behulp van het DC-model naar het molecuul *omega-1*. *Omega-1* is een enzym dat RNA kan knippen (dit wordt RNase-activiteit genoemd) en dat suikermoleculen op zijn oppervlak heeft (glycosylering). Zowel na het inactiveren van de RNase-activiteit als na het weghalen van de glycosylering bleek *omega-1* niet meer in staat DCs aan te zetten tot Th2-differentiatie. Nader onderzoek wees uit dat *omega-1* zijn suikermoleculen gebruikt om te binden aan de mannosereceptor op het oppervlak van DCs, zodat het kan worden opgenomen door deze cellen. Eenmaal in de cellen bleek de RNase-activiteit van *omega-1* van belang. Op basis van informatie uit het DNA maakt een cel eiwitten met behulp van RNA. Door RNA te knippen, belemmerde *omega-1* de eiwitproductie in de DCs. In het kort blijkt glycosylering dus nodig te zijn voor de opname van *omega-1* via de mannosereceptor, waarna de RNase-activiteit essentieel was om de DCs aan te zetten tot Th2-differentiatie.

Hoe het belemmeren van eiwitproductie door *omega-1* precies leidt tot een signaal voor Th2-differentiatie werd onderzocht in **hoofdstuk 3**, wederom met het DC-model. We bestudeerden de mTOR-signaleringsroute, een keten van regelprocessen die signalen van

binnen en buiten de cel integreert en daardoor celgroei en activatie van witte bloedcellen kan beïnvloeden. Deze signaleringsroute kan worden geblokkeerd door het geneesmiddel rapamycin. Dit medicijn wordt gebruikt om afstoting na orgaantransplantatie te voorkomen, omdat het middel het immuunstelsel onderdrukt. Rapamycin bleek, net als omega-1, DCs aan te zetten tot Th2-differentiatie. Dit leidde tot de hypothese dat stimulatie met omega-1 wellicht een effect heeft op de activiteit van de mTOR-signaleringsroute. Dit was echter niet het geval: omega-1 had geen effect op activatie van het mTOR-eiwit of op andere eiwitten binnen de mTOR-signaleringsroute. Bovendien leidde co-stimulatie van DCs met rapamycin en omega-1 tot een sterkere Th2-differentiatie dan stimulatie met alleen rapamycin of omega-1. Uit deze resultaten kan geconcludeerd worden dat DCs op verschillende manieren aangezet kunnen worden tot Th2-differentiatie: via mTOR-afhankelijke en -onafhankelijke mechanismen.

In **hoofdstuk 4** werden DCs na stimulatie met omega-1 bestudeerd met behulp van massaspectrometrie, een techniek voor het identificeren en kwantificeren van eiwitfragmenten. In de gestimuleerde cellen werden in totaal 208 verschillende eiwitten geïdentificeerd en gekwantificeerd. Uit een nadere analyse bleek dat de aanwezigheid van omega-1 een sterk effect had op de eiwitten betrokken bij antigeenpresentatie: in vergelijking met DCs die niet waren gestimuleerd, bezaten DCs na stimulatie met omega-1 minder van deze eiwitten. Eerder is al aangetoond dat een zwakke interactie tussen DCs en T-helpercellen tijdens de antigeenpresentatie kan leiden tot Th2-differentiatie. Omdat omega-1 zorgt voor een verlaging van de eiwitten betrokken bij antigeenpresentatie, suggereren de resultaten dat Th2-differentiatie door omega-1 wellicht ook tot stand komt door een zwakke interactie tussen DCs en T-helpercellen. Om deze hypothese te toetsen is verder onderzoek nodig.

Zoals in de inleiding beschreven, is recent aangetoond dat een infectie met de worm *N. brasiliensis* de insulinegevoeligheid kan bevorderen in muizen met overgewicht. Echter, *N. brasiliensis* is een worm die alleen knaagdieren voor een korte duur kan infecteren. In **hoofdstuk 5** is onderzocht of *Schistosoma*-wormen, die wereldwijd meer dan 200 miljoen mensen chronisch infecteren, hetzelfde effect hebben op het glucosepijl. Om dit te bestuderen zijn muizen met obesitas blootgesteld aan *Schistosoma mansoni*. Muizen op een hoog-vetdieet met een chronische *S. mansoni* infectie werden minder dik, de cellen in het lichaam namen glucose sneller op en de muizen waren gevoeliger voor insuline, in vergelijking met niet-geïnfecteerde soortgenoten. Dit ging gepaard met een type 2-afweerreactie in het vetweefsel. Het positieve effect van *S. mansoni*-wormen op de insulinegevoeligheid bleek te reproduceren door de muizen te injecteren met enkel SEA, wat perspectief biedt voor een eventuele therapeutische toepassing van wormen als bescherming tegen diabetes type 2.

Tot slot is in **hoofdstuk 6** gekeken naar de rol van de mannosereceptor (MR) in het ontstaan van insulineresistentie. In hoofdstuk 2 was met behulp van omega-1 al aangetoond dat de MR een belangrijke rol speelt in Th2-differentiatie. Daarnaast was ook al bekend dat de MR in grote mate aanwezig is op M2-macrofagen (onderdeel van de type 2-afweerreactie), en juist laag tot expressie komt op M1-macrofagen (onderdeel van de type 1-afweerreactie). Om de rol van de MR in het ontstaan van insulineresistentie te onderzoeken, zijn muizen waarin de MR door middel van genetische manipulatie werd uitgeschakeld (MR-*knockout* muizen)



blootgesteld aan een hoog-vet-dieet. In vergelijking met gewone muizen, waren er in de *MR-knockout* muizen tegen de verwachting in juist minder M1-macrofagen te vinden in het vetweefsel en in de lever. Dit ging gepaard met een verhoging van de insulinegevoeligheid. Hoe de afwezigheid van de mannosereceptor een positief effect op de suikerhuishouding veroorzaakt, is nog onduidelijk en vraagt om verder onderzoek.

Conclusie

Het onderzoek beschreven in dit proefschrift draagt bij aan een beter begrip van de mechanismen die ten grondslag liggen aan Th2-differentiatie. Daarnaast laten de studies zien dat wormmoleculen in muizen met obesitas bijdragen aan een gezonde suikerhuishouding. Er is echter nog veel onbekend over het ontstaan van type 2-afweerreacties. Daarom is het noodzakelijk om verder onderzoek te verrichten naar wormmoleculen, DCs en Th2-differentiatie. Dit is niet alleen relevant voor het verschaffen van inzichten in basale immunologische processen, maar draagt ook bij aan het ontwikkelen van therapieën voor ziekten waarbij een type 2-afweerreactie wenselijk is, zoals diabetes type 2.



CURRICULUM VITAE

Leonie Hussaarts was born on 19 September 1987 in Delft, the Netherlands. At the age of nine, she moved to Emmeloord where she completed grammar school (gymnasium; *cum laude*) at the Zuyderzee College. In 2008, she graduated *cum laude* with a Bachelor of Science (B.Sc.) in Liberal Arts and Sciences from University College Utrecht, after which she moved to Leiden to study Biomedical Sciences. In the summer of 2009, Leonie worked as a research assistant at the department of Parasitology at the Leiden University Medical Center. She stayed at the department as a graduate intern, and studied regulatory B cells in collaboration with the department of Rheumatology at Imperial College London, where she also spent three months. In February 2011, she obtained her degree of Master of Science (M.Sc.). Leonie started her PhD program on dendritic cell modulation by *Schistosoma mansoni* antigens under the supervision of Prof. Dr. Maria Yazdanbakhsh at the department of Parasitology in January 2011. Halfway through her program, Dr. Bruno Guigas joined the department, and Leonie took the opportunity to study the effect of helminths and their products on high-fat diet-induced metabolic disorders under his supervision. In addition to her scientific experience, Leonie has a minor in Art History and a minor in Journalism and New Media. She worked as a freelance science journalist for Leiden University and has been a member of various boards and committees, including the LUMC PhD-Day committee (2012), while working towards her PhD degree. Leonie currently works as a Scientific Communication Officer at CTMM-TI Pharma.



LIST OF PUBLICATIONS

Hussaarts L, García-Tardón N, van Beek L, Heemskerk MM, Haeberlein S, van der Zon GC, Ozir-Fazalilikhan A, Berbée JFP, Willems van Dijk K, van Harmelen V, Yazdanbakhsh M, Guigas B. *Chronic helminth infection and helminth-derived egg antigens promote adipose tissue M2 macrophages and improve insulin sensitivity in obese mice*. FASEB J. 2015 Apr 7 [Epub ahead of print]

Hussaarts L, Yazdanbakhsh M, Guigas B. *Priming dendritic cells for Th2 polarization: lessons learned from helminths and implications for metabolic disorders*. Front Immunol. 2014 Oct 20;5:499.

Bos E, **Hussaarts L**, van Weering JR, Ellisman MH, de Wit H, Koster AJ. *Vitrification of Tokuyasu-style immuno-labelled sections for correlative cryo light microscopy and cryo electron tomography*. J Struct Biol. 2014 May;186(2):273-82.

Sattler S, Ling GS, Xu D, **Hussaarts L**, Romaine A, Zhao H, Fossati-Jimack L, Malik T, Cook HT, Botto M, Lau YL, Smits HH, Liew FY, Huang FP. *IL-10-producing regulatory B cells induced by IL-33 (Breg(IL-33)) effectively attenuate mucosal inflammatory responses in the gut*. J Autoimmun. 2014 May;50:107-22.

Hussaarts L, Smits HH, Schramm G, van der Ham AJ, van der Zon GC, Haas H, Guigas B, Yazdanbakhsh M. *Rapamycin and omega-1: mTOR-dependent and -independent Th2 skewing by human dendritic cells*. Immunol Cell Biol. 2013 Aug;91(7):486-9.

Everts B, **Hussaarts L***, Driessen NN*, Meevissen MH, Schramm G, van der Ham AJ, van der Hoeven B, Scholzen T, Burgdorf S, Mohrs M, Pearce EJ, Hokke CH, Haas H, Smits HH, Yazdanbakhsh M. *Schistosome-derived omega-1 drives Th2 polarization by suppressing protein synthesis following internalization by the mannose receptor*. J Exp Med. 2012 Sep 24;209(10):1753-67, S1.

* These authors contributed equally

Sattler S, van der Vlugt LE, **Hussaarts L**, Smits HH, Huang FP. *Regulatory B Cells - Implications in Autoimmune and Allergic Disorders*. In J.R. Kanwar, Recent Advances in Immunology to Target Cancer, Inflammation and Infections, InTech Open Access, 2012 May:177-200.

Hussaarts L, van der Vlugt LE, Yazdanbakhsh M, Smits HH. *Regulatory B-cell induction by helminths: implications for allergic disease*. J Allergy Clin Immunol. 2011 Oct;128(4):733-9.



